ANALYSIS OF CORNER EFFECTS ON IN-SITU WALLS SUPPORTING DEEP EXCAVATIONS: COMPARISON OF PLANE STRAIN AND THREE DIMENSIONAL ANALYSIS

A THESIS SUBMITTED TO
THE GRADUATE SCHOOL OF NATURAL AND APPLIED SCIENCES
OF
MIDDLE EAST TECHNICAL UNIVERSITY

BY

GÜLİZ ÜNLÜ

IN PARTIAL FULFILLMENT OF THE REQUIREMENTS
FOR
THE DEGREE OF MASTER OF SCIENCE
IN
CIVIL ENGINEERING

NOVEMBER 2008

Approval of the thesis:

ANALYSIS OF CORNER EFFECTS ON IN-SITU WALLS SUPPORTING DEEP EXCAVATIONS: COMPARISON OF PLANE STRAIN AND THREE DIMENSIONAL ANALYSIS

Submitted by **GÜLİZ ÜNLÜ** in partial fulfillment of the requirements for the degree of Master of Science in **Civil Engineering Department, Middle East Technical University** by,

Prof. Dr. Canan Özgen _____
Dean, Graduate School of **Natural and Applied Sciences**

Prof. Dr. Güney Özcebe _____
Head of Department, **Civil Engineering**

Prof. Dr. Orhan Erol _____
Supervisor, **Civil Engineering Dept., METU**

Examining Committee Members:

Prof. Dr. Erdal Çokça _____
Civil Engineering Dept., METU

Prof. Dr. Orhan Erol _____
Civil Engineering Dept., METU

Assoc. Prof. K. Önder Çetin _____
Civil Engineering Dept., METU

Dr. Kartal Toker _____
Civil Engineering Dept., METU

M.S. Mustafa Toker _____
Toker Drilling and Cons. Co.

Date: November 25, 2008

I hereby declare that all information in this document has been obtained and presented in accordance with academic rules and ethical conduct. I also declare that, as required by these rules and conduct, I have fully cited and referenced all material and results that are not original to this work.

Name, Last name: Güliz ÜNLÜ

Signature :

ABSTRACT

ANALYSIS OF CORNER EFFECTS ON IN-SITU WALLS
SUPPORTING DEEP EXCAVATIONS:
COMPARISON OF PLANE STRAIN AND THREE DIMENSIONAL ANALYSES

Ünlü, Güliz
M. Sc., Department of Civil Engineering
Supervisor: Prof. Dr. Orhan Erol

November 2008, 196 pages

In this thesis, hypothetical cases of in-situ walls, that are supported at one, two and four levels, as well as cantilever walls, are analyzed using plane strain and 3D finite element programs. A parametric study is performed by varying the soil stiffness. Deflection, moment, anchor loads and effective lateral earth pressures acting on the walls are examined to understand corner effect. Comparisons are made between plane strain and 3D without corner analysis results to confirm that two programs yield similar results. Moreover, two deep excavation case histories namely: i) Ankara Çankaya trade center and residence and, ii) Ekol construction are analyzed using calibrated models. Calibrations of the models are made using inclinometer data.

In hypothetical models, it is found that corner effects on deflections diminish after 20m distance from the corner for excavations that are 8m and 12m deep. Corner effects on deflection decrease as elastic modulus of soil or stiffness of the system increase. Moment diagram pattern changes along the excavation side in cantilever case study. Moment diagram obtained around a corner in 3D analysis and diagrams obtained from the plane strain analyses by modeling the corner as a strut are quite similar. The anchor loads increase until 10-15m distance from the corner. After this distance they become nearly constant.

In the analysis of case histories, a trial error solution is adopted to fit the deformed shape of piled wall obtained from 3D analysis to the deformations recorded by inclinometers. These results are compared with the results of plane strain analyses. Ankara-Çankaya project is solved by modeling the corner as strut in plane strain analyses. Results of this analyze agrees with field monitoring data, indicating that corner effects could be simulated by modeling the perpendicular pile wall as a strut in plane strain analysis.

Keywords: Corner Effect, Finite Element Method, 3D Analyses, Plane Strain Analyses, Deep Excavations

ÖZ

DERİN KAZI DUVARLARINDAKİ KÖŞE
ETKİLERİNİN ANALİZLERİ:
İKİ BOYUTLU VE ÜÇ BOYUTLU ANALİZLERİN KARŞILAŞTIRILMASI

Ünlü, Güliz
Yüksek Lisans, İnşaat Mühendisliği Bölümü
Tez Yöneticisi: Prof. Dr. Orhan Erol

Kasım 2008, 196 sayfa

Bu tezde iki boyutlu ve üç boyutlu sonlu elemanlar yöntemi kullanılarak ankastre, bir sıra ankrajlı, iki sıra ankrajlı ve dört sıra ankrajlı hipotetik kazılar analiz edilmiştir. Farklı elastik modülüs değerleri kullanılarak parametre çalışması yapılmıştır. Köşe etkisinin anlaşılabilmesi için deformasyon, moment, ankraj yükleri ve uzun dönem yanal basınç dayanımı değerleri incelenmiştir. Üç boyutlu ve iki boyutlu programlardan benzer sonuçlar elde edilip edilmediğini doğrulamak için üç boyutlu köşesiz modeller analiz edilmiştir. Ayrıca, i) Ankara Çankaya Konut ve İş Merkezi ve ii) Ekol İnşaat projeleri için uygulanan iksa sistemleri kalibre edilmiş modeller kullanılarak analiz edilmiştir. Modellerin kalibrasyonları inklinometre verilerine göre yapılmıştır.

Hipotetik modellerde, köşe etkisi köşeden 20m uzaklıkta kaybolmaktadır. Köşenin deformasyon üzerindeki etkisi, zeminin deformasyon modülü ve iksa sistemin rijitliği arttıkça azalmaktadır. Ankastre sistemlerde, moment grafiklerinin tipi kazı cephesi boyunca değişiklik göstermektedir. Üç boyutlu analizlerde, iksa sisteminin köşe noktalarında elde edilen moment grafiklerin tipi, köşelerin destek olarak iki boyutlu modellenmesinden elde edilen grafiklerle benzerlik göstermektedir. Ankraj yükleri köşeden 10-15m uzaklığa kadar artmakta, bu mesafeden sonra sabitlenmektedir.

Vaka analizlerinde, deneme yanılma yöntemi kullanılarak üç boyutlu analizler yapılarak inklinometre ölçümlerinden elde edilmiş deformasyon şekillerine ulaşılmıştır. Bu sonuçlar, iki boyutlu analiz sonuçları ile mukayese edilmiştir. Ankara-Çankaya projesi köşelerin destek olarak iki boyutlu modellenmesi yöntemi ile çözülmüştür. Bu analizin sonuçları, saha ölçümleri ile benzerlik göstermektedir. Bu durum köşe etkisinin, dik kazıkların destek olarak modellenmesi ile iki boyutlu analizlere yansıtılabileceğini göstermektedir. .

Anahtar kelimeler: Köşe Etkisi, Sonlu Elemanlar Yöntemi, Üç Boyutlu Analiz, İki Boyutlu Analiz, Derin Kazılar

To My Parents

ACKNOWLEDGMENTS

I express my appreciation to Prof. Dr. Orhan Erol for his supervision, concern and precious suggestions during the whole period of the study. Thanks go to the staff of Toker Drilling and Construction Company, and especially to Mustafa Toker for providing data for the study and their great encouragement. I express my appreciation to Sevilay Kahveci, Hande Işık Öztürk and Levent Ünkap for their great aids. I also like to express my deepest gratitude to my family for their great encouragement and financial helps for providing programme.

TABLE OF CONTENTS

LIST OF TABLES

TABLES

LIST OF FIGURES

FIGURES

CHAPTER 1

INTRODUCTION

Due to the scarcity of land in big cities, basements and car parking facilities below existing ground level are constructed. To this end, deep excavations are carried out in close proximity to existing buildings. Mostly, plane strain analyses are performed to obtain deflection, moment and effective horizontal stresses. However, excavations behave in a manner described as three dimensional. Especially, corner effect on in-situ wall behavior cannot be modeled by using two dimensional programs. Consequently, Plane strain analyses of such excavations may mislead the designers.

Corner effect on deflection is studied by many researchers. In these studies, plane strain and three dimensional analyses are performed, and calculated results are compared with measured ones. However, in these researches, moments and effective horizontal stresses are not studied.

The subject of this thesis is to define corner effect on deflection, moment, effective horizontal stress and anchor loads, and compare the results of plane strain and three dimensional analyses. For the hypothetical cases, only comparisons between analysis results and theories are made. Two case histories; support systems of ‘Ankara Çankaya Trade Center and Residence’ and ‘Ekol Construction’ are modeled and comparisons between measured and calculated deflections are made. In addition to that, moment and effective horizontal stresses of these in-situ wall systems are obtained.

Also a literature review on plane strain and three dimensional numerical analyses of excavations is presented. Hypothetical study on corner effect in deep excavations, and two case histories, namely; i) Ankara- Çakaya Trade Center and Residence excavation, ii) Ekol construction are studied in scope of this thesis.

CHAPTER 2

LITERATURE REVIEW ON NUMERICAL ANALYSIS OF EXCAVATIONS

2.1. Plane Strain Analyses

Lateral deflections, lateral earth pressures and moments of in situ walls are important research subjects of geotechnical researchers. According to field observations some predictions about lateral deflections of in-situ walls were being made. As computer capacities increased, numerical analysis programs were also developed. Firstly, plane strain analyses of in-situ walls were performed by these programs, later three dimensional analyses was also possible.

In previous studies, based on field observations, some predictions about lateral deflections of in-situ walls are made by Clough and O'Rourke (1990), Ou et al. (1993), Wong at al. (1997), Carder (1995), Fernie and Suckling (1996).

Clough and O'Rourke (1990) consider two main categories of soils: i) stiff clays/residual soils/sands and, ii) soft to medium clay. For first category, it is predicted that maximum lateral movement of wall is 0.2% of excavation depth. For the second category, by considering effects of excavation base heave and system stiffness, a chart is presented by Clough and O'Rourke as shown in Figure 1. In this chart, system stiffness is defined as

$$\text{System Stiffness} = \frac{EI}{\gamma_w s^4} \quad \text{.....Eq. 1.}$$

where E=Young's modulus, I=moment of inertia, γ_w=unit weight of water, and s=average prop spacing.

Ten high quality case histories are studied by Ou et al. (1993). Suggested maximum wall deflections of in-situ walls are within 0.2%-0.5% of excavation depth.

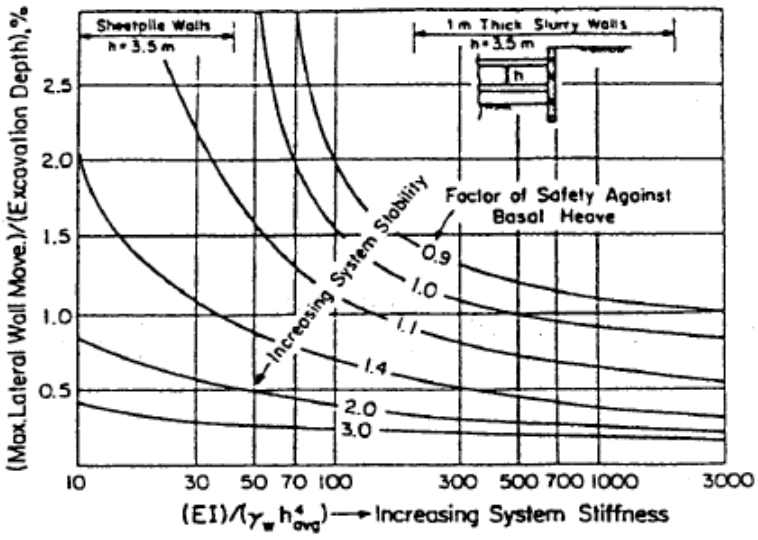

Figure 1. Charts for predicting wall movements for soft to medium clays (Cloug and O'Rourke (1990))

Maximum horizontal deflections of in-situ walls made in largely stiff soils are studied by Carder (1995). He suggested that maximum lateral wall movement depend on system support stiffness. Upper limits of maximum wall deflections are demonstrated; for high support stiffness; 0.125% of excavation depth, for moderate stiffness; 0.2% of excavation depth, for low stiffness; 0.4% of excavation depth.

Fernie and Suckling (1996) studied on U.K. soils and showed that maximum lateral wall deflection values varied between 0.15% to 0.2% of the excavation depth.

The construction of the tunnels in the Central Expressway (CTE) Phase II of Singapore is studied by Wong, Poh, Chuah (1997). General layout of Central Expressway Phase II is demonstrated in Figure 2. In the scope of the project deep excavations for construction of 2.4km of cut and cover tunnels and 0.5 km of open cut depress roadways are opened. These excavations are monitored by 1400 instruments that include inclinometers, settlement points, piezometers, water standpipes and tilt gauges.

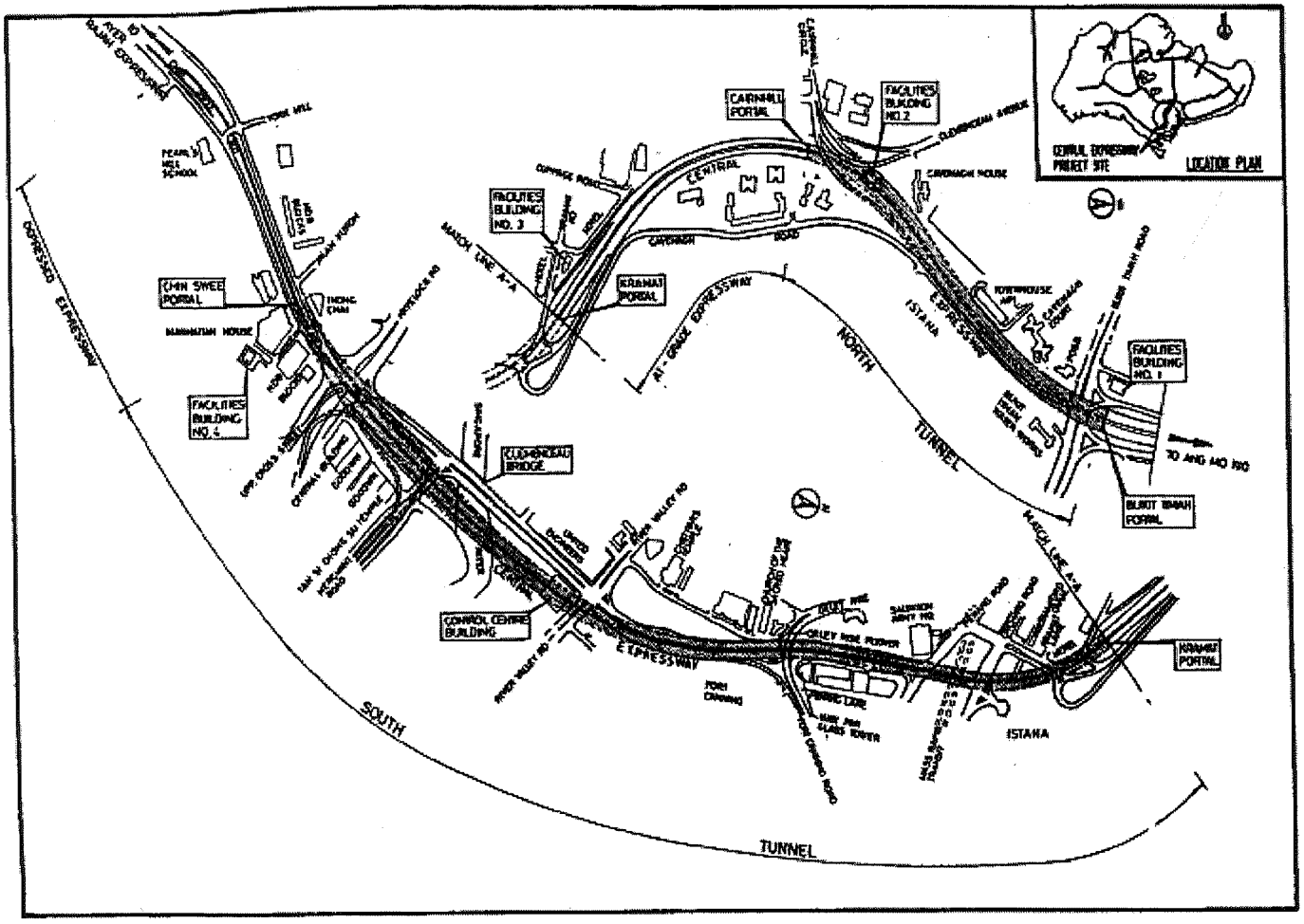

Figure 2. General layout of central expressway phase II (Wong, Poh, Chuah (1997))

Diaphragm walls, contiguous bored pile walls, arbed walls, composite sheet pile and H pile walls and soldier pile walls are used as support systems. The soil profile is composed of softer soils underlain by the residual soils and weathered rocks of the sedimentary Jurong Formation as well as the residual soils and weathered rocks of the Bukit Timah Granite.

Excavations are classified into two groups: soft soil thickness is smaller than 90% of excavation depth in first group and 60% of excavation depth in second group. Observed lateral wall deflections and lateral earth pressures are studied by researchers.

It is deduced that, for excavations with a combined thickness of soft soil layers of less than 0.9H and 0.6H overlying stiff soils, the movements are less than 0.5% of H and 0.35% of H, respectively as shown in Figure 3.

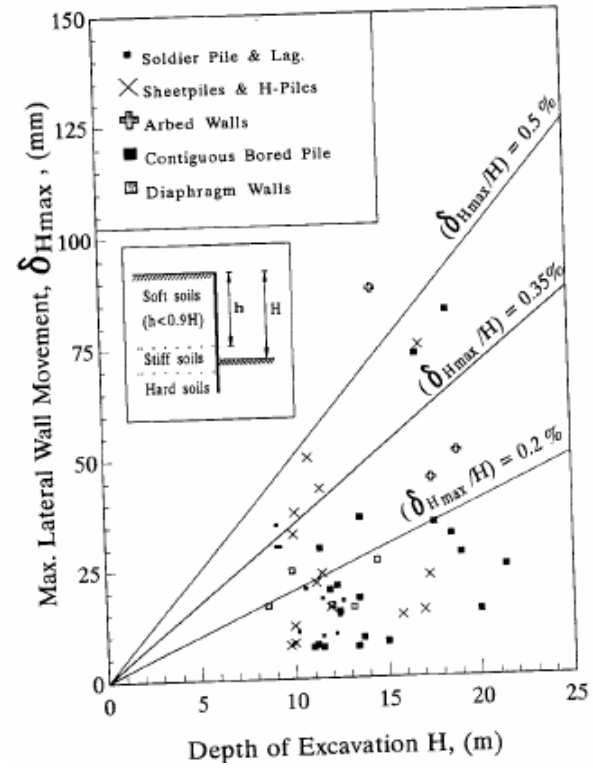

b)

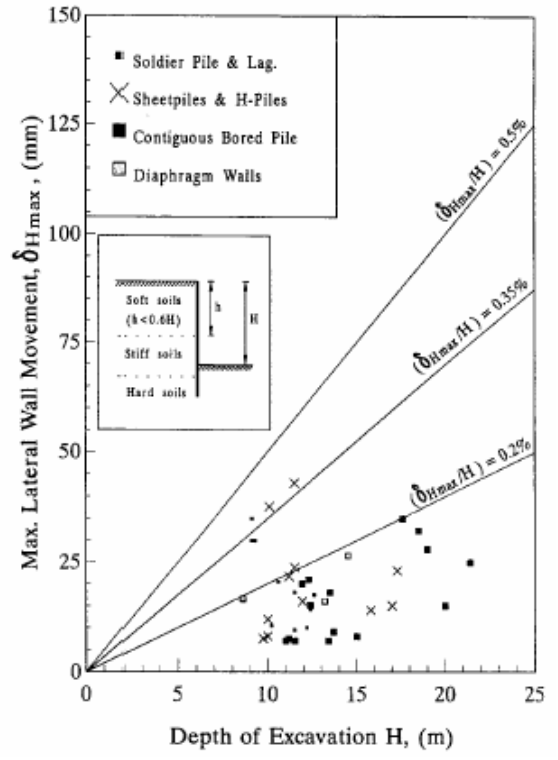

Figure 3. Observed maximum lateral wall deflections for excavations supported by five types of walls (a) for h<0.9H; (b) for h<0.6H in the construction of CTE Phase II (Wong, Poh, Chuah (1997))

Effect of support types on lateral wall movement is also studied by the researchers (see Figure 4). It is observed that maximum lateral wall movements for cases that are supported by anchors are smaller than the ones that are propped by struts. The reason of this is explained by researchers as to the smaller relief of overburden stress prior to the installation of anchors and the higher prestress level that is used in the anchors compared to that for the strutted excavations (Wong, Poh, Chuah (1997)).

For excavations with combined thickness of soft soil layers of less than 0.9H and 0.6H overlying stiff soils, maximum apparent earth pressures are less than 0.6γH and 0.25γH (see Figure 5). It is noted that at the top few meters, observed lateral earth pressures are more than estimated values. This trend may be a result of the high position of the first prop level (Wong, Poh, Chuah (1997)).

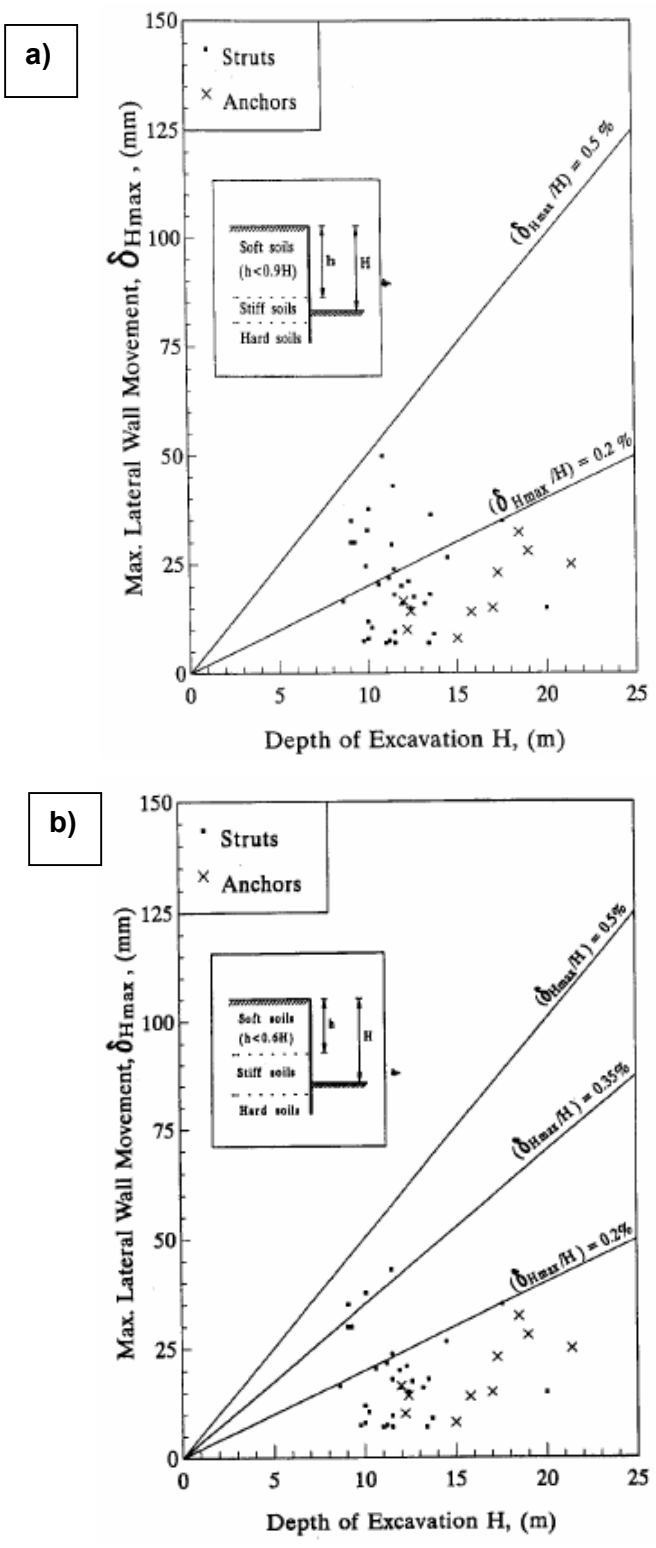

Figure 4. Effect of prop type on maximum lateral wall movement for excavations supported by walls (a) for h<0.9H; (b) for h<0.6H in the construction of CTE Phase II (Wong, Poh, Chuah (1997))

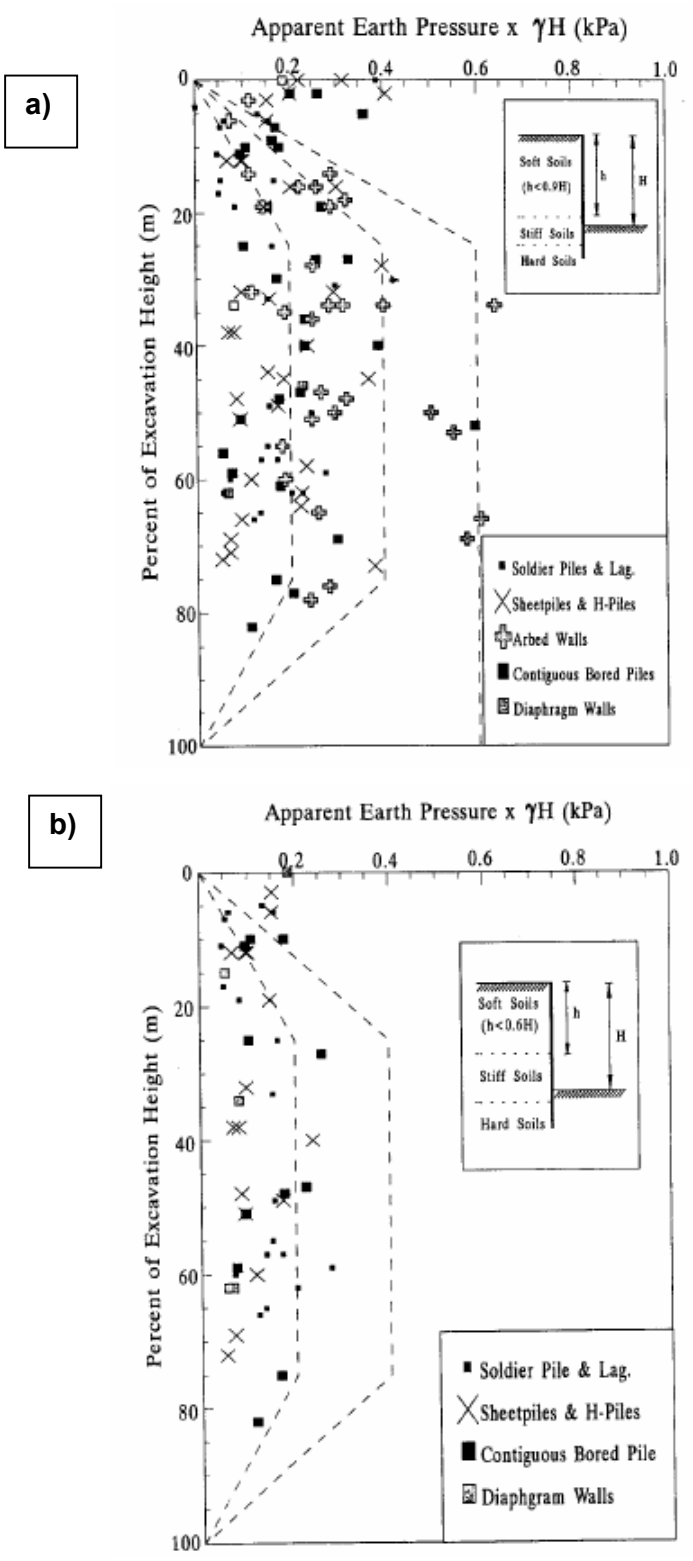

Figure 5. Apparent earth pressure diagram for excavations supported by walls in stiff soil profiles (a) for h<0.9H; (b) for h<0.6H in the construction of CTE Phase II (Wong, Poh, Chuah (1997))

Difficulties in achieving reliable analytical predictions of soil deformation are mentioned by Whittle, Hashash, Whitman (1993). Causes of these difficulties are listed as follows: i. limitations in the site investigation and geometric approximation used in the analytical model, ii. uncertainties in the selection of engineering properties because of inadequate laboratory and field studies; iii. approximate representations of constitutive behavior used in the finite element model; iv. some activities of construction process that cannot be easily analyzed by using finite element model.

Whittle, Hashash, Whitman's (1993) case study is a good example of comparison of finite element analysis results and field observation. Underground parking garage at Post Office Square in Boston which is composed of seven stories is analyzed using finite element analysis. Plan area of the building is 6880 m^2. The garage is surrounded by important buildings and streets of Boston (see Figure 6). Fifteen boreholes are opened in the site. Through the boreholes, fill, low plasticity clay, dense to very dense sand, severely weathered argillite deposit and sound rock are observed. The ground water is at 2.3-2.9m depth from the ground surface.

ABAQUS, two dimensional finite element code, is used for analysis. Fill, sand and rock are modeled by using Drucker-Prager failure criterion with a no associated flow rule; on the other hand, clay is modeled by using MIT-E3 effective stress soil model.

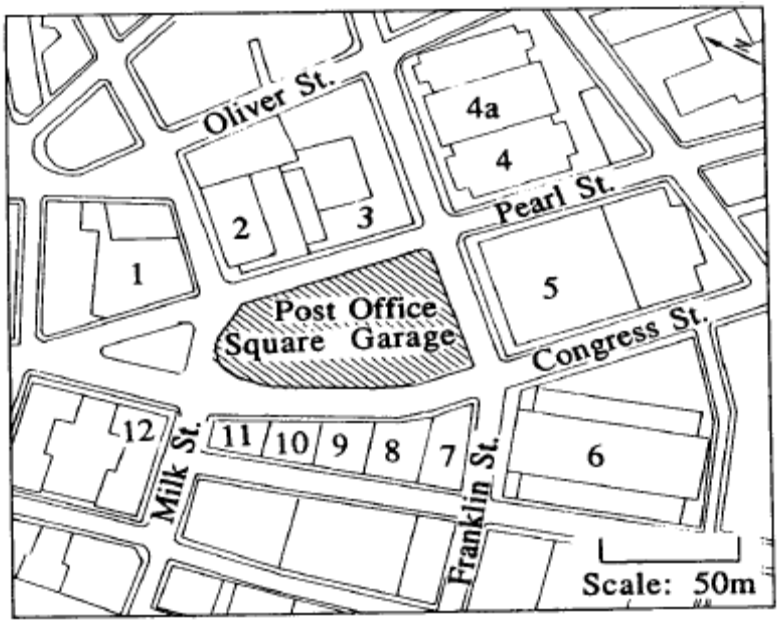

Key (1)	Stories (2)	Foundation type (3)	Bearing soil (4)
1	14	Piers/caissons	Till
2	40	PIFs	Till
3	5	Footings	Clay
4	12	Footings/caissons	Clay
4a	34	Mat	Till
5	21	Footings	Till
6	38	Mat	Till
7	7	Mat/footings	Clay
8	11	Footings	Clay
9	7	Footings (?)	Clay (?)
10	12	Strip footings	Clay
11	11	Mat/footings	Clay
12	17	Mat	Clay

Figure 6. Site location, adjacent buildings and adjacent buildings foundations (Whittle, Hashash, Whitman (1993))

Top-down construction is simulated by three stages like: undrained excavation, time delay for simulation of curing and partial drainage time, and installation of structural properties. Finite element mesh used in calculations is shown in Figure 7.

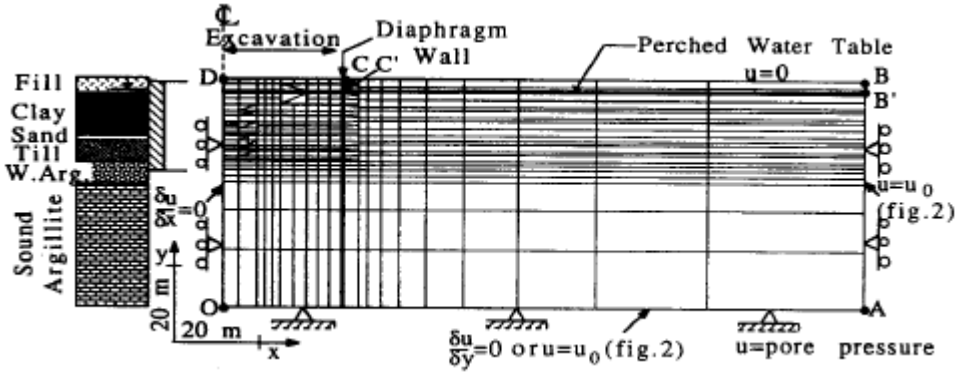

Figure 7. Finite element mesh and boundary conditions, Post Office Square (Whittle, Hashash, Whitman (1993))

Taken field measurements at roof slab (stage 10), third floor (stage 19) and sixth floor (stage 28) steps are compared with predictions in Figure 8. In roof slab stage, diaphragm wall deforms in a cantilever mode and in this stage predictions are close to measured values. In third floor stage, maximum movement is observed at third floor elevation. Finally in sixth floor stage maximum movement is noticed at elevation of clay layer. It should be noted that in the last two steps, there are discrepancies between predicted and measured values. It is claimed that the most important cause of this differences is unmodeled post construction behavior of the roof and floor slabs. By considering this effect, analyses are modified by authors and modified analysis results are also demonstrated in Figure 8.

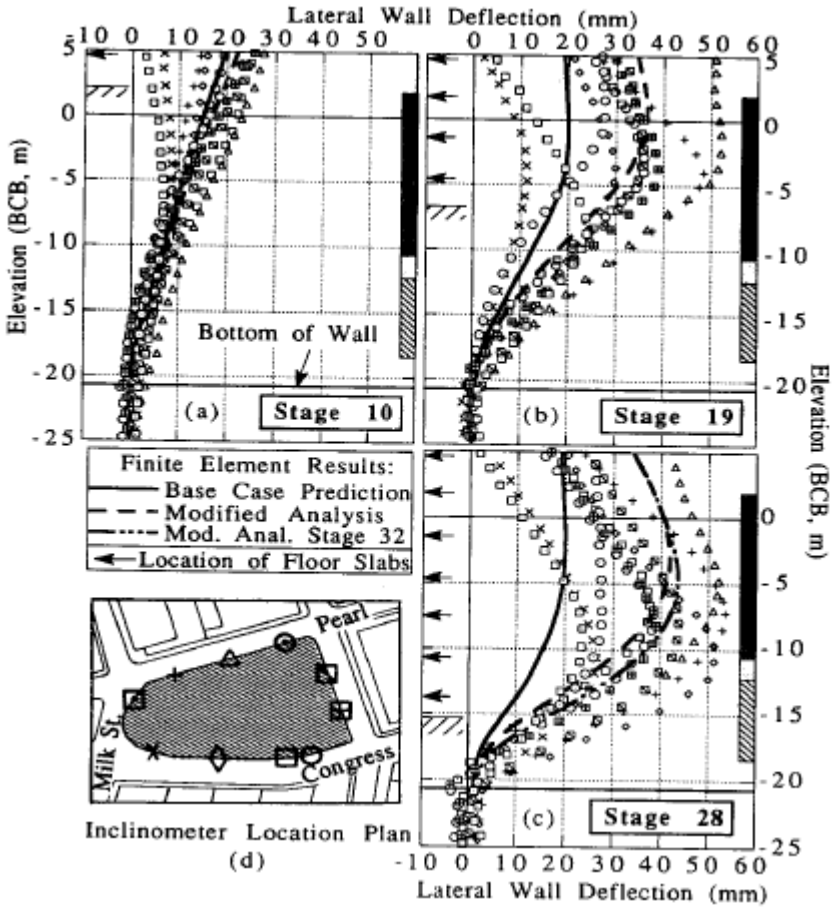

Figure 8. Comparison of predicted and measured lateral wall deflections (Whittle, Hashash, Whitman (1993))

Another example of comparison of plane strain analysis results with field observations is performed by Ou and Lai (1994). Deep excavations in layered sandy and clayey soil deposits are studied using finite element analysis. Analyses are done by using JFEST program which is developed by Finno (1983). Modified Cam Clay Model is used for modeling cohesive soils, whereas hyperbolic model as proposed by Duncan and Chang (1970) is used for modeling cohesionless soil type. Three case histories are modeled; The Chi-Ching Building, the Chi-Chyang Building and The Taipei World Trade Center Office Building.

For construction of The Chi-Ching building 13.2m deep excavation is retained by 70cm thick 28m long diaphragm wall. Top-down method of construction in four stages is used. The excavation is performed through silty sand and silty clay. The ground water level was originally 3m below ground surface and is lowered to 12m depth. Inclinometers are placed near the center of each side, also hydraulic earth pressure cells are installed at four different depths. In order to measure moment values, rebar strain meters are installed on the reinforcement cages at three sections.

The eight-noded quadrilateral finite element is used. The diaphragm wall and lateral support are assumed to behave as a linear elastic material.

The strength parameters of hyperbolic model except the stiffness modulus are obtained from laboratory tests. However stiffness modulus values are obtained from back analysis because this parameter is affected by sample disturbance. Finite element mesh for the Chi-Ching excavation project is demonstrated in Figure 9. Predicted and measured wall displacements, moments and lateral earth pressures are shown in Figures 10, 11.

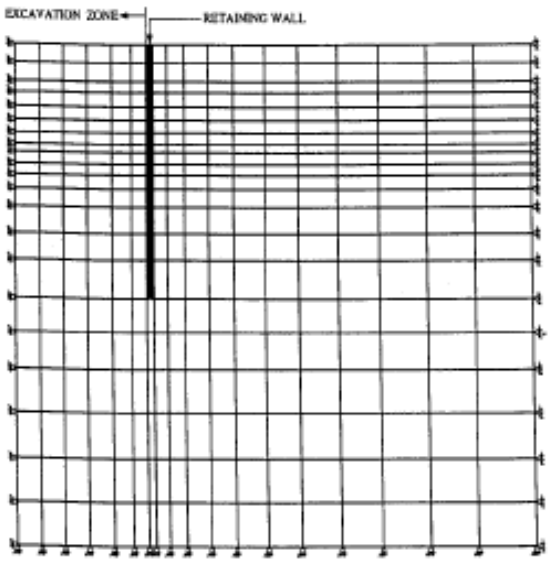

Figure 9. Finite element mesh for the Chi-Ching excavation (Ou and Lai (1994))

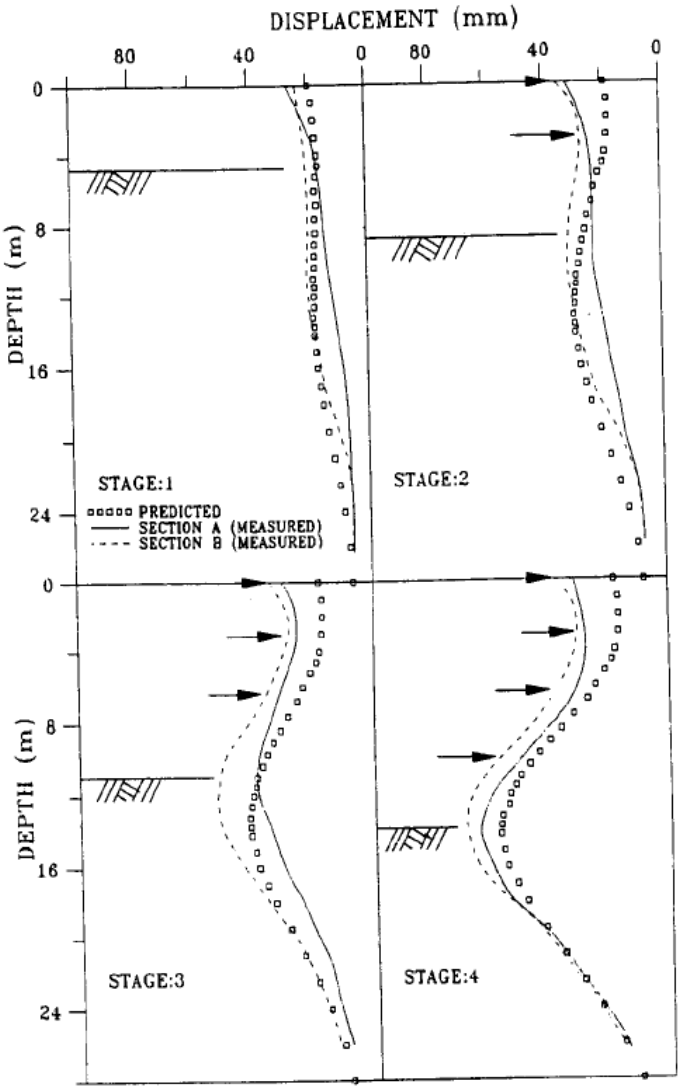

Figure 10. Predicted and measured wall displacements for the Chi-Ching excavation (Ou and Lai (1994))

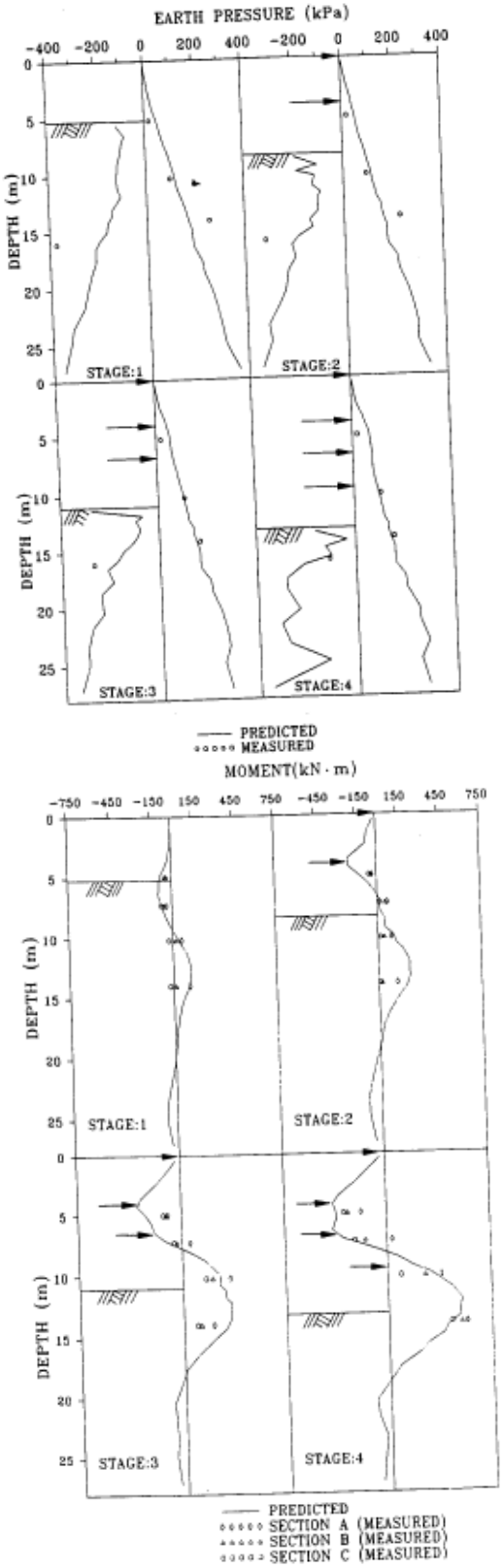

Figure 11. Predicted and measured lateral earth pressures; predicted and measured moment of the wall for the Chi-Ching excavation (Ou and Lai (1994))

For construction of The Chi-Chyang building, a 13.6m deep excavation is retained by 70cm thick 28m long diaphragm wall. Excavation is made through silty sand and silty clay layers. Top-down method of construction in four stages is used. The ground water level is originally 3m below ground surface and is lowered to 12m depth. Inclinometers are placed near the center of each side. Predicted and measured wall displacements are shown in Figure 12.

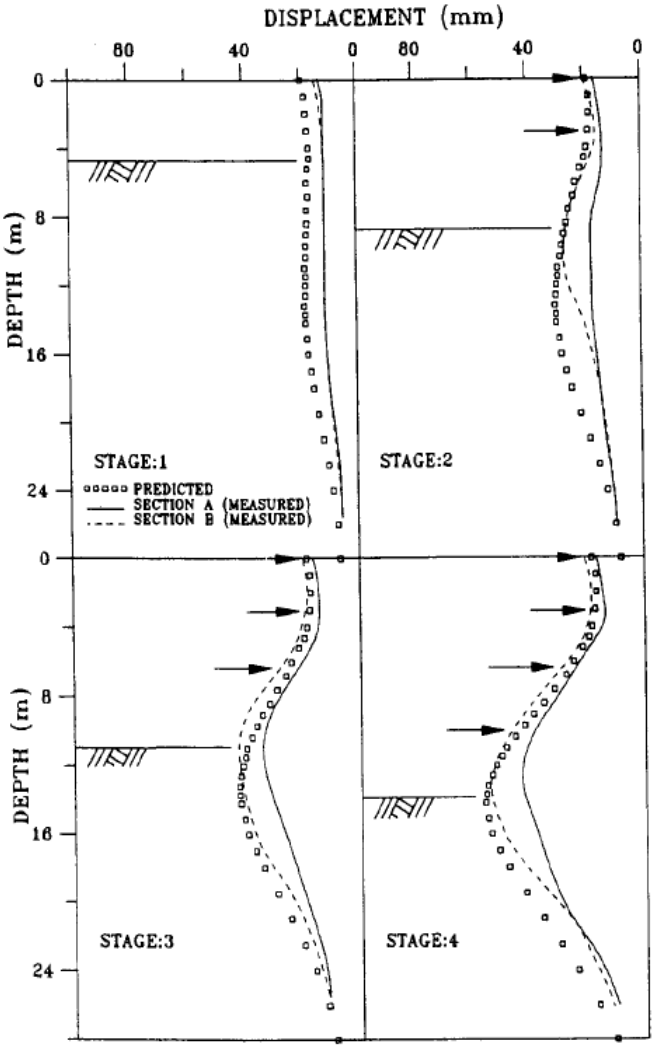

Figure 12. Comparison of predicted and measured wall displacements for the Chi-Chyang excavation project (Ou and Lai (1994))

For construction of The Taipei World Trade Center Office building, a 14.1 m deep excavation is retained by 70cm thick 30m long diaphragm wall. Excavation is made through clayey silt and silty clay. Top-down method of construction in four stages is used. An inclinometer is placed near the center of one side. Predicted and measured wall displacements are also shown in Figure 13.

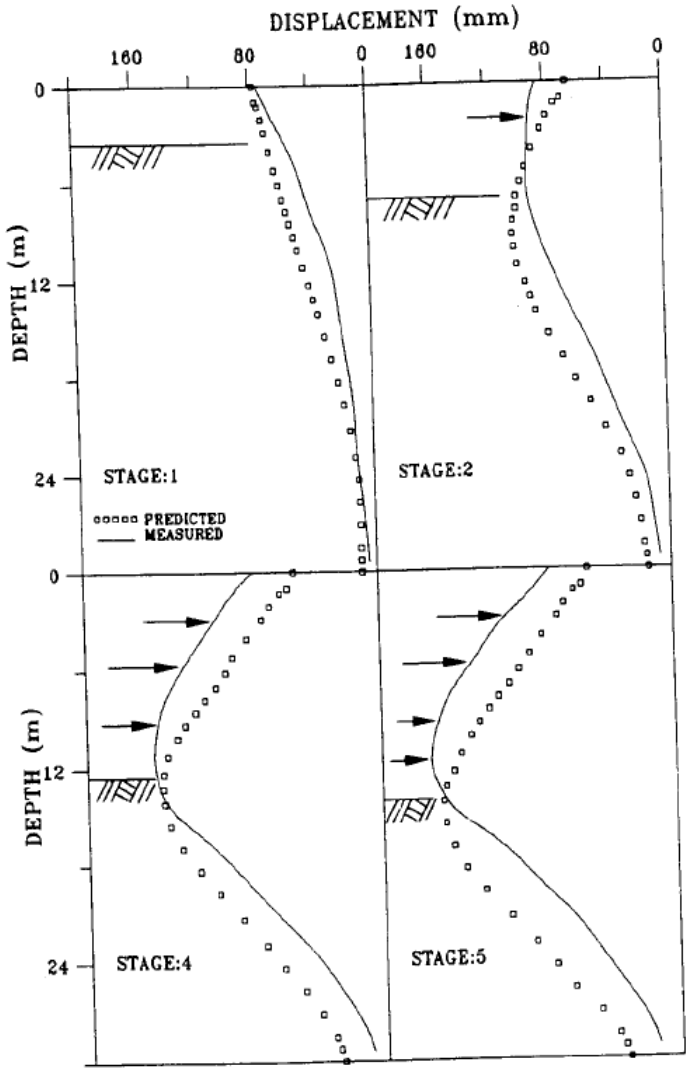

Figure 13. Comparison of predicted and measured wall displacements for the Taipei World Trade Center Office Building excavation project (Ou, Lai (1994))

In conclusion, results obtained by using hyperbolic and modified cam-clay model are fairly close to those from field observations. It should also be noted that measurements are taken nearly at the middle of the sides to avoid the corner effects.

Another case study comparing plane strain analysis with field observations is performed for an excavation through Ankara Clay by Çalışan (2005). For construction of a hotel in Gaziosmanpaşa-Ankara, 27m deep excavation is opened. Plane strain analyses are performed by using REWARD and PLAXIS programs.

Construction site with 1100 m^2 plan area, is surrounded by buildings and roads (see Figure 14). Eighty cm piles with 100cm spacing is used for the sides that are in the neighbor of buildings; and sixty-five cm piles with 120cm spacing is used for other sides. Pile walls are propped by nine levels anchors which are applied with 120 cm lateral spacing. Moreover cross section view of the excavation system is demonstrated in Figure 15.

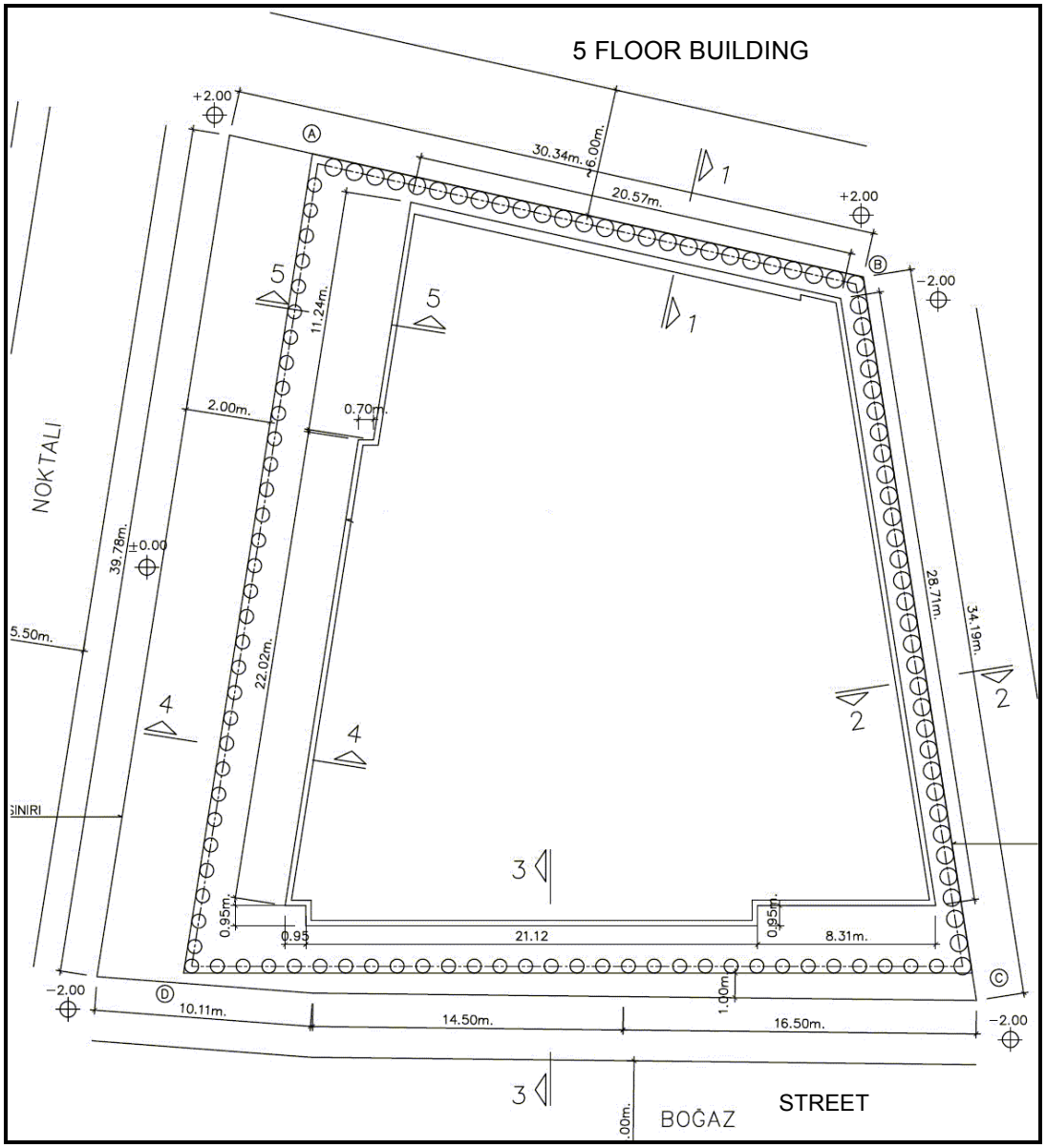

Figure 14. Plan view of hotel construction site (Çalışan (2005))

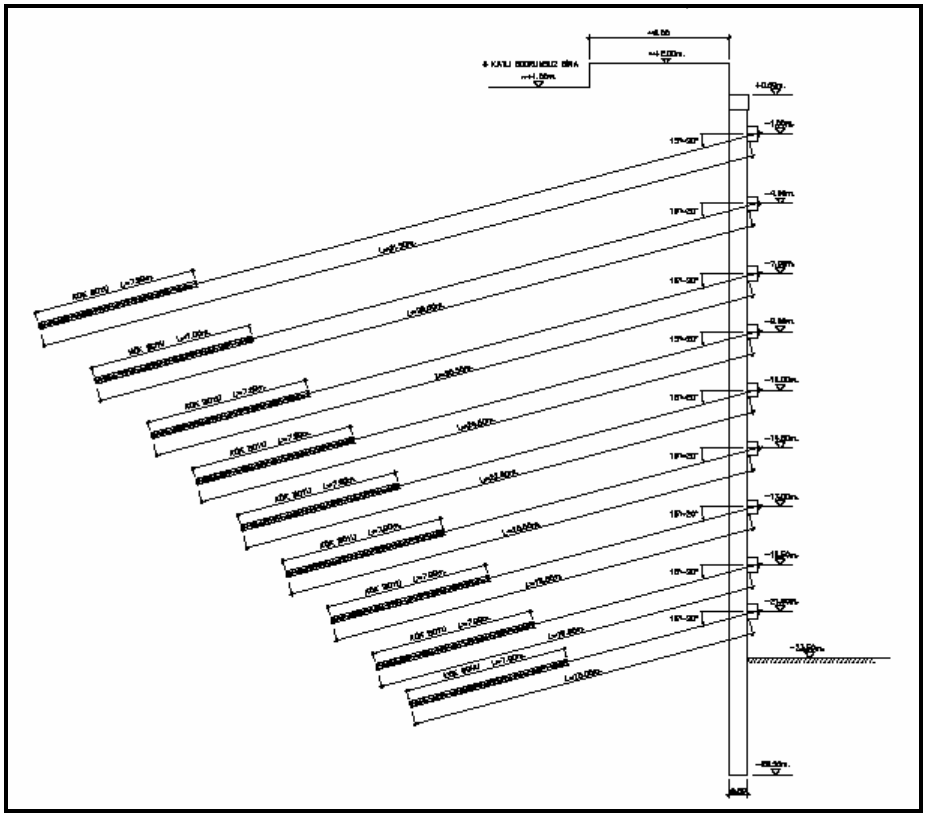

Figure 15. Cross section view of in-situ wall (Çalışan (2005))

Maximum observed and predicted lateral displacements are summarized in Table 1. It is concluded that values obtained from Plaxis analysis are quite higher than field observations and this can be caused by plane strain analysis, which ignores corner effects (Çalışan (2005)).

Table 1. Estimated and observed deflections (Çalışan (2005))

Side	Excavation Depth (m)	Estimated Deflections (mm)		Observed Maximum Deflection (mm)	δ/H (%)		
		Plaxis	Reward		Plaxis	Reward	Observed
A-B	29,5	108,5	88	20	0,36	0,29	0,07
B-C	23	-	76	35	-	0,33	0,15
C-D	25	-	76	17	-	0,3	0,07
D-A	26,5	-	81	29	-	0,31	0,11

2.2. Three Dimensional Analyses

In order to investigate three dimensional behaviors of excavations, researchers perform three dimensional analyses with different computer programs such as FLAC, CRISP, CUT3D, etc. In these analyses lateral movement of the excavation and ground surface settlements are examined. Also some suggestions are made for mesh types and convergence boundaries of models.

Corner effect in excavations are studied by Ou, Chiou, Wu (1996), Lee, Yong, Quan, Chee (1998), Ou, Shiau and Wang (2000), Lin, Chung, Phien-wej (2003) and others.

Different mesh types are performed during convergence study of Ou, Chiou and Wu (1996). It is concluded that meshes should be dense at the excavation zone, and behind the wall, of which deformation is evaluated. Suggested mesh configuration is demonstrated in Figure 16.

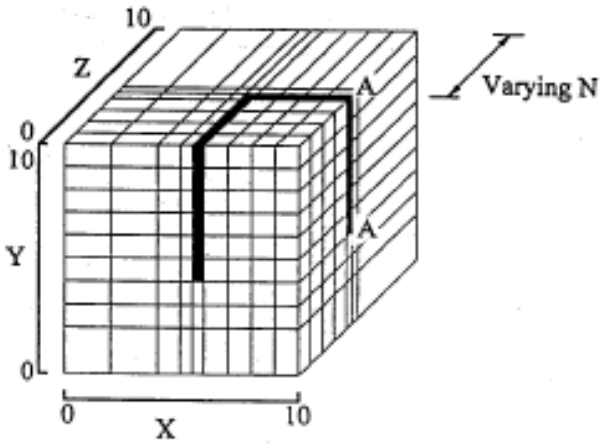

Figure 16. Suggested mesh configuration (by Ou, Chiou and Wu,1996)

Convergence boundary conditions of three dimensional models are examined by Lin, Chung, Phien-wej (2003). To expedite the 3D analysis without sacrificing the numerical accuracy, the geometry boundary and the mesh density should be approximately arranged (Lin, Chung, Phien-wej (2003)). For various geometry boundaries, lateral wall movements and ground settlements are investigated as shown in Figure 17, 18. According to these investigations, the geometry boundary is suggested to extend from diaphragm wall by three times the excavation depth (3H; where H is excavation depth) (Lin, Chung, Phien-wej (2003)). Suggested geometry boundary is demonstrated in Figure 19.

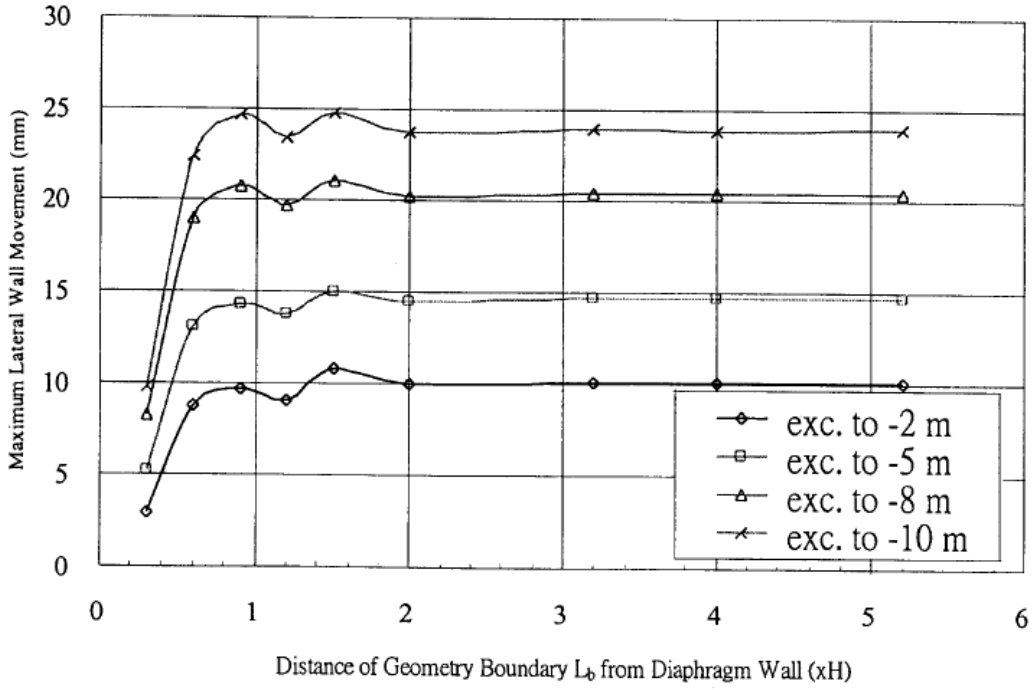

Figure 17. Effect of geometry boundary on numerical convergence in 3D analysis, Lateral Wall Movement (by Lin, Chung and Phien-wej, 2003)

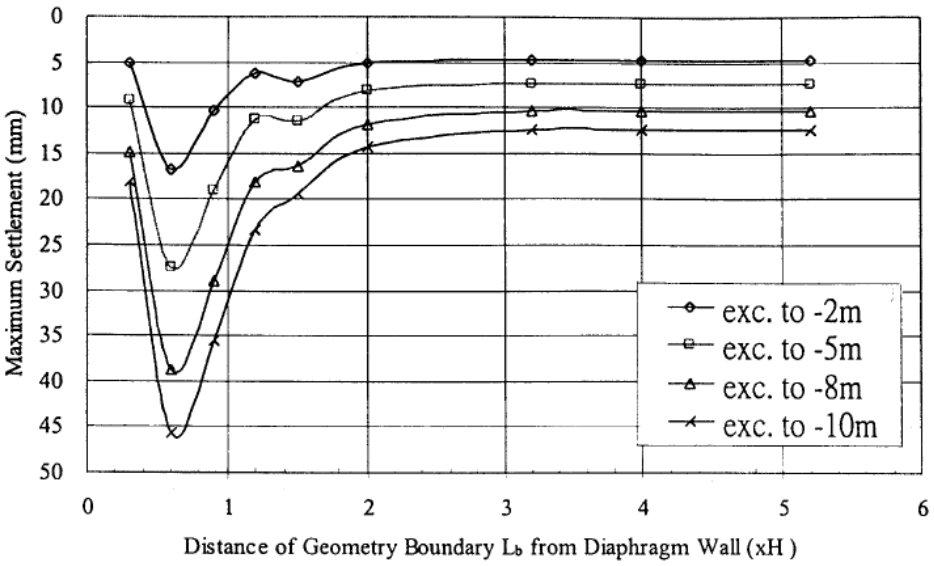

Figure 18. Effect of geometry boundary on numerical convergence in 3D analysis, Maximum Settlement (by Lin, Chung and Phien-wej, 2003)

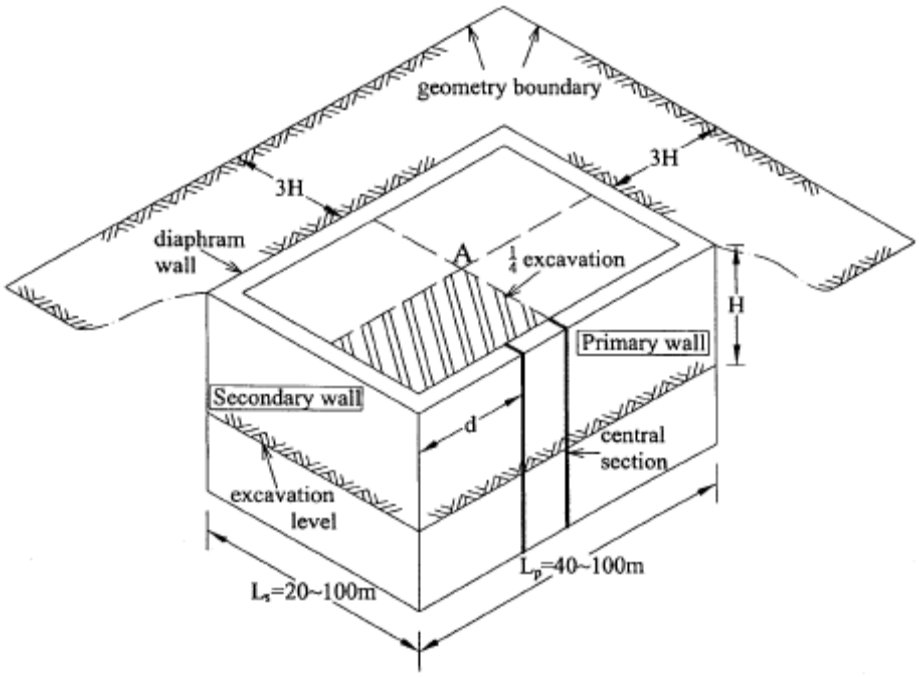

Figure 19. Illustration of primary wall, secondary wall, the evaluated section at a distance d from the corner and the central section of d=Lp/2 (by Lin, Chung and Phien-wej, 2003)

Moreover observed wall deformations and excavation surface heaves are symmetric in symmetric excavations. Therefore, a quarter of the excavations can be modeled to gain computing time.

Effect of primary and secondary (complementary) wall lengths of a rectangular excavation site on lateral wall movement is studied by Ou, Chiou and Wu (1996). In the convergence studies by changing the primary and complementary wall lengths, numbers of rectangular excavations are analyzed. In these analyses, primary wall varied in between 40m to 100m; while complementary wall varied in between 20m to 100m (see Figure 20).

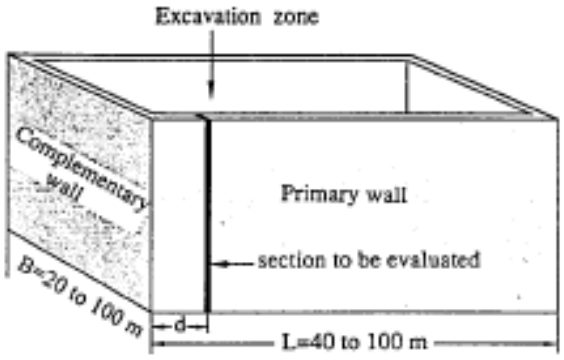

Figure 20. Configurations of hypothetical excavation case (by Ou, Chiou and Wu, 1996)

Hypothetical excavations are modeled in low to medium plasticity of silty clayey subsoil stratum in Taipei. A diaphragm wall with 70cm thick and 32m depth is modeled. Top down structure technique is used for the model. The steps of this technique; first excavate up to 4m depth then construct the first floor, then before second and third steps respectively excavate up to 8m and 12m depth, construct the second and the third floor, lastly excavate up to 16m depth and construct the fourth floor.

Primary wall deflections at every 10m distance from the corner are determined from the analyses. Maximum deflections of the primary walls vs. distance from the corner graphs are formed for constant complementary and various primary wall lengths (see Figure 21).

As it can be seen from the figures, the changes in primary wall length has nearly no effect on maximum displacement of the wall for B=20m. For other complementary wall lengths, maximum displacement of the walls reduces as primary wall length reduces. It should also be noticed that maximum displacements near the corners are smaller than the distant points and as primary wall length increases the 3D analysis results get closer to the plane strain results.

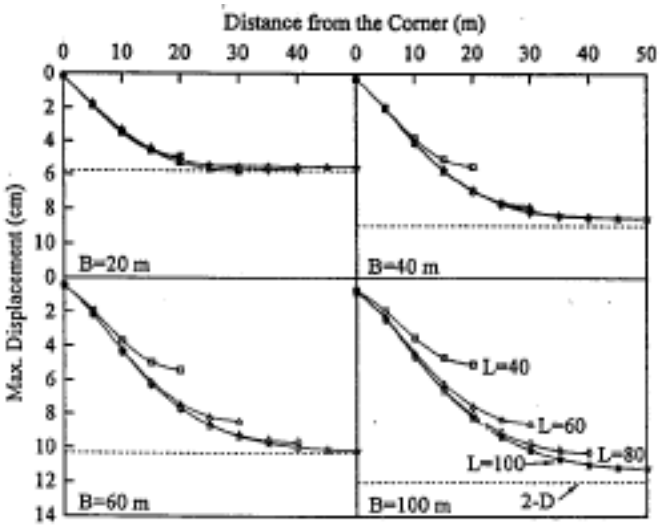

Figure 21. Variations of maximum wall displacement with the distance for constant sizes of complementary wall (B) and various sizes of primary wall (L) (by Ou, Chiou and Wu, 1996)

For describing deflection behavior of a wall section, plane strain ratio (PSR), which is the ratio of maximum wall displacement of a section to the maximum wall displacement for the same excavation width, is used. For the purpose of discussing the length effect of complementary wall PSR is used. In the graphs (see Figure 22) PSR values are plotted for constant primary wall lengths with various complementary wall lengths. As the complementary wall length increases, corner effect becomes more pronounced. As the primary wall length increases deformation of the wall at the center approaches to plane strain condition.

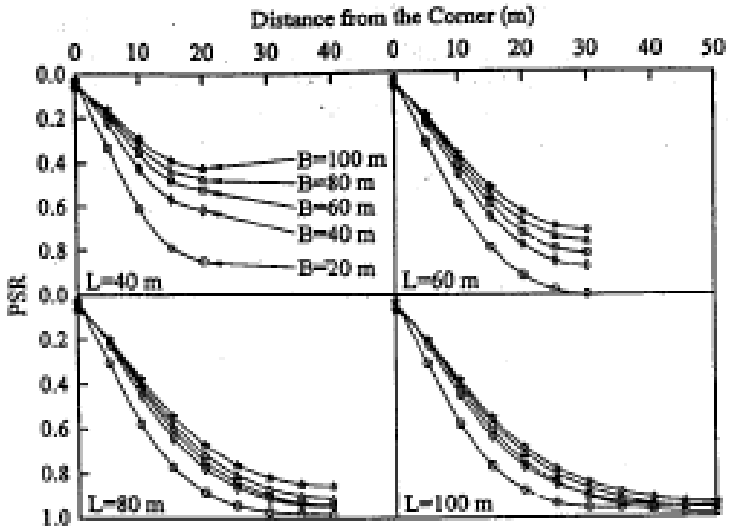

Figure 22. Variation of PSR for maximum wall displacement with distance for constant size of primary wall (L) and various sizes of complementary wall (B) (by Ou, Chiou and Wu, 1996)

To summarize the effects of primary and complementary wall on the displacement along the primary wall, the relationship between length ratio of complementary wall to primary wall (B/L) and distance from corner for various PSR is plotted in Figure 23.

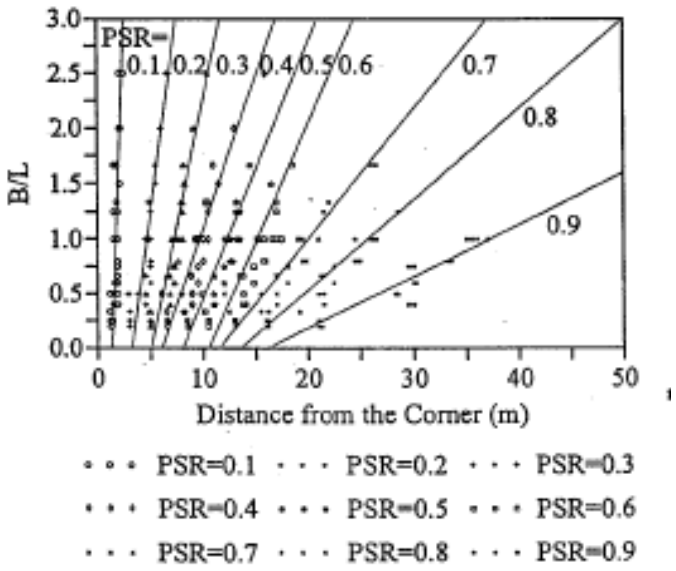

Figure 23. Relationship between B/L and distance from the corner for various PSR (by Ou, Chiou and Wu, 1996)

It should be noted that in general there are a lot of factors effecting the displacement behavior of the wall, such as: excavation sequence, method of excavation, method of wall support, excavation depth, penetration depth of excavation wall, excavation geometry, wall stiffness, soil strength, and so on. Therefore relationship between wall lengths and PSR should be obtained for every unique case. As a first order approximation, the ratio of the three dimensional to the plane strain analysis results for any excavation could be assumed similar.

PSR method obtained from convergence studies is used for excavation analysis of The Hai-Hua Building Site. At the site shown in Figure 24, a 20.3m deep excavation is planned to be supported by 110cm thick and 42m long wall. For the corner section of the excavation top down construction method composed of seven stages is used. The site is composed of silty clay and silty sand layers. For silty sand layers, drained; for silty clay layers, undrained behavior is assumed. Two dimensional and three dimensional analyses are performed for the corner of the site and also measurements are taken at the site after construction.

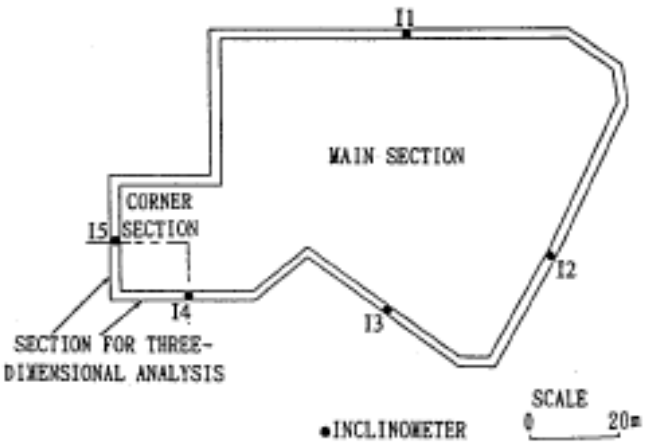

Figure 24. The Hai-Hua Building Site

Results obtained from three dimensional analyses are very close to measured displacement values. On the other hand results from two dimensional finite element analyses are very conservative (see Figure 25, 26). Displacement values obtained from 2D analyses are multiplied by the PSR values which were found from convergence studies. In Figure 27 maximum wall displacements obtained from field measurements, PSR method, 2D and 3D analyses are comparatively demonstrated. It should be noted that PSR method results are very similar to 3D analysis results and also measured values.

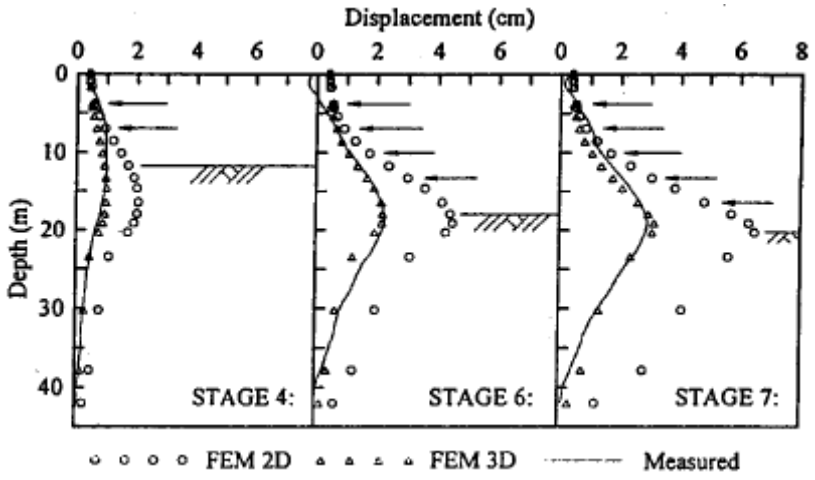

Figure 25. Measured and predicted wall displacement for corner excavation sections (Inclinometer I4) (Arrows indicate locations of bracing levels) (by Ou, Chiou and Wu, 1996)

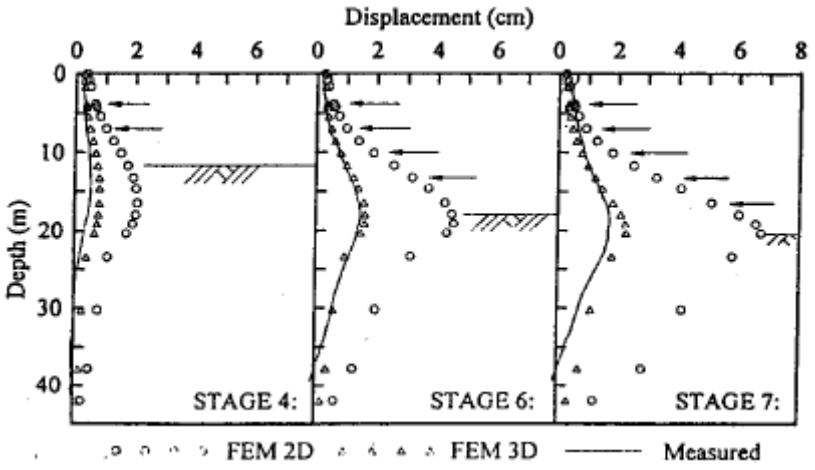

Figure 26. Measured and predicted wall displacements for corner excavation sections (Inclinometer I5) (Arrows indicate location of bracing levels) (by Ou, Chiou and Wu, 1996)

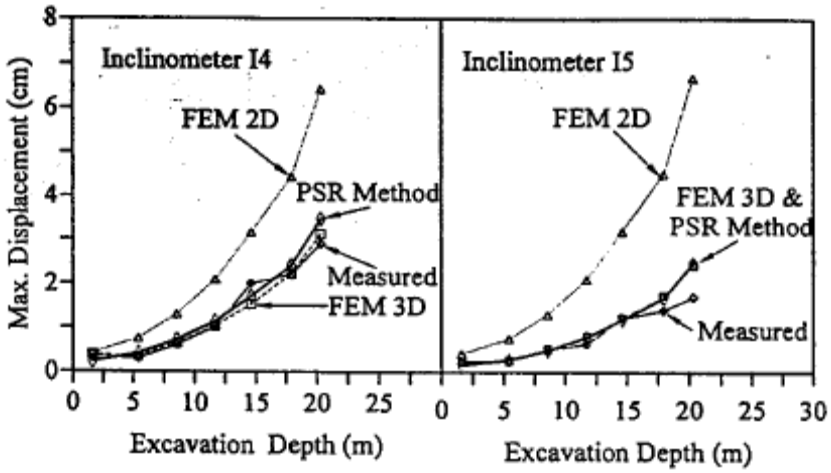

Figure 27. Comparison of measured and calculated maximum wall displacements from PSR method (by Ou, Chiou and Wu, 1996)

In order to discuss the effects of corners on wall deflection and ground movement around multi level strutted deep excavations, 2D and 3D analyses are performed and field monitoring exercise was conducted by Lee, Yong, Quan and Chee (1998). For the construction of Immigration Building, its 17.3m deep excavation is supported by a 1m thick diaphragm wall with internal steel strutting. The site is composed of marine clay underlain by clayey silt-sand and an old alluvium formation under that.

For the purpose of monitoring wall displacement four wall inclinometers and three soil inclinometers are installed at the site (see Figure 28). During the excavation stages regular measurements are taken (see Figure 29). Largest wall deflection is observed at Section-C; followed by Section-A and Section-B, all of which are installed very close to the midspan of the edges. On the other hand, relatively small displacements are observed at Section-E and Section-D, which are placed closer to the corners.

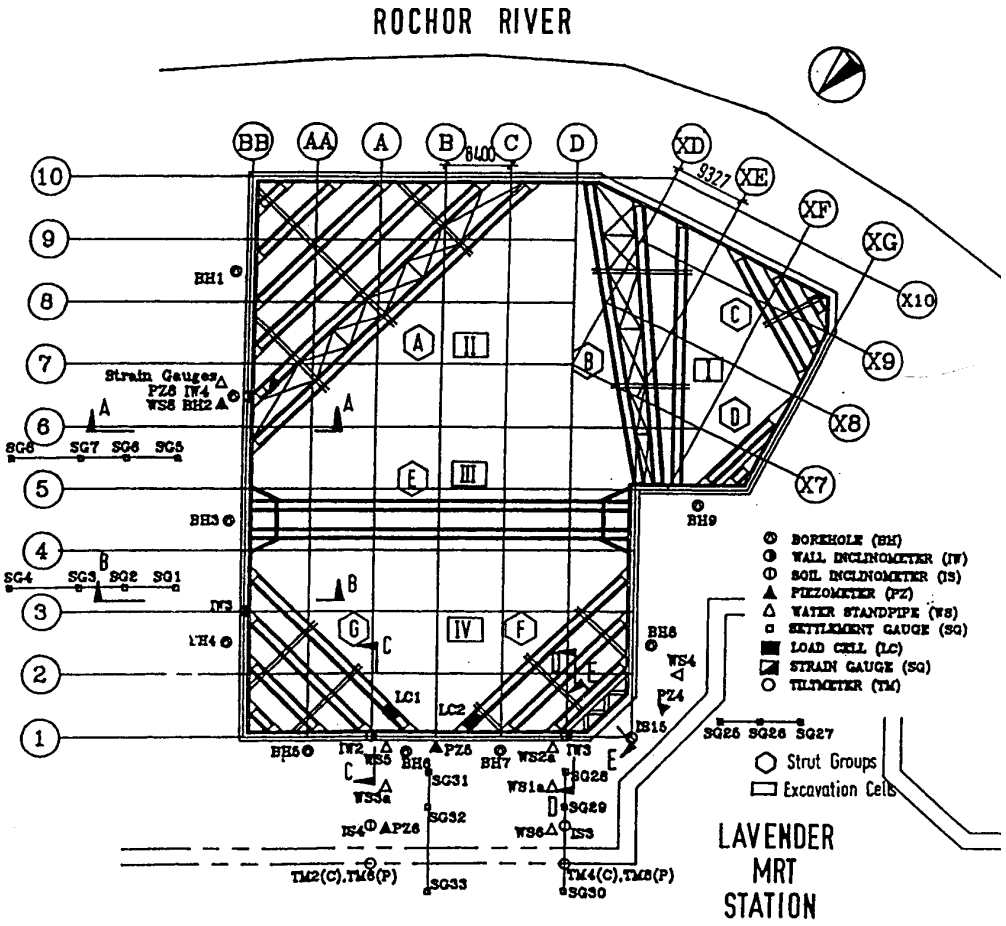

Figure 28. Plan View of IMM Building Excavation (by Lee, Yong, Quan and Chee (1998))

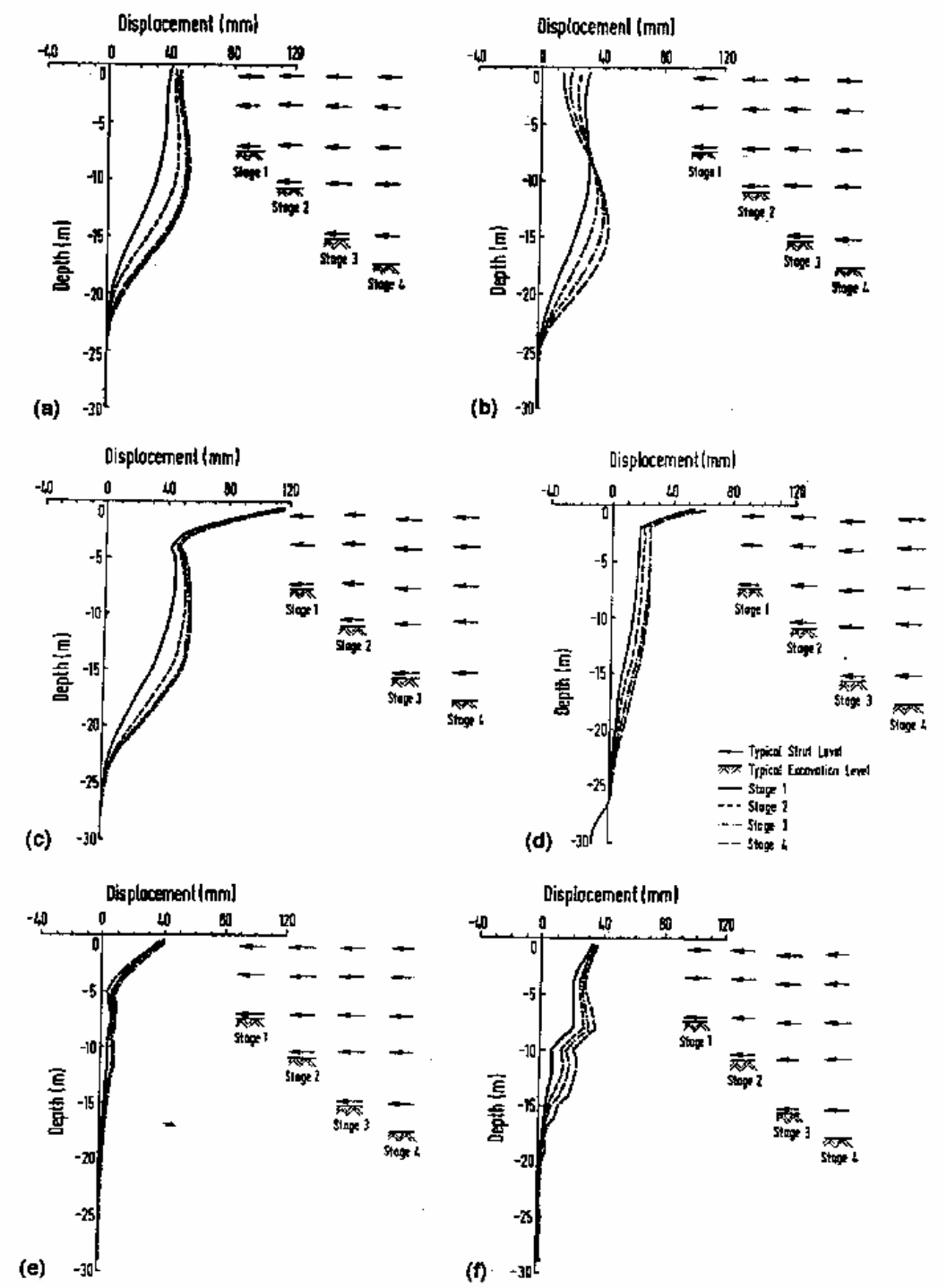

Figure 29. Measured diaphragm wall deflection at four stages of excavation (a) IW4 at section A (b) IW3 at section B (c) IW2 at section C (d) IW1 at section D (e) IS15 at section E (f) IS4 at section C (g) IS3 at section D (by Lee, Yong, Quan and Chee (1998))

In this study beside monitoring lateral movements, ground settlement is monitored as well. Maximum settlement is observed at Section-C followed by Section-A and Section-B. The lowest settlement is monitored at Section-D which is the closest one to the corner (see Figure 30).

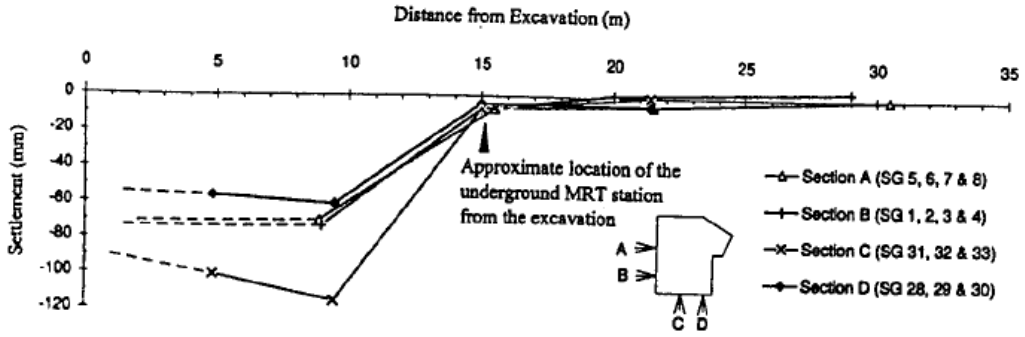

Figure 30. Ground surface settlement profiles in retained soil at sections A to D at final excavation level (by Lee, Yong, Quan and Chee (1998))

The program CRISP developed at Cambridge University is used for 3D finite element analyses. Because of the limitation of computer capacity, several idealizations and simplifications without affecting the accuracy of the solution are made. In Figures 31, 32, 33; plan views of the modeled corner with and without simplification and the idealized section of the region is demonstrated. In modeling Cam Clay model is preferred for modeling the soils, elasto-plastic material is used for the diaphragm wall and 3D spring elements are applied for modeling diagonal struts by the researchers. The typical mesh of 3D analysis is demonstrated in Figure 34.

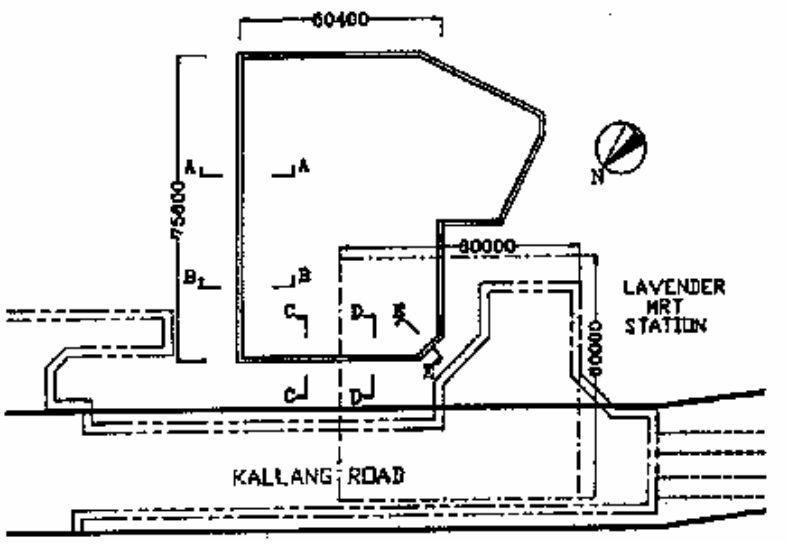

Figure 31. Plan view showing dimensions and locations of region modeled by 3D finite element method (by Lee, Yong, Quan and Chee (1998))

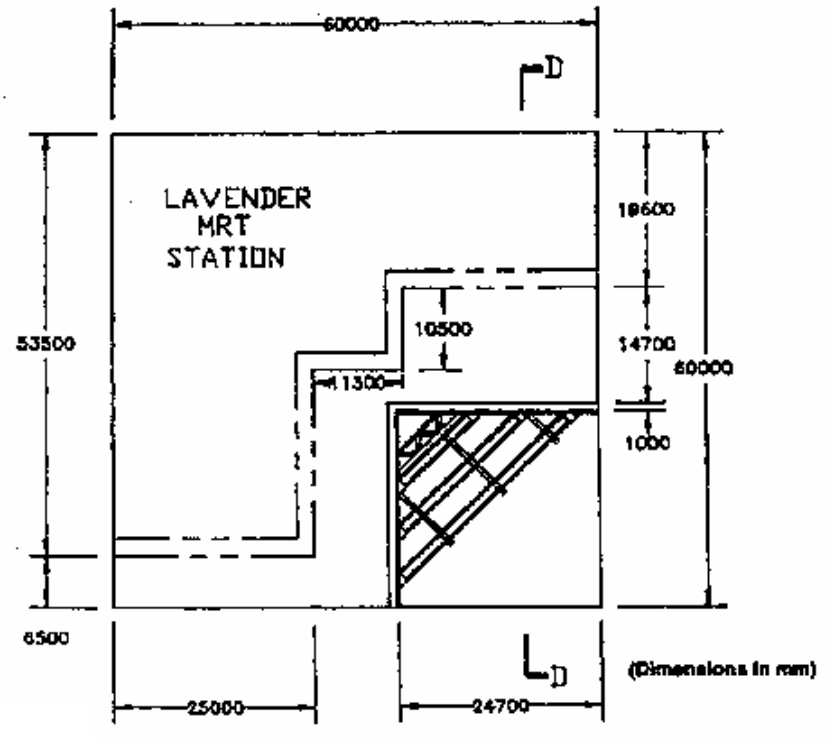

Figure 32. Plan view showing simplified geometry of excavation corner and station used in 3D finite element analysis (by Lee, Yong, Quan and Chee (1998))

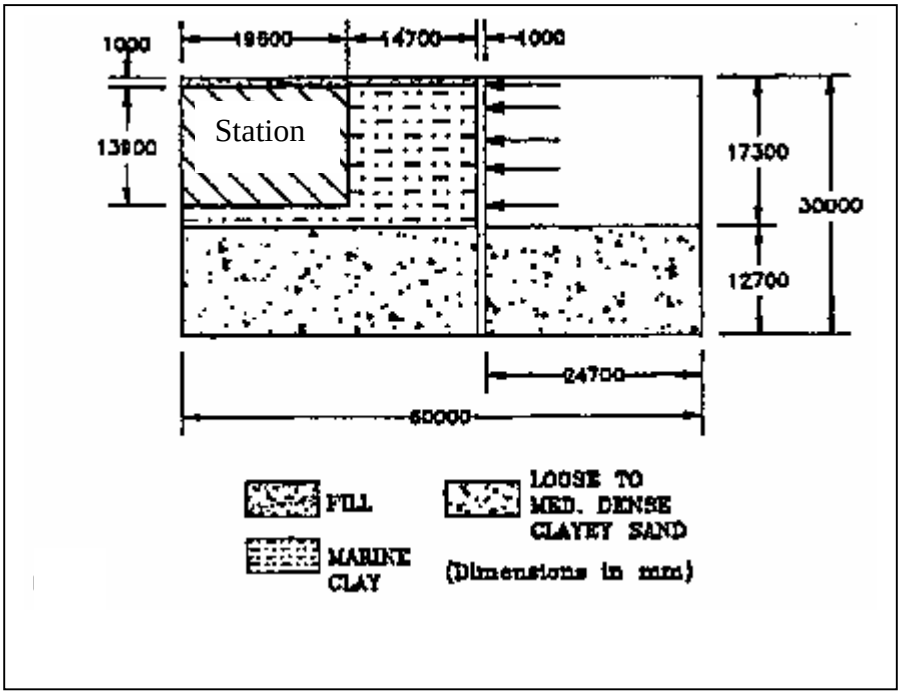

Figure 33. Idealized section used in 3D finite element analysis (by Lee, Yong, Quan and Chee (1998))

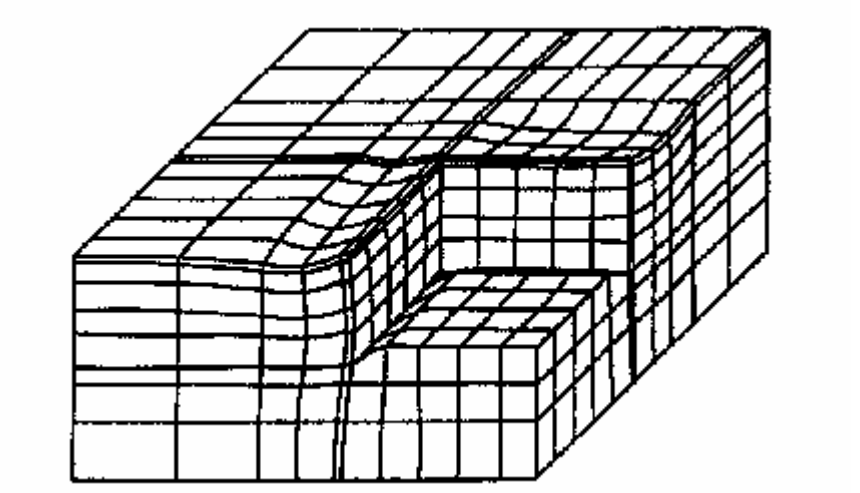

Figure 34. Typical deformed mesh of 3D analysis (by Lee, Yong, Quan and Chee (1998))

2D finite element analyses are also performed for comparing the results with 3D analyses ones. For this purpose, same material properties as 3D analyses are used for modeling except out of plane strut forces. Only the components of strut stiffness and preloads in the direction perpendicular to the diaphragm wall can be modeled.

Measured values for section C and D are compared with 2D and 3D analysis results. Neither 3D nor 2D results are found to match the measured deflection profile completely. However, very well predicted deflection results are obtained from 3D analysis. The deflection measured in section-C, which is nearly at the midspan of the edge, does not match the 2D results. This means that even at the midspan of the edges plane strain conditions do not completely represent the behavior. For section-D, the deflection obtained from 2D dimensional analysis is two times more than the measured deformation profile. On the other hand, the deflections obtained from 3D results are only %30 more than the measured values (see Figure 35).

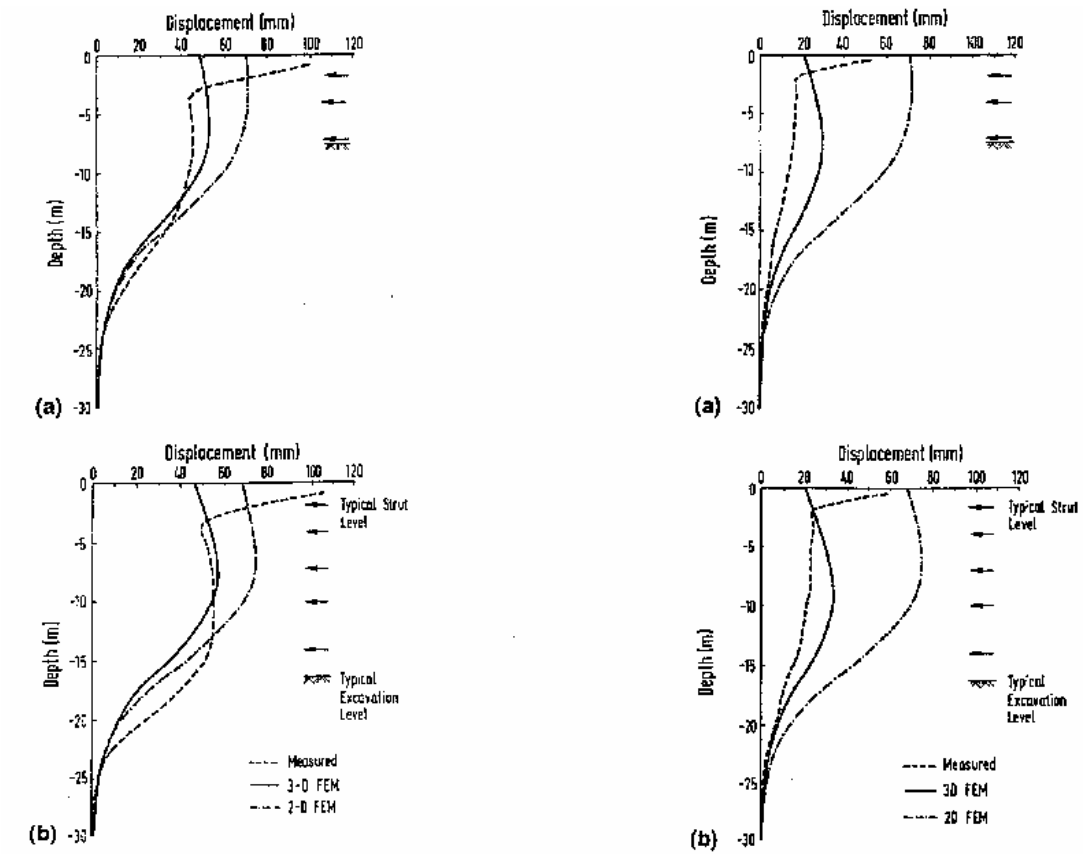

SECTION-C ***SECTION-D***

Figure 35. Comparison of computed and measured wall deflections for section-C and section-D (by Lee, Yong, Quan and Chee (1998))

Diaphragm wall deformations and ground surface settlements are measured during and after Taipei National Enterprice Center (TNEC) excavation by Ou, Shiau and Wang (2000). Moreover finite element analyses are performed for this site. TNEC building is composed of 18 stories and 5 basements. For construction of the basement up to 19.7m depth, top down construction method is used. Ninety cm thick diaphragm wall is supported by concrete floor slabs and temporary steel struts, cross sectional view of construction site is demonstrated in Figure 37. During and after the construction stages regular measurements are taken by inclinometers, heave gauges and settlement gauges (see Figure 36).

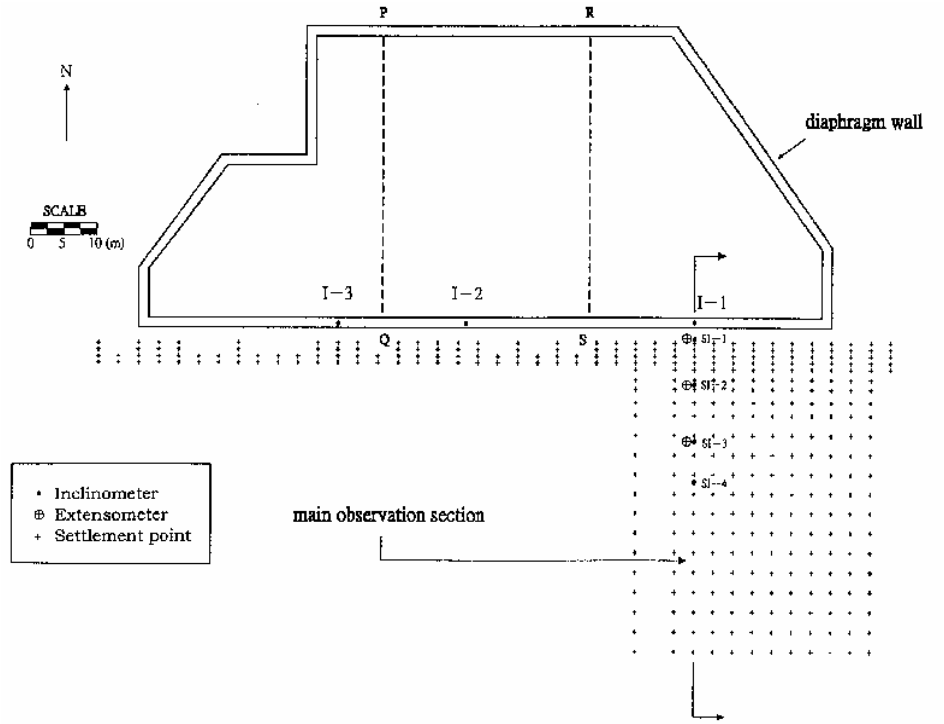

Figure 36. Geometry and instrumentation of the Taipei National Enterprise Center (TNEC) excavation project (by Ou, Shiau, Wang (2000))

The excavation is performed in Silty Clay and Silty Sand underlained by gravel (see Figure 38).

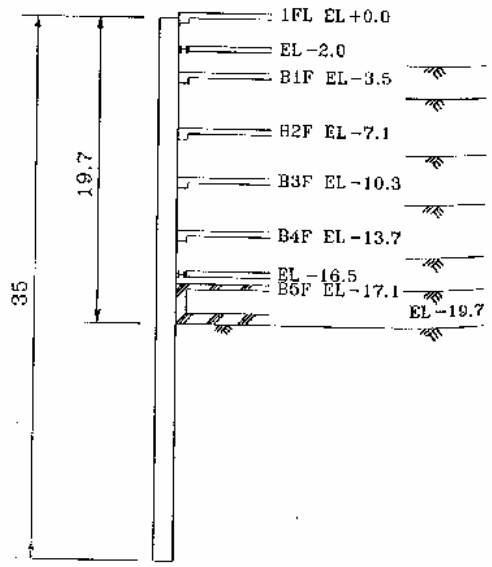

Figure 37. Construction sequence for the TNEC excavation project. All values are in meters. EL, elevation. (by Ou, Shiau, Wang (2000))

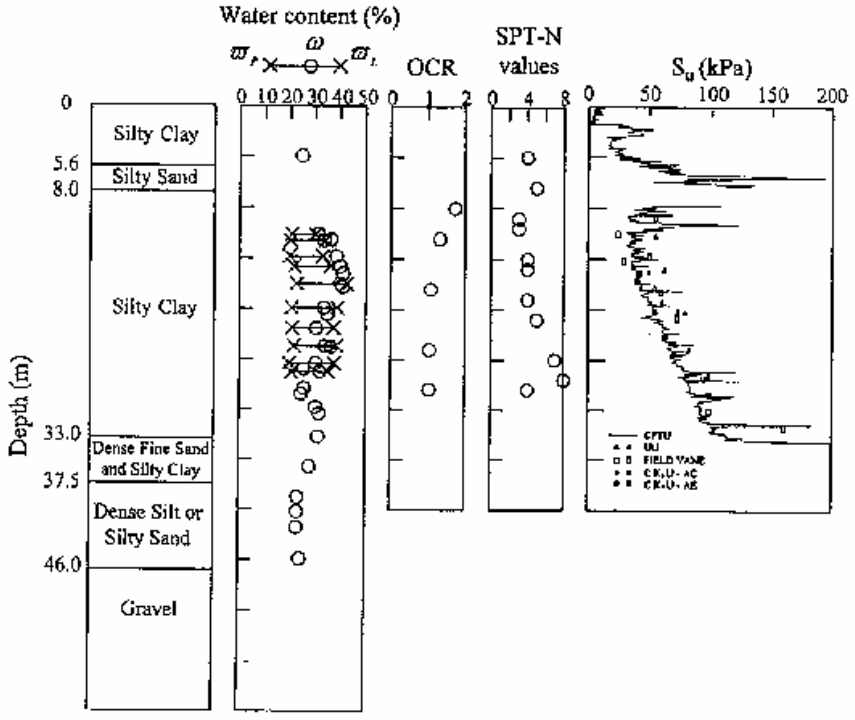

Figure 38. Subsurface ground conditions and characteristics of soils (by Ou, Shiau, Wang (2000))

During and after the construction stages, regular measurements are taken from inclinometers (see Figure 39). Latitudinal measurements show that I-1 tends to deflect toward west; on the other hand I-3 tends to deflect toward east. This indicates that there is a tendency of soil that is not in the center of the site, for moving toward the excavation center.

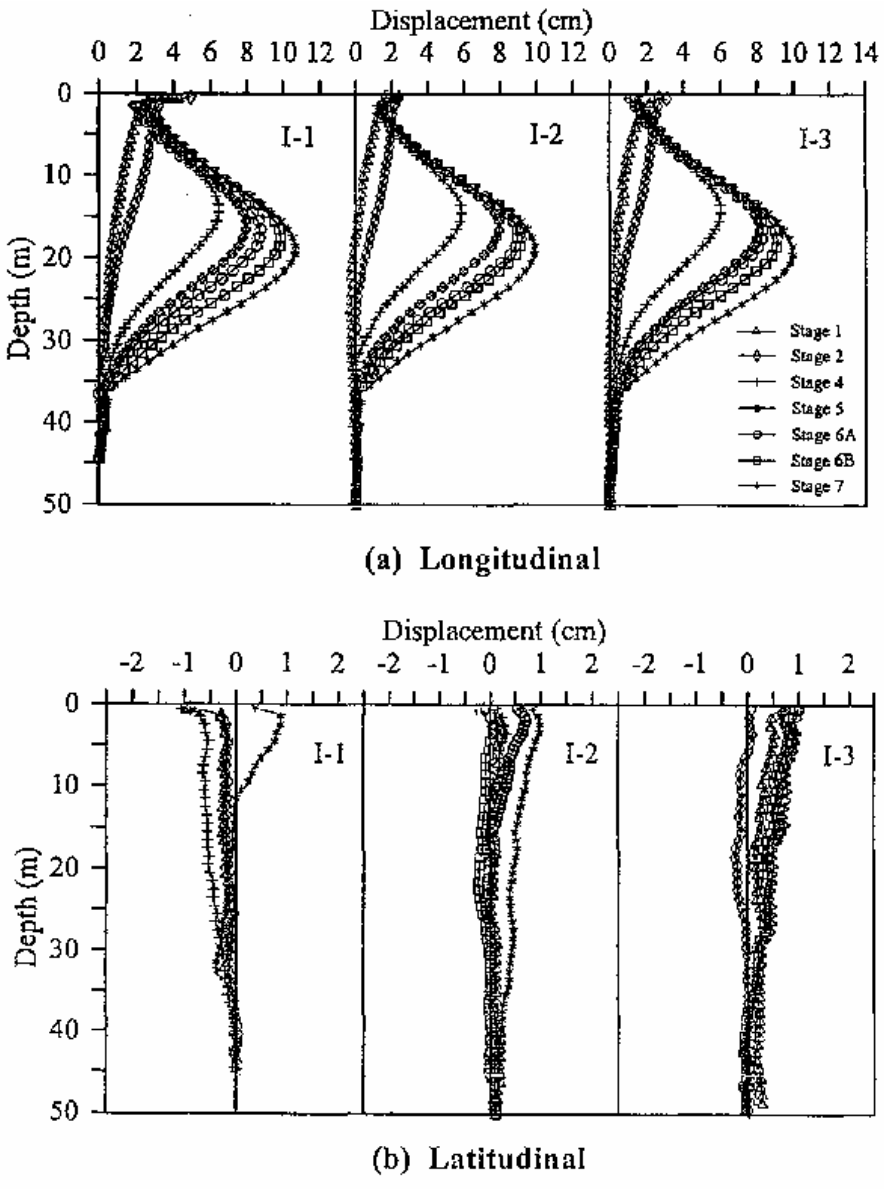

Figure 39. Longitudinal and Latitudinal Wall Deformations at I-1, I-2 and I-3 (by Ou, Shiau, Wang (2000))

Researchers concluded that ground surface settlements are decreased with decreasing the distance to the southeast corner and increasing distance to the diaphragm wall. Contours showing ground surface settlements, which are drawn according to heave gauge and settlement gauge measurements, are shown in Figure 40.

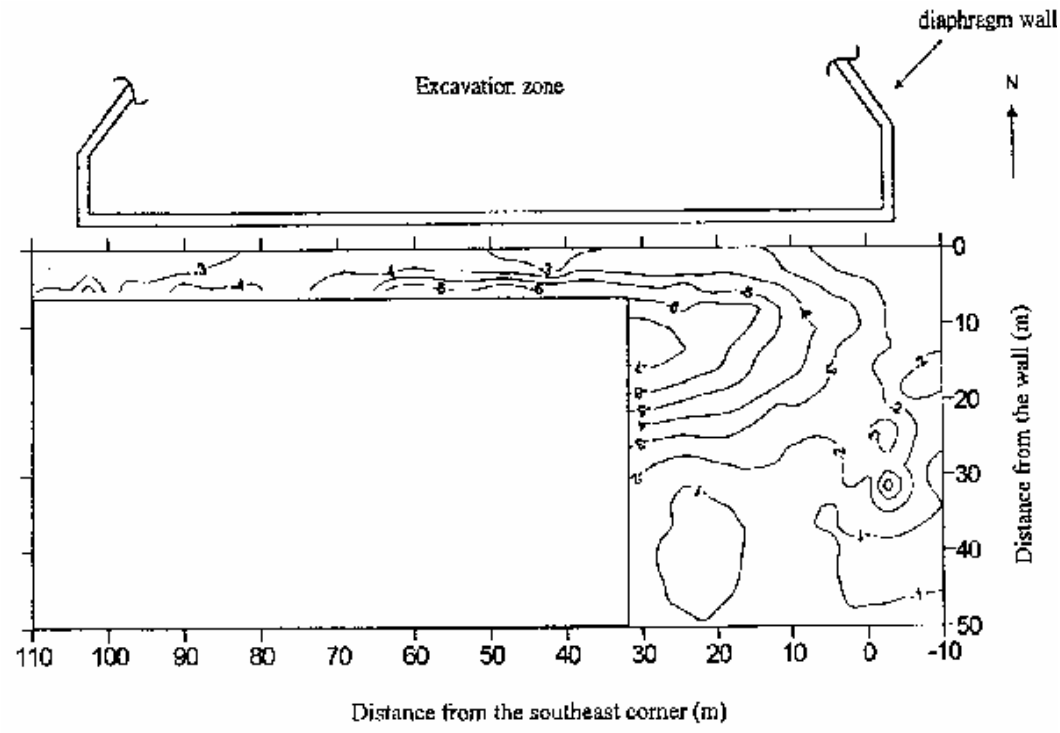

Figure 40. Contours (in cm) of the ground surface settlement at the final stage of excavation (by Ou, Shiau, Wang (2000))

Three dimensional finite element analyses are also performed for the site by using the program CUT3D. For simulation of soil the hyperbolic model by Duncan and Chang (1970) which assumes nonlinear, inelastic, and strain dependent soil behavior. Observed wall deformation and computed wall deflections are consistent. At I-3 and I-2 competed values are slightly bigger than the observed ones. However at I-1 observed values are larger then the computed ones. Furthermore observed ground settlements are bigger than the computed ones (see Figure 41, 42).

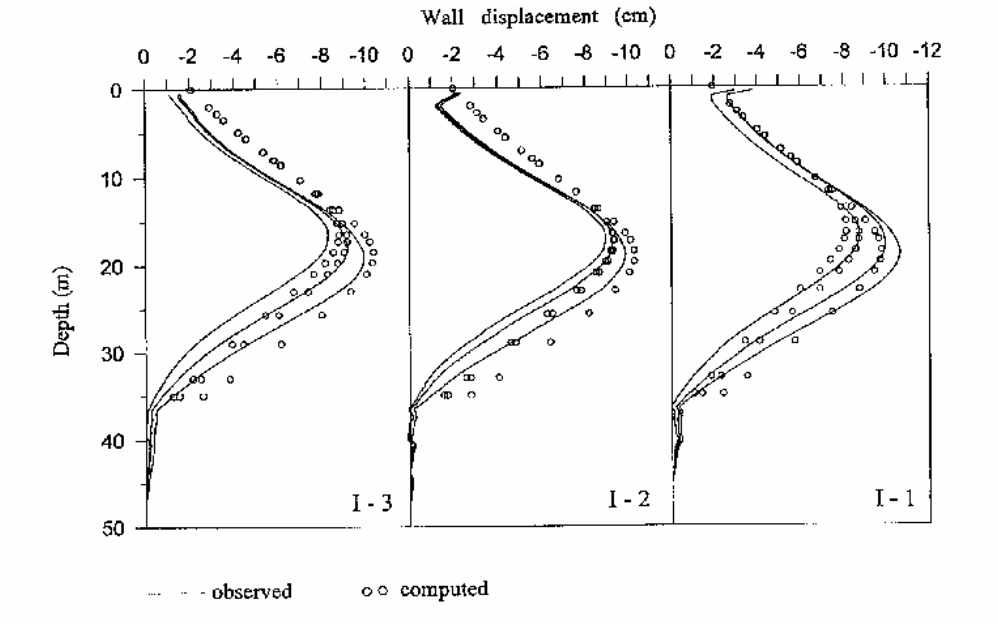

Figure 41. Comparison of the observed and computed wall deflections at the last three stages of excavation for I-1, I-2 and I-3 (by Ou, Shiau, Wang (2000))

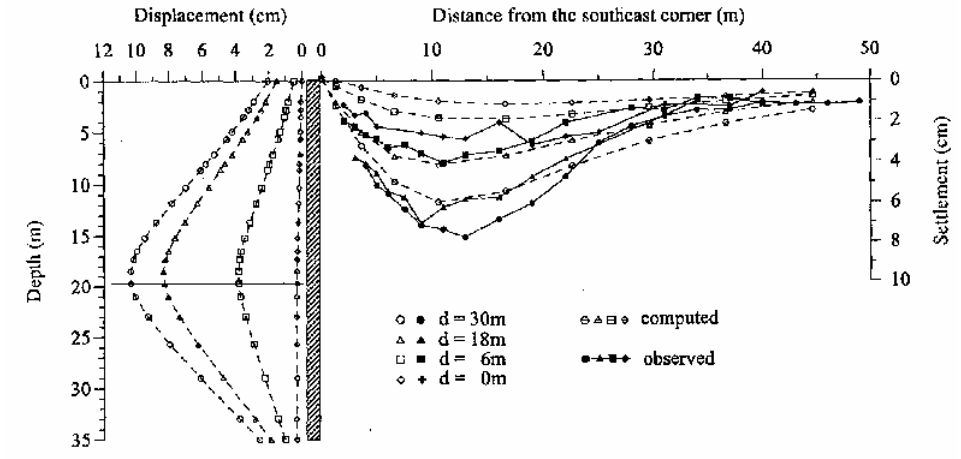

Figure 42. Comparison of the observed and computed ground surface settlements at some representative sections and corresponding computed wall displacements (by Ou, Shiau, Wang (2000))

The effects of stiff stratum of soil and stiffness of the strutting system on corner effect are studied by Liu (1995). He concludes that maximum lateral movement of the supporting system is observed above excavation depth in stiff soil stratum, whereas it occurs below the excavation depth in soft clay stratum. Moreover it is mentioned that as effectiveness of the supporting system increases, the corner effect decreases, and the results of 2D and 3D analyses become closer.

A deep excavation in Bangkok Metropolitan Area is studied by Lin, Chung, and N. Phien-wej (2003). The soil profile of the site from the ground surface is; 1-2m soft clay layer then 9-12m thick marine clay layer underlain by medium clay to stiff to hard clay and medium dense sand. 100m wide, 20m long and 0.8m thick wall is supported by four struts at 1m, 4m, 7m and 10m depths.

To clarify a quantitative relationship of lateral wall movement between 3D and 2D analyses, multi strutted diaphragm wall is modeled by using FLAC which is 3D Finite Difference Method (FDM) program. 2D analyses are performed by using FLAC program by taking the unit width of cross section of 3D mesh along X direction.

For investigating corner effect in a deep excavation in Bangkok Subsoil, a study similar to Ou et al's (1993-1996) study is performed. The plane strain ratios (PSR) for this specific case are obtained as shown in Figure 43.

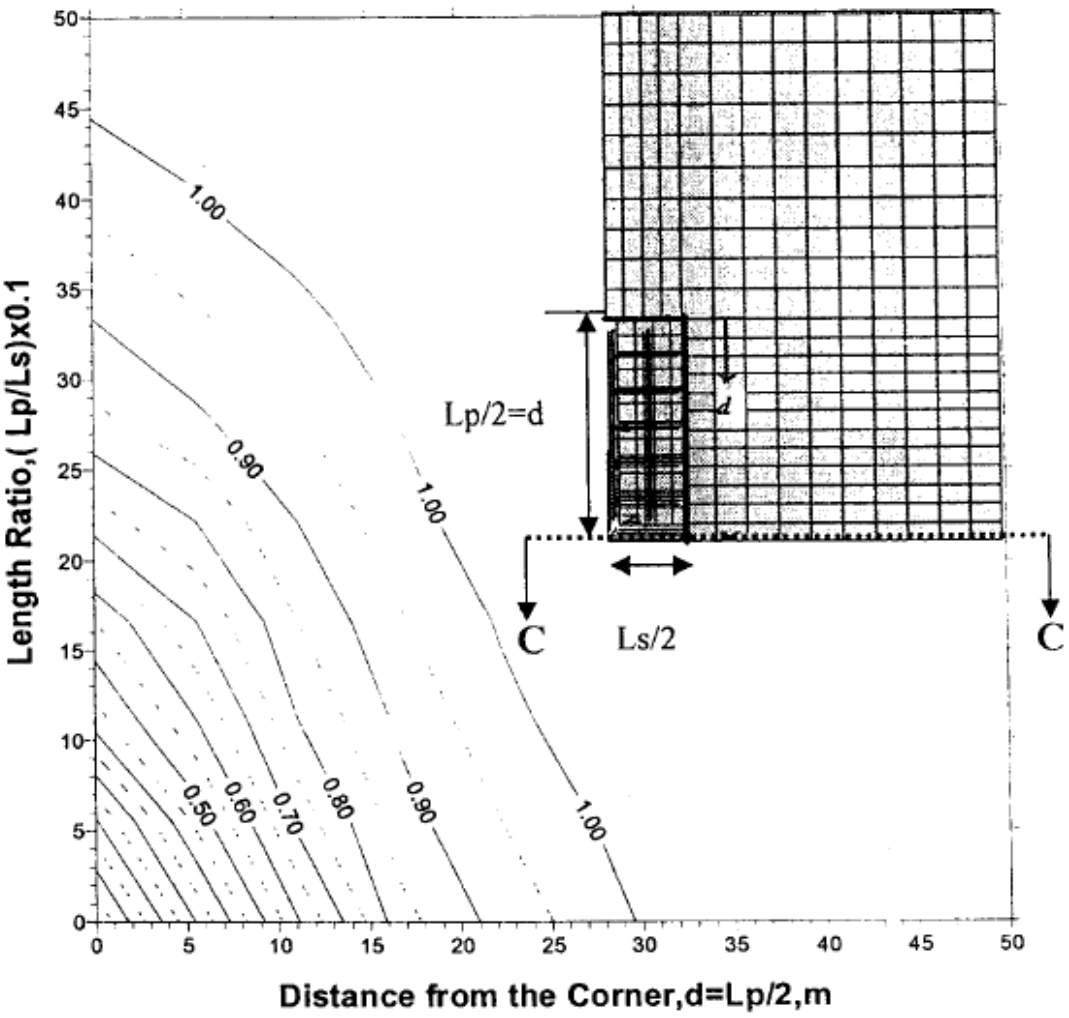

Figure 43. Relationship of width ratio Lp/Ls, distance d of the evaluated C-C section from the corner and plane strain ratio PSR (by Lin, Chung, Phien-wej (2003))

Rajavej Hospital Project is also examined by Lin, Chung, Phien-wej. A 14.4m deep excavation is supported by a 21m long and 0.8m thick diaphragm wall. Excavation's width and lengths are 28m and 36m, respectively. Measurements obtained from the site are compared with 2D and 3D predictions, as well as with PSR predictions. Comparisons are demonstrated in Figure 44 PSR predictions are very close the field observations. However it should be noted that the PSR graphs do not include all the factors affecting the lateral movement of the system. It is suggested that for similar excavations with this study, PSR predictions should be made and by using field instrumentation the predictions should be checked.

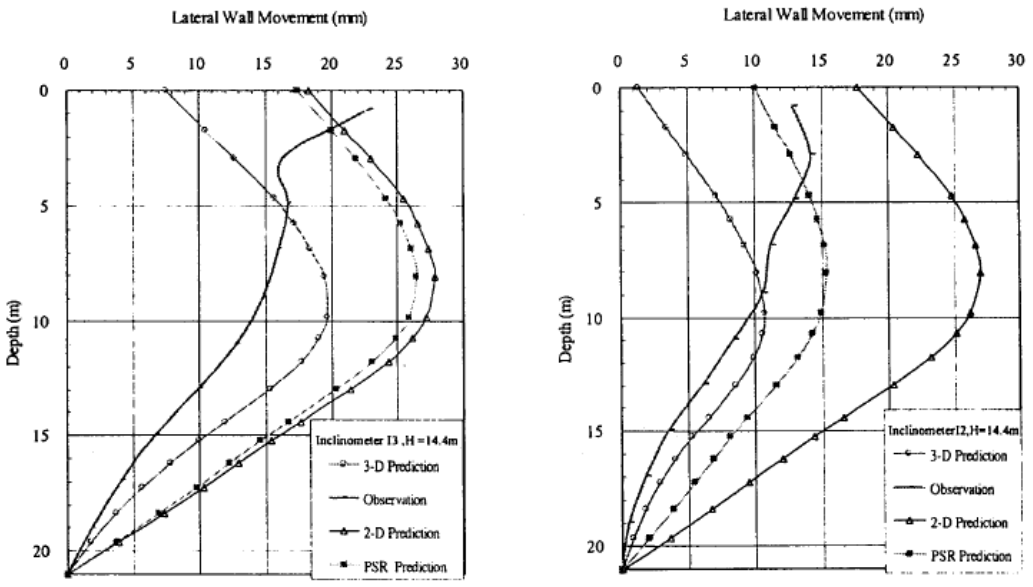

Figure 44. Comparison of lateral wall movement between numerical predictions (3D,2D and PSR) and field observation of Rajavej Hospital excavation (by Lin, Chung, Phien-wej (2003))

CHAPTER 3

PARAMETRIC STUDY ON CORNER EFFECT IN DEEP EXCAVATIONS

3.1. General

The accuracy of predicted deflection, moment and lateral stresses are affected by the presence of a corner in an excavation. In order to examine the corner effects, 8m deep excavation having 20m by 100m dimensions is modeled as shown in Figure 45. To reduce the calculation time, only quarter of the excavation is analyzed as shown in Figure 46. Cantilever, pile walls anchored wall at one level and anchored wall at two levels pile walls are considered. In order to analyze the anchor loads, an excavation anchored wall at four levels is also investigated.

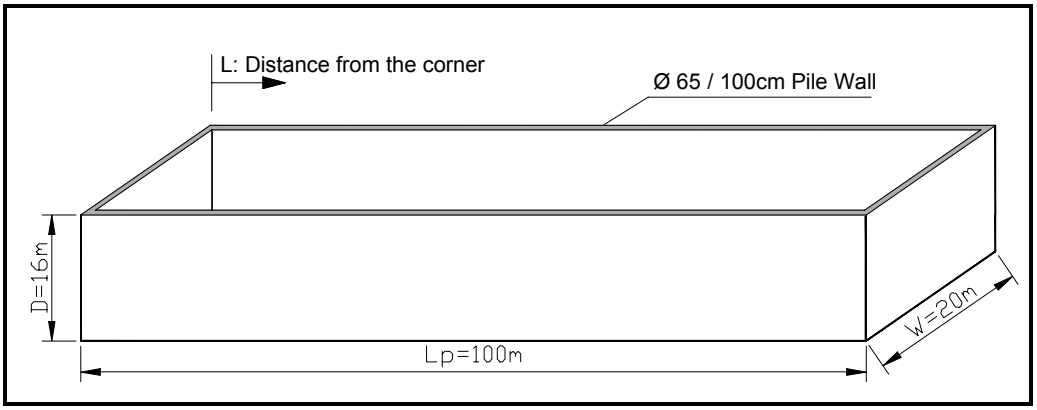

Figure 45. Configurations of excavation cases

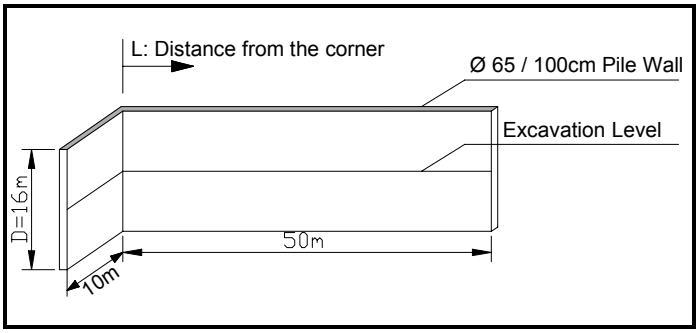

Figure 46. Configuration used in 3D (with corner) analyses

For comparison of deflections, moments and effective horizontal stresses along the excavation side, 2D, 3D with corner, and 3D without corner models are studied.

3.2. Support System

Eight meter deep excavations having 20m by 100m dimensions are modeled. Following cases are analyzed;

i) Cantilever Case: (as shown in Figure 47)

- Pile diameter: 65cm
- Pile spacing: 100cm
- Pile Length: 16m
- Excavation Depth: 8m

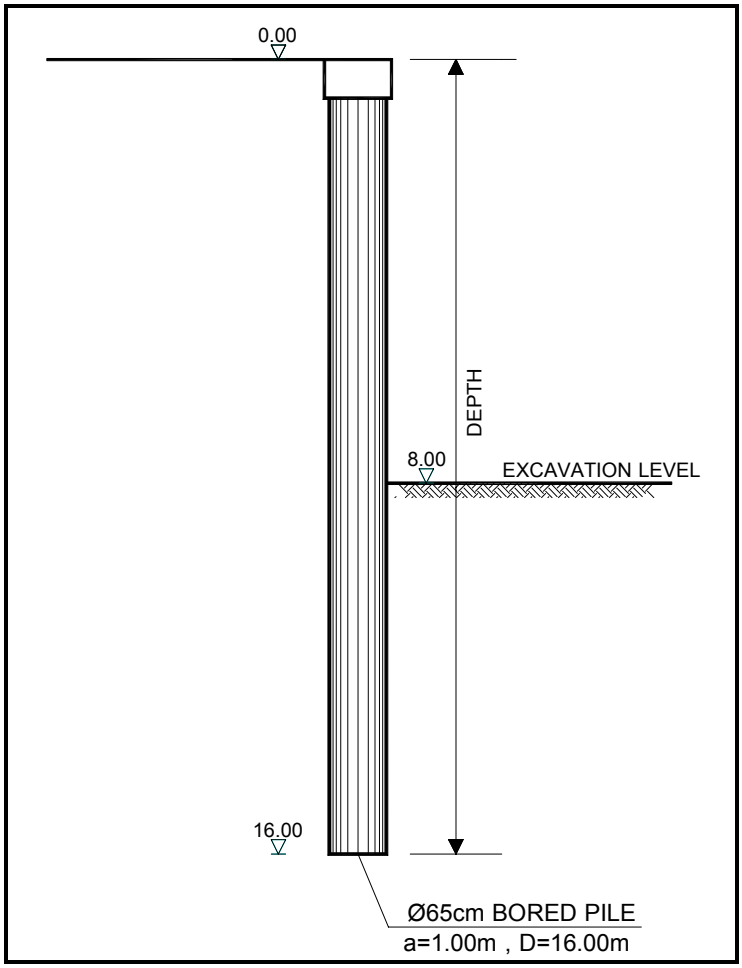

Figure 47. Cross sectional view of cantilever case

ii) Single level anchored wall (as shown in Figure 48)

- Pile diameter: 65cm
- Pile spacing: 100cm
- Pile Length: 16m
- Excavation depth: 8m
- Anchor level / length: -2.0m / 13.5m
- Lateral anchor spacing: 2m

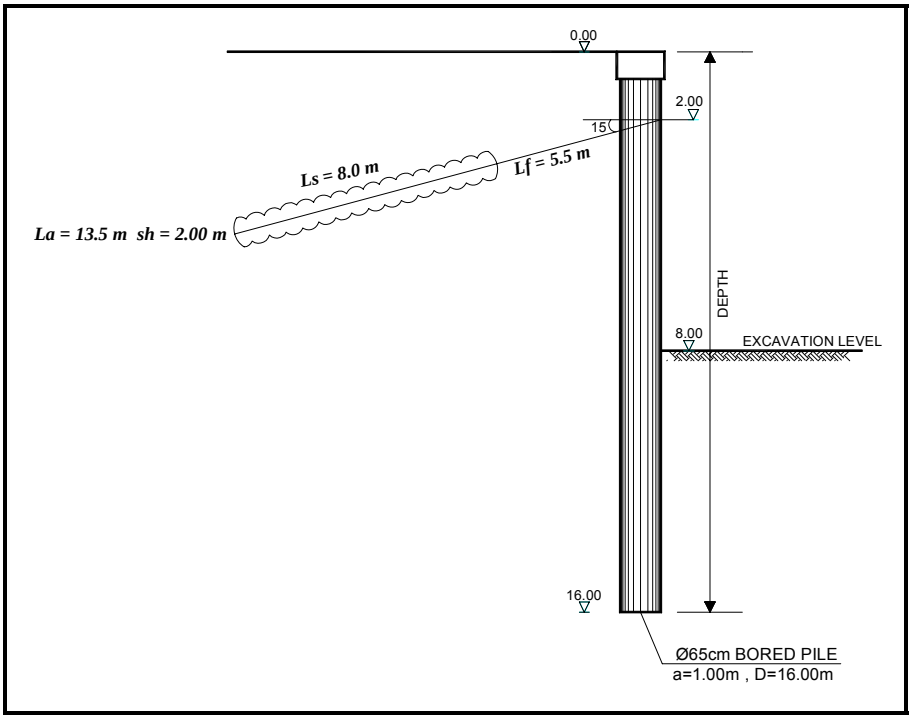

Figure 48. Cross sectional view of single level anchored wall

iii) Two level anchored wall (as shown in Figure 49)

- Pile diameter: 65cm
- Pile spacing: 100cm
- Pile Length: 16m
- Excavation depth: 8m
- Anchor level / length: -2.0m / 13.5m
  -4.5m / 12.0m
- Lateral anchor spacing: 2m

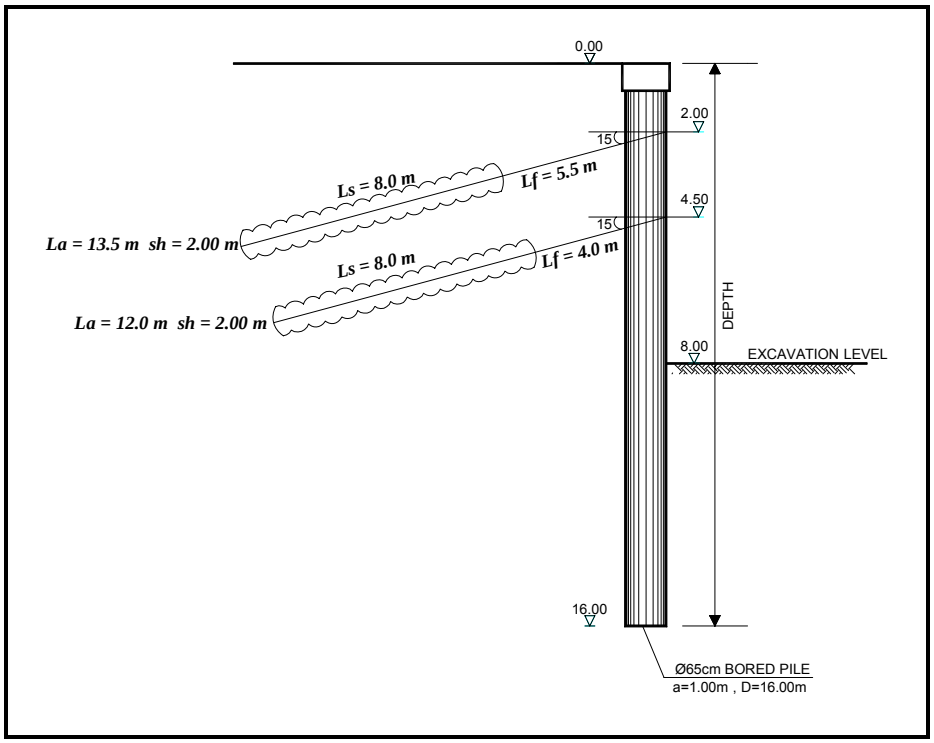

Figure 49. Cross sectional view of two level anchored wall

iii) Four level anchored wall (as shown in Figure 50)

- Pile diameter: 65cm
- Pile spacing: 100cm
- Pile Length: 16m
- Excavation depth: 12m
- Anchor level / length: -1.5m / 15.5m
  -4.0m / 14.0m
  -6.5m / 12.5m
  -9.0m / 11.0m
- Lateral anchor spacing: 2m

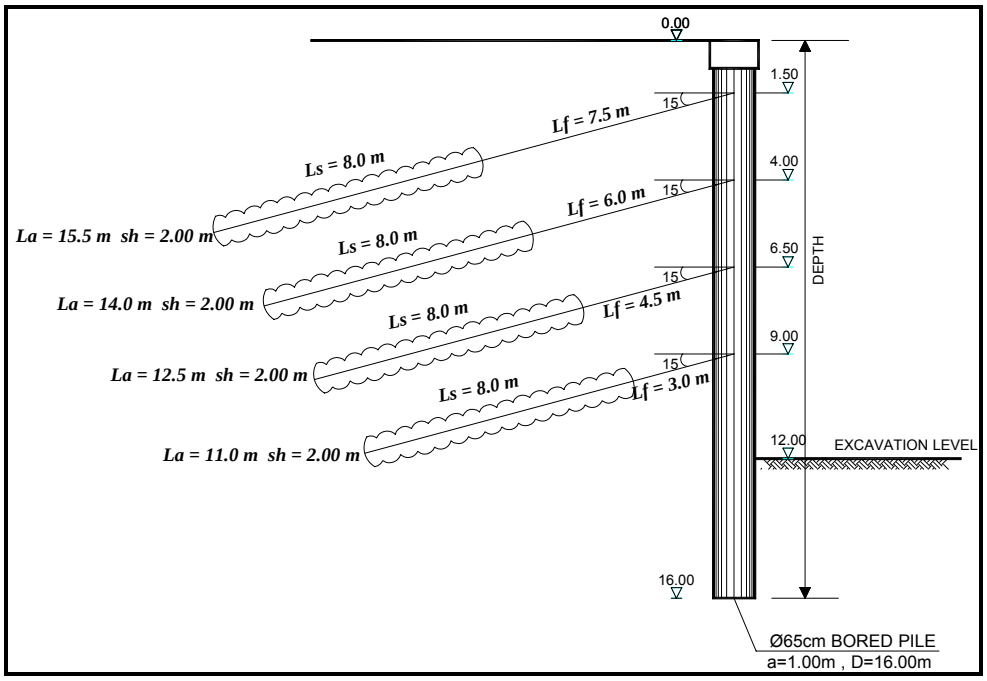

Figure 50. Cross sectional view of four level anchored wall

3.3. Subsoil Conditions

Parametric studies are performed for clays with different elastic modulus values. No water table case was considered in parametric study. Constant cohesion, internal friction angle, unit weight, poissons ratio and interface constant are used in the calculations.

Parameters used in calculations are summarized in Table 2.

Table 2. Parameters used in parametric study

PARAMETER	***NAME***	***CLAY***	***UNIT***
Material Model	*Model*	HSM	-
Material Behavior	*Type*	Drained	-
Unsaturated Soil Weight	γ_{unsat}	19	kN/m^3
Saturated Soil Weight	γ_{sat}	19	kN/m^3
Secant Stiffness for CD Triaxial Test	E_{50}^{ref}	3500-8500-16500-25000-33500	kN/m^2
Tangent Oedometer Stiffness	E_{oed}^{ref}	3500-8500-16500-25000-33500	kN/m^2
Unloading/Reloading Stiffness	E_{ur}^{ref}	10000-25000-50000-75000-100000	kN/m^2
Power Stress Level Dependency of Stiffness	*Model*	0.5	-
Cohesion	c_{ref}	15	kN/m^2
Friction Angle	ϕ	24	°
Dilatancy Angle	ψ	0	°
Poisson's Constant	ν_{ur}	0.2	-
Interface Reduction Factor	R_{inter}	0.7	-

Note: HSM: Hardening soil model

3.4. Finite Element Analyses

Plaxis 2D Analyses and Plaxis 3D Foundation programs are used for analyses of parametric studies and also the cases mentioned in this thesis. Plaxis is a finite element program used for computation of stresses and strains in geotechnical design. In Plaxis 2D the third direction of the system is assumed as infinite and parameters for structural elements are given for per meter. Also a plane strain model with a uniform cross section is used for modeling, for this reason some simplifications for real cases have to be made in 2D analyses. On the other hand in Plaxis 3D Foundation program the third direction of the systems can be defined. However data entry and processing times are much longer compared to 2D one.

In 2D and 3D analyses Hardening Soil Model (HSM), which is an elastoplastic type of hyperbolic model formulated in the framework of friction hardening plasticity, is used. The model let the users to simulate behavior of sand, gravel and clays in excavation phases. The most important advantage of HSM is taking into account of increase of stiffness with pressure. Furthermore some more advantages compared to Mohr-Coulomb model are distinction between primary loading and unloading/reloading, memory of preconsolidation stress and well suited for unloading situations with simultaneous deviatoric loading.

For simulation of soil behavior by using HSM, the friction angle, ϕ, cohesion, c , the dilatancy angle, ψ , triaxial loading stiffness, E_{50} , triaxial unloading stiffness, E_{ur} and oedometer loading stiffness E_{oed} are used. There is a relation between stiffness values as $E_{ur} \cong 3E_{50}$ and $E_{50} \cong E_{oed}$.

According to availability of water and permeability of soil, behavior (drained or undrained) of soil is assessed. No excess pore pressures are produced in drained behavior. On the other hand in undrained behavior excess pore water pressures are generated. Drained condition is appropriate for dry soils and high permeable soil types like sand and gravels. Also it should be noted that drained analyses simulate long term soil behavior. Undrained condition is suitable for low permeable soil types like clays. No matter which permeability constants are used, if drained type material is used.

In order to model pile walls, plate element is used in 2D analyses and wall element is used for 3D analyses. For this simulation equivalent thickness are determined

and are used both for the plate and the wall. In 3D model, interfaces that are modeling interaction between structure and soil are automatically placed when the wall is defined. On the other hand in 2D model, interfaces are also determined by the user. In order to obtain identical models, interfaces are placed in both 2D and 3D models and same interface factors are utilized.

Node to node anchors for free length and geogrid for fixed length are used for modeling anchors in 2D analyses. On the contrary, ground anchor option is available to determine anchors in 3D analyses. Same stiffness values for both fixed and free length are assigned in both analyses except the skin resistance value. Since skin resistance can be defined only in 3D analyses.

According to finite element method the continuum is divided into volume elements called meshes. To get more precise results from the program, finer meshes should be assigned. However as the fineness of the mesh increases, required calculation time increases as well. Because of this reason much finer mesh can be assigned in 2D analyses but coarser meshes have to be assigned in 3D analyses. 3D analyses give a chance to generate both 2D mesh and 3D mesh individually. By using this advantage, finer mesh is utilized in X-Z plane that is used for defining plan view of the site. However coarser mesh is used in the third direction (Y direction) which is used for modeling the layering in soil skeleton, the levels used for defining pile length and anchor places. This mesh type is recommended by Ou, Chiou, Wu (1996).

A typical mesh generation used in 3D analyses is demonstrated in Figure 51.

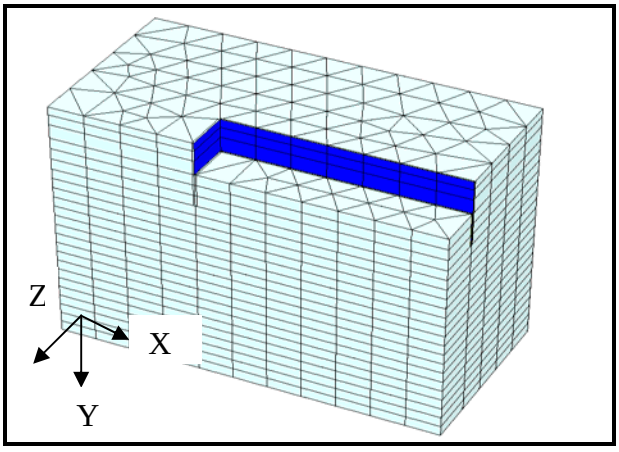

Figure 51. A typical finite element mesh used in 3D analyses

3.5. Results

In the parametric study, cantilever, anchored wall at one level, anchored wall at two levels, and anchored wall at four levels cases are studied for five different soil modulus values. For these cases deflection, moment, and effective horizontal forces versus depth graphs are prepared. To understand the effects of the corner on deflection of the pile wall, various cross sections of which distances from the corner are 5m, 10m, 15m, 20m, 30m, 40m and 50m are studied. Only the sections taken from 7m, 21m, 35m and 50m distances from the corner are used, in order to avoid the crowdedness of moment vs. depth and effective horizontal stresses vs. depth graphs.

A quarter of 20m wide 100m long excavation is modeled by using 3D finite element program. The variations of deflection, moment and effective horizontal stresses along the long side of the excavation are determined. To compare the 3D analyses with corner, with 2D one, 2D finite element analyses are performed. Moreover, to compare the results of plane strain analyses and 3D with corner analyses, long excavation side without a corner is also modeled by using 3D analyses program.

Because of difference in mesh coarseness between 2D and 3D analyses, number of obtained data along the pile wall is different. As a result of this fact more smoother lines are formed for 2D analyses; on the other hand sharp broken lines are obtained in 3D analyses.

3.5.1. Cantilever Cases

Cantilever cases for elastic modulus values of 8500, 16500, 25000, and 33500 kPa are studied. The finite element meshes used in 2D analyses, 3D analyses with and without corners are demonstrated in Figures 52, 53, 54, respectively.

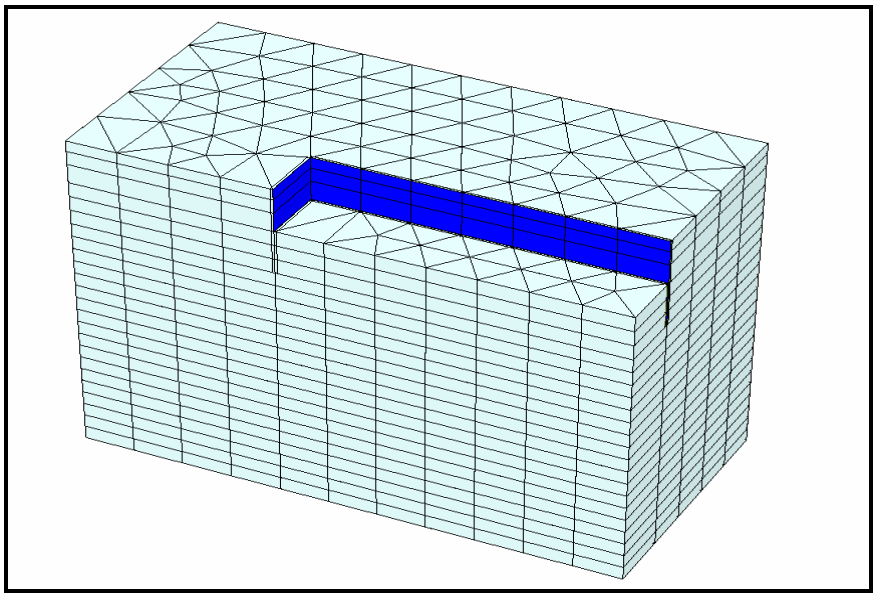

Figure 52. Finite element mesh used in 3D analyses (with corner) of cantilever case

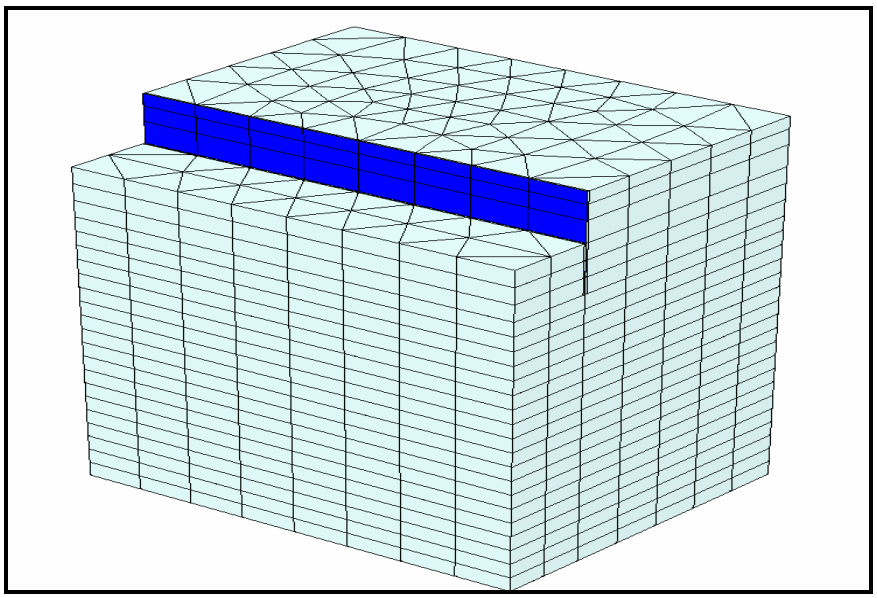

Figure 53. Finite element mesh used in 3D analyses (without corner) of cantilever case

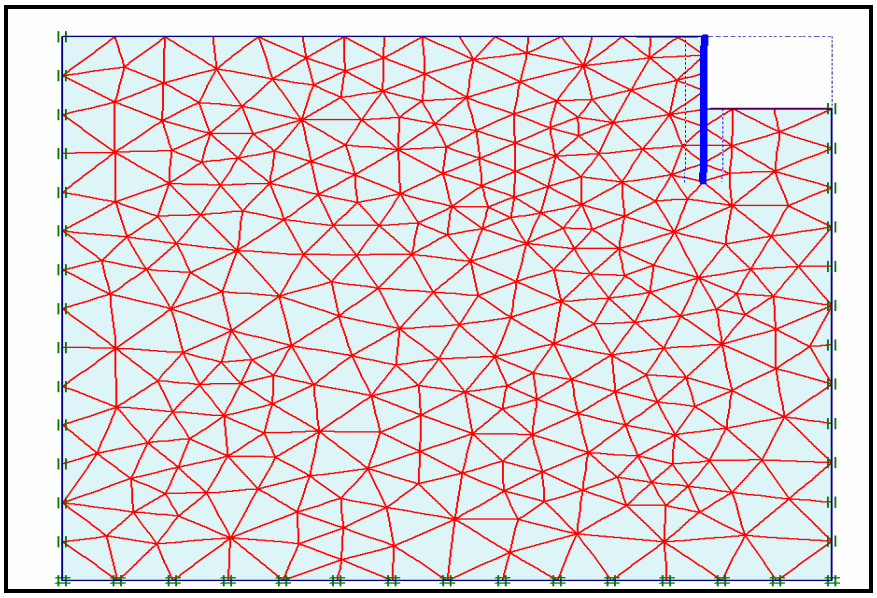

Figure 54. Finite element mesh used in 2D analyses of cantilever system

Deflection for various sections vs. depth graphs are demonstrated in Figures 55, 56, 57, 58, respectively.

Following results are obtained;

- Comparisons of various sections taken from 3D with corner analyses;

  For all elastic modulus values, corner effect on deflections is observed up to 20m distance from the corner. After this distance deflections become nearly constant.

- Comparisons of 3D with and without corner analyses;

  - *0-4m depth*: Deflections of 3D without corner analyses are 3-5mm smaller than deflections of sections, distance of which are bigger than 20m from corner. This deflection difference may be a result of mesh generation disparity between models.

  - *4-16m depth*: The deflections of sections, distance of which are bigger than 20m from corner, are similar with deflection of 3D without corner analyses.

- Comparisons of 3D without corner and plane strain analyses;

  - Maximum deflections obtained from plane strain analyses are nearly two times of the ones obtained from 3D analyses.

  - Under the excavation level, plane strain deflections match the ones obtained from 3D analyses.

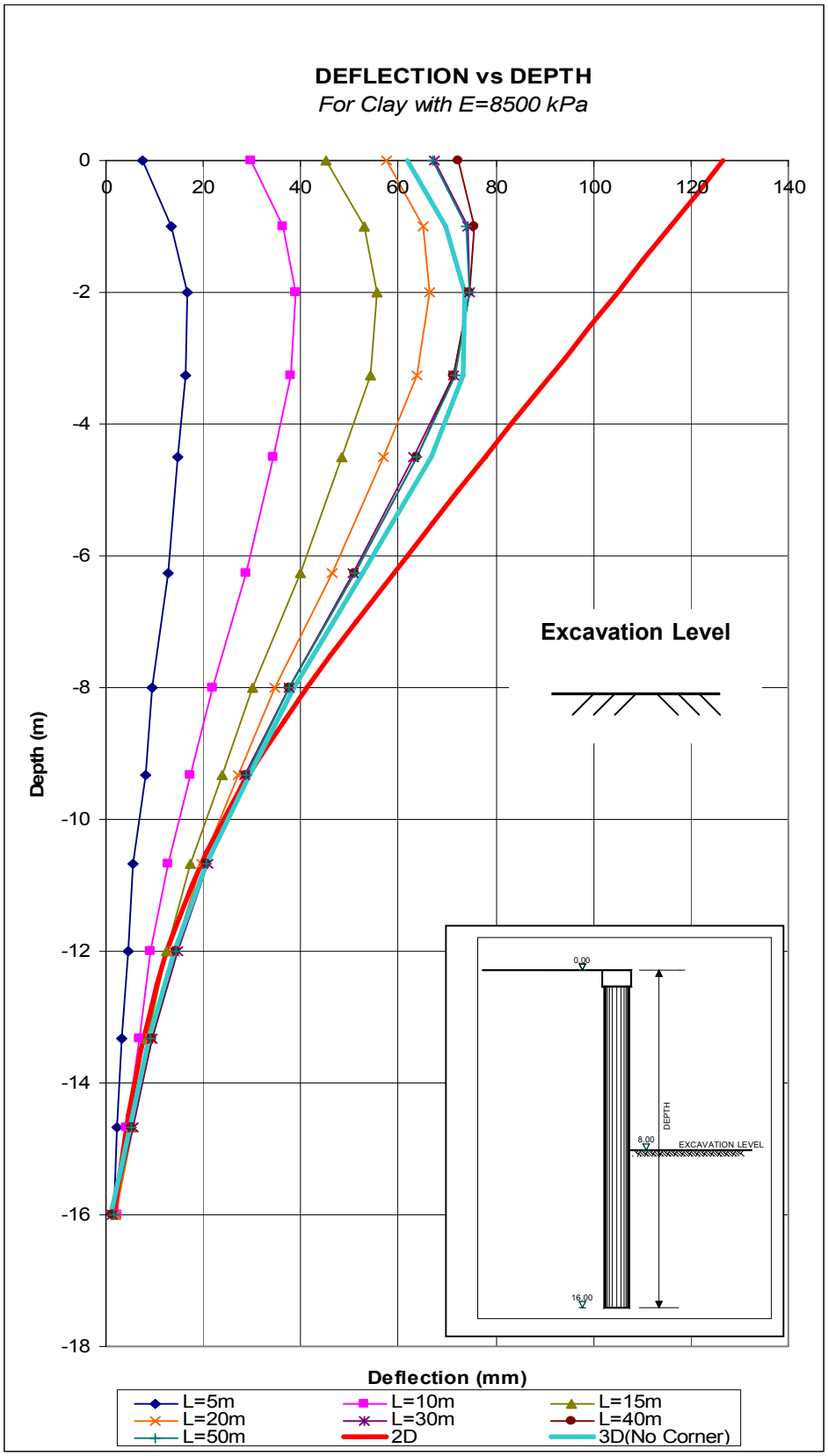

Figure 55. Deflection of cantilever system vs. depth for clay with E=8500kPa

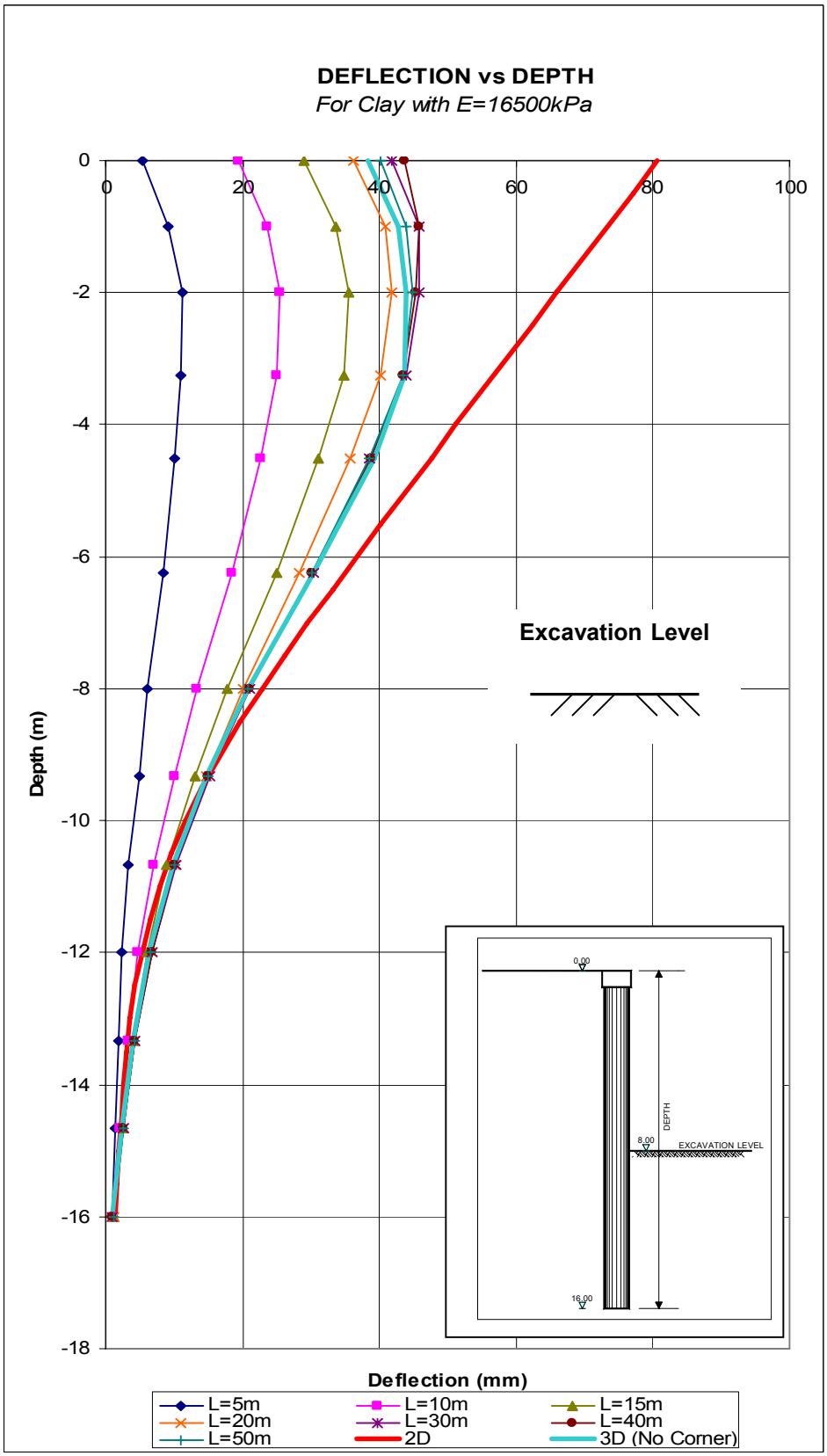

Figure 56. Deflection of cantilever system vs. depth for clay with E=16500kPa

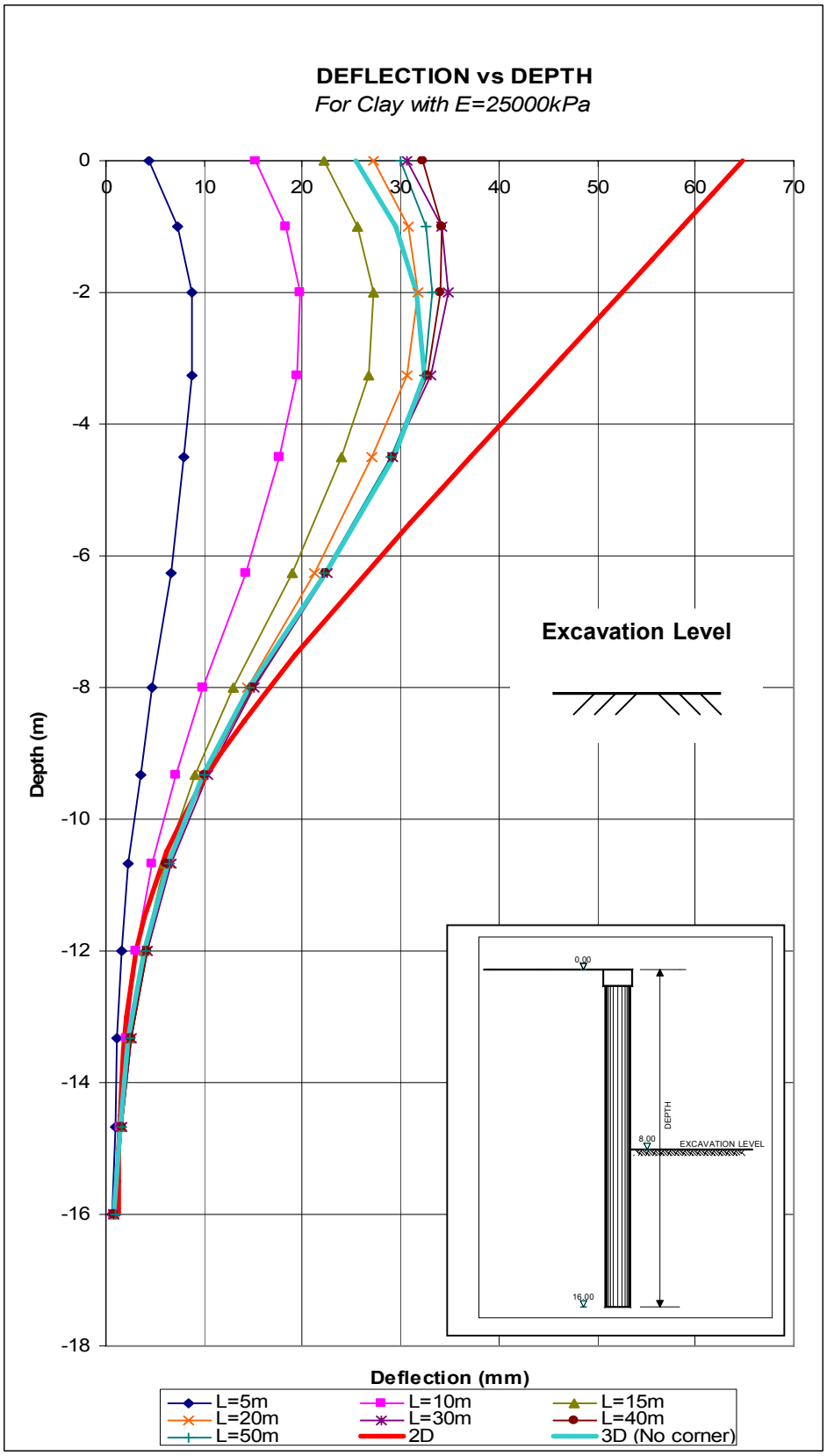

Figure 57. Deflection of cantilever system vs. depth for clay with E=25000kPa

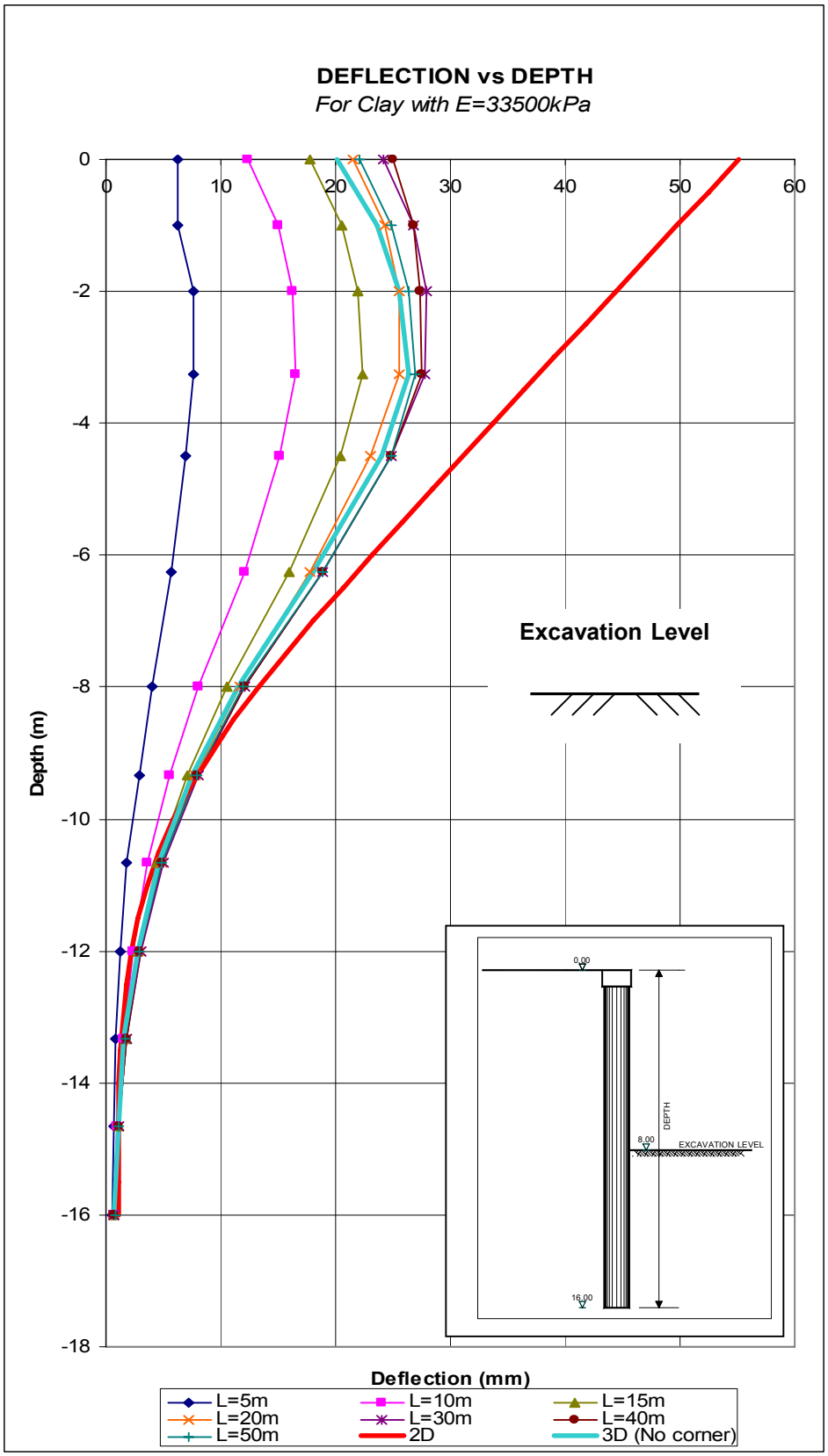

Figure 58. Deflection of cantilever system vs. depth for clay with E=33500kPa

In order to describe deflection behavior of a wall section, Deflection / Maximum Deflection ratio is used in this study. This ratio is the ratio of maximum wall displacement of a section to maximum wall displacement of in-situ wall.

‘’Maximum deflection vs. distance from the corner’’ and ‘’ ‘Deflection / Maximum Deflection’ vs. distance from the corner’’ plots are shown in Figures 59, 60, respectively. The following results are obtained from these figures;

- As elastic modulus decreases, maximum deflection of the excavation side increases.

- For all elastic modulus values it is found that corner effects on deflections diminish at 20m distance from the corner. After this distance maximum deflections are nearly constant.

- Some uncommon decreases in deflection/maximum deflection ratio are observed after 30m distance from the corner. It is predicted that these decreases are a result of mesh generation process and sensitivity of the program.

- For the same distance from the corner, as elastic modulus increase, deflection over maximum deflection ratio increase slightly. Average ratios for various distances are as follows;

  Distance from the corner; 5m → 0.25
  Distance from the corner; 10m → 0.55
  Distance from the corner; 15m → 0.77
  Distance from the corner; 20m → 0.90
  Distance from the corner; 30m → 1.00
  Distance from the corner; 40m → 1.00
  Distance from the corner; 50m → 1.00

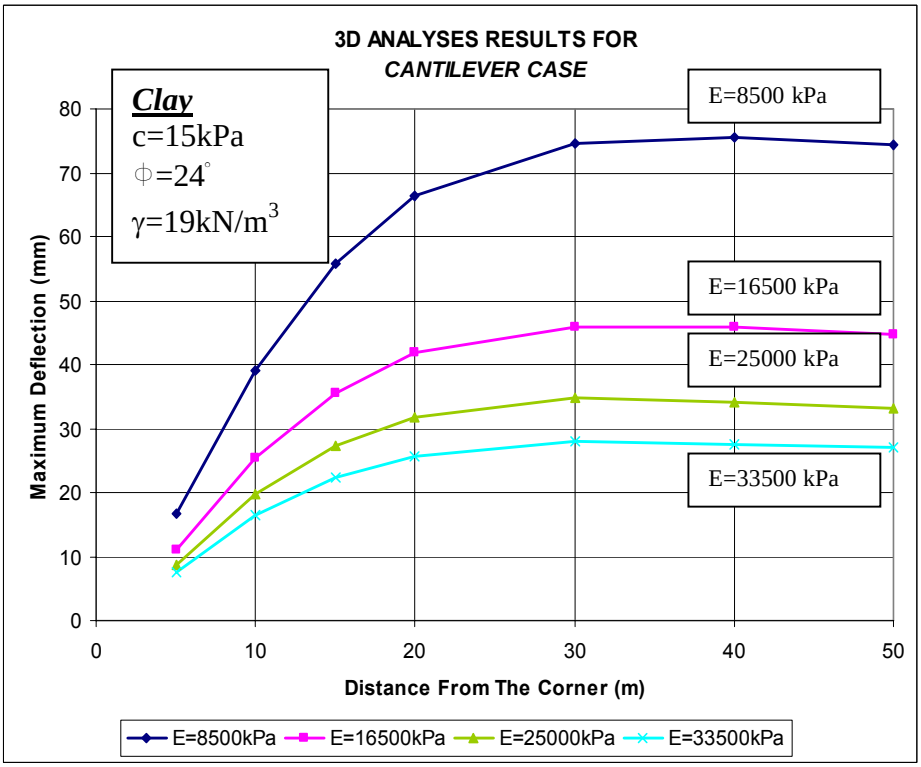

Figure 59. Maximum deflections vs. distance from the corner for cantilever case in 3D analyses

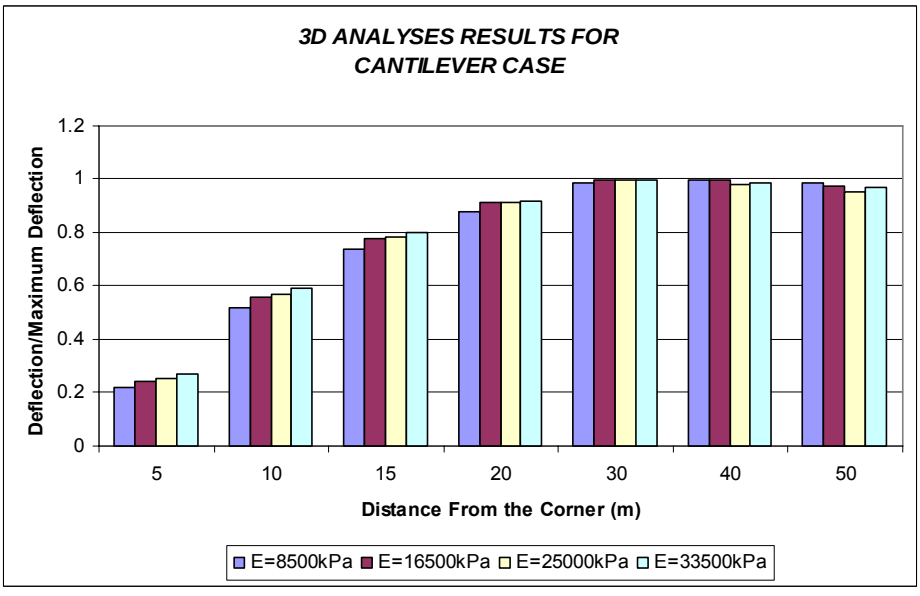

Figure 60. 'Deflection / Maximum Deflection ratios vs. distance from the corner for cantilever case in 3D analyses

Beside deflection, moments for different cross sections of excavation side are also studied. Moment vs. depth graphs are shown in Figures 61, 62, 63, 64. Moment diagrams are drawn for four different sections;

A-A Section: Distance from the corner = 7m
B-B Section: Distance from the corner = 21m
C-C Section: Distance from the corner = 35m
D-D Section: Distance from the corner = 50m

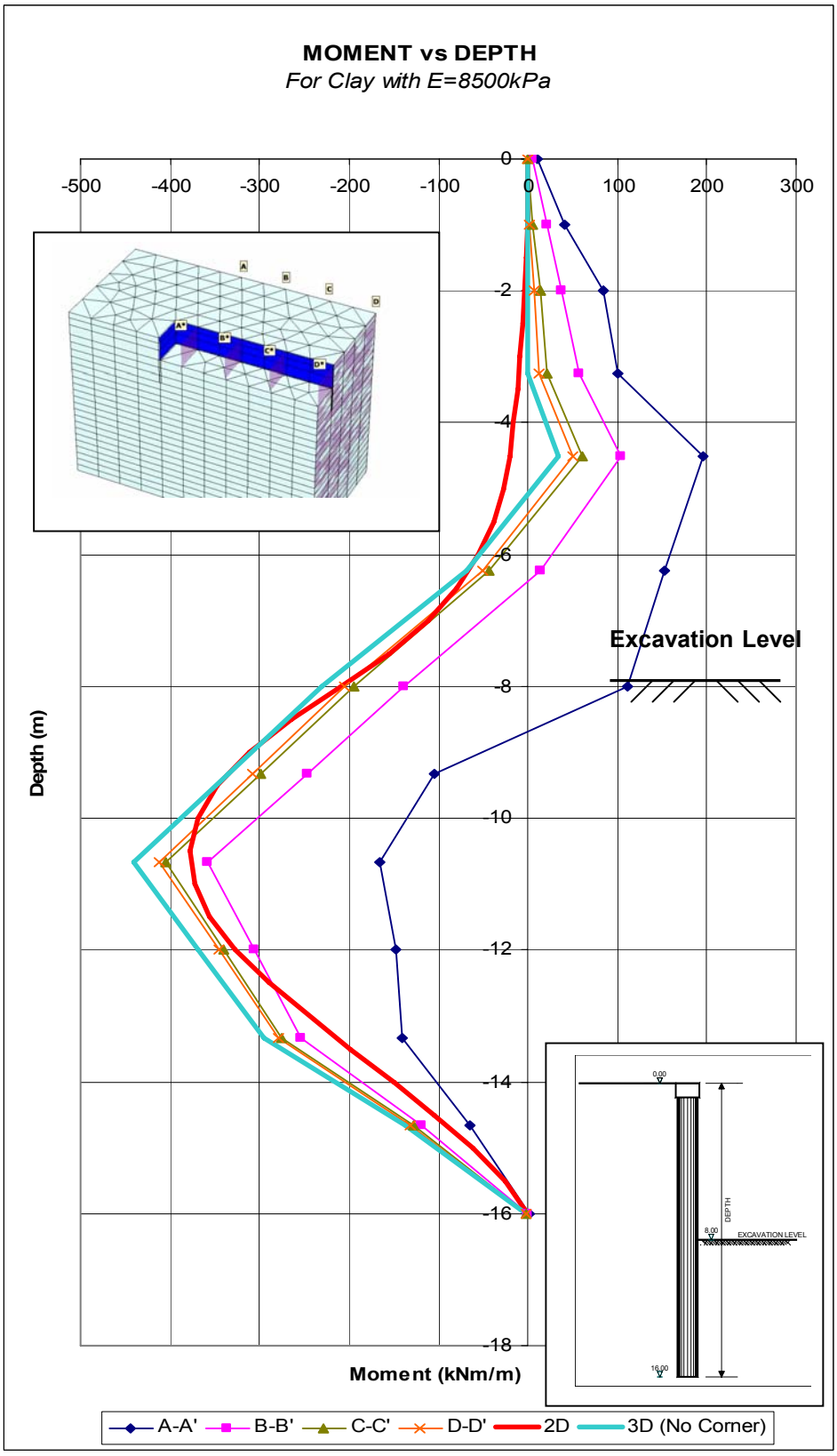

Figure 61. Moment of cantilever system vs. depth for clay with E=8500kPa

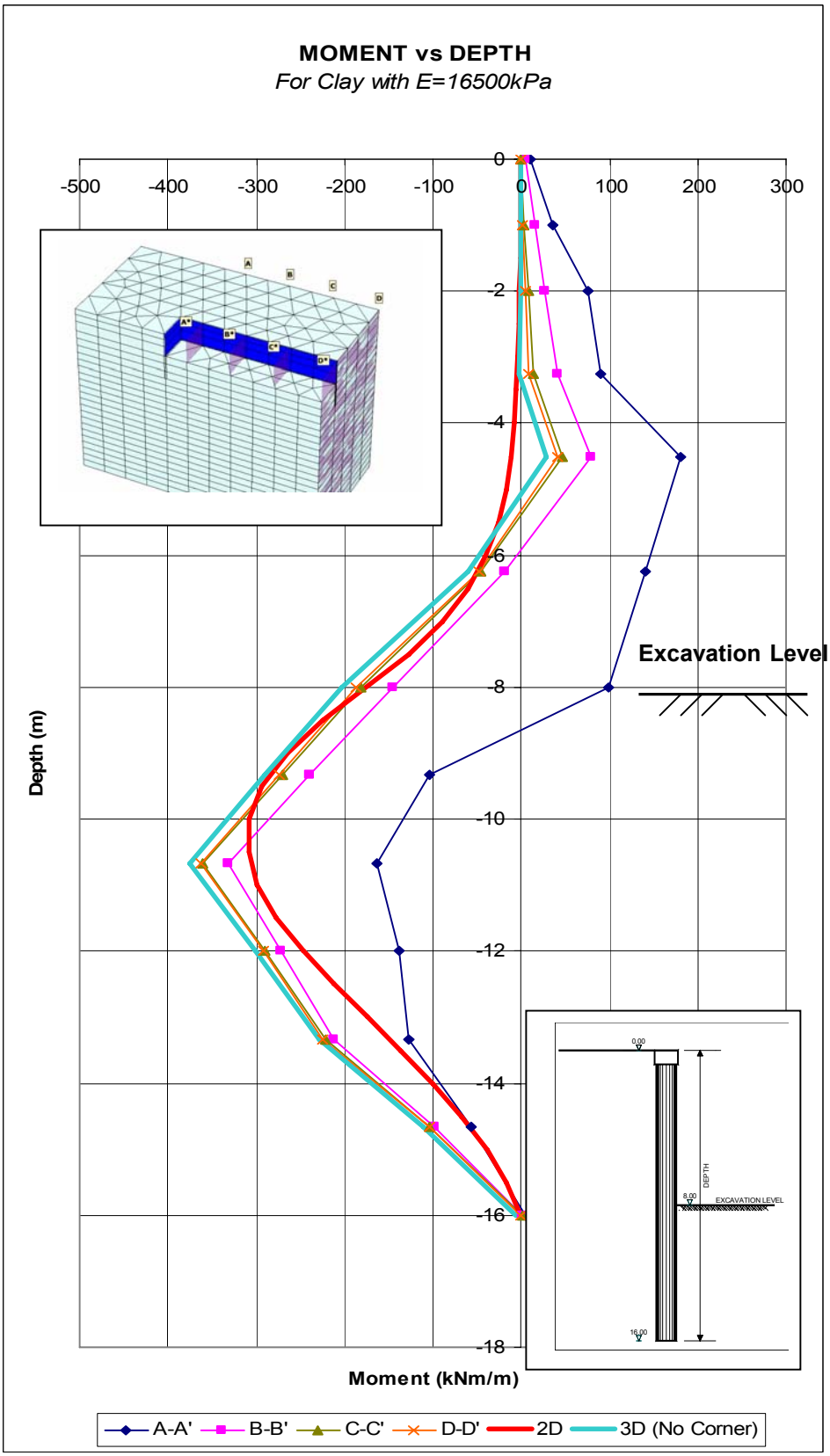

Figure 62. Moment of cantilever system vs. depth for clay with E=16500kPa

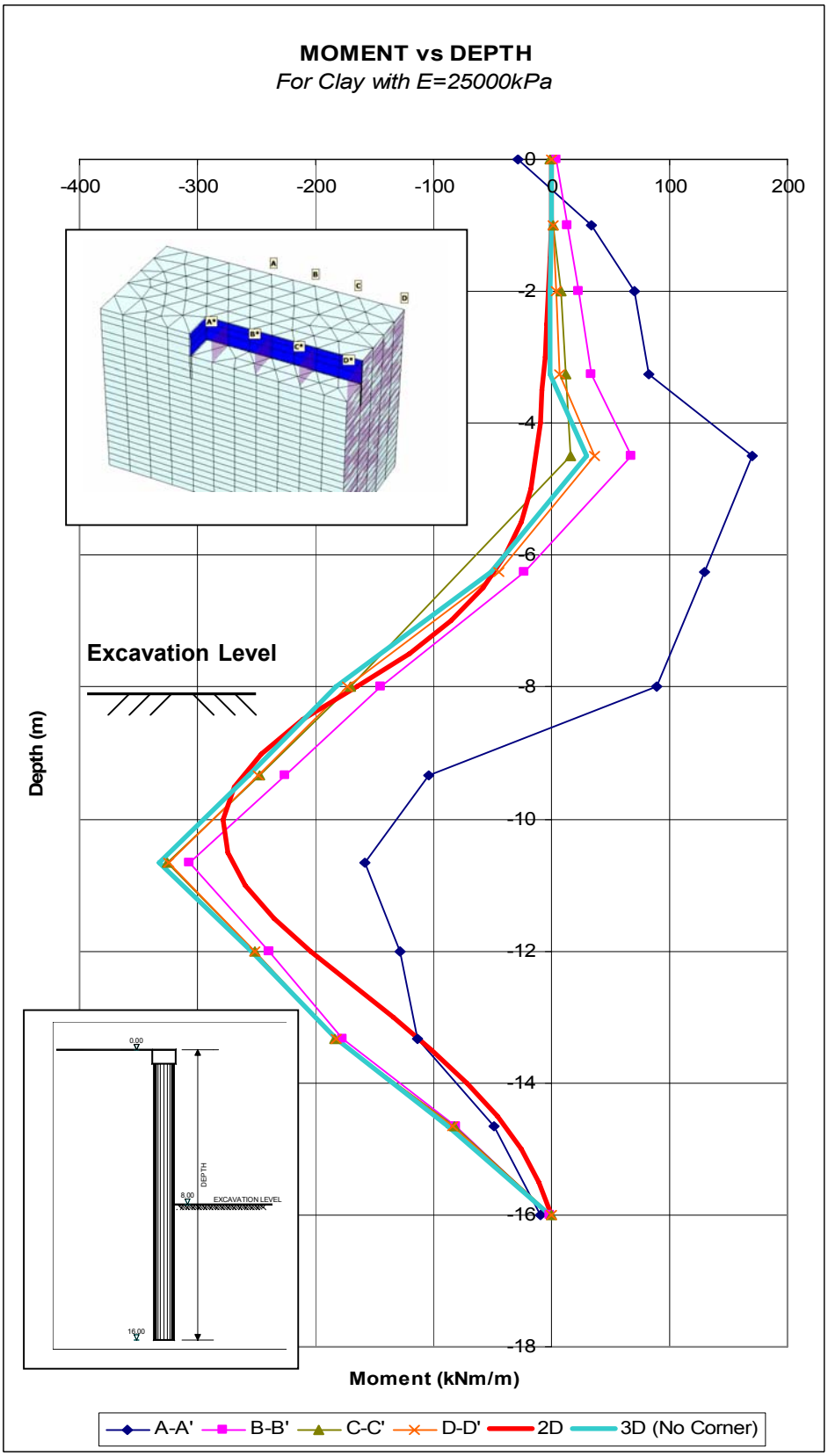

Figure 63. Moment of cantilever system vs. depth for clay with E=25000kPa

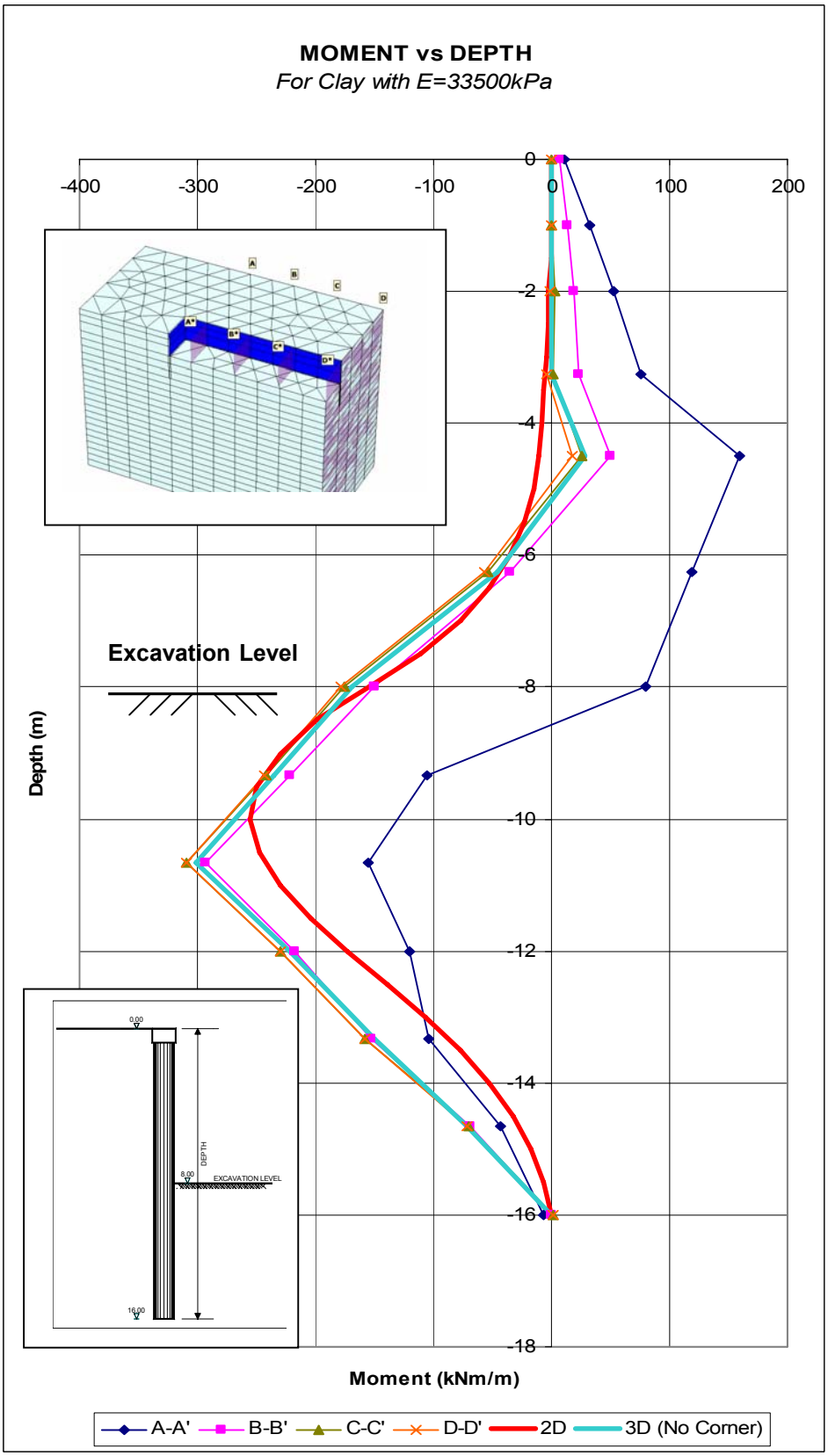

Figure 64. Moment of cantilever system vs. depth for clay with E=33500kPa

Following results are obtained;

- Two types of moment diagrams are observed from the analyses. Typical appearance of observed moment diagrams are demonstrated in Figure 65.

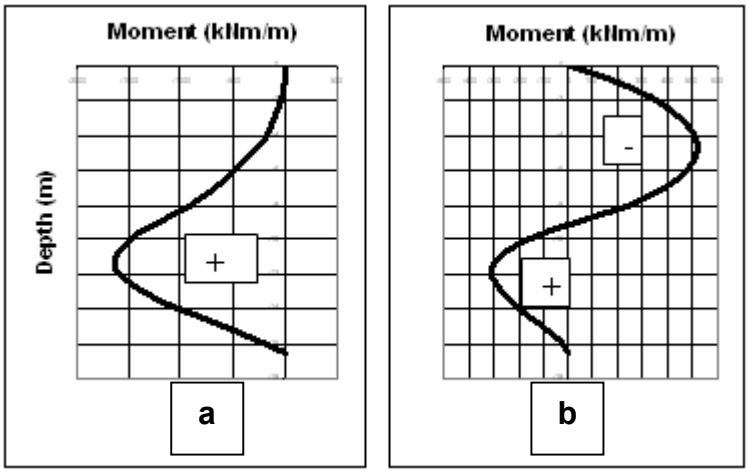

Figure 65. Observed moment distribution patterns from the analyses

In Type-a, moment sign (+) is constant. On the other hand, in Type-b, moment sign changes through the pile. Above excavation level; minus sign, below excavation level plus sign is observed. Plus sign is used to define the moment toward retained soil side; on the other hand minus sign is used for defining the moment toward excavation side. It should be noted that Type-b is a typical moment diagram of in-situ walls supported by struts and Type-b is typical for unsupported / cantilever walls.

- <u>Comparisons of various sections taken from 3D with corner analyses;</u>

  - In all sections, moment modes are alike Type-b; above excavation level minus sign, below excavation level plus sign is observed.

  - As distance from the corner increase, absolute moment value of minus sign part decrease, and absolute moment value of plus sign part increase. So that as distance from corner increase, moment type mode is getting similar to Type-a.

- Corner effect is observed at A-A (Distance from corner: 7m) and B-B (distance from corner: 14m) sections. After B-B section moment values are nearly constant.

- Comparisons of 3D with and without corner analyses;

  Moment values of 3D without corner analyses are similar to moment values of C-C (distance from corner: 21m) and D-D (distance from corner: 50m) sections.

- Comparisons of 3D without corner and plane strain analyses;

  Moment diagrams obtained from plane strain analyses are similar with Type-a. Maximum moments of plane strain analyses are 45-65 kNm/m smaller than the maximum values of 3D without corner analyses.

It is observed that as elastic modulus increases, maximum moment decrease as shown in Figure 66.

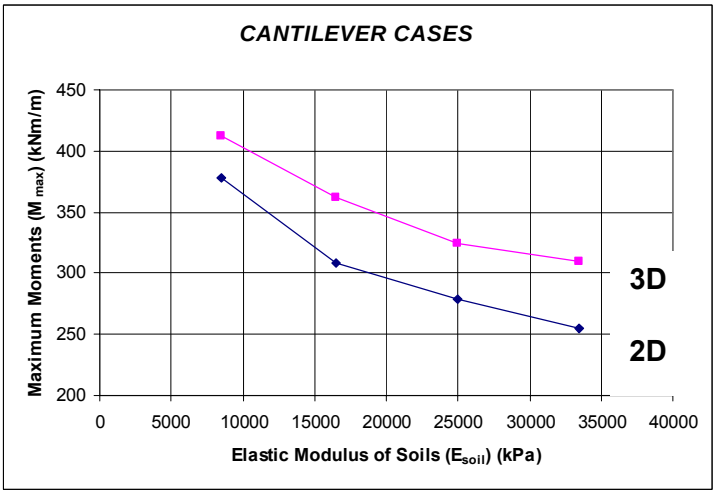

Figure 66. Maximum moments vs. elastic modulus of soils for cantilever case

Difference between maximum moment of A-A (7m from the corner) and maximum moment of D-D (50m from the corner) sections decrease, as elastic modulus of soil increase as shown in Figure 67. In other words, corner effect on magnitude moment decreases as elastic modulus of soil increases.

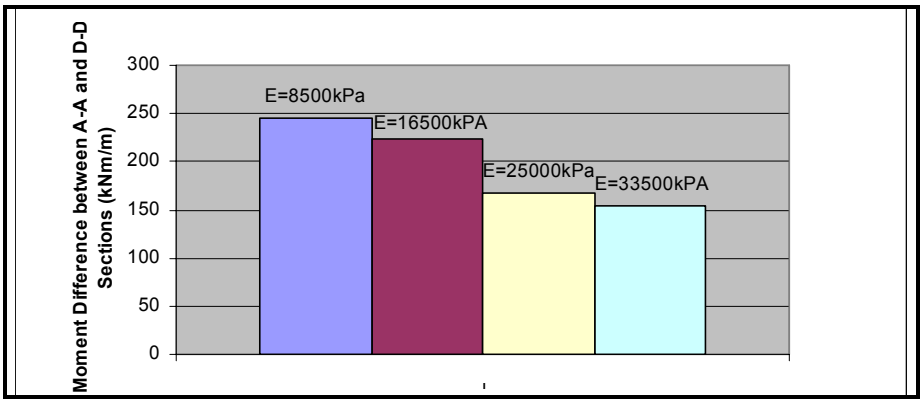

Figure 67. Difference between maximum moments of A-A and D-D Sections for cantilever case

For all elastic modulis of soils; maximum moments increase as distance from the corner increase up to 20m distance from the corner. After this distance moment values become nearly constant, as shown in Figure 68.

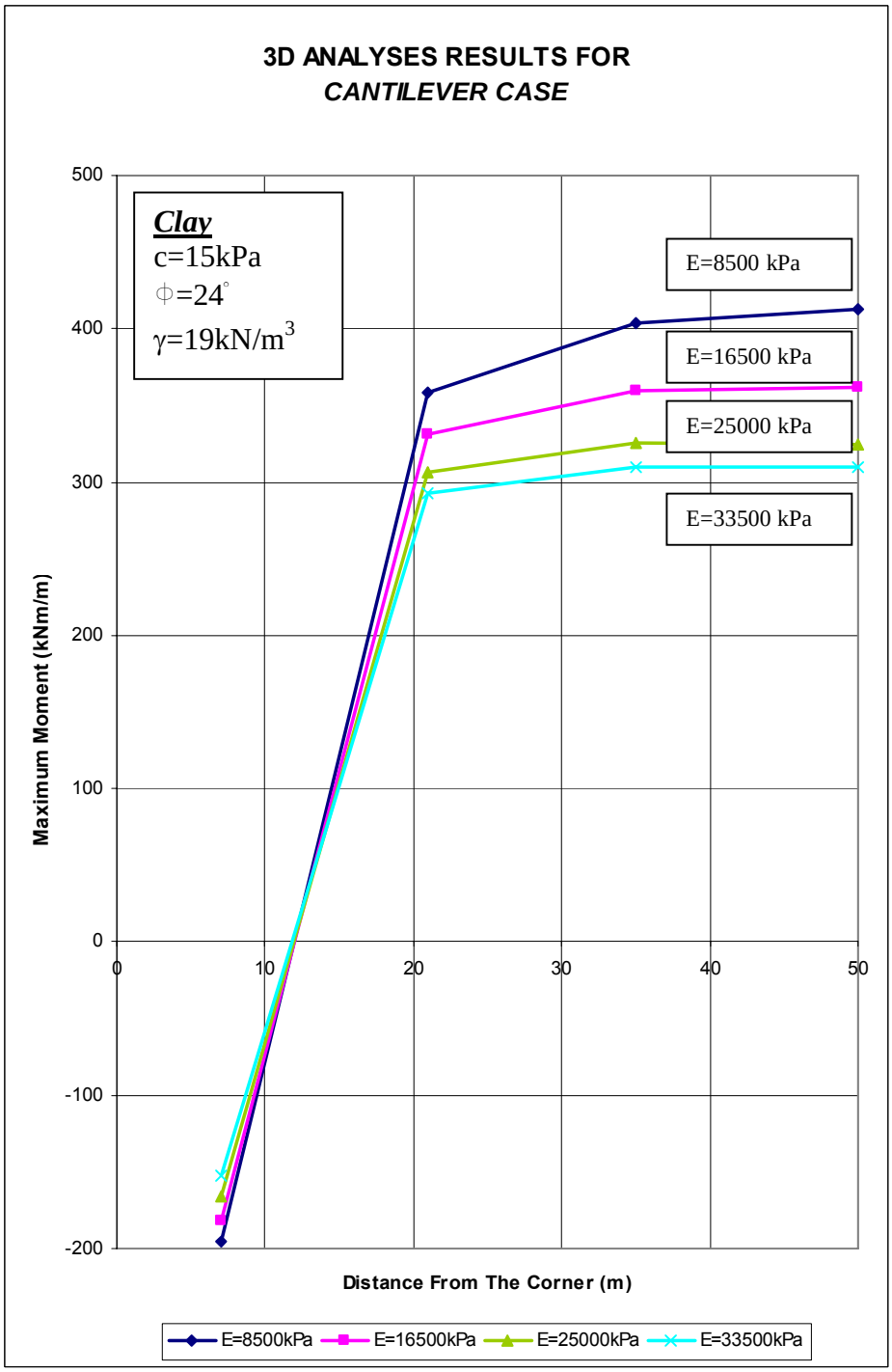

Figure 68. Maximum moment vs. distance from the corner for cantilever case

In addition to moments and deflections, effective horizontal soil stresses on the soil side are also examined. Calculated effective horizontal stresses are compared with Rankine's active earth pressure envelope and earth pressure at rest theory.

Active Earth Pressure Envelope= $\gamma' z K_A - 2 c' \sqrt{K_A}$ where;

$K_A = \tan^2(45° - \Phi'/2)$

γ': Drained unit weight of the soil =19kN/m^3

z: Depth (m)

c': Drained cohesion =15kPa

Φ': Drained friction angle =24°

So Active earth pressure (AEP);

At z=0.0m → AEP=19 * 0 * 0.4217 * (2 * 15 * √0.4217)

→ AEP ≅ -19.5 kPa

At z=2.43m → AEP=19 * 2.43 * 0.4217 – (2 * 15 * √0.4217)

→ AEP ≅ 0 kPa

At z=16.0m → AEP=19 * 16 * 0.4217 – (2 * 10 * √0.4217)

→ AEP ≅ 109 kPa

As negative lateral pressure is not possible in soil structure interaction behavior, negative pressures are omitted and negative pressures are assumed to be zero in lateral earth pressure diagrams.

At rest earth pressure envelope= $\gamma' z K_o$

$K_o = 1 - \sin \Phi'$

γ': Drained unit weight of the soil =19kN/m^3

z : Depth (m)

Φ': Drained friction angle =24°

So At Rest Earth Pressure (REP);

At z=0.0m → REP= 19 * 0 * 0.593

→ REP ≅ 0kPa

At z=16.0m → REP= 19 * 16 * 0.593

→ REP ≅ 180 kPa

Effective horizontal stresses obtained from 3D and plane strain analyses are demonstrated in Figures 69, 70, 71, 72. Effective horizontal stress diagrams are drawn for four different sections;

A-A Section: Distance from the corner = 7m
B-B Section: Distance from the corner = 21m
C-C Section: Distance from the corner = 35m
D-D Section: Distance from the corner = 50m

Following results are obtained;

- According to 3D with corner analyses results, it can be said that effective horizontal stresses for different sections are similar.

- When the results of plane strain and 3D with corner analyses are compared, it is seen that effective horizontal stresses in 3D analyses are 10-20kPa bigger than plane strain ones.

- Below comparisons between theories and results of analyses are obtained;

  Above excavation level: Active approximate stresses above excavation level.

  Below excavation level: Effective horizontal stresses are upper bounded by at rest earth pressures and lower bounded by active earth pressures.

- Similar effective horizontal stresses are obtained for all sections; it shows that there is no significant corner effect on effective horizontal stresses.

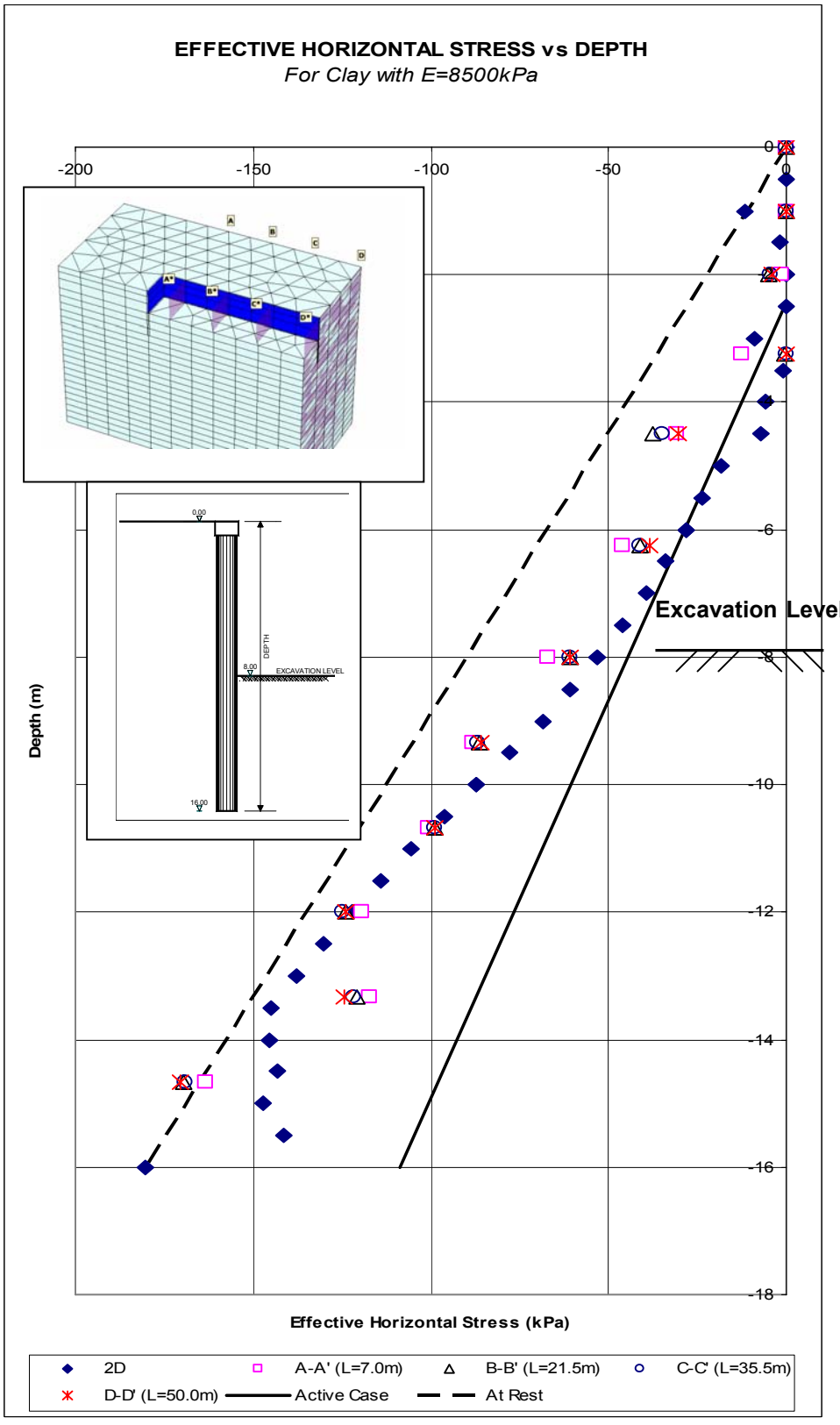

Figure 69. Effective horizontal stresses of cantilever case vs. depth for clay with E=8500kPa

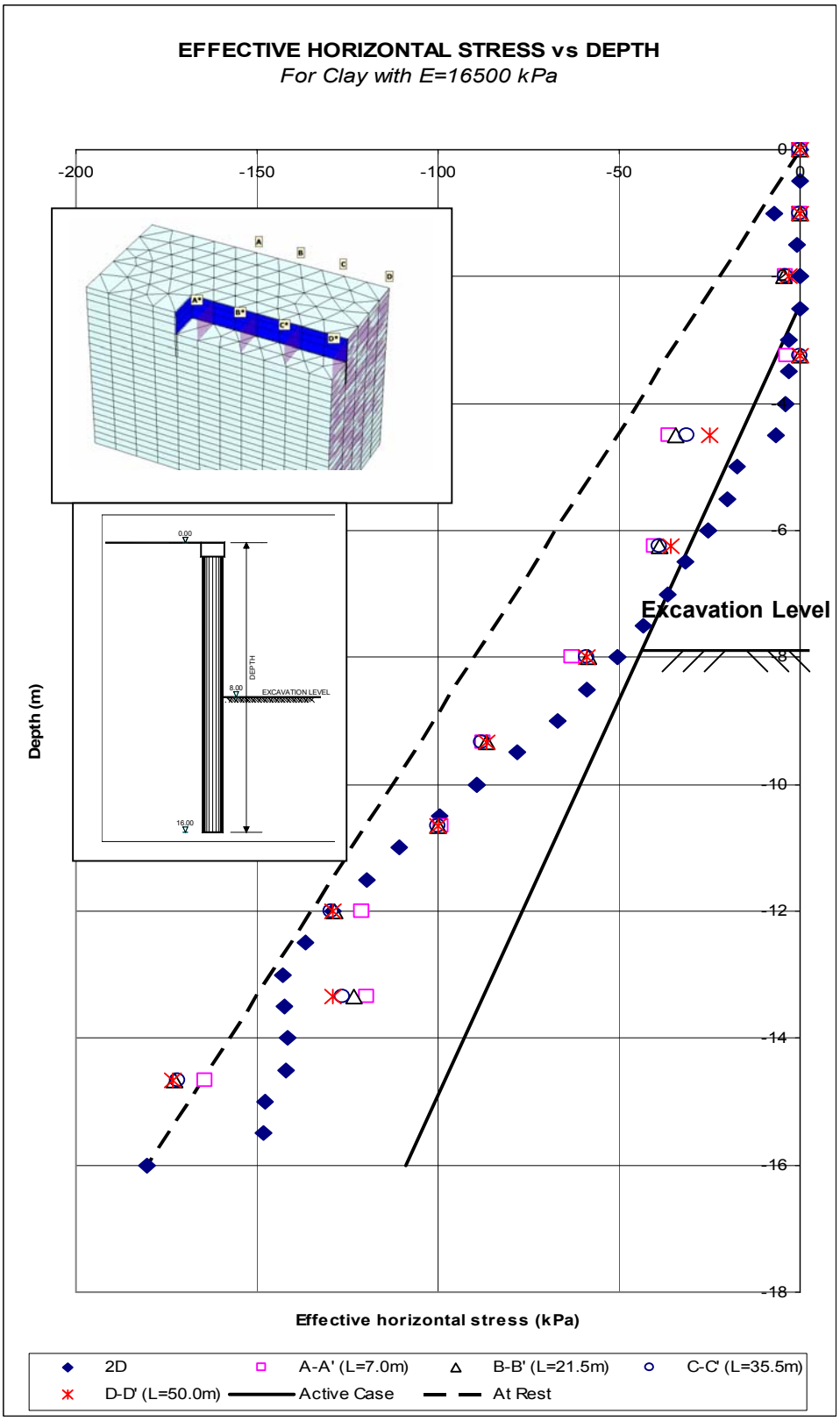

Figure 70. Effective horizontal stresses of cantilever case vs. depth for clay with E=16500kPa

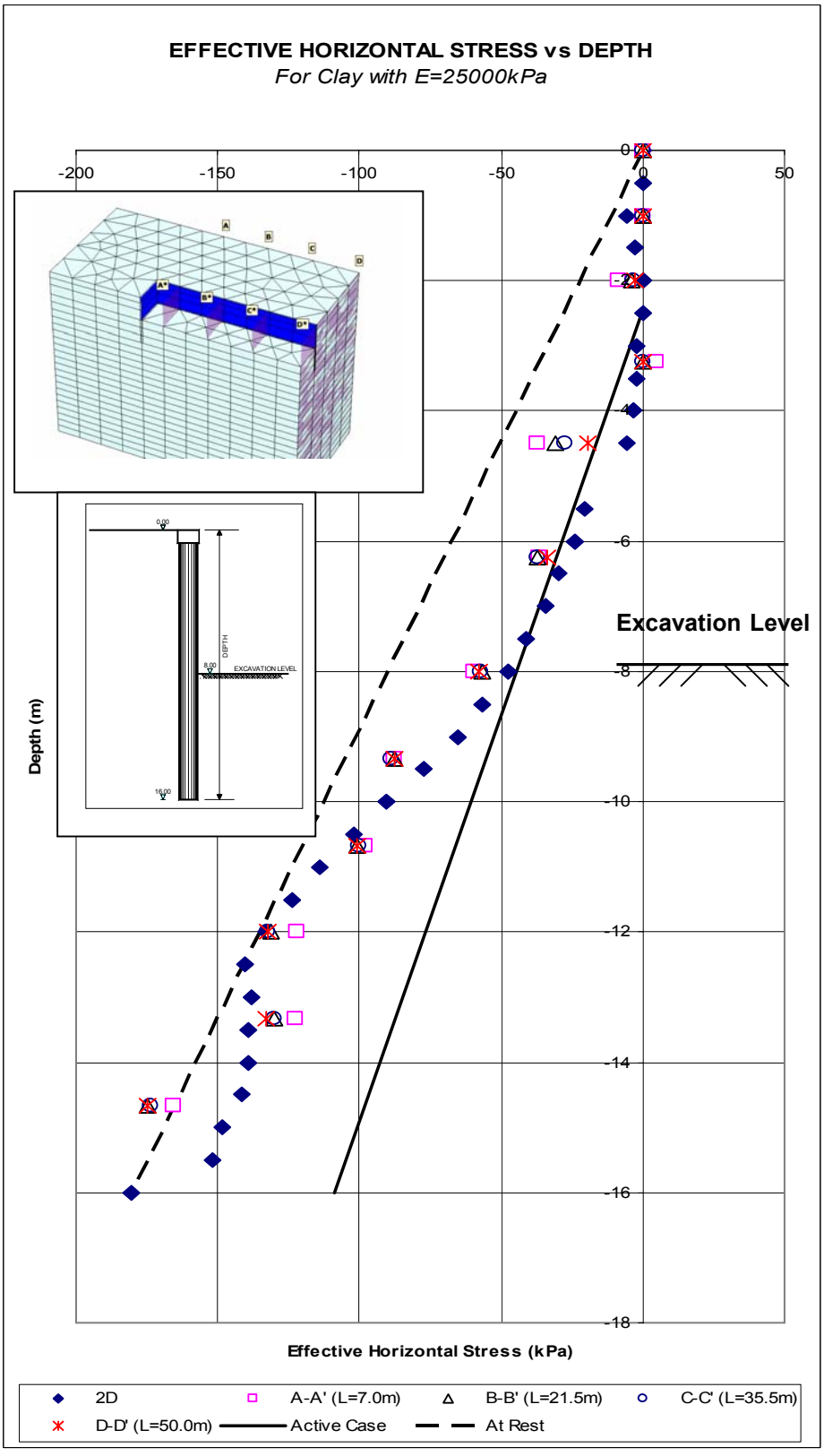

Figure 71. Effective horizontal stresses of cantilever case vs. depth for clay with E=25000kPa

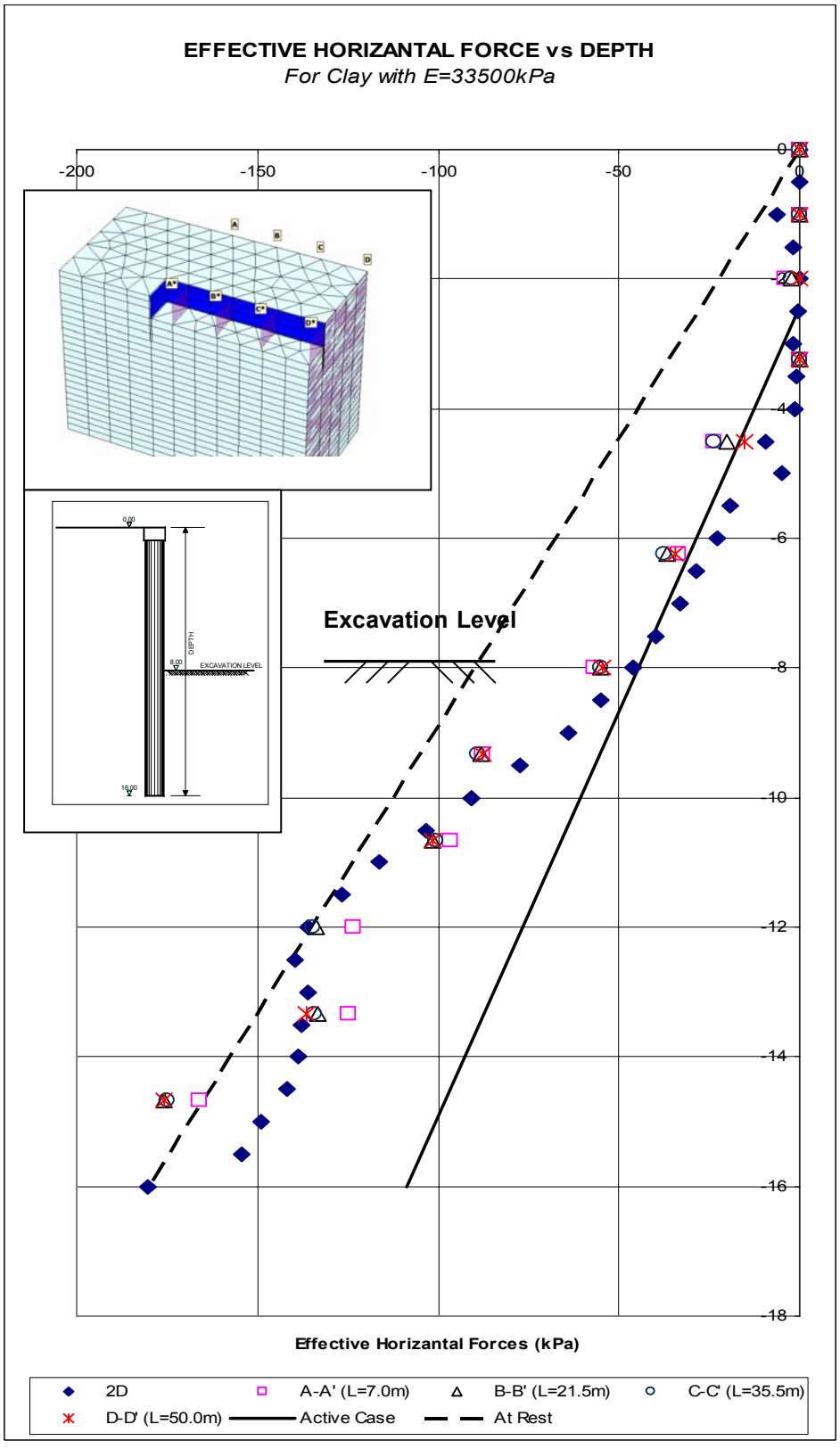

Figure 72. Effective horizontal stresses of cantilever case vs. depth for clay with E=25000kPa

3.5.2. Anchored Wall at One Level Cases

A series of plane strain analyses are performed by changing the prestress values to investigate the deflection behavior of pile wall anchored wall at one level;. This study is performed only for elastic modulus values of 3500, 8500 and 16500kPa. 100 to 250 kN prestresses are applied to anchors and deflection of pile wall are investigated. The finite element meshes used is demonstrated in Figure 73.

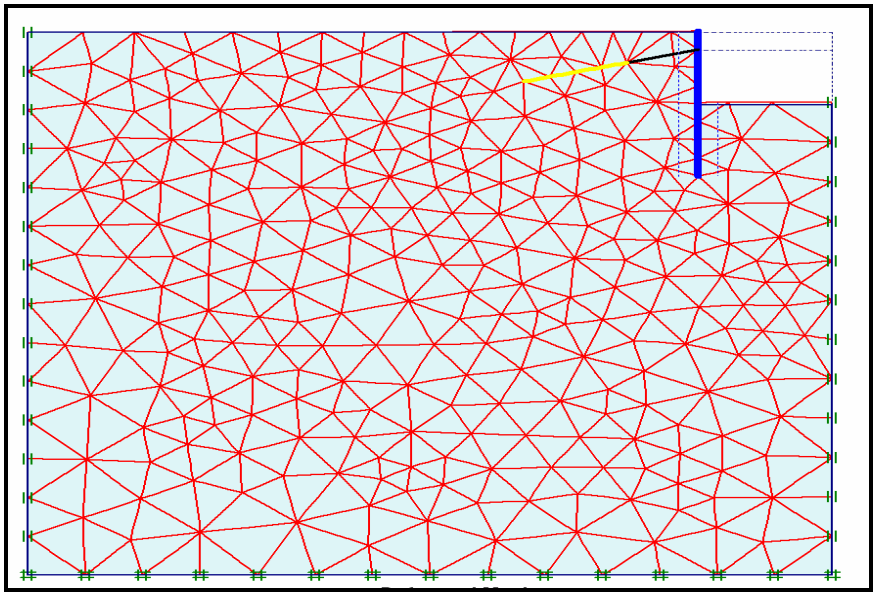

Figure 73. Finite element mesh used in 2D analyses of one layer anchor system

When the top few meters of the pile wall is examined, it is seen that the deflection is toward retained soil side (see Figures 74, 75, 76). This reverse movement is a result of prestress loads applied to the anchors. As the prestressing force increase, movement toward retained soil side increases. On the other hand, as the elastic modulus values increase, the movement toward retained soil side decreases. To overcome this back movement in plane strain analyses, prestress values were reduced from 250 kN/anchor to 100 kN/anchor but the deformation pattern did not change.

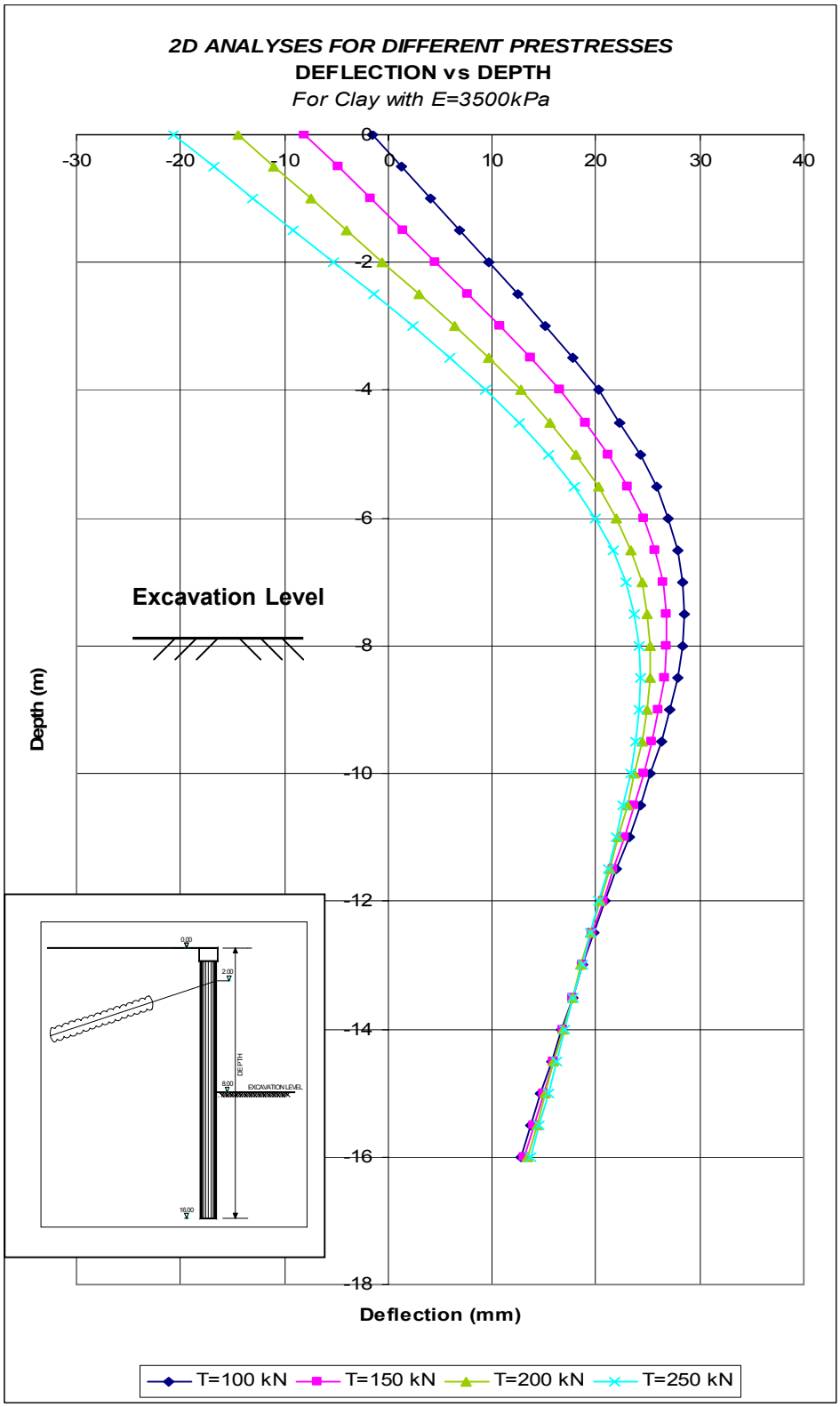

Figure 74. Deflection of anchored wall at one level system vs. depth for various prestresses (clay with E=3500kPa)

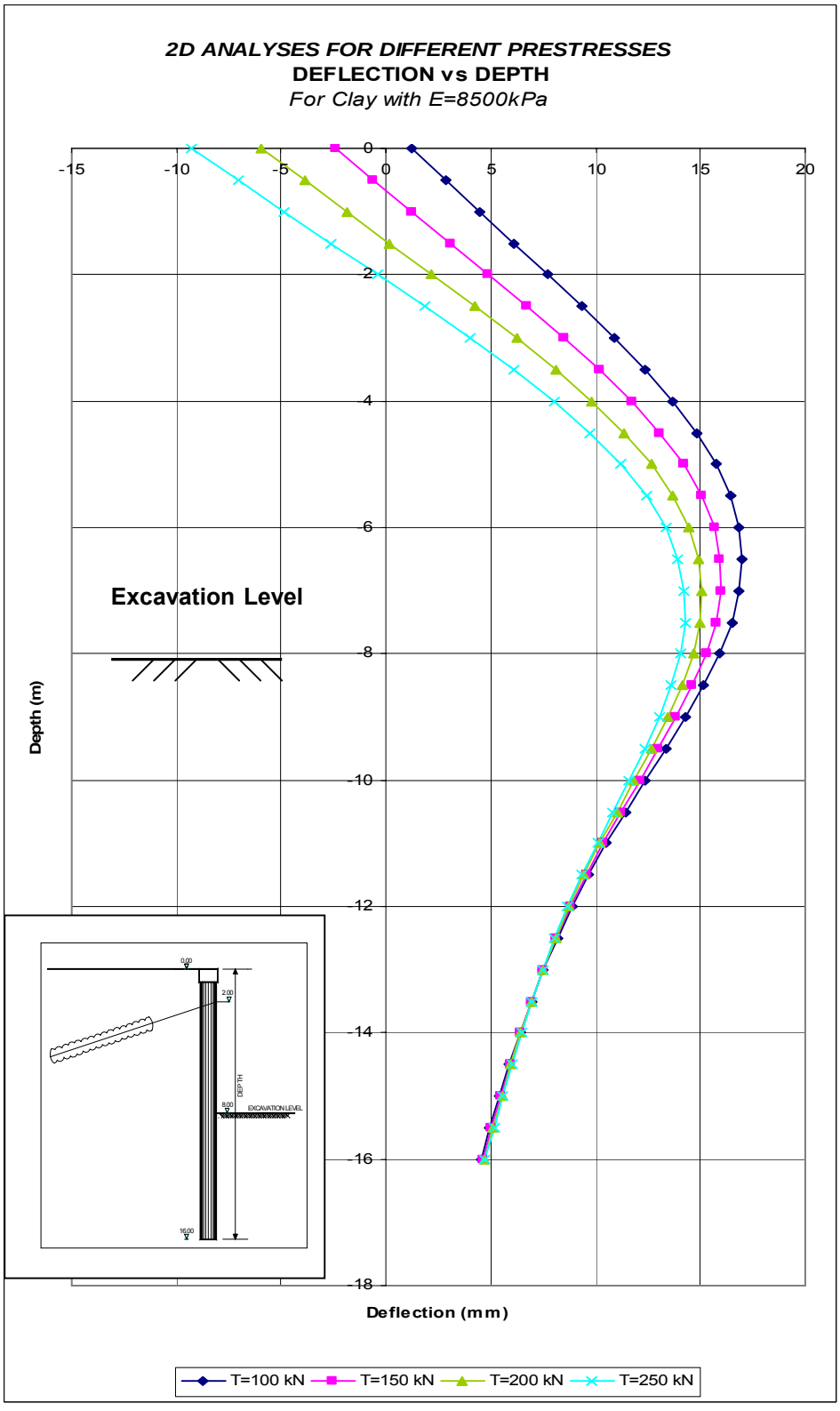

Figure 75. Deflection of anchored wall at one level system vs. depth for various prestresses (clay with E=8500kPa)

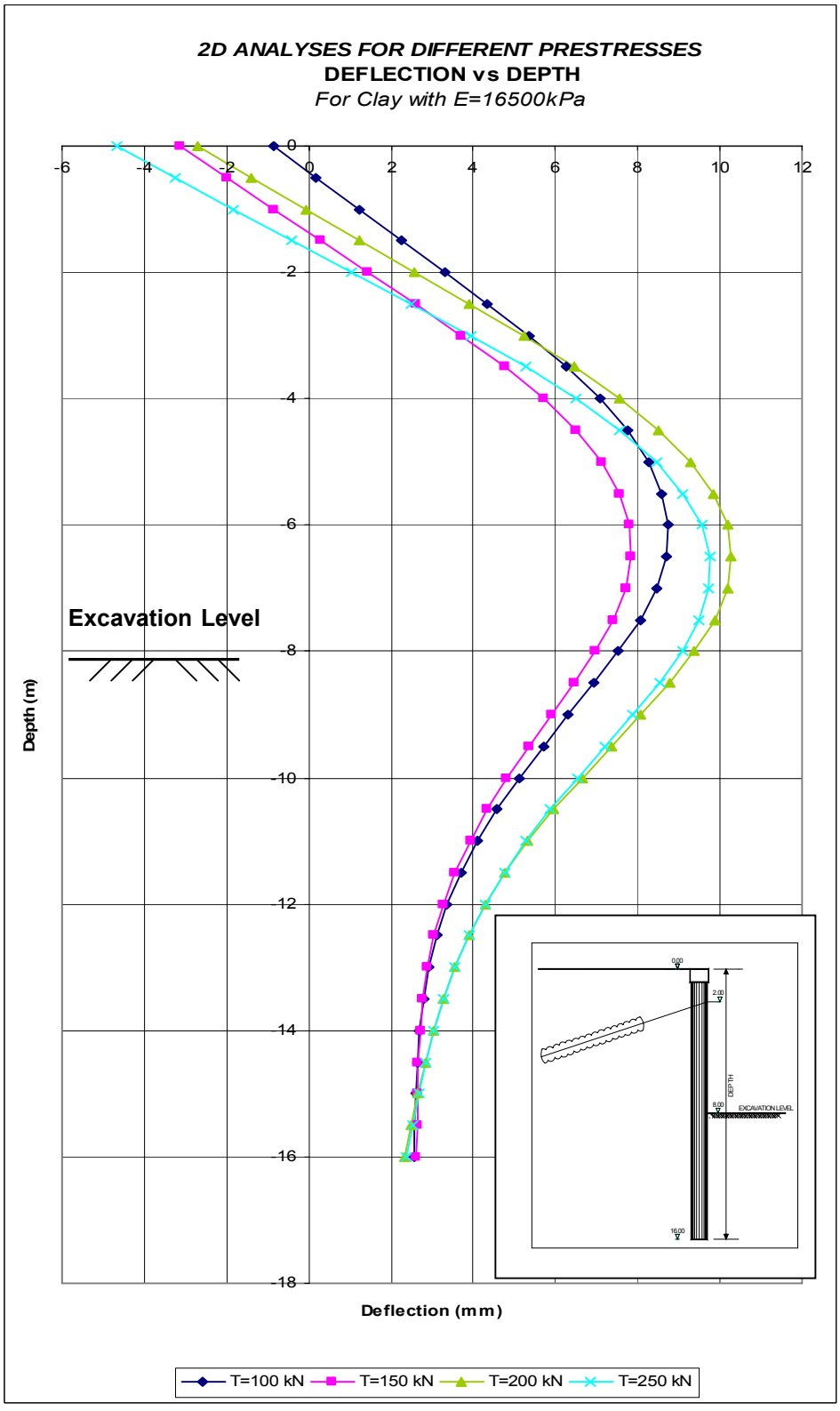

Figure 76. Deflection of anchored wall at one level system vs. depth for various prestresses (clay with E=16500kPa)

Deflection vs. elastic modulus of soil graphs are demonstrated in Figure 77. Following results are obtained;

- As elastic modulus of soil increase, maximum deflection toward retained soil side and toward excavation side decrease.
- As pretension increase, deflection toward retained soil side increase. On the other hand, deflection toward excavation side decreases.

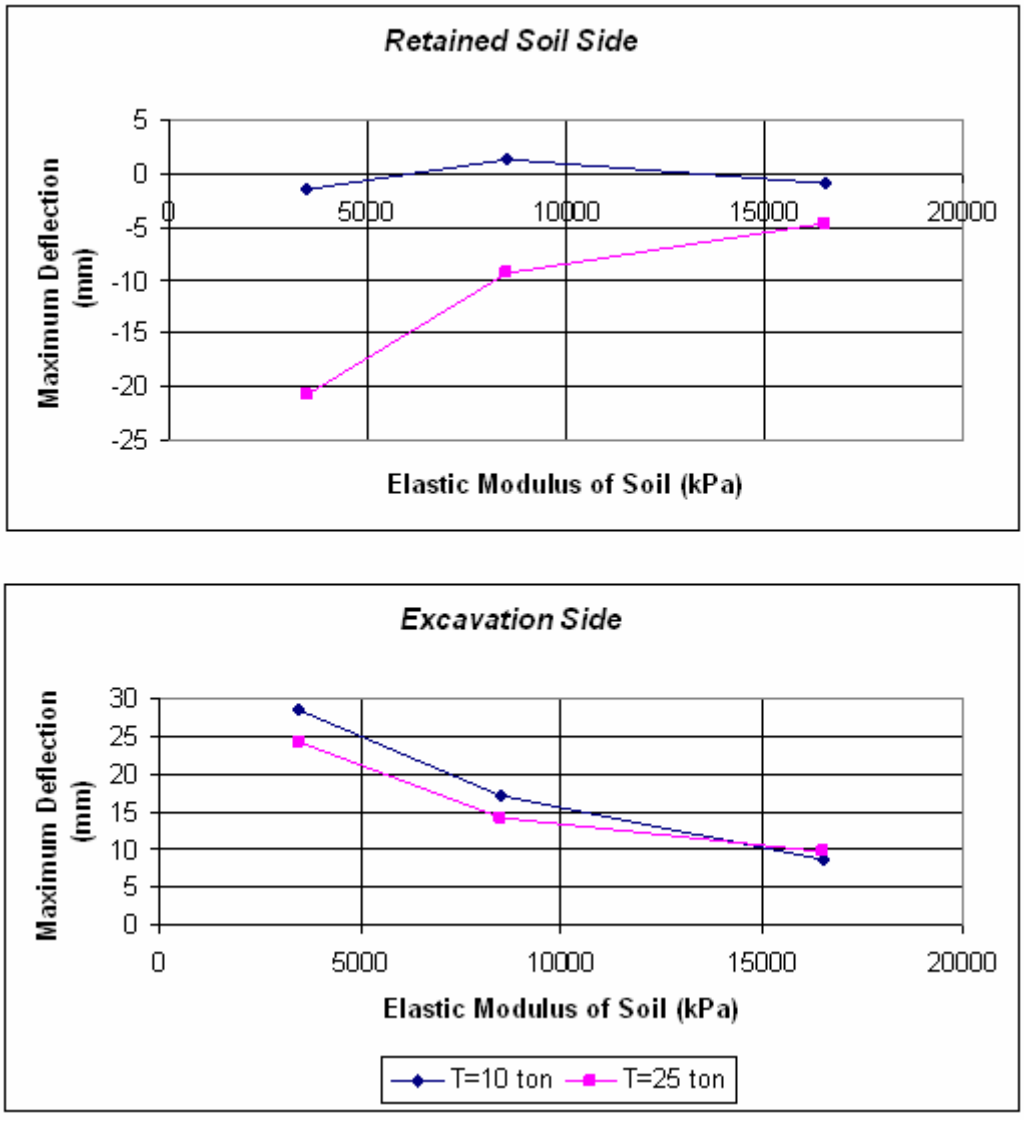

Figure 77. Maximum deflection vs. Elastic modulus of soil for various prestresses

Pile wall anchored wall at one level cases are studied in 3D model for elastic modulus values of 3500, 8500, 16500 and 25000 kPa. The finite element meshes used in 3D analyses with and without corners are demonstrated in Figures 78, 79.

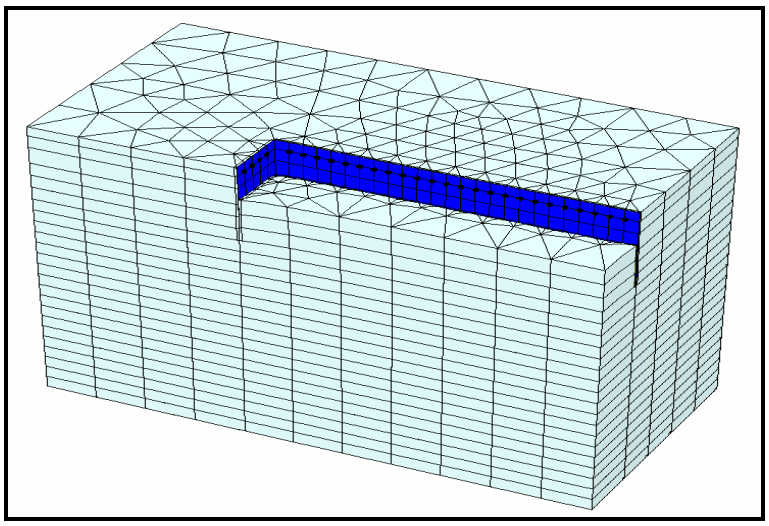

Figure 78. Finite element mesh used in 3D analyses of one layer anchor case

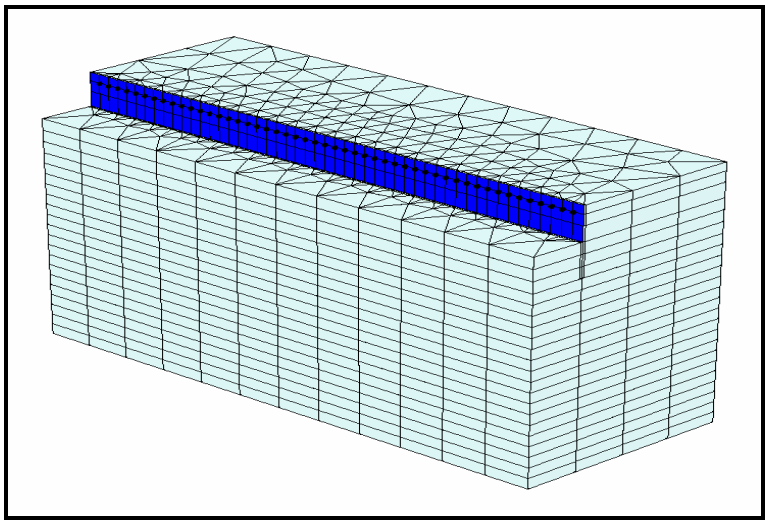

Figure 79. Finite element mesh used in 3D analyses (without corner) of one layer anchor case

Deflection for various sections vs. depth graphs are demonstrated in Figures 80, 81, 82, 83. In 3D analyses 250 kN/anchor prestresses are applied. Even though prestresses as high as 250 kN/anchor are applied, no movement toward the retained soil side is observed for even elastic modulus as small as 3500kPa as shown in Figure 80. Therefore it is concluded that the deformation patterns of plane strain and 3D analyses are different for piles anchored wall at one level. Because of this mode difference plane strain and 3D analyses results are not shown in the same graphs.

Following results are obtained;

- Comparisons of various sections taken from 3D with corner analysis;

  For all elastic modulus values it is seen that corner effects on deflections diminish at 20m distance from the corner. After this distance deflections become nearly constant with increasing distance away from the corner.

- Comparisons of 3D with and without corner analysis;

  After 20m distance from the corner, deflections of 3D with corner analyses match with 3D without corner ones. However it should be noted that, 3D without corner analyses results are 2-5mm smaller than the with corner ones. This may be as a result of mesh generation disparity between models.

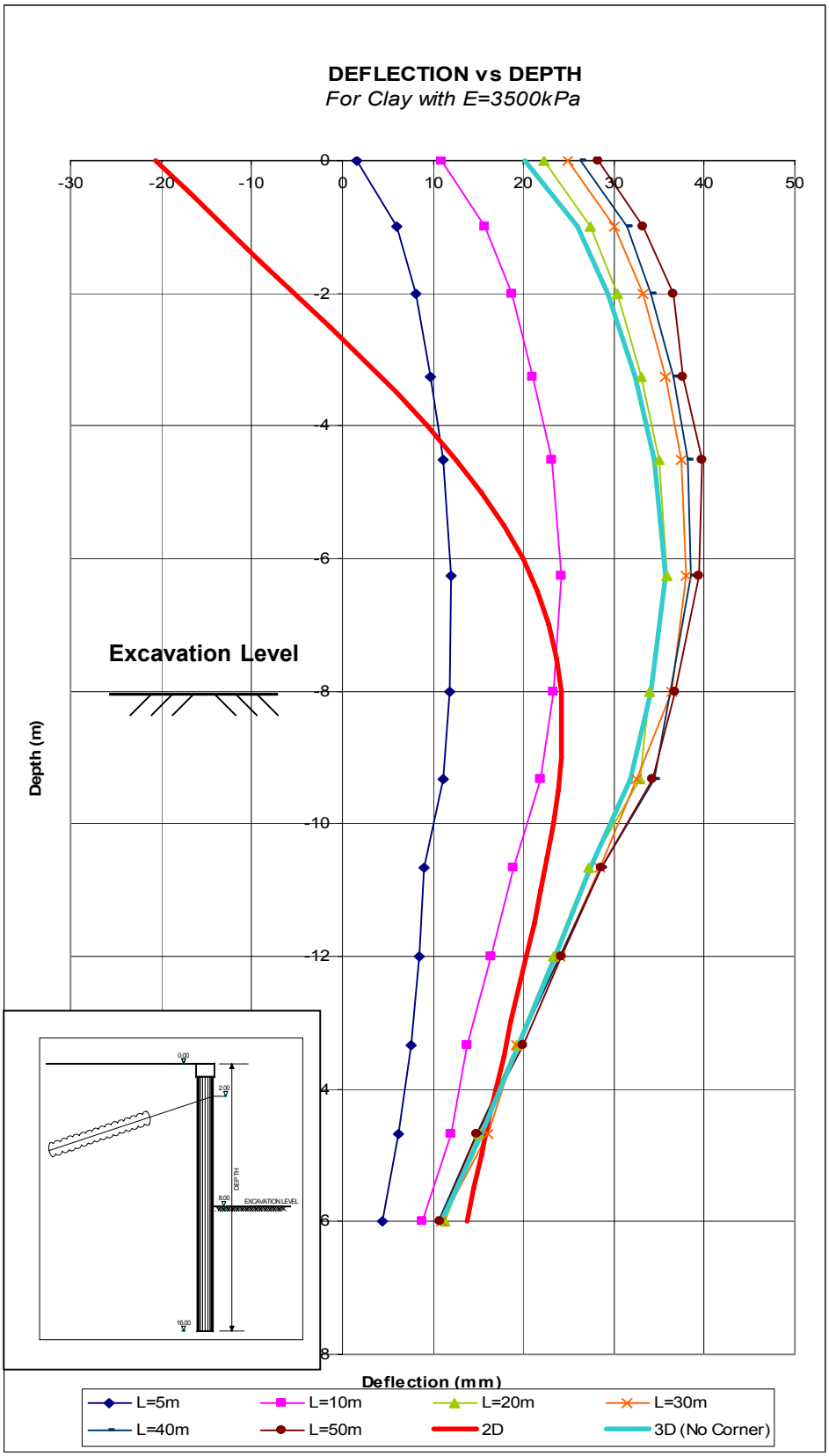

Figure 80. Deflection of anchored wall at one level case vs. depth for clay with E=3500kPa

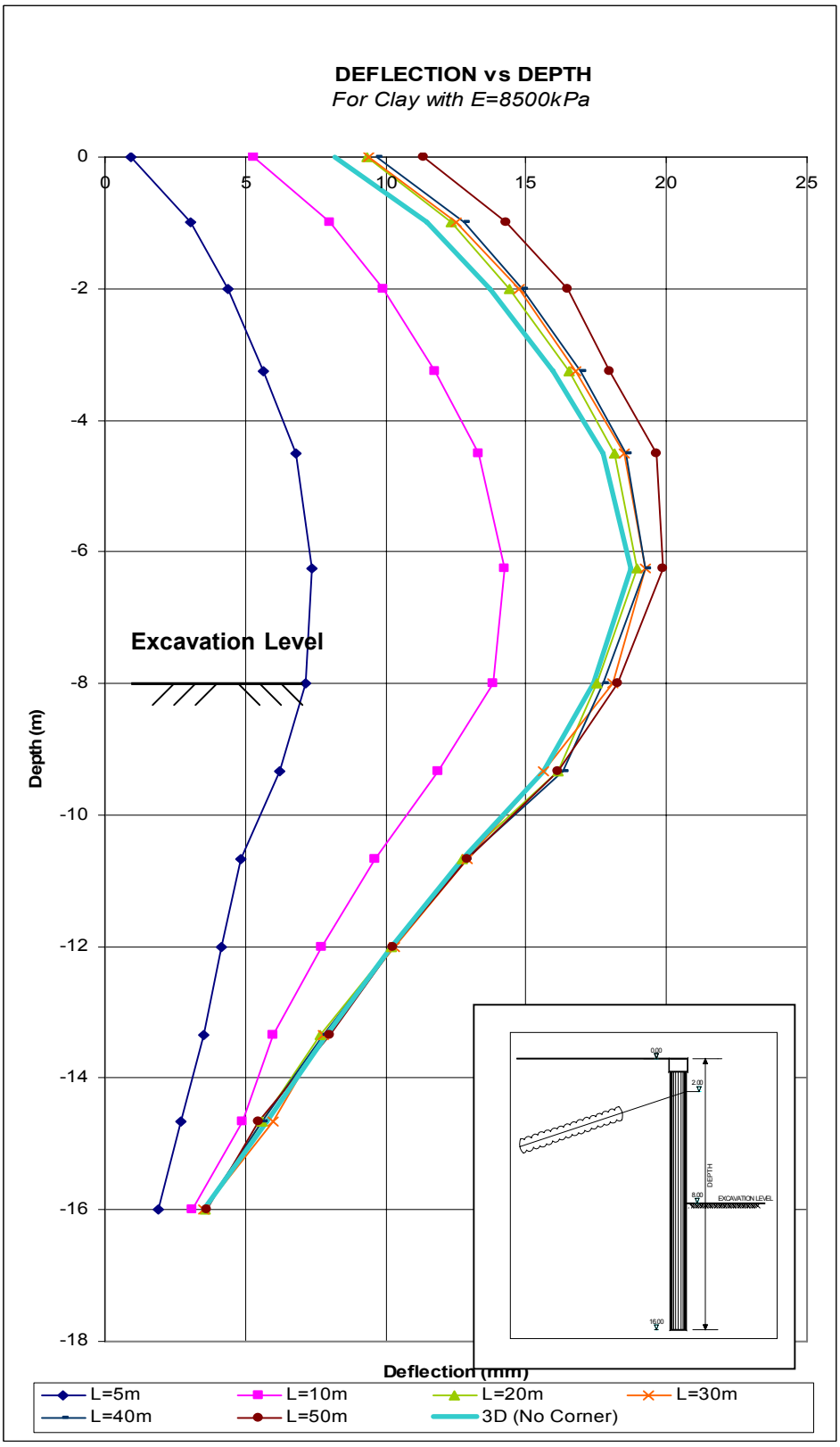

Figure 81. Deflection of anchored wall at one level case vs. depth for clay with E=8500kPa

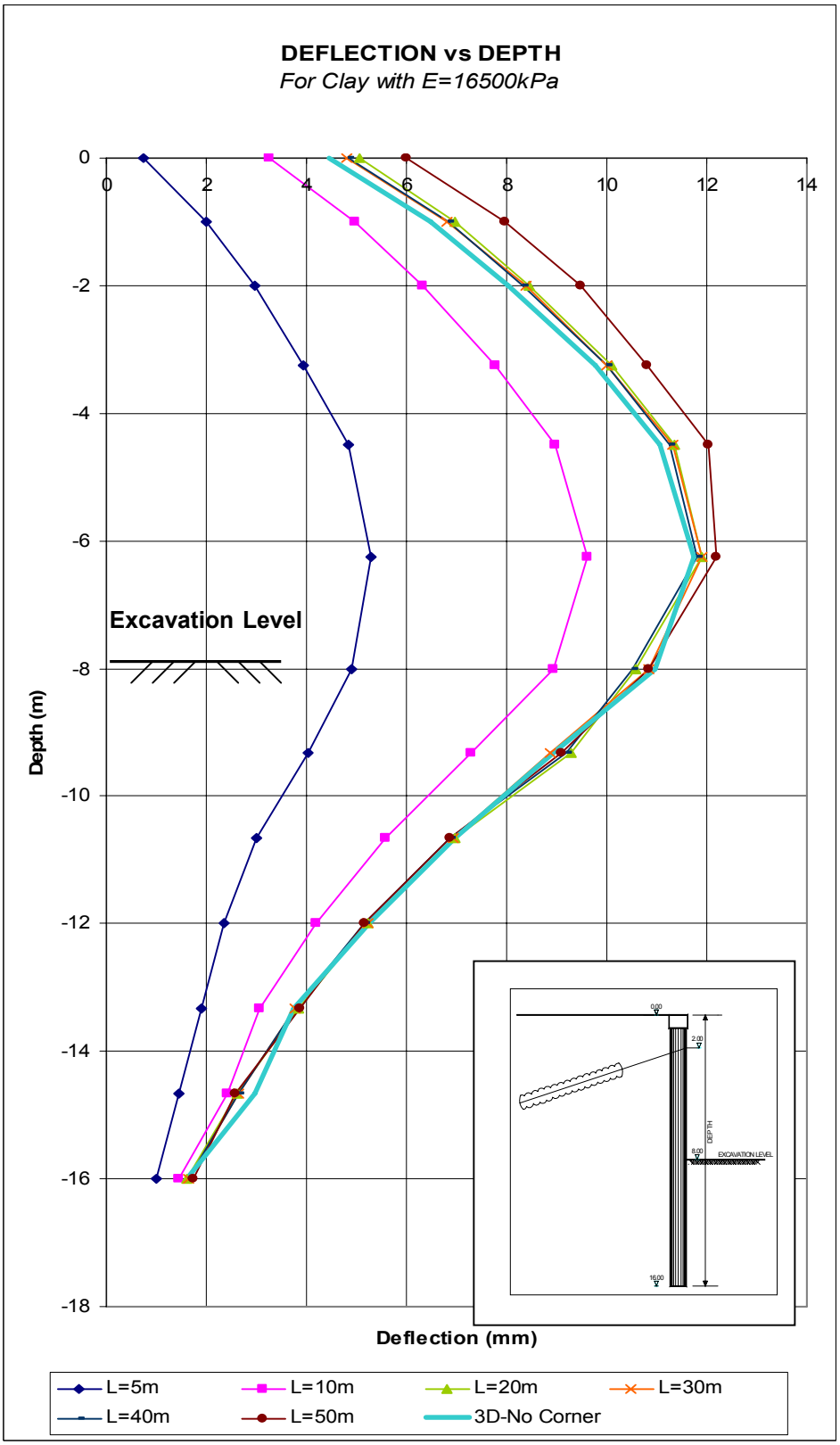

Figure 82. Deflection of anchored wall at one level case vs. depth for clay with E=16500kPa

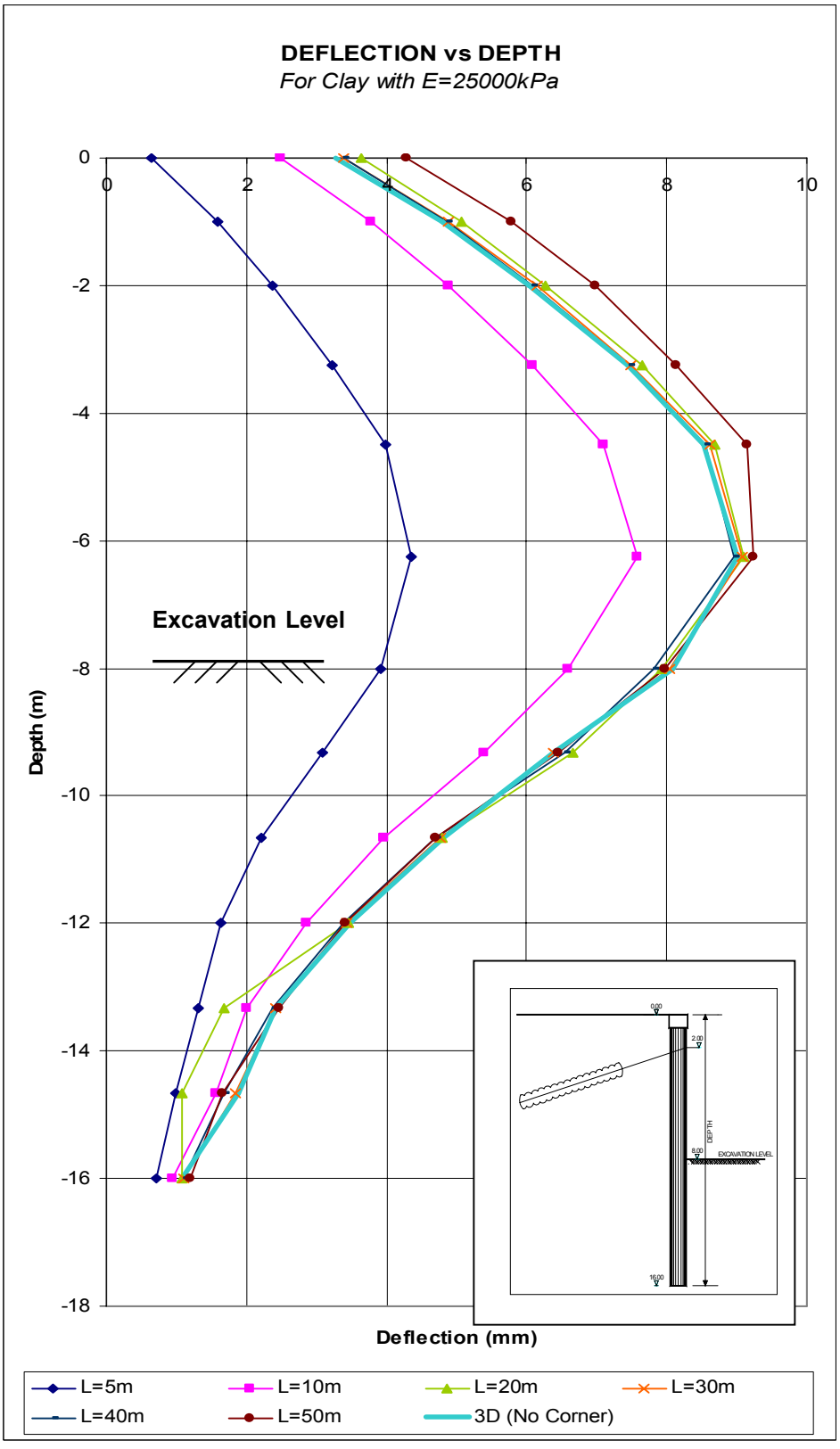

Figure 83. Deflection of anchored wall at one level case vs. depth for clay with E=25000kPa

‘’Maximum deflection vs. distance from the corner’’ and ‘’ ‘Deflection / Maximum Deflection’ vs. distance from the corner’’ graphs are shown in Figures 84, 85, respectively. According to these graphs following results are obtained;

- As elastic modulus decrease, maximum deflection throughout the excavation side increase.

- For all elastic modulus values, corner effect is observed up to 20m distance from the corner. Beyond this distance maximum deflections are nearly constant. It should also be noted that significant corner effect is observed up to 10m distance from the corner.

- For the same distance from the corner, as elastic modulus increase, deflection over maximum deflection ratio, which is the ratio of maximum wall displacement of a section to maximum wall displacement of in-situ wall, increase slightly. Average ratios for different distances are as follows;

  Distance from the corner; 5m → 0.25
  Distance from the corner; 10m → 0.73
  Distance from the corner; 20m → 0.95
  Distance from the corner; 30m → 0.97
  Distance from the corner; 40m → 0.97
  Distance from the corner; 50m → 1.00

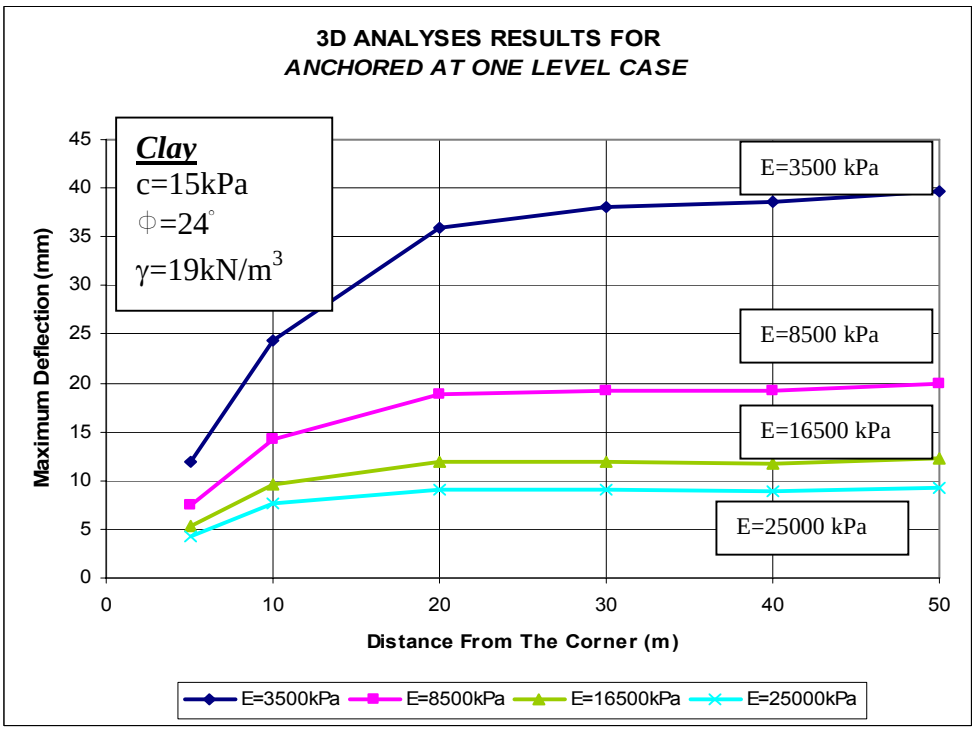

Figure 84. Maximum deflections vs. distance from the corner for anchored wall at one level case in 3D analyses

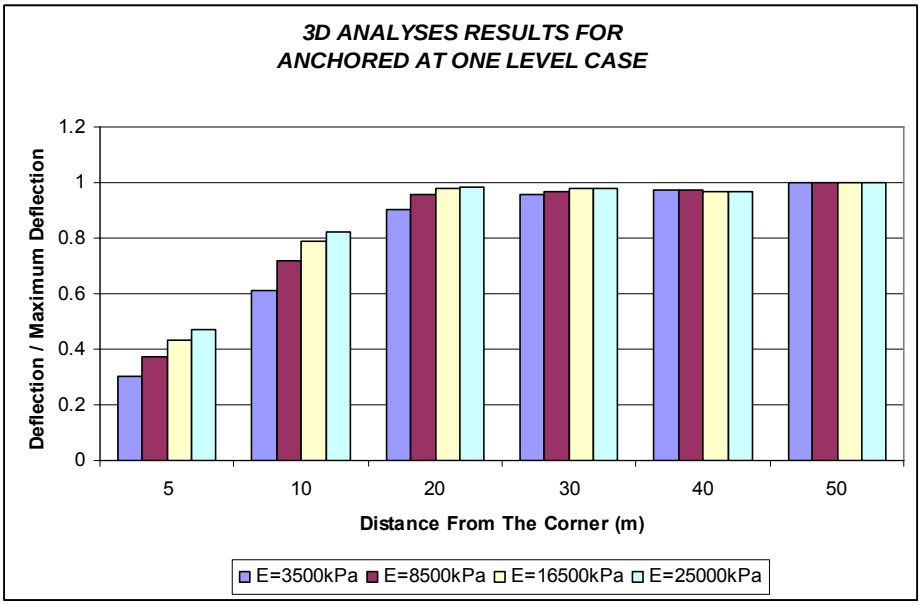

Figure 85. 'Deflection / Maximum Deflection ratios vs. distance from the corner for anchored wall at one level case in 3D analyses

Beside deflection, moments are also studied. 3D with and without corner, and plane strain analyses' results are plotted in the same graphs. Moment vs. depth graphs are shown in Figure 86, 87, 88, 89. Moment diagrams are drawn for four different sections;

A-A Section: Distance from the corner = 7m
B-B Section: Distance from the corner = 21m
C-C Section: Distance from the corner = 35m
D-D Section: Distance from the corner = 50m

Following results are obtained;

- Moment diagram patterns do not change through the excavation side. However, because of the mesh coarseness difference between 2D and 3D analyses, smooth moment lines are obtained from 2D analyses; sharp broken lines are obtained from 3D ones.

- Comparisons of various sections taken from 3D with corner analyses;

  - Moments of B-B (distance from corner=21m), C-C (distance from corner=35m) and D-D (distance from corner=50m) sections are similar. On the other hand moment of A-A (distance from the corner=7m) is 50-150kNm/m smaller than the other values.

  - Similar maximum moment values are found at similar depths of the pile wall.

- Comparisons of 3D with and without corner analyses;

  Moment values of 3D without corner analyses are similar to moment values of B-B, C-C and D-D sections.

- Comparisons of 3D without corner and plane strain analyses;

  Maximum moments of plane strain analyses are 30-60 kNm/m smaller than the maximum values of 3D without corner analyses. Therefore, it can be claimed that moments of these two analyses are similar.

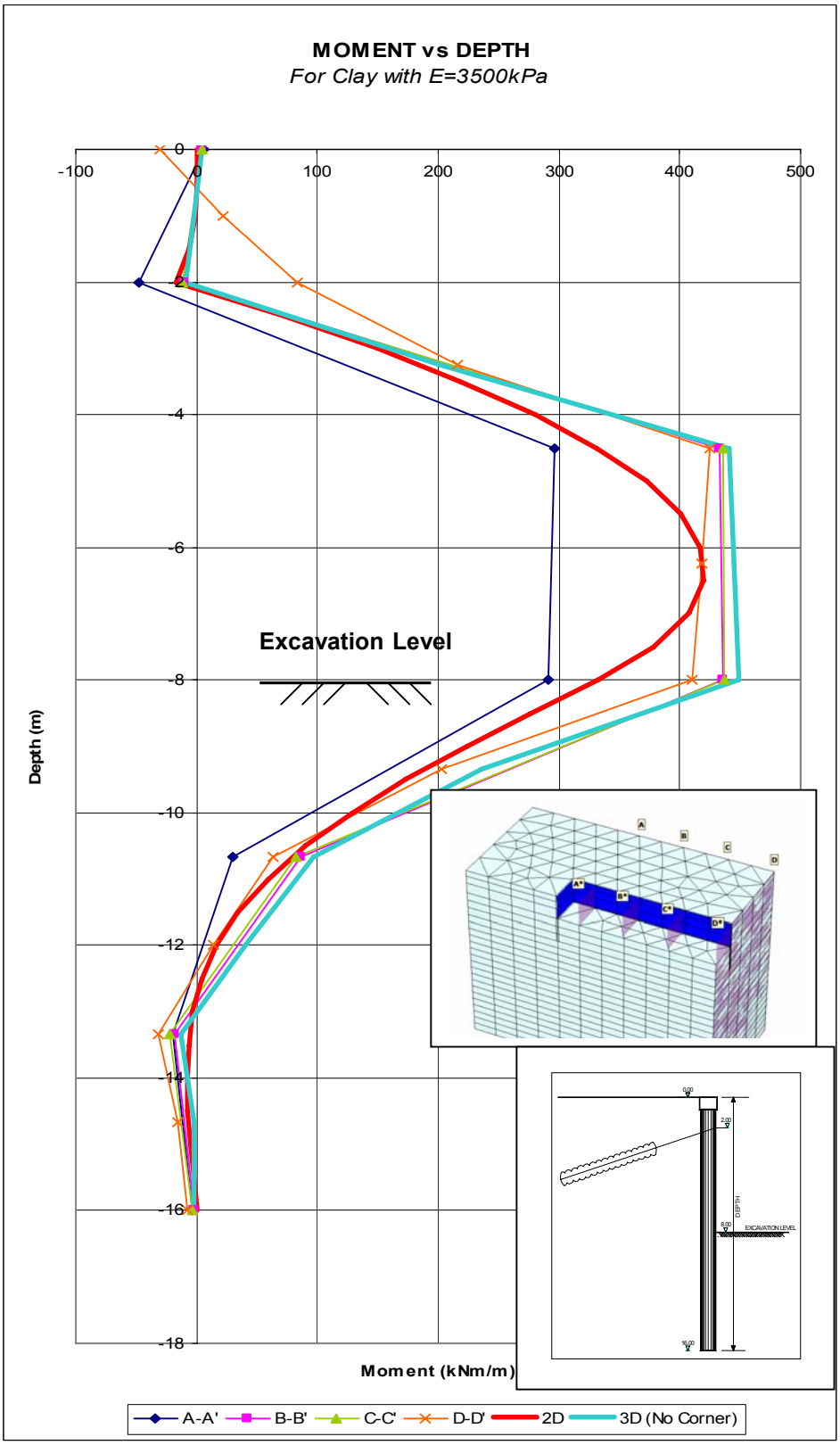

Figure 86. Moment of anchored wall at one level case vs. depth for clay with E=3500kPa

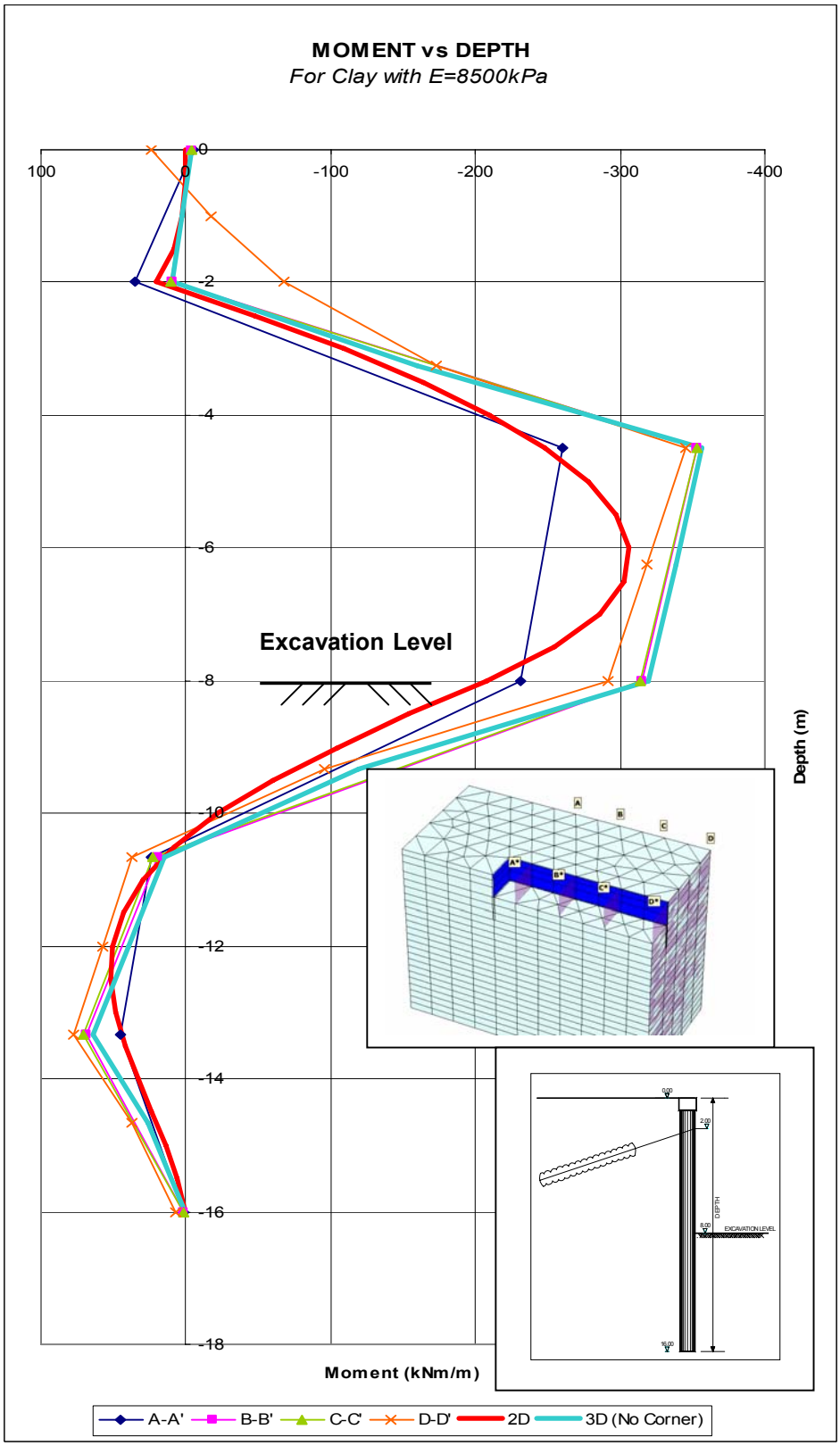

Figure 87. Moment of anchored wall at one level case vs. depth for clay with E=8500kPa

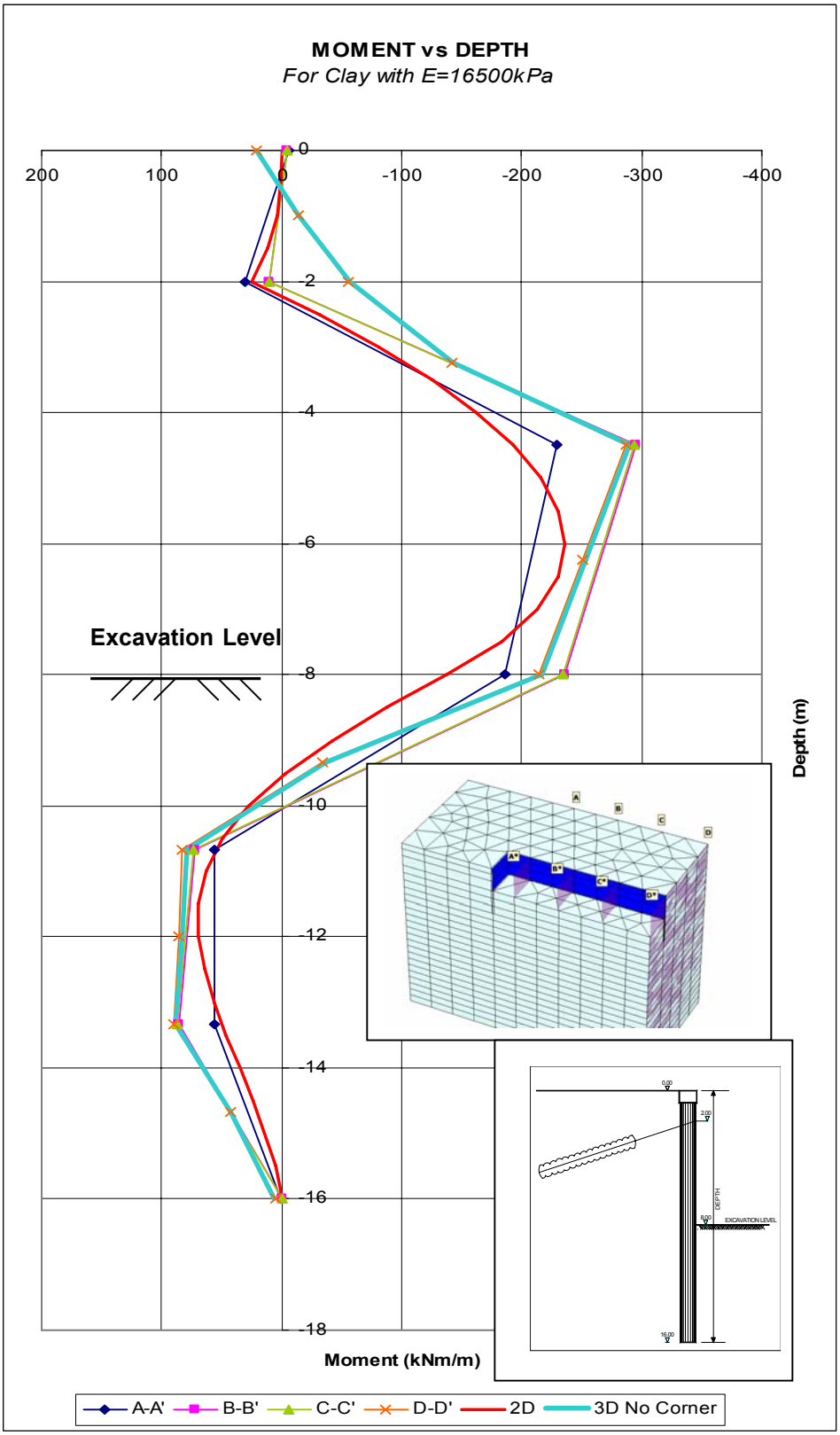

Figure 88. Moment of anchored wall at one level case vs. depth for clay with E=16500kPa

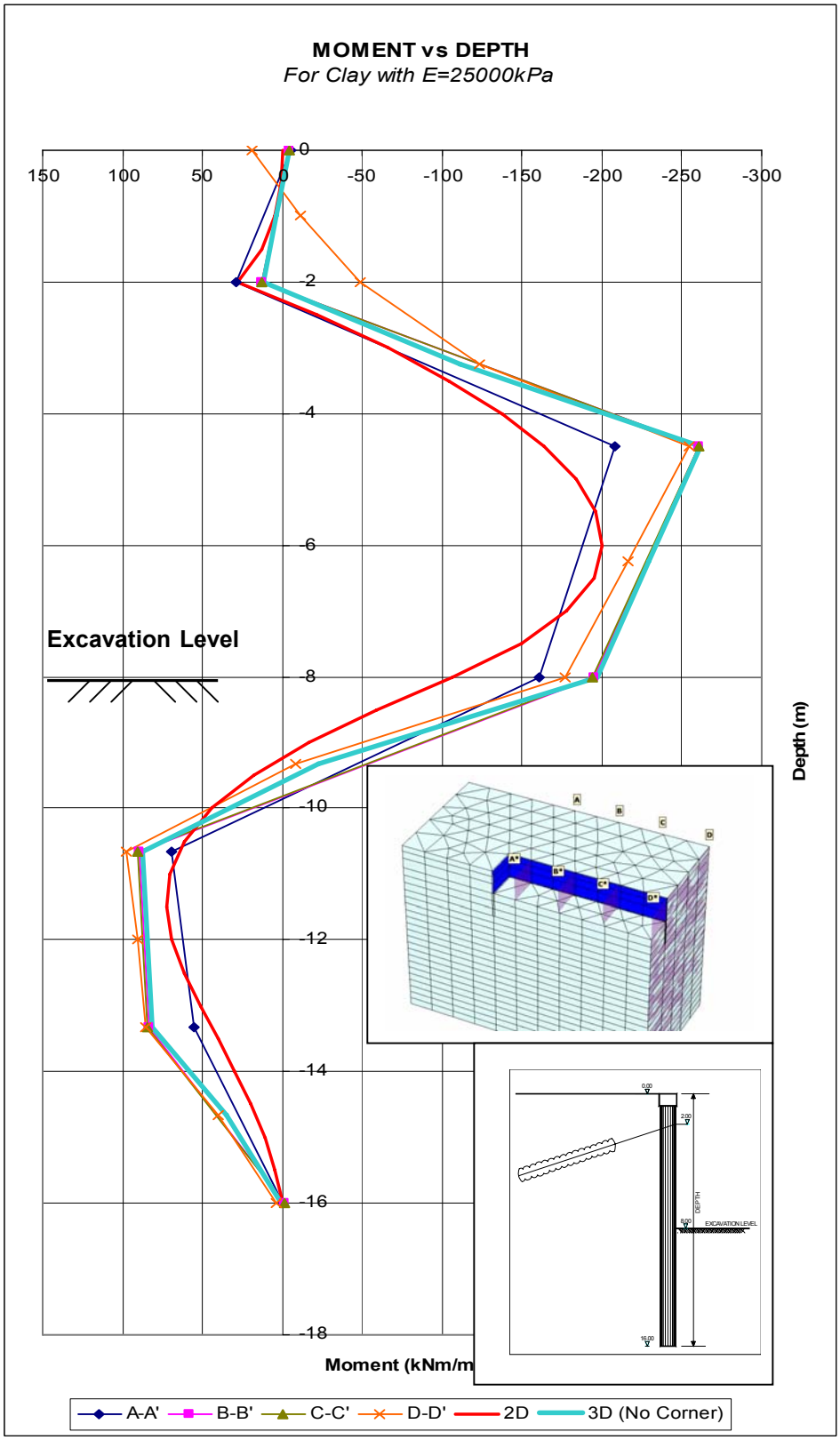

Figure 89. Moment of anchored wall at one level case vs. depth for clay with E=25000kPa

It is observed that as elastic modulus increases, maximum moments of sections decrease as shown in Figure 90.

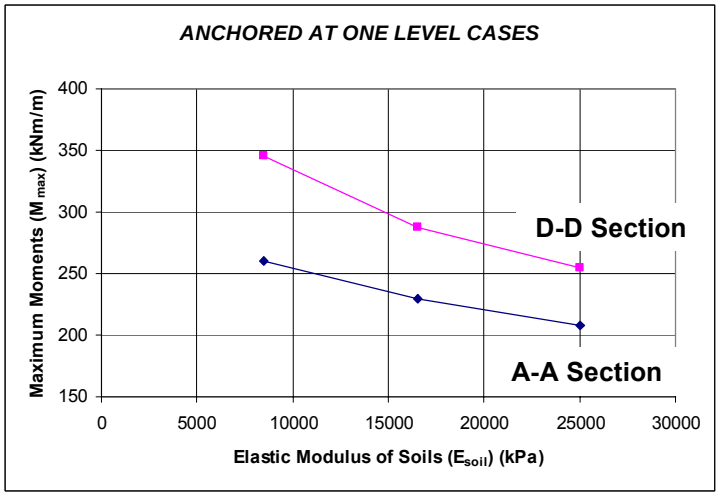

Figure 90. Maximum moments vs. elastic modulus of soils for anchored wall at one level case

Difference between maximum moment of A-A (7m from the corner) and maximum moment of D-D (50m from the corner) sections decreases, as elastic modulus of soil increases as demonstrated in Figure 91. In other words, it can be said that corner effect on magnitude of moment decreases as elastic modulus of soil increases.

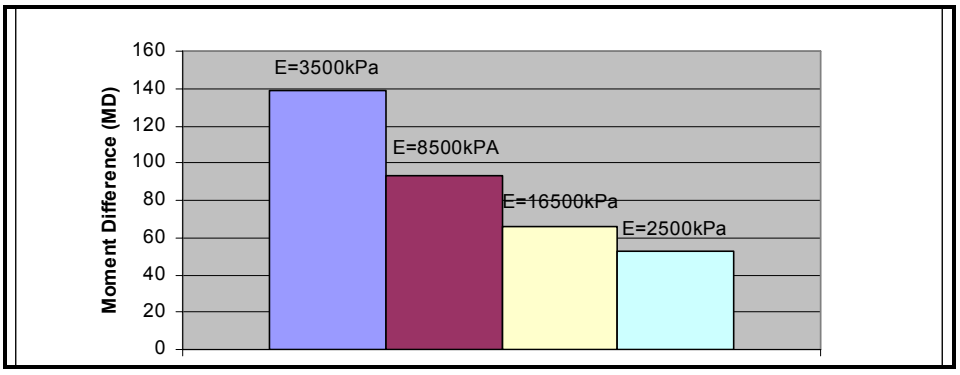

Figure 91. Difference between maximum moments of A-A and D-D Sections for anchored wall at one level case

For all elastic modulis of soils; maximum moments increase as distance from the corner increase up to 20m distance from the corner. After this distance moment values become nearly constant, as shown in Figure 92.

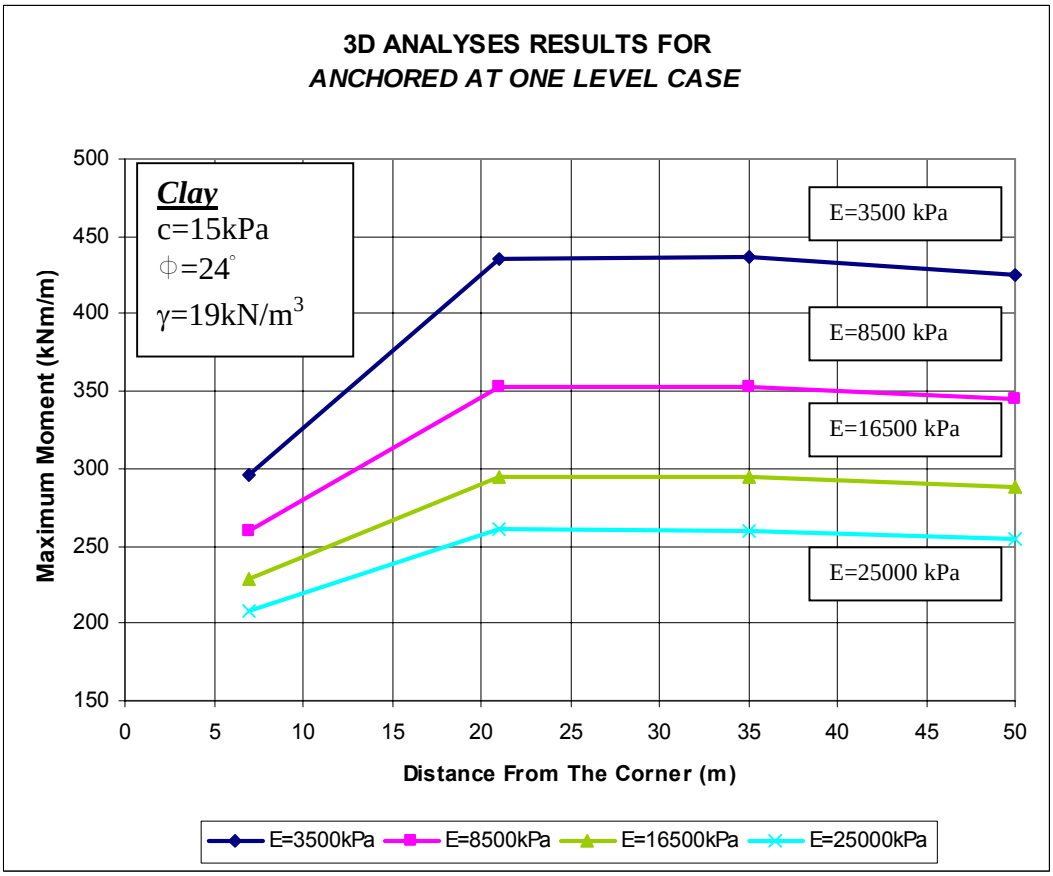

Figure 92. Maximum moments vs. distance from the corner for anchored wall at one level case in 3D analyses

In addition to moments and deflections, effective horizontal stresses of the cases are also examined. Calculated effective stresses are compared with Rankine's active pressures and at rest earth pressures as shown in Figures 93, 94, 95, 96. The effective horizontal stress diagrams are drawn for four different sections;

A-A Section: Distance from the corner = 7m
B-B Section: Distance from the corner = 21m
C-C Section: Distance from the corner = 35m
D-D Section: Distance from the corner = 50m

Following results are obtained;

- According to 3D with corner analysis results, it can be said that effective horizontal stresses for different sections are similar. It shows that there is no significant corner effect on effective horizontal stresses.

- When the results of plane strain and 3D with corner case are compared, generally similar results are seen but 10-20 kPa differences are observed.

- Below comparisons between theories and calculated results are obtained;

  Between Surface and Anchor Level: Effective horizontal stresses are bigger than at rest earth pressures because anchors restrict deflections. As elastic modulus of soil increase, effective horizontal stresses also increase.

  Between Anchor Level and Excavation Level: Effective horizontal stresses are upper bounded by at rest earth pressure line and lower bounded by active earth pressure line. As elastic modulus of soil increase, effective earth pressures get closer to active earth pressure line.

  Below Excavation Level: Effective horizontal stresses of all elastic modulus of soils are similar and very close to at rest earth pressure line.

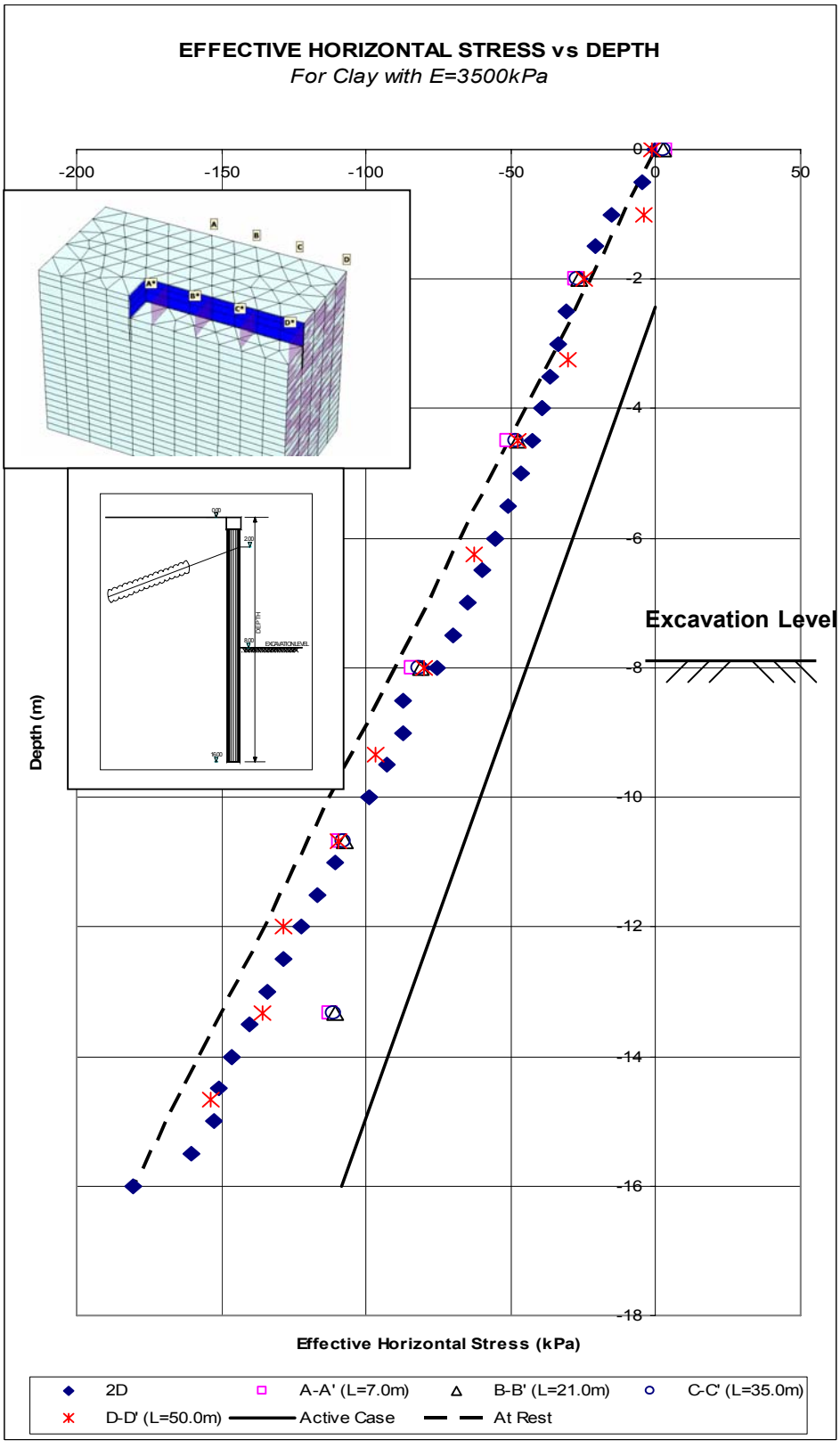

Figure 93. Effective horizontal stress of anchored wall at one level case vs. depth for clay with E=3500kPa

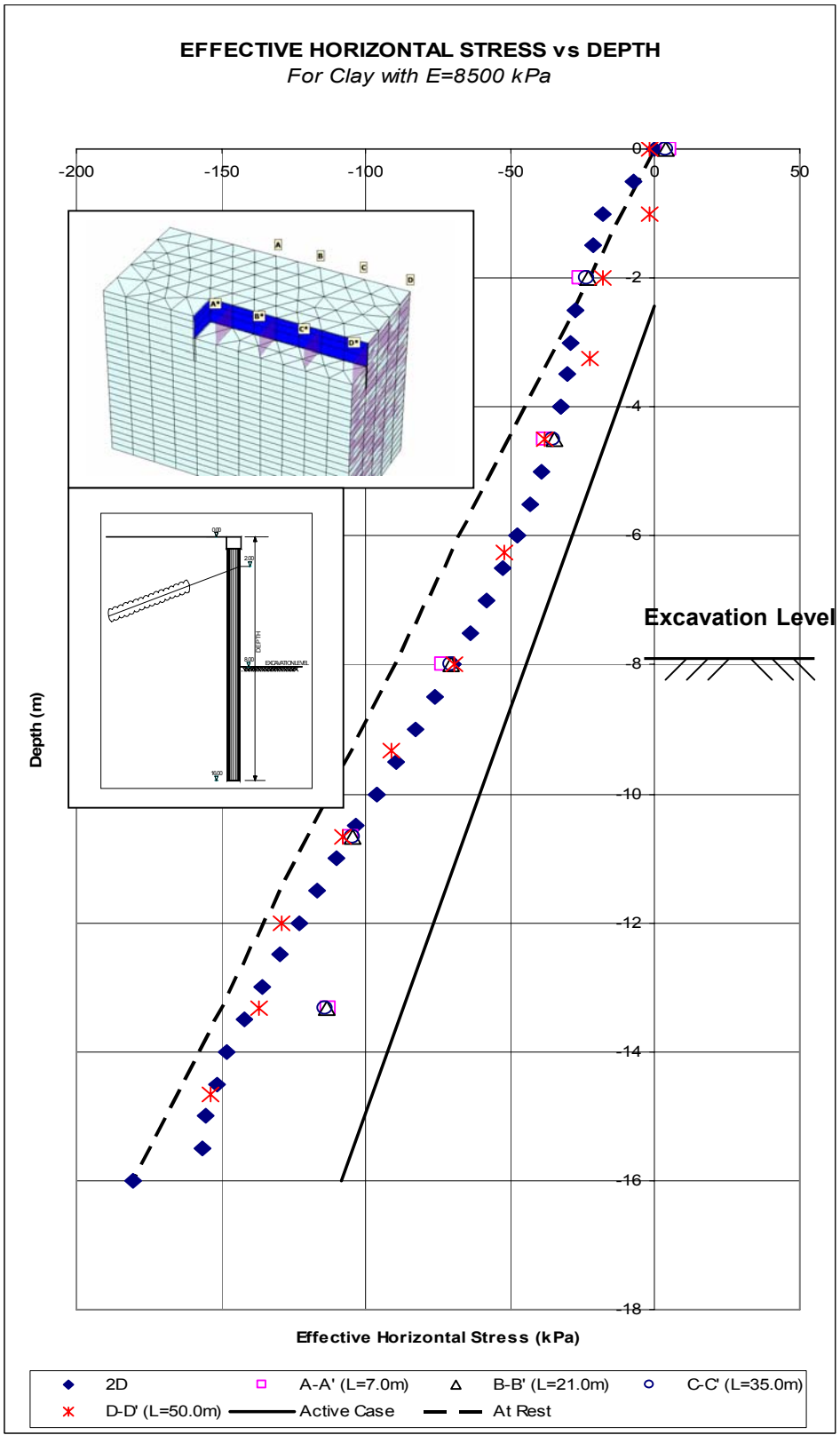

Figure 94. Effective horizontal stress of anchored wall at one level case vs. depth for clay with E=8500kPa

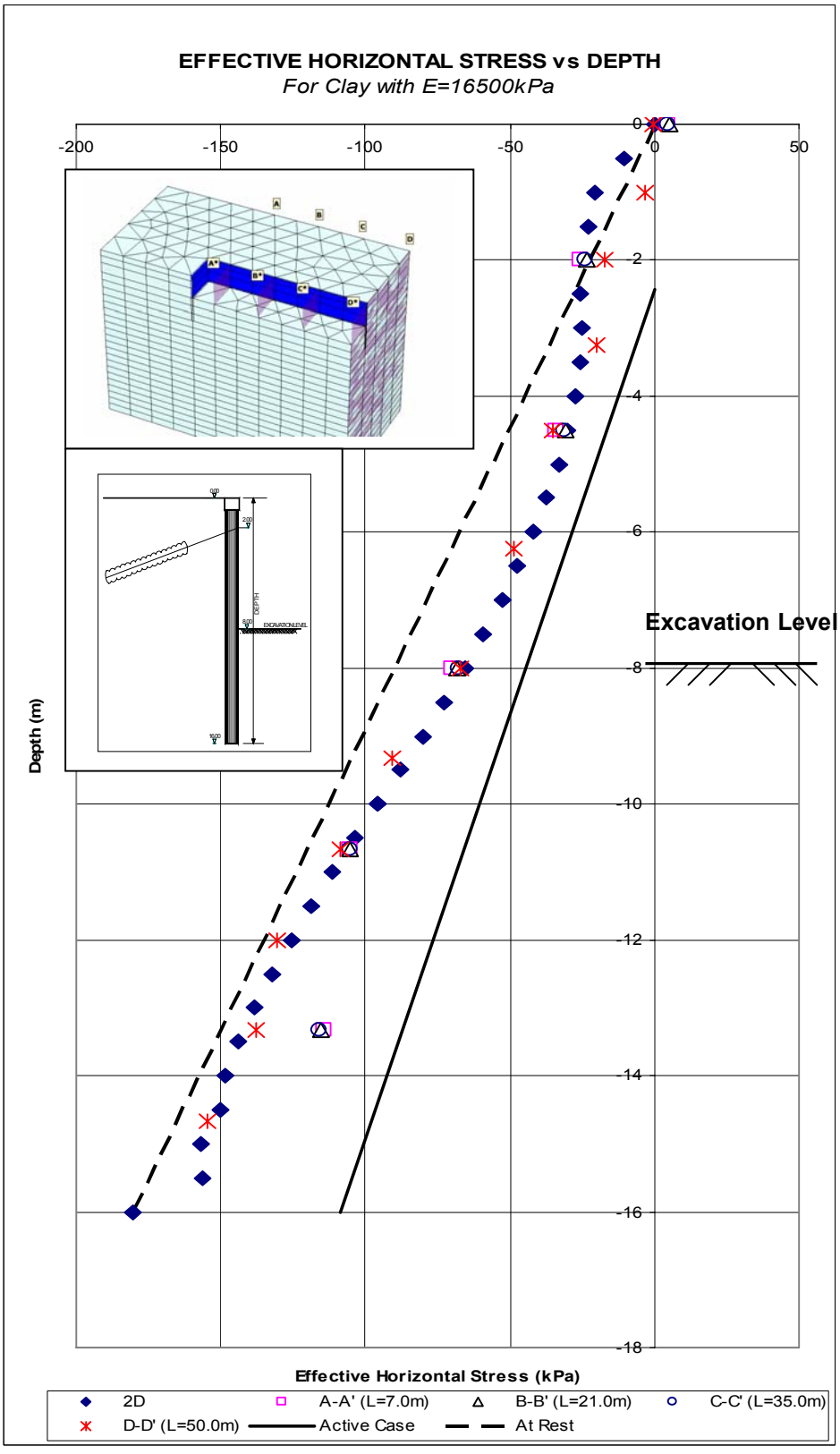

Figure 95. Effective horizontal stress of anchored wall at one level case vs. depth for clay with E=16500kPa

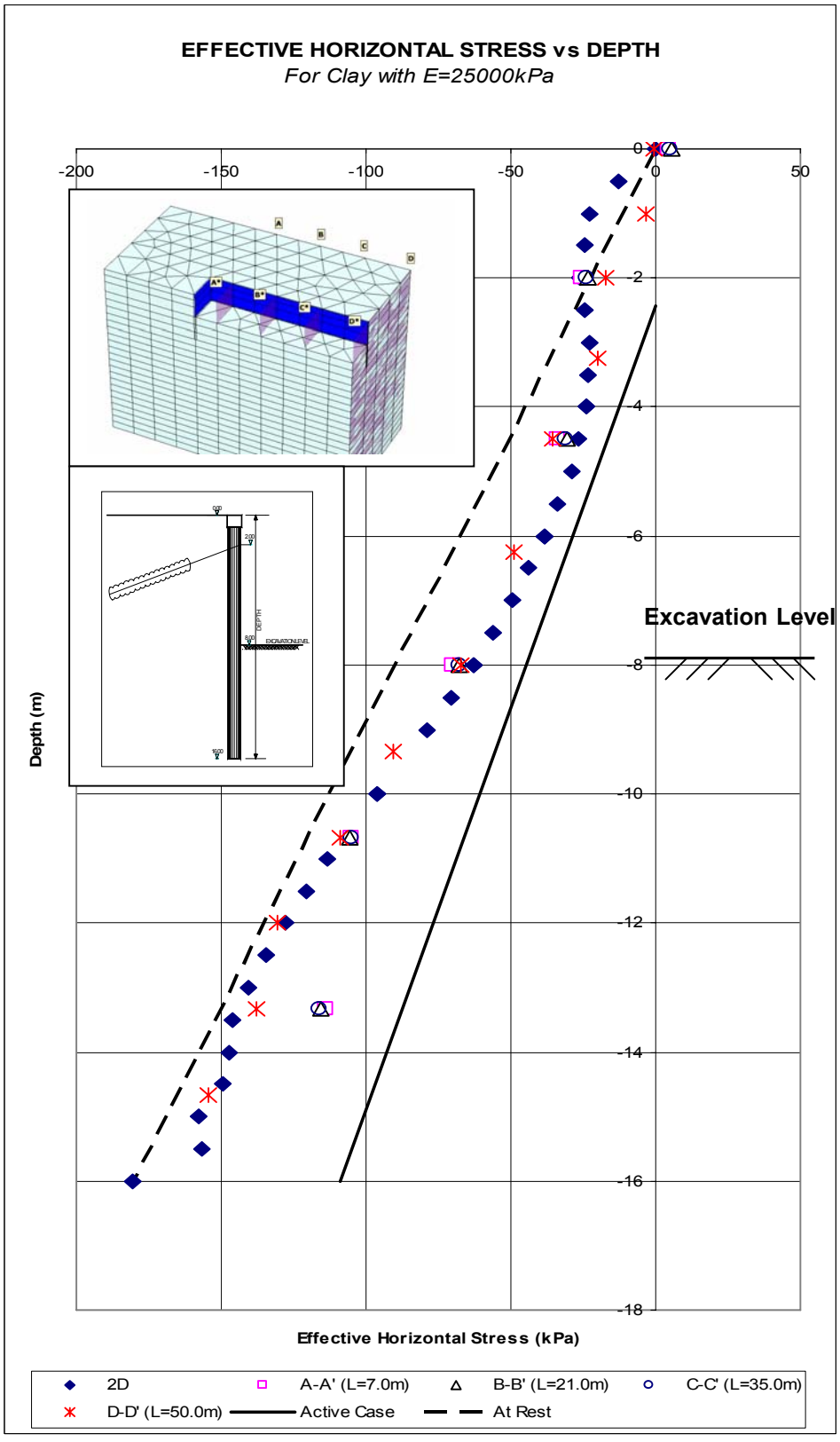

Figure 96. Effective horizontal stress of anchored wall at one level case vs. depth for clay with E=25000kPa

3.5.3. Anchored Wall at Two Levels Cases

Pile wall anchored wall at two levels cases are studied for elastic modulus values of 3500 and 8500 kPa. The finite element meshes used in 3D with and without corner analyses and plane strain analyses are demonstrated in Figures 97, 98, 99.

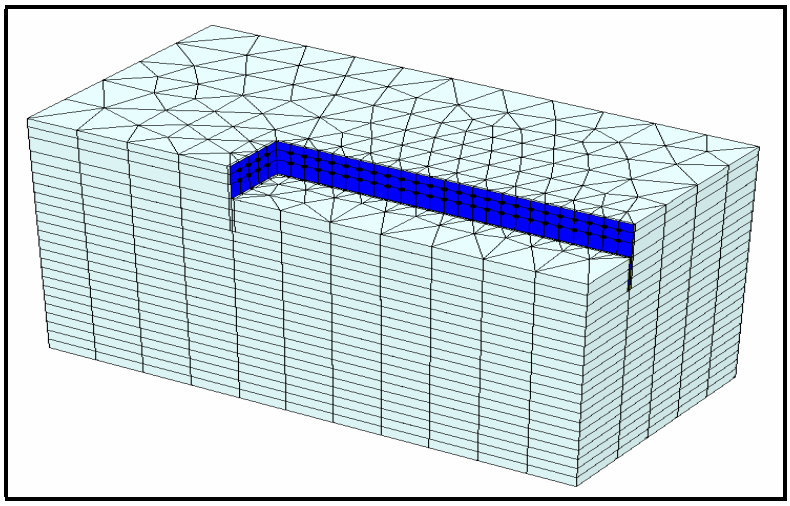

Figure 97. Finite element mesh used in 3D analyses of two level anchor case

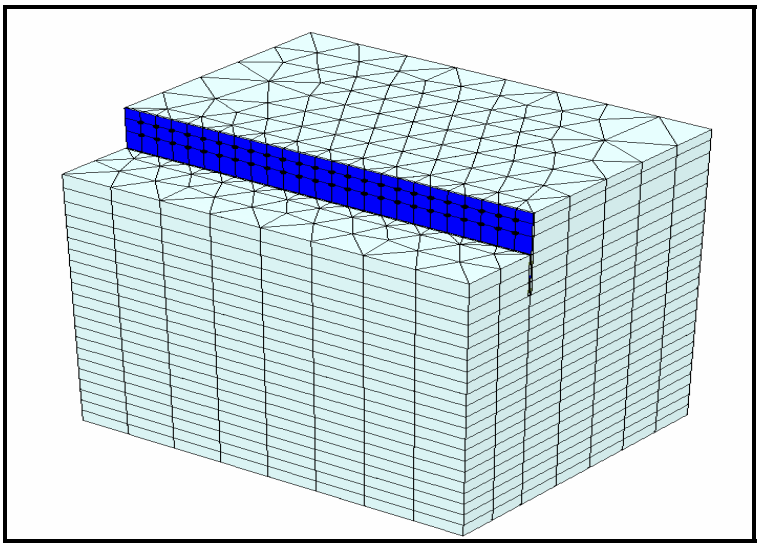

Figure 98. Finite element mesh used in 3D analyses of two level anchor case (For no corner condition)

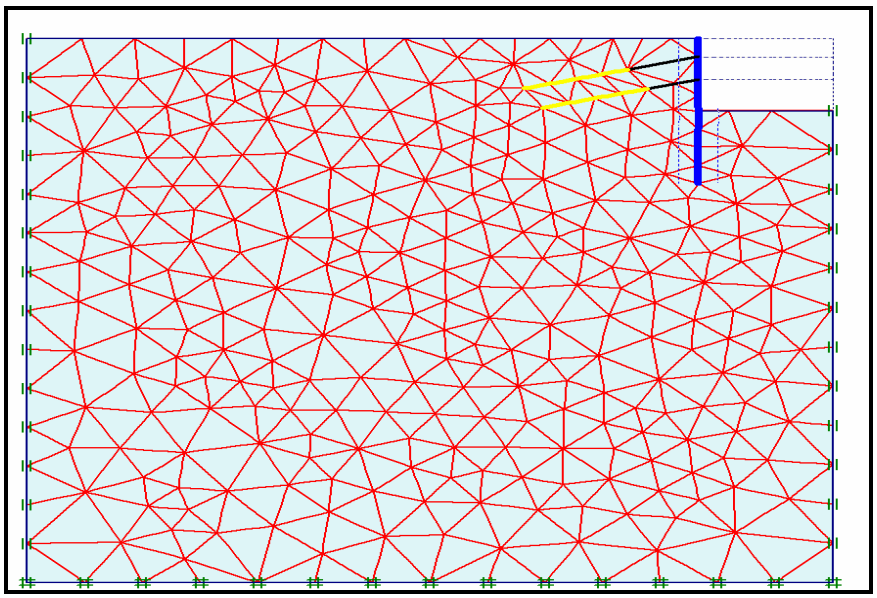

Figure 99. Finite element mesh used in 2D analyses of anchored wall at two levels case

Deflection toward retained soil side caused by prestress force is also observed in plane strain analyses results of anchored wall at two levels cases, as shown in Figure 100. Because of this mode difference, plane strain and 3D analyses results are not shown in the same graphs.

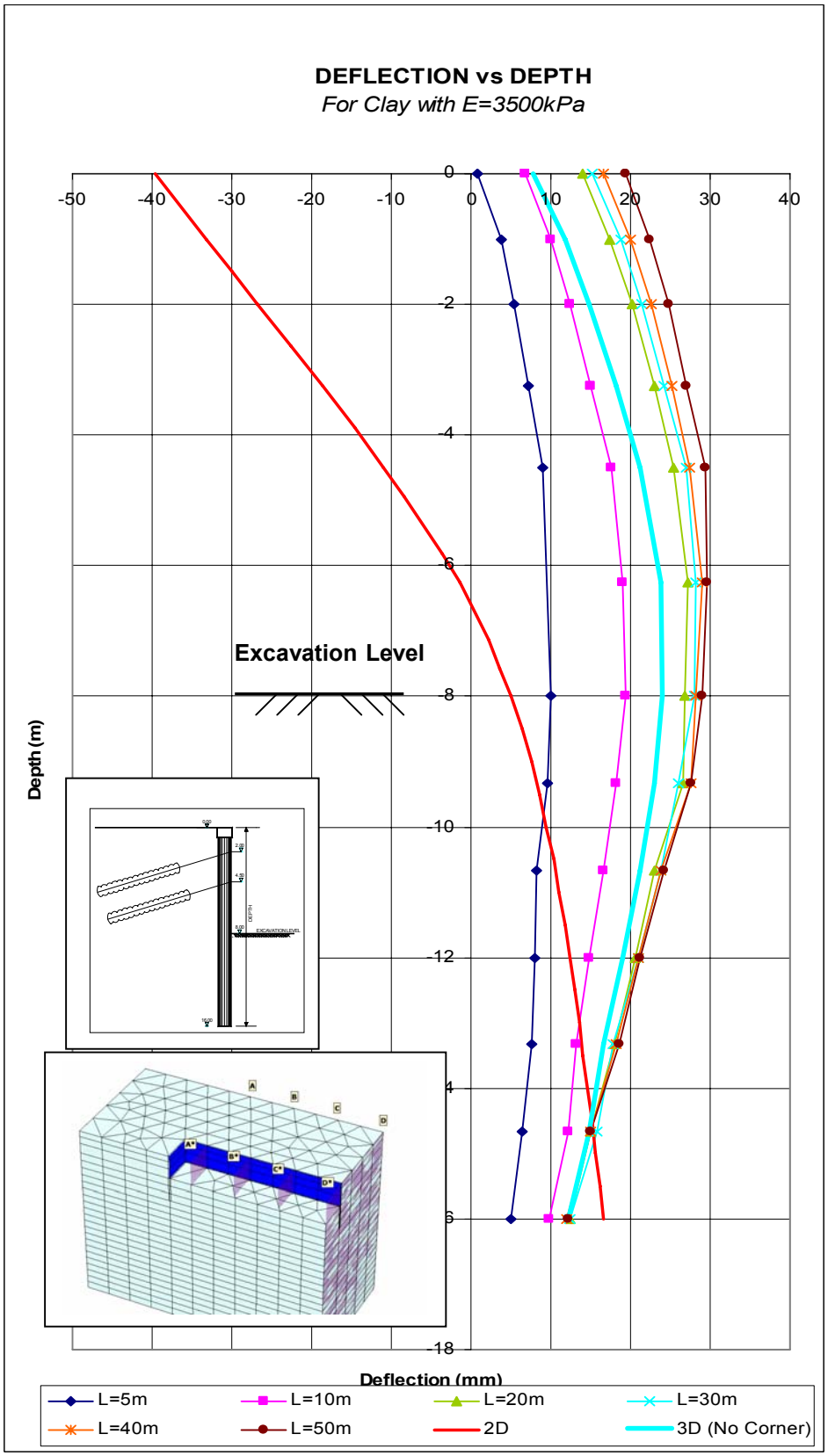

Figure 100. Deflection of anchored wall at two levels case vs. depth for clay with E=3500kPa (with 2D analyses results)

Deflection for various sections vs. depth graphs are demonstrated in Figures 101, 102. Following results are obtained;

- Comparisons of various sections taken from 3D with corner analyses;

  For both elastic modulus values it is seen that corner effects on deflections diminish at 20m distance from the corner. After this distance deflections become nearly constant.

- Comparisons of 3D with and without corner analysis;

  Deflections of 3D without corner analyses are 5-10mm smaller than maximum deflections of with corner analyses. This unexpected disparity is predicted to be an effect of mesh generation difference between models.

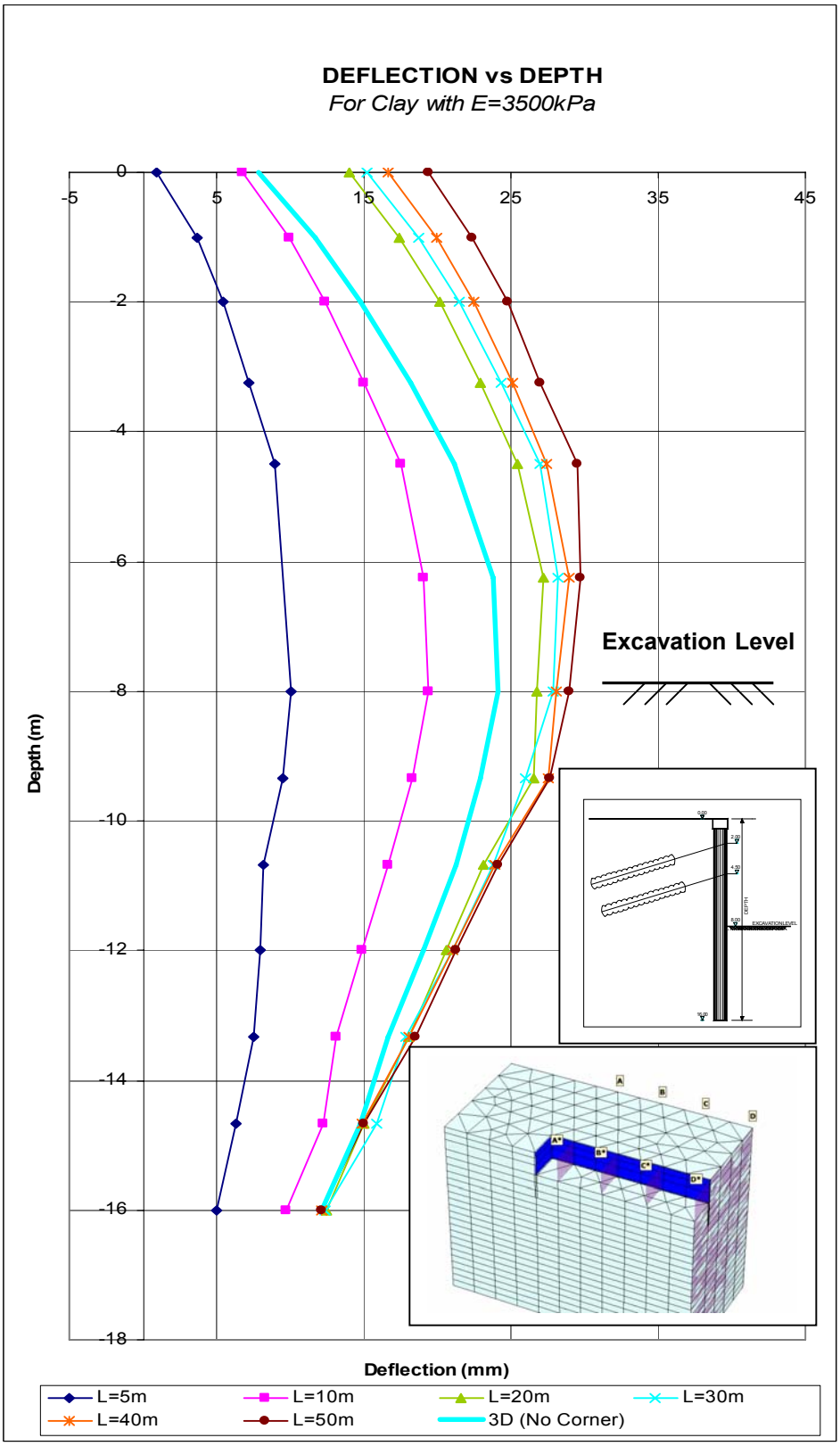

Figure 101. Deflection of anchored wall at two levels case vs. depth for clay with E=3500kPa

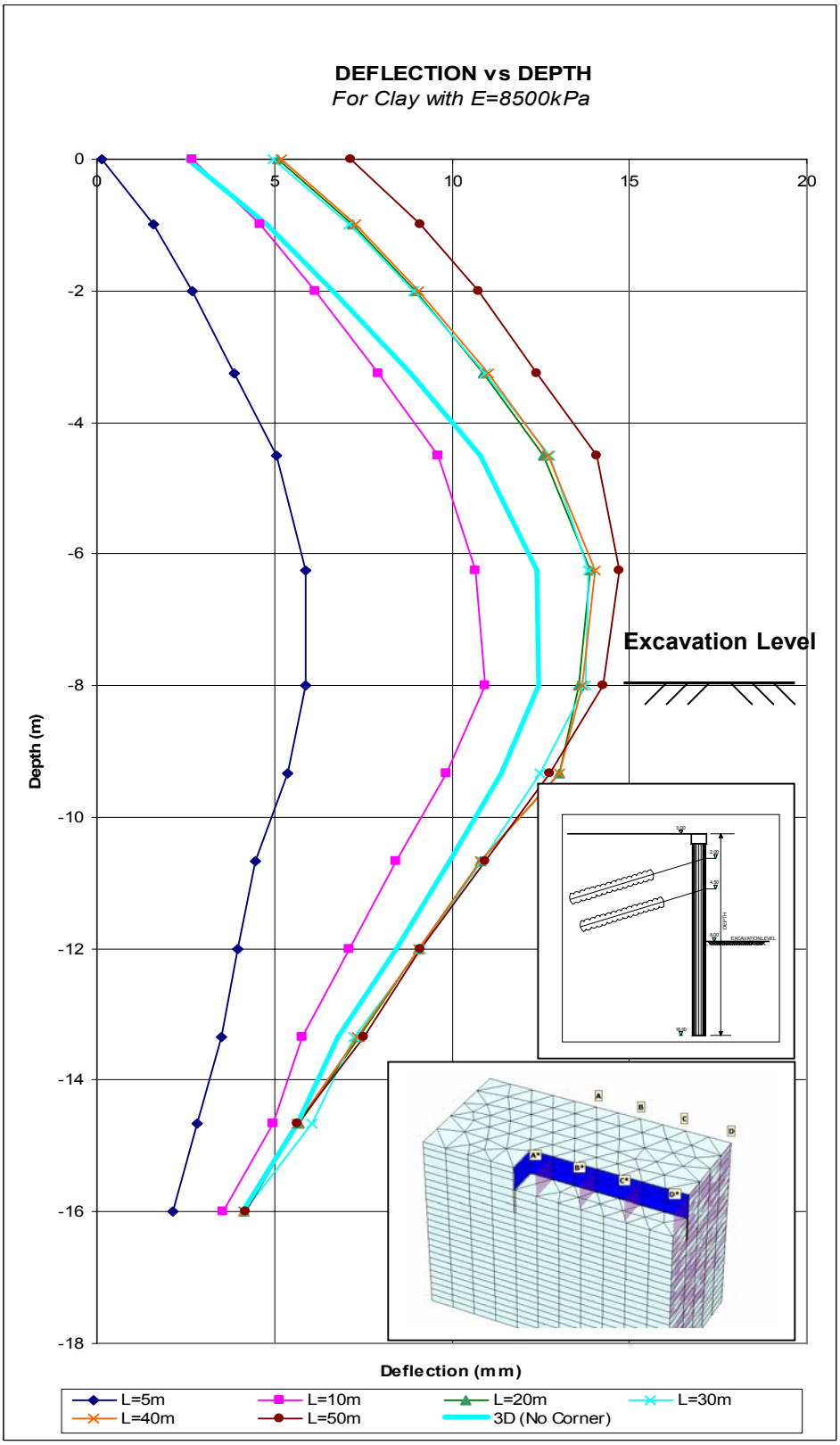

Figure 102. Deflection of anchored wall at two levels case vs. depth for clay with E=8500kPa

‘’Maximum deflection vs. distance from the corner’’ and ‘’ ‘Deflection / Maximum Deflection’ vs. distance from the corner’’ graphs are demonstrated in Figures 103, 104, respectively. According to these graphs following results are obtained;

- As elastic modulus decreases, maximum deflections towards the excavation side increase.

- For all elastic modulus values, corner effect is observed up to 20m distance from the corner. After this distance maximum deflections are nearly constant.

- For the same distance from the corner, as elastic modulus increases, deflection over maximum deflection ratio, which is the ratio of maximum wall displacement of a section to maximum wall displacement of in-situ wall, increases slightly up to 20m distance from the corner as shown in Figure 103. Average ratios for different distances are as follows;

  Distance from the corner; 5m → 0.37
  Distance from the corner; 10m → 0.70
  Distance from the corner; 20m → 0.93
  Distance from the corner; 30m → 0.95
  Distance from the corner; 40m → 0.97
  Distance from the corner; 50m → 1.00

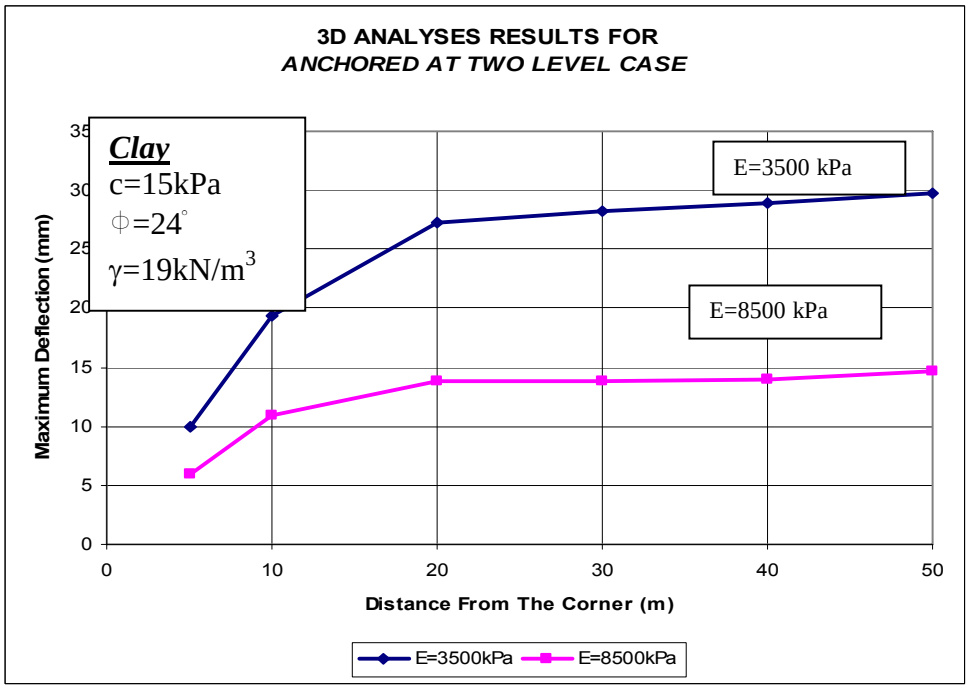

Figure 103. Maximum deflections vs. distance from the corner for anchored wall at two levels case in 3D analyses

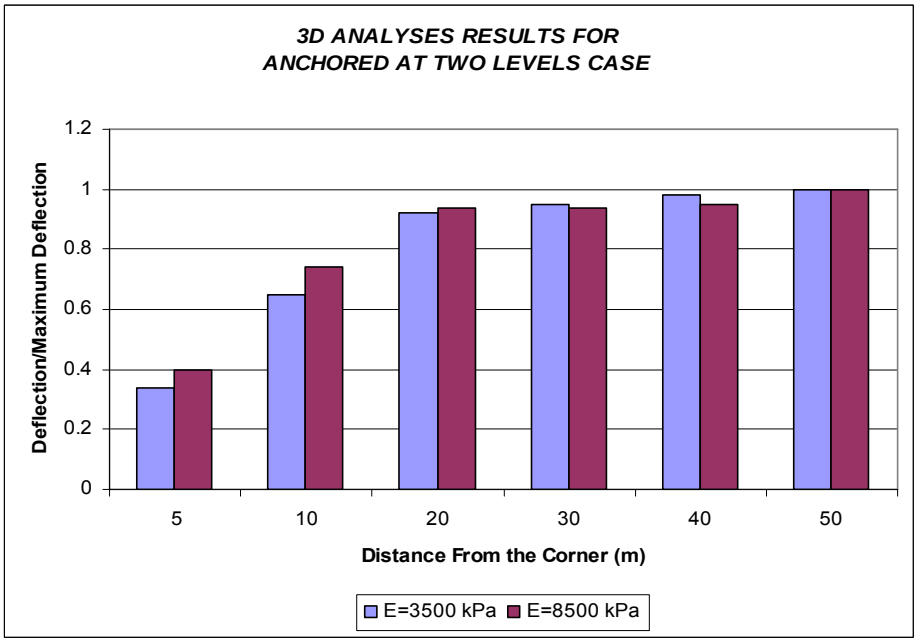

Figure 104. 'Deflection / Maximum Deflection ratios vs. distance from the corner for anchored wall at two levels case in 3D analyses

Beside deflection, moments for different cross sections of excavation site are also studied. 3D with and without corner, and plane strain analyses' results are plotted in the same graphs. 'Moment vs. depth' graphs are shown in Figures 105, 106. Moment diagrams are drawn for three different sections;

A-A Section: Distance from the corner = 7m
B-B Section: Distance from the corner = 21m
C-C Section: Distance from the corner = 35m

Following results are obtained;

- Moment diagram patterns of plane strain and 3D analyses are different. Sudden decreases and increases in moment diagrams are observed at anchor levels in plane strain analyses. On the other hand, this kind of decreases and increases are not observed in 3D analyses. This disparity can be as a result of number of node difference between two programs; as number of nodes in plane strain analyses are more than 3D analyses, more sensitive moment lines are obtained from 2D analyses.

- <u>Comparisons of various sections taken from 3D with corner analyses;</u>

  - Moments of B-B (distance from corner=21m) and C-C (distance from corner=35m) sections are similar. On the other hand moment of A-A (distance from the corner=7m) is 60-110kNm/m smaller than the other values.

  - Similar maximum moment values are found at similar depths of the pile wall.

- <u>Comparisons of 3D with and without corner analyses;</u>

  Moment values of 3D without corner analyses are similar to moment values of B-B and C-C sections.

- <u>Comparisons of 3D without corner and plane strain analyses;</u>

  Maximum moments of plane strain analyses are 100-150 kNm/m smaller than the maximum values of 3D without corner analyses.

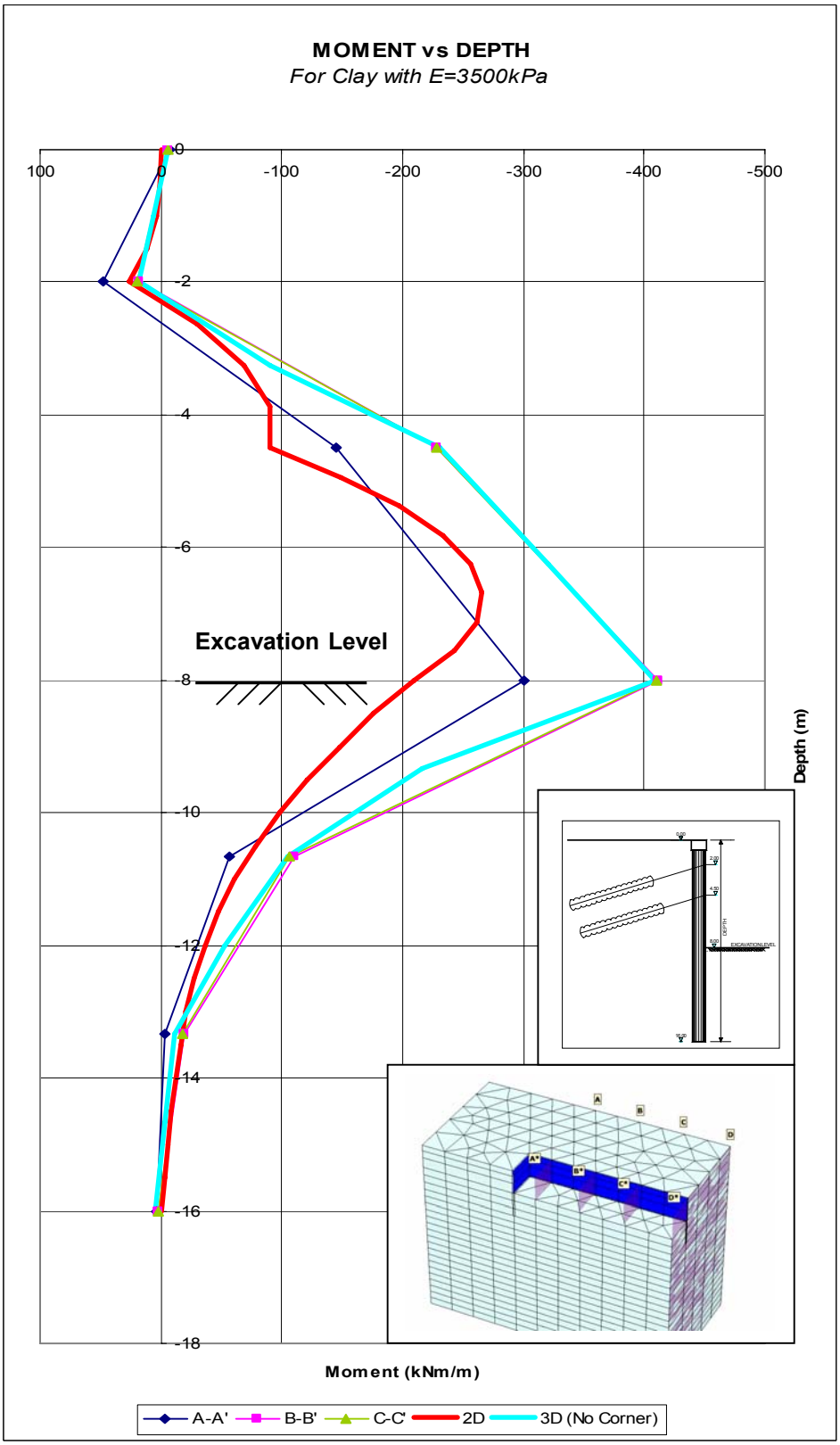

Figure 105. Moment of anchored wall at two levels case vs. depth for clay with E=3500 kPa

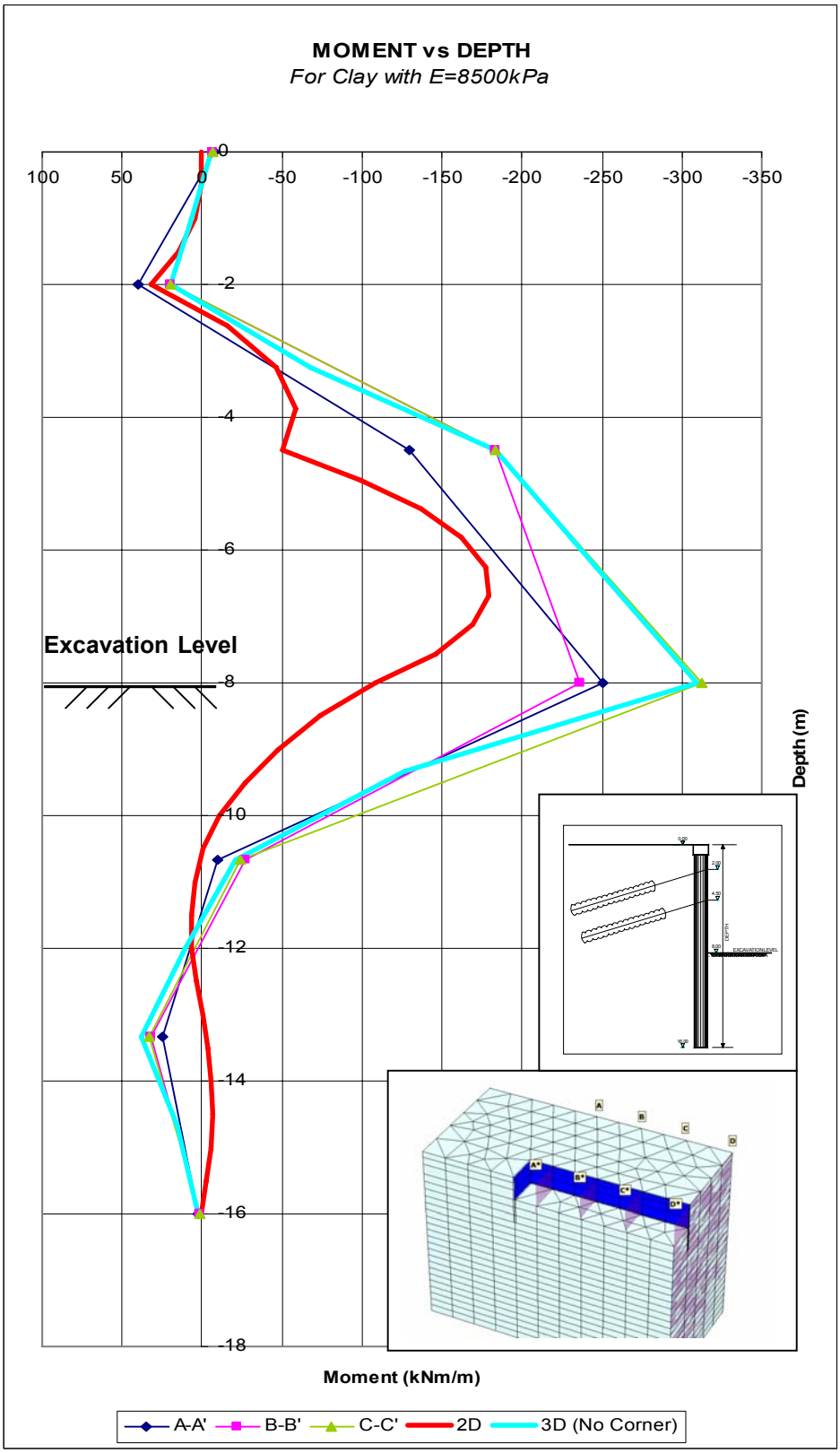

Figure 106. Moment of anchored wall at two levels case vs. depth for clay with E=8500kPa

It is observed that as elastic modulus increase, maximum moments of sections decrease as shown in Figure 107.

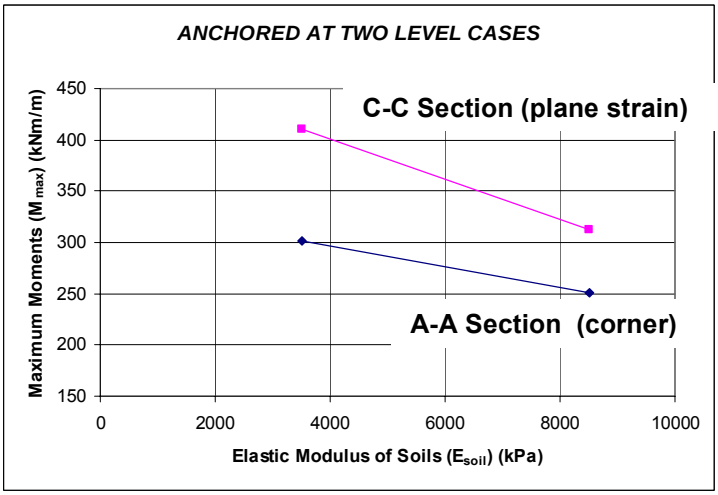

Figure 107. Maximum moments vs. elastic modulus of soils for anchored wall at two level case

Difference between maximum moment of A-A (7m from the corner) and maximum moment of C-C (35m from the corner) sections decrease, as elastic modulus of soil increase as demonstrated in Figure 108. In other words, it can be said that corner effect on magnitude of moment decreases as elastic modulus of soil increases.

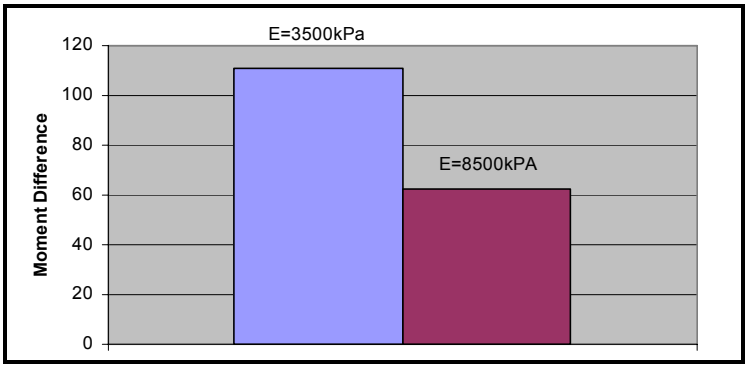

Figure 108. Difference between maximum moments of A-A and D-D Sections for anchored wall at two level case

For all elastic modulis of soil; maximum moments increase as distance from the corner increase up to 20m distance from the corner. After this distance moment values become nearly constant, as shown in Figure 109.

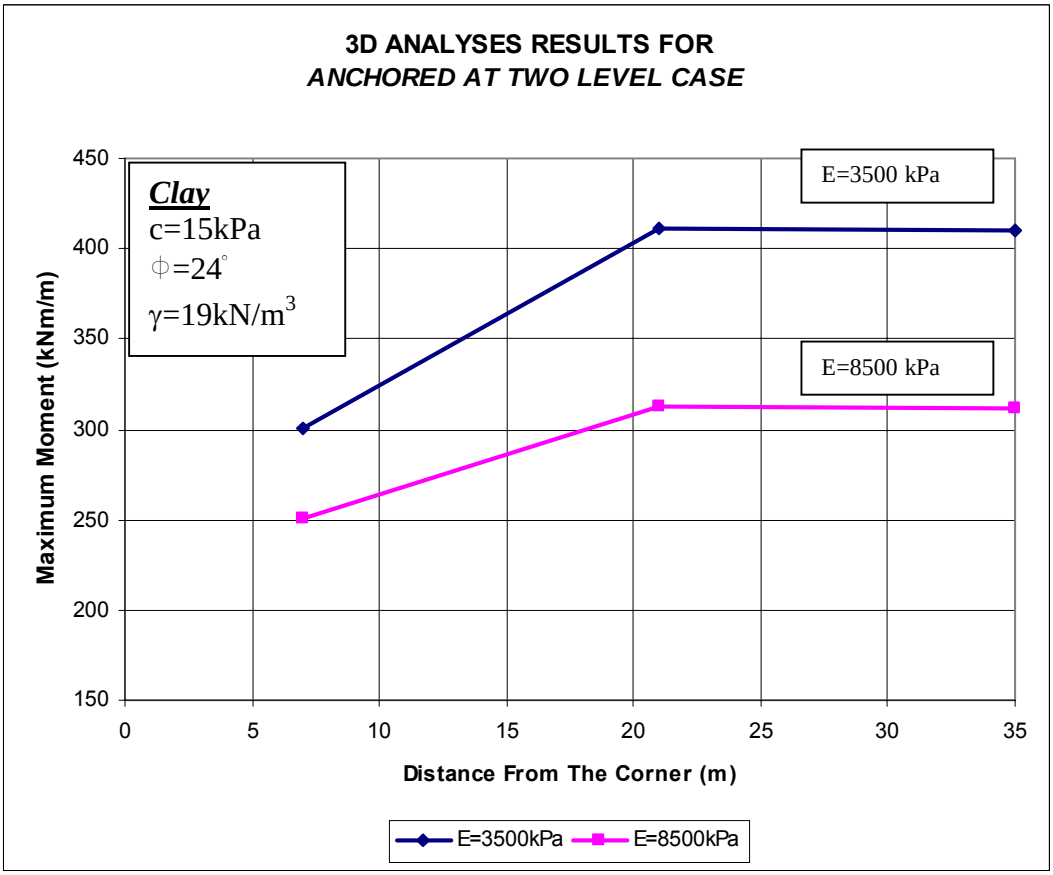

Figure 109. Maximum moments vs. distance from the corner for anchored wall at two level case in 3D analyses

In addition to moments and deflections, effective horizontal stresses of the cases are also examined. Calculated effective stresses are compared with Rankine's active pressures and at rest earth pressures as demonstrated in Figures 110, 111. Effective horizontal stress diagrams are drawn for four different sections;

A-A Section: Distance from the corner = 7m
B-B Section: Distance from the corner = 21m
C-C Section: Distance from the corner = 35m
D-D Section: Distance from the corner = 50m

Following results are obtained;

- According to 3D with corner analyses results, it can be said that effective horizontal stresses for different sections are similar. It shows that there is no significant corner effect on effective horizontal stresses.

- When results obtained from plane strain and 3D with corner analyses are compared, generally similar results are seen but 5-10 kPa differences are observed.

- Below comparisons between theories and results of analyses are obtained;

  0 – 5~6 m: Effective horizontal stresses are bigger than at rest earth pressures. Anchors placed at 2m and 4m depths, restrict the deflections. This restriction is predicted to cause an increase in effective horizontal stresses. As elastic modulus of soil increase, effective horizontal stresses also increase.

  5~6 – 16 m: Effective horizontal stresses are upper bounded by at rest earth pressure line. As elastic modulus of soil increase, effective earth pressures decrease.

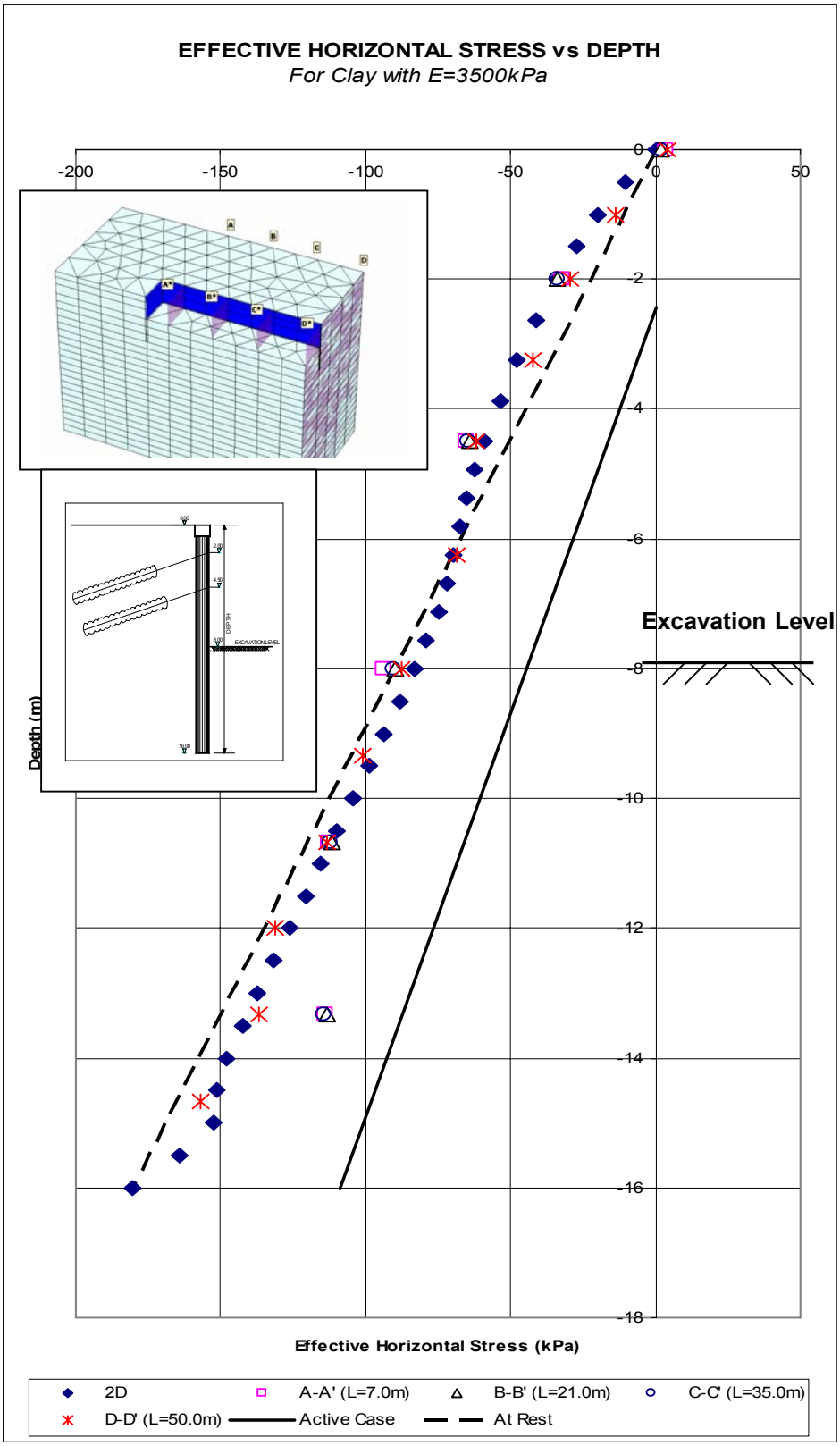

Figure 110. Effective horizontal stress of anchored wall at two levels case vs. depth for clay with E=3500kPa

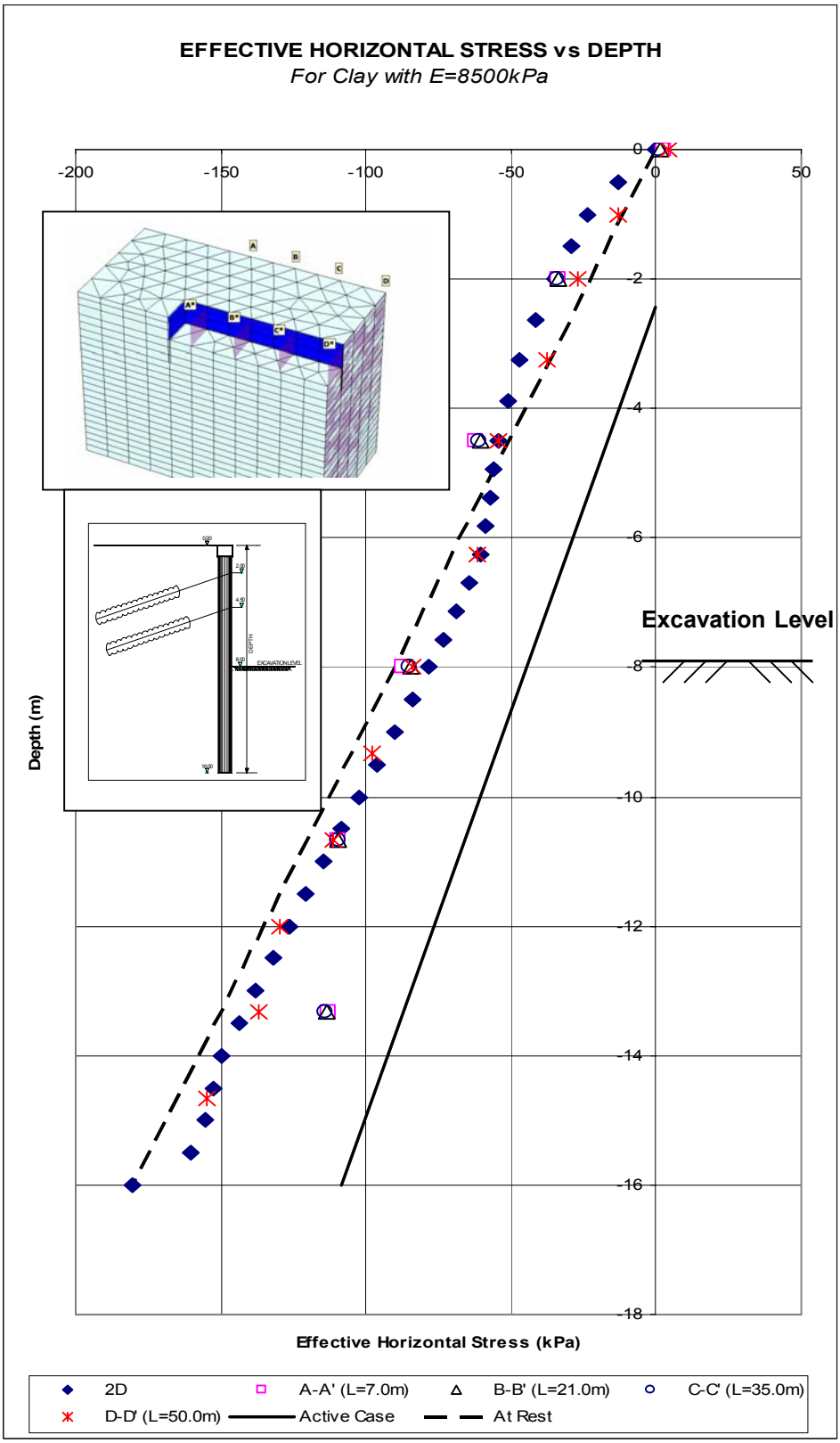

Figure 111. Effective horizontal stress of anchored wall at two levels case vs. depth for clay with E=8500kPa

3.5.3. Anchored Wall at Four Levels Cases

In order to examine anchor loads, a pile wall anchored wall at four levels is modeled. This analysis is performed for soil having 25000kPa elastic modulus value. 200 kN/anchor prestresses are applied to anchors. Anchor loads are obtained from 3D with corner and plane strain analyses. Mesh distributions used in the analysis are demonstrated in Figures 112, 113.

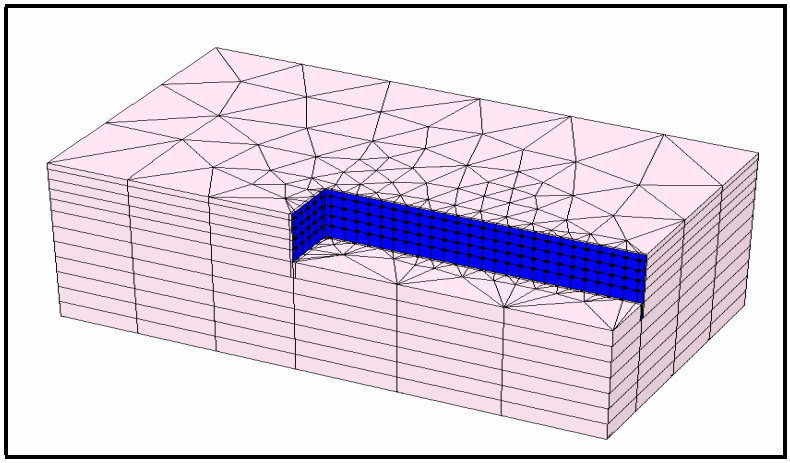

Figure 112. Finite element mesh used in 3D analyses of anchored wall at four levels case

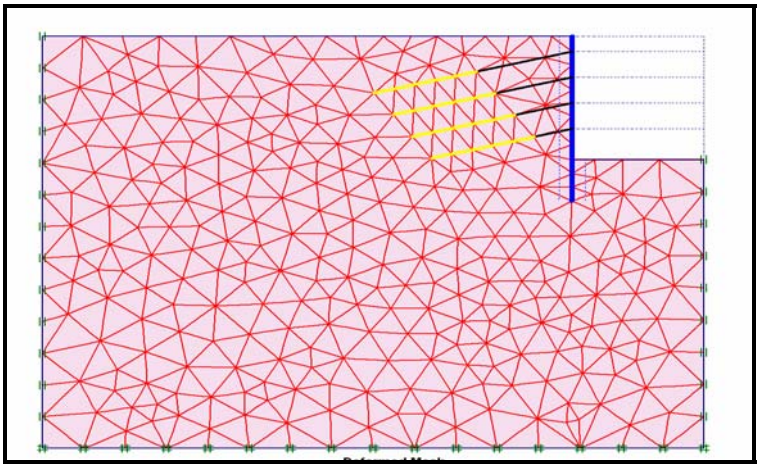

Figure 113. Finite element mesh used in 2D analyses of anchored wall at four levels case

Anchor loads dispersion through the excavation side is shown in Figure 114. Following results are obtained;

- Anchor loads obtained from 3D analyses, shows an increasing trend up to 15m distance from the corner. After 15m distance from the corner, anchor loads are nearly constant. The corner effect on anchor loads diminishes at 10-15m distance from the corner.

- It is found that some fluctuations in the magnitude of anchor loads occur after 30m distance from the corner in 3D analyses. However, the best line of anchor loads can be seen easily. It is predicted that these fluctuations are results of mesh generation process and sensitivity of the programme.

- When results of plane strain and 3D analyses are compared, it is found that first and second level anchor forces are higher, third level forces are comparable to 2D analysis. The magnitude of fourth level anchor force however is slightly smaller in 3D analysis as compared to plane strain case.

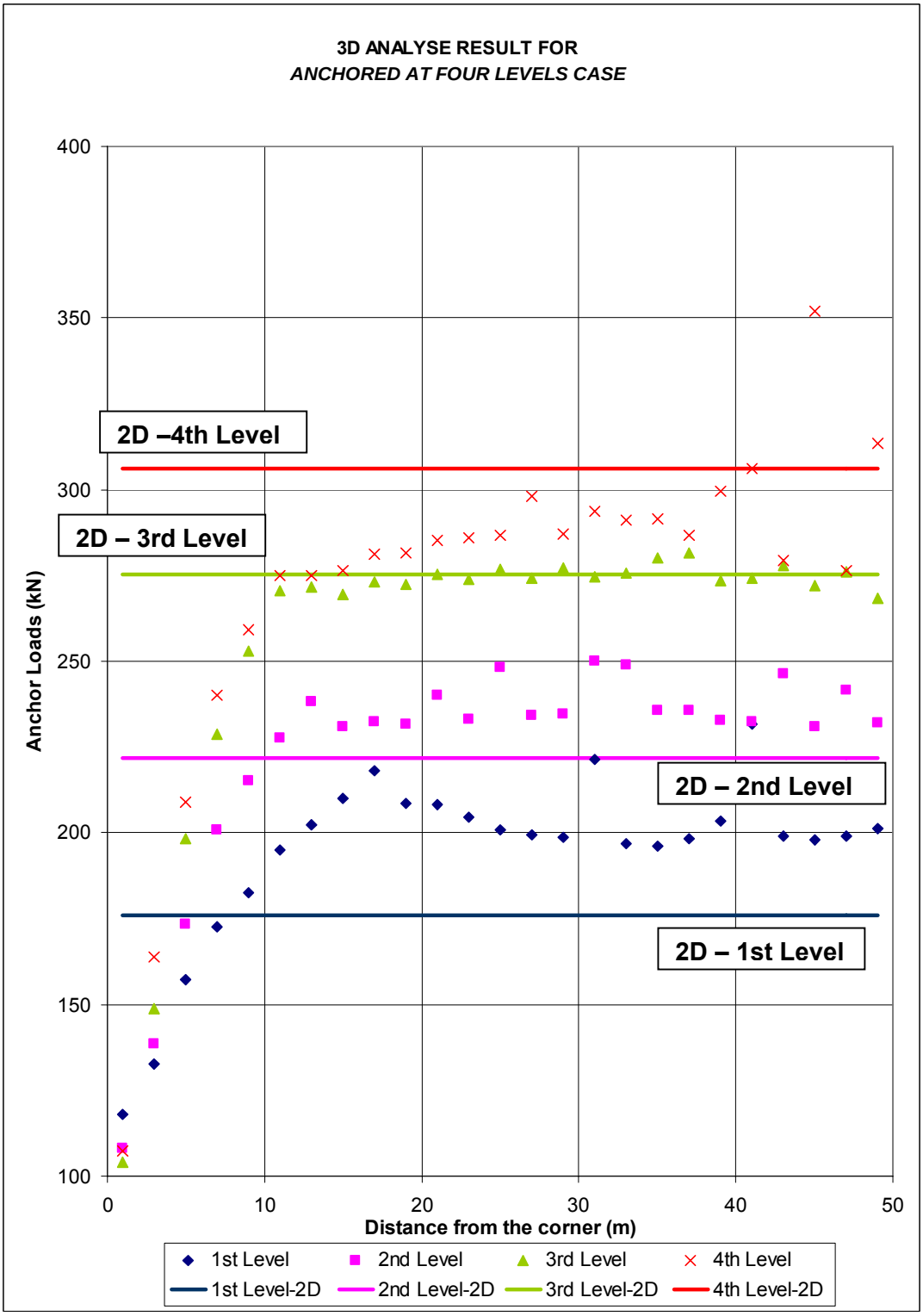

Figure 114. Anchor loads vs. distance from the corner for anchored wall at four levels

In addition to anchor loads, deflection behavior of this case is studied. Deflection vs. depth plots are shown in Figure 115. Following results are obtained,

- Up to 20m distance from the corner, as distance from the corner increase, deflections increase. After 20m distance, deflections become nearly constant. Therefore it can be said that corner effect on deflection is observed up to 20m distance from the corner.

- The deflection patterns of plane strain and 3D analyses are similar. However observed maximum deflections of plane strain analyses are 5-10mm smaller than the 3D ones.

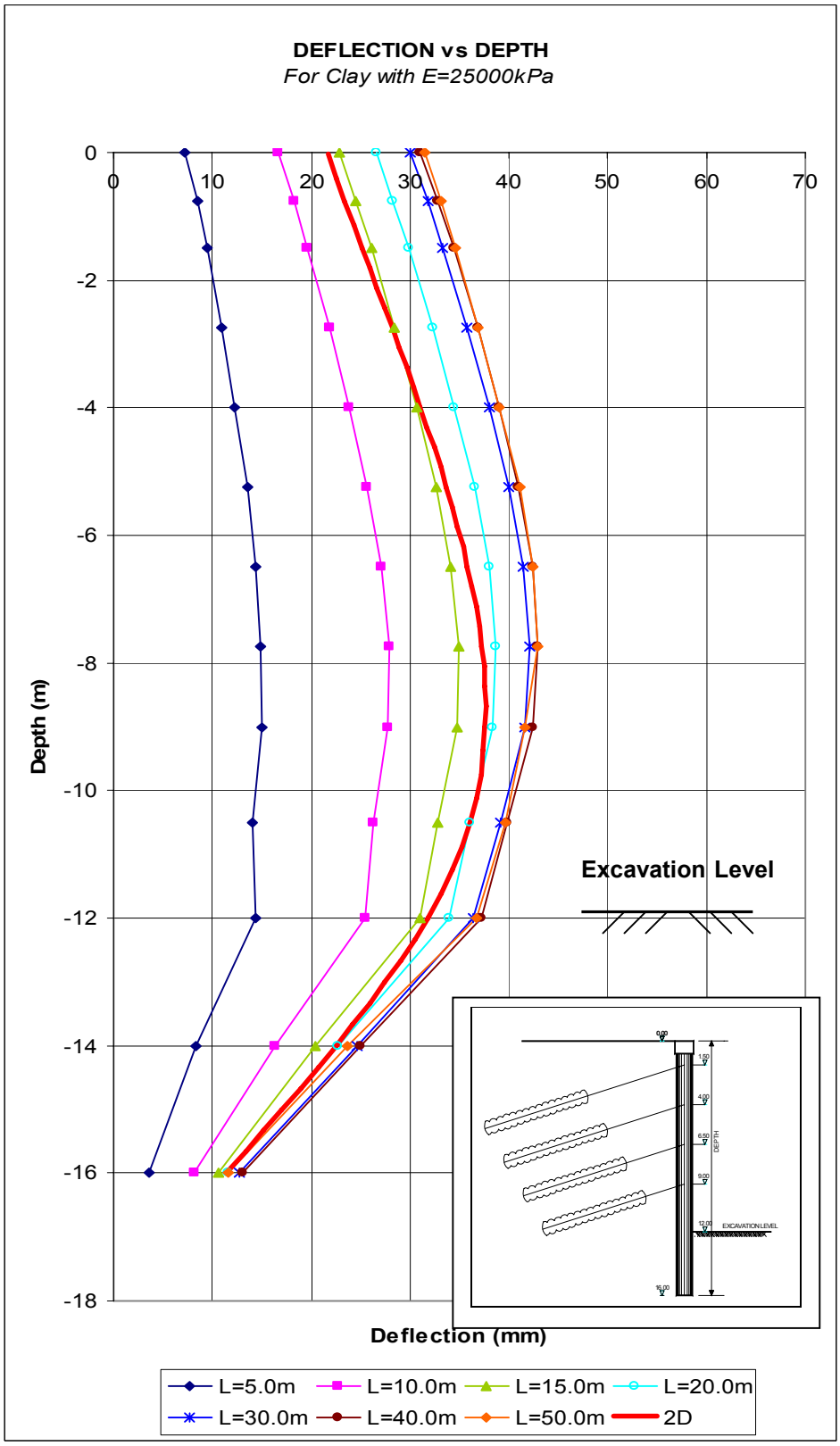

Figure 115. Deflection of anchored wall at four levels case vs. depth for clay with E=25000kPa

Deflection over maximum deflection ratios, which is the ratio of maximum wall displacement of a section to maximum wall displacement of in-situ wall, increase up to 20m distance from the corner. After this distance the ratio become nearly constant as shown in Figure 116.

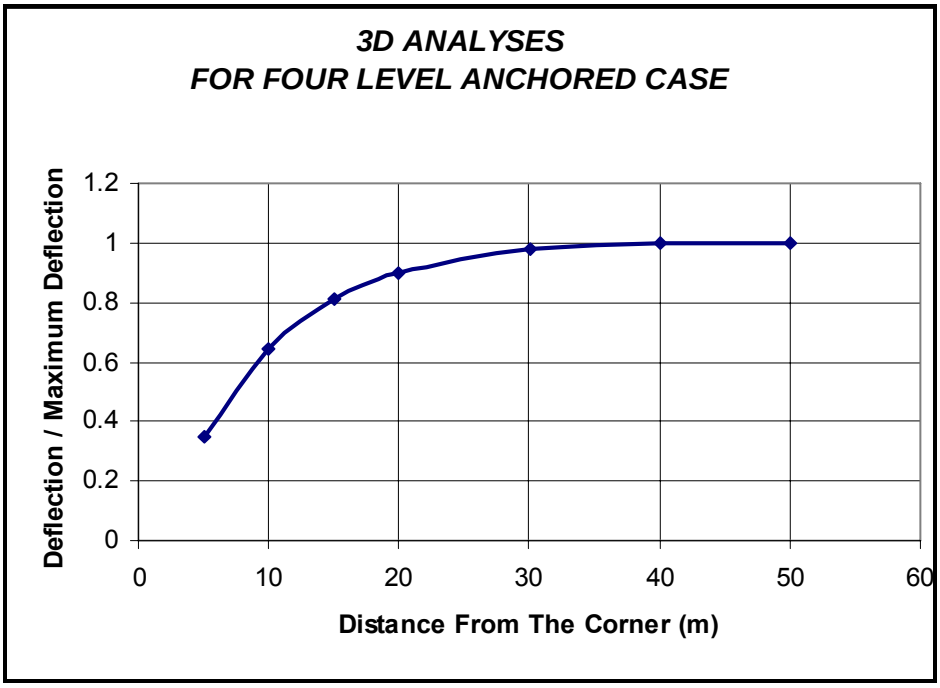

Figure 116. 'Deflection / Maximum Deflection ratios' vs. distance from the corner for anchored wall at four level case in 3D analyses

Moment behavior of the case is also studied, and demonstrated in Figure 117. Following results are obtained;

- Significant corner effect on moment is observed up to 15m distance from the corner. After this distance, moments are nearly constant.

- Moment diagram patterns of plane strain and 3D analyses are different. Sudden decreases and increases in moment diagrams are observed at anchor levels in plane strain analyses.

- Moment obtained from plane strain analyses is 200 kNm/m smaller than maximum moment of 3D analyses.

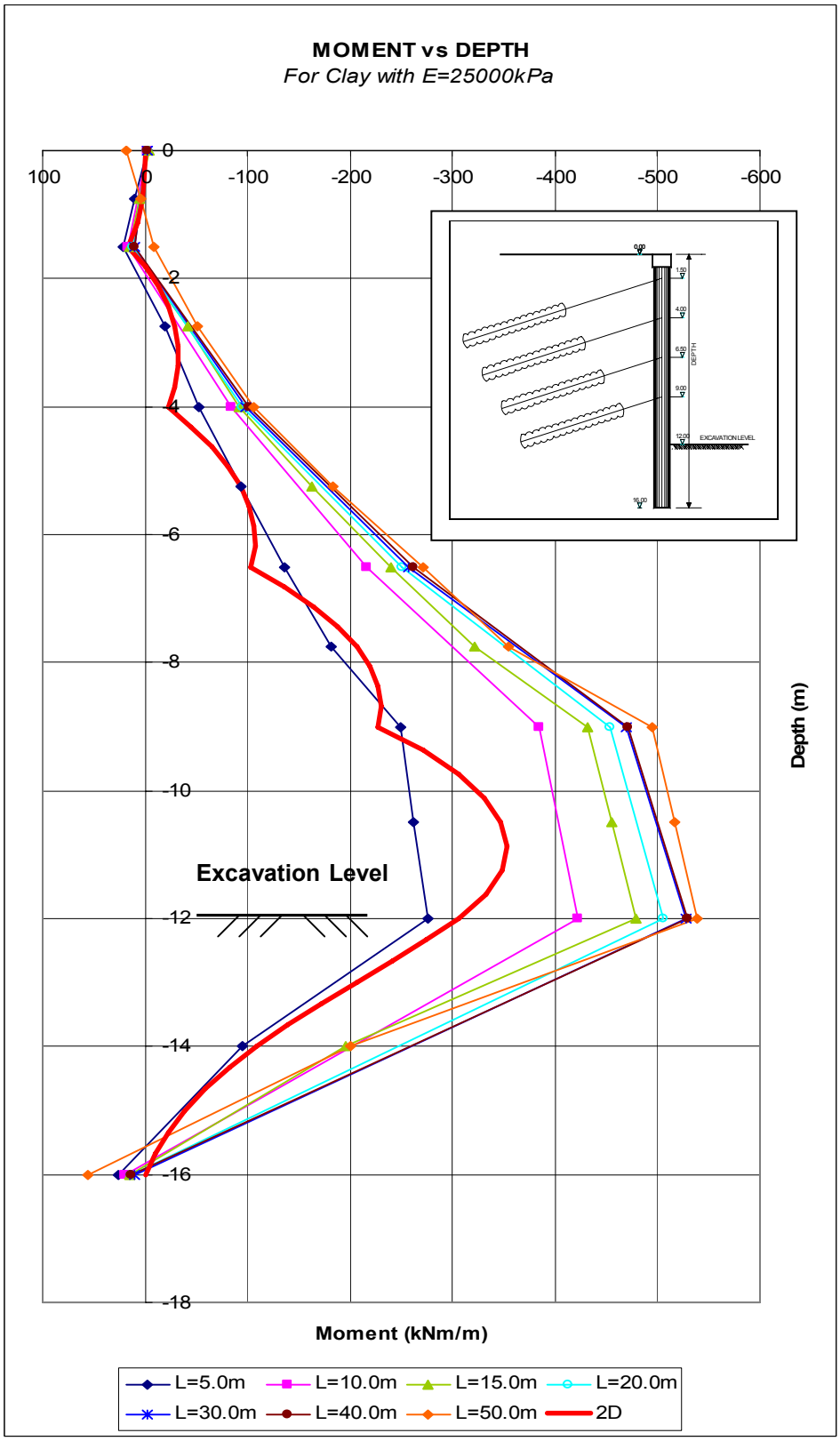

Figure 117. Moments of anchored wall at four levels case vs. depth for clay with E=25000kPa

3.5.4. Conclusions and Discussions

- Deformation

- For all support systems and all elastic modulus of soil values, it is observed that corner effect is observed up to 20m distance from the corner, after this distance deflection is nearly constant.

- As elastic modulus of soil decrease, maximum deflection throughout the excavation side increase. Moreover, as elastic modulus of soil decrease, 'deflection over maximum deflection ratio' also decreases.

- When deflection results of plane strain and 3D analyses are compared, it is seen that in cantilever cases; maximum deflections of plane strain analyses are two times of 3D results. In anchored wall at one level and two levels cases; the deflection of plane strain analyses is toward retained soil side at top few meters of the piles. This kind of a movement is not observed in 3D analyses.

- Deflection toward retained soil side is not observed in plane strain analyses of anchored wall at four levels case. Therefore it can be said that as excavation depth and number of anchor levels increase, deflection toward retained soil side decrease and deformation pattern of the plane strain and 3D analyses becomes similar.

- In order to describe deflection behavior of a wall section, Deflection / Maximum Deflection ratio is used in this study. This ratio is the ratio of maximum wall displacement of a section to maximum wall displacement of this in-situ wall. For the same distance from the corner, as elastic modulus increase, deflection over maximum deflection ratio increase. Therefore, it can be claimed that as elastic modulus increase, corner effect on deflection decrease.

- As stiffness of the system increase, deflection / maximum deflection ratio increase as shown in Figure 118. Therefore it can be claimed that as stiffness of the system increase, corner effect on deflection decrease.

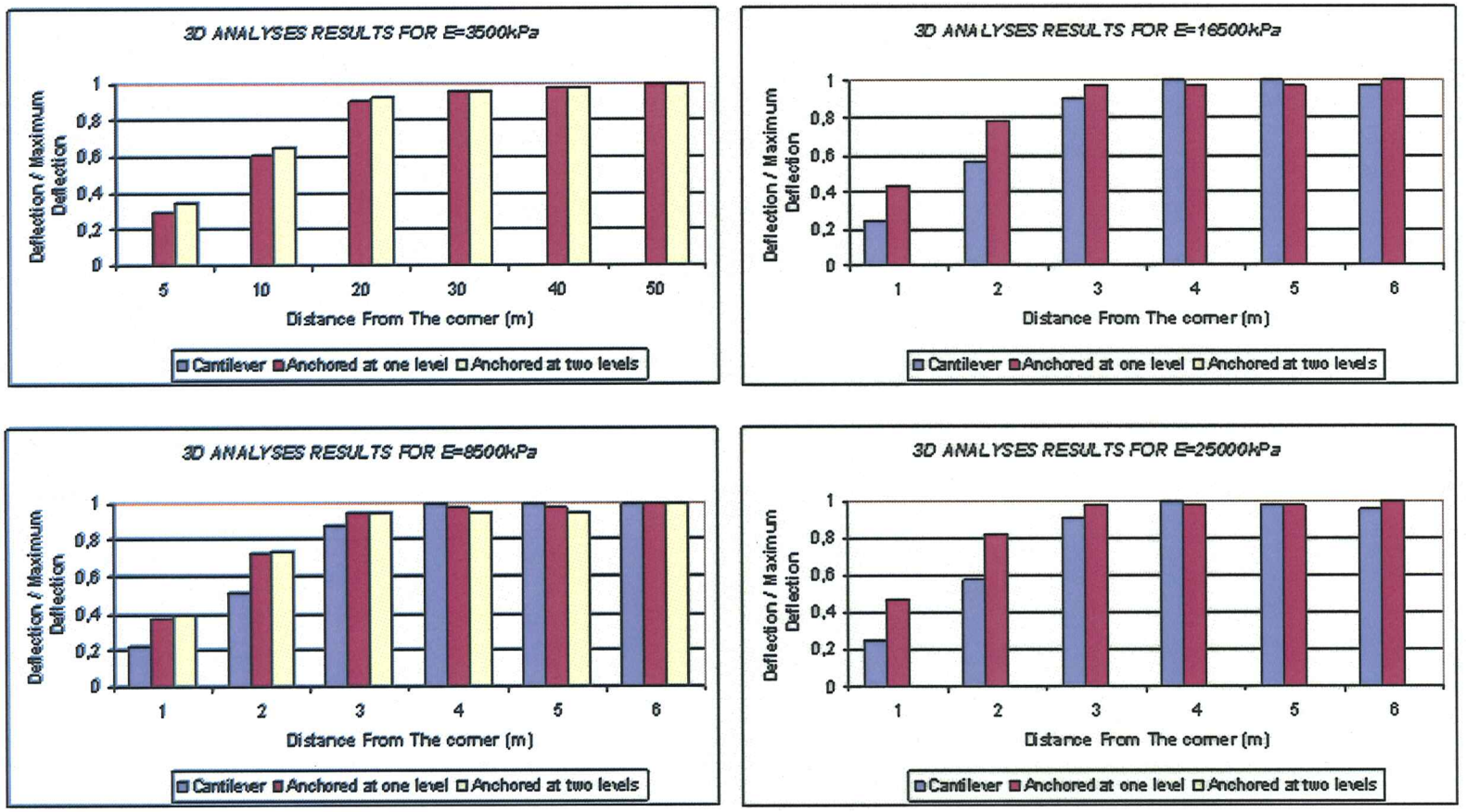

Figure 118. 'Deflection / Maximum Deflection values vs. distance from the corner for all cases in 3D analysis

- Moment

  - It is found that corner effect on moment diminish at nearly 20m distance from the corner.

  - As elastic modulus of soil increases, moment difference between A-A (distance from the corner: 7m) and D-D (distance from the corner:50m) decreases. Therefore it can be claimed that as elastic modulus of soil increases, corner effect on moment decreases.

  - Two types of moment diagrams are obtained from cantilever analyses; type-a: typical moment diagram of cantilever case, type-b: typical moment diagram of in-situ walls supported by struts. Results of 3D analyses are similar to type-b, but as distance from corner increase, moment type is getting similar to type-a. Therefore, it is claimed that moment diagram obtained around corner in 3D analyses and diagrams obtained from plane strain analyses by modeling the corner as a strut are quite similar.

  - In anchored one, two, and four levels cases; corners do not affect moment patterns. It shows that as effectiveness of the supporting system increases, the corner effect decreases (claimed by Liu (1995)).

- Anchor Loads

  - The anchor loads increase until 10-15m distance from the corner. After this distance they become nearly constant.

  - When results of plane strain and 3D analyses are compared, It is found that first and second level anchor forces are higher, third level forces are comparable to 2D analysis. The magnitude of fourth level anchor force however is slightly smaller in 3D analysis as compared to plane strain case.

- Effective Horizontal Stresses

  - Effective horizontal stresses of different cross sections are close to each others. Corner effect on effective horizontal stresses is not apparent. Also plane strain and 3D results are similar.

- Generally the effective horizontal stresses are upper bounded by at rest earth pressure line and lower bounded by active earth pressure line. However, at anchor levels, as deflection is restricted, effective horizontal stresses are bigger than at rest earth pressures. Moreover, in cantilever case, effective horizontal stresses above excavation level are upper bounded by active earth pressure line.

- As elastic modulus of soil increases: above anchor level, effective horizontal stresses increase; below anchor level, effective horizontal stresses decrease.

CHAPTER 4

BEHAVIOR OF ANKARA-ÇANKAYA TRADE CENTER AND RESIDENCE EXCAVATION

4.1. General

Ankara Çankaya Trade Center and Residence Construction is surrounded by İran Avenue, 8 story building, open land and embassy site as demonstrated in Figure 119. The area of the excavation pit is about 5540 m^2 in plan view as shown in Figure 120. Elevation of the site changes between 945-950m and excavation level is fixed to 938.7m. Therefore excavation depth of the site changes from 6 to 11m. The deepest part of the excavation is near the embassy site.

4.2. Subsoil Conditions

Seven boreholes for foundation design (S1-S7) and three boreholes (S8-S10) for in-situ wall design of embassy site part are drilled (see Figure 120). Fill, Alluvium, Ankara Clay and altered Greywacke are observed in S1-S7 borings. On the other hand, between S8 and S10 borings only altered Greywacke is observed. Since the behavior of the excavation near the embassy site is concerned in scope of this chapter, only relevant soil parameters for altered Greywacke are derived.

Green, gray and brown colored; slightly to moderately weathered Greywacke with quartz is observed at the site. Total core recovery of the material changes between 12-100%; rock quality designation (RQD) of the Greywacke changes between 0-38% but mostly 0% is observed. Cores obtained from S8-10 borings are demonstrated in Figure 121 and boring logs of S8-10 are given in Appendix A.

Figure 119. Views of the site

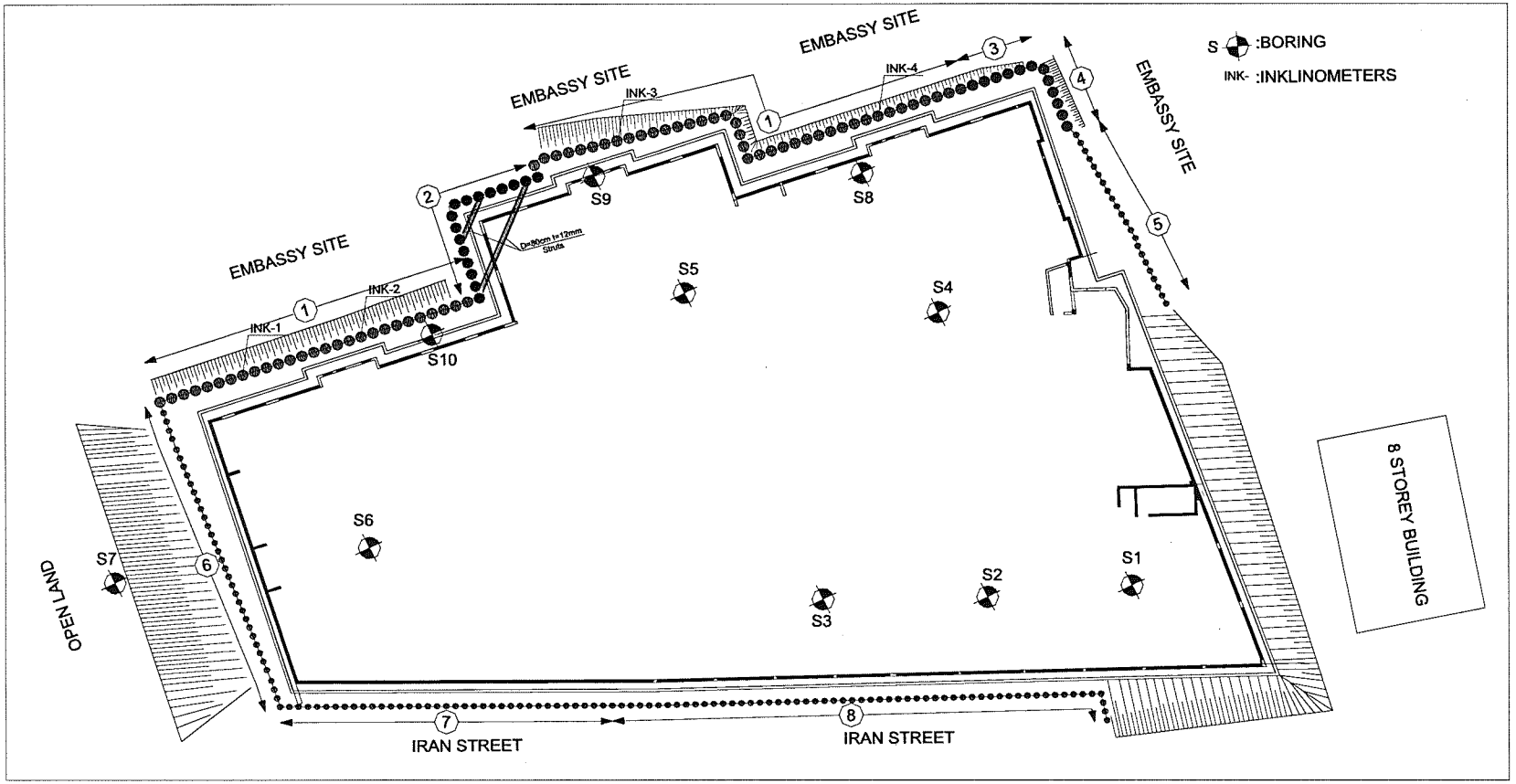

Figure 137. Plan view of the site, location of borings and inclinometers, support system types

Figure 121. Core samples taken from S8, S9, S10

Back analyses of wall deformation are performed for the retaining system near the embassy site. Numerous modulus of elasticity, friction angle and cohesion values are entered to 3D Analyses program until the measured and calculated deformations matches. According to the back analyses soil profile and soil parameters are derived. Resulting soil profile is demonstrated in Figure 122.

4.3. Support System

Elevation differences at the site, diplomatic problems with embassy and limitations of architecture forced designers to design eight types of support systems for this site as summarized in Table 3. Assigned type numbers to support systems are demonstrated in Figure 120.

At the side that neighbors the embassy site (Types 1, 2, 3, 4); there is no chance to support the piled wall by anchors due to diplomatic reasons. Consequently 120cm piles with 135cm spacing are constructed with no supporting for this part. For Type-5, a composite system composed of wall and bored piles have to be constructed, because of architectural limitations of a garage entry.

Cross sectional views of Type-1 and Type-6, which are modeled for analyses, are shown in Figure 123.

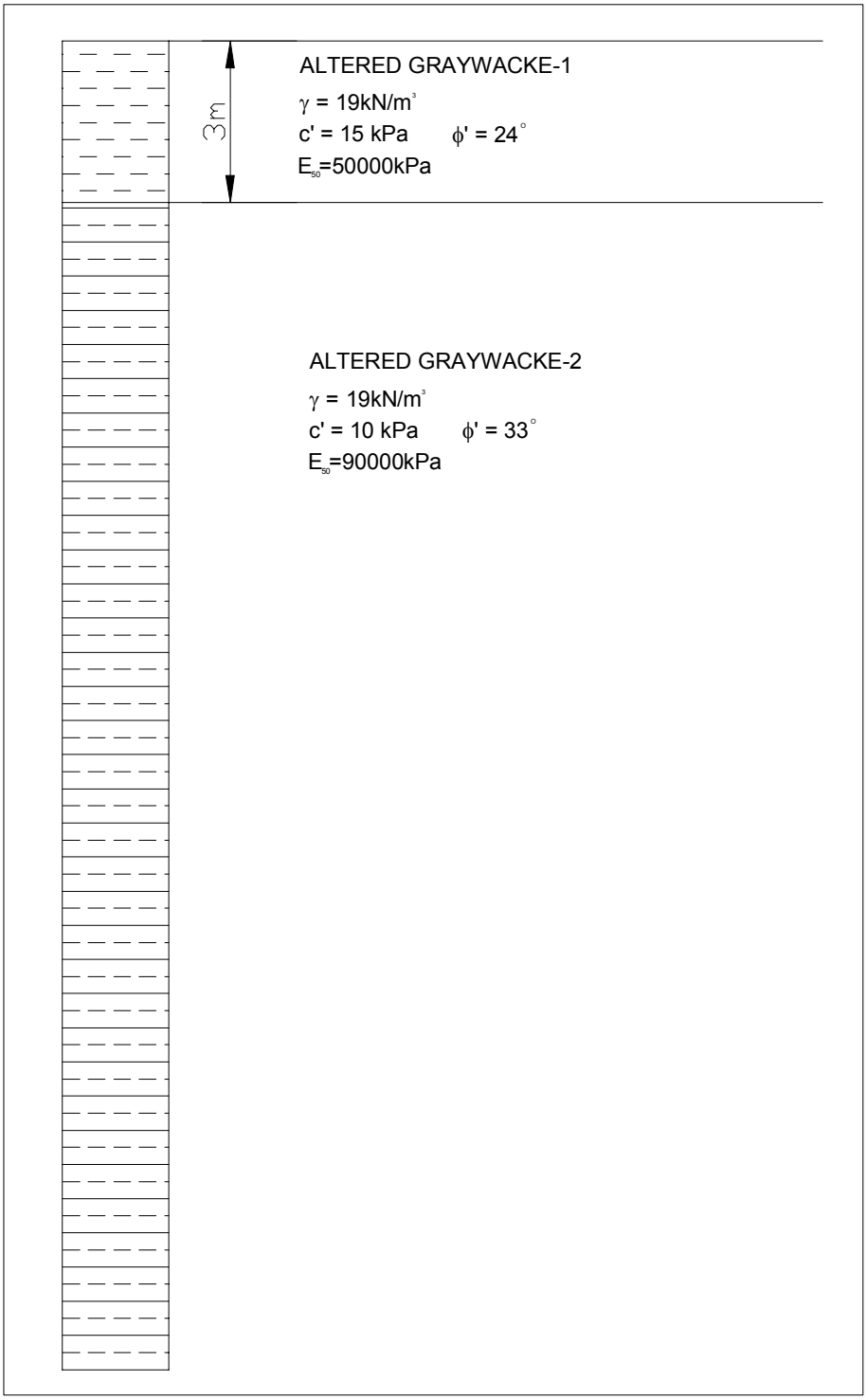

Figure 122. Back calculated soil profile

Table 3. Properties of support system type

Type number of the systems	Top elevation of the system	Bored pile diameter / spacing	Pile Length	Anchor / strut levels	Surcharge effect near the system
1	947.5	120cm/135cm	16.5m	Not applicable	100kPa
2	949.0	120cm/135cm	18.0m	Strut Level: 949.0	100kPa
3	947.5	120cm/135cm	21.0m	Not applicable	100kPa
4	946.0	120cm/135cm	16.5m	Not applicable	-
5	946.0	65cm/100cm and wall	15.5m	Not applicable	-
6	945.0	65cm/100cm	12.0m	Anchor levels: 943.5 and 941.5	-
7	947.0	65cm/100cm	12.0m	Anchor levels: 945.0 and 942.5	-
8	945.0	65cm/100cm	12.0m	Anchor levels: 943.5 and 941.0	-

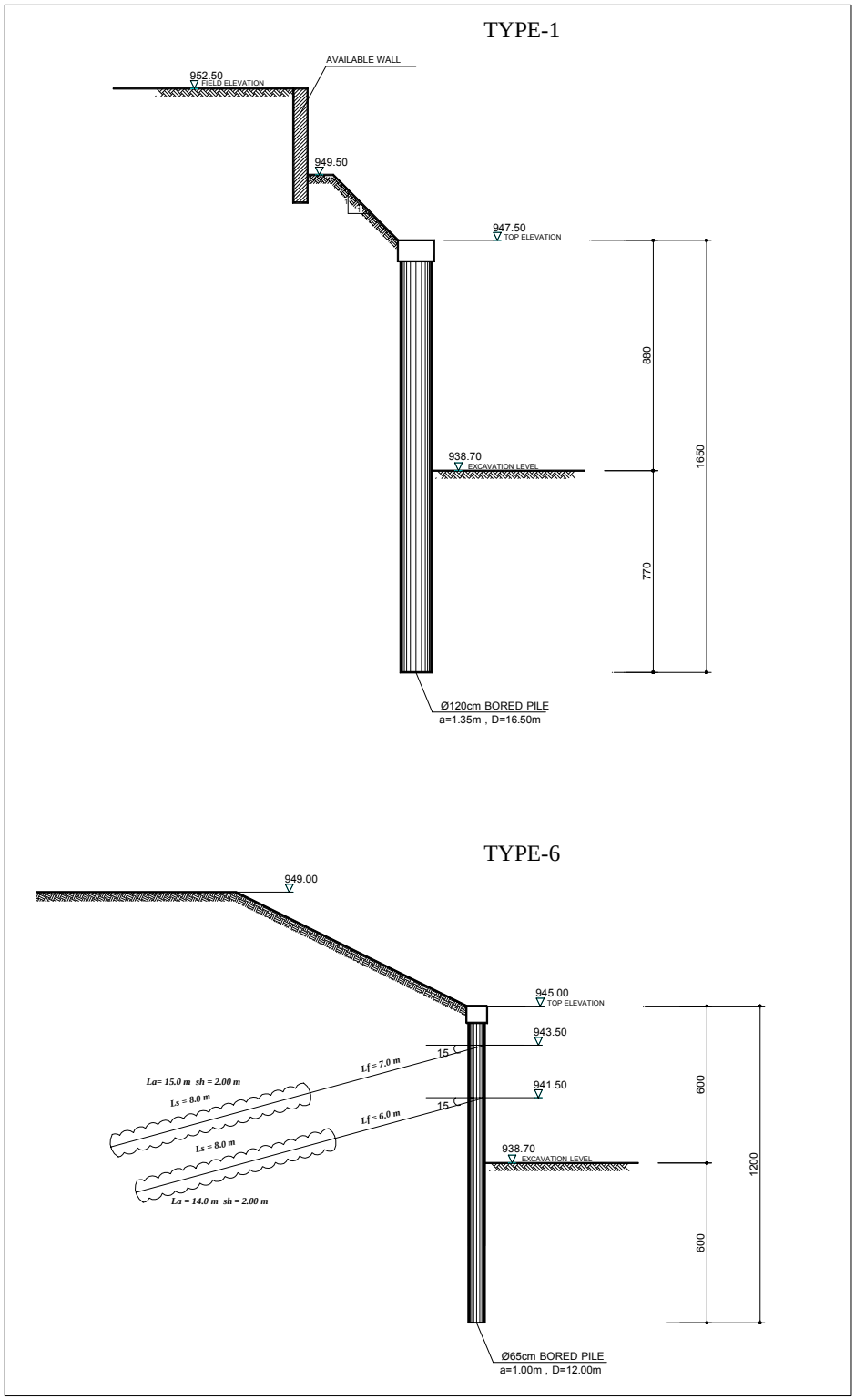

Figure 123. Cross-sections of Type-1 and Type-6

4.4. Monitoring System

The deflection behavior of type-1 system is monitored by using four inclinometers placed inside the 120cm piles as shown in Figure 67. Distances of inclinometer pipes (from INK-1 to INK-4) to the corner, which is the intersection point of type-1 and type-6, are 9.25m, 27.25m, 56.50m, 88.00m, respectively. Frequent sets of readings are taken from inclinometers;

INK-1 → Two sets of readings (after second reading, inclinometer pipe is broken by mistake during construction)

INK-2 → Six sets of readings

INK-3 → Four sets of readings

INK-4 → Four sets of readings

Inclinometer measurements are given in Appendix B.

4.5. Finite Element Analyses

Plane strain and 3D analyses are made to model the part near the embassy site. In plane strain analyses only type-1, where inclinometers are placed is modeled. In 3D Analyses, in addition to type-1; type-2, type-3, type-4, type-5 and type-6 are also simulated in the same model by using the advantages of 3D analyses.

Some simplifications are made for modeling. There was a beveled excavation and a wall near the embassy site before the construction. This wall was constructed because of the elevation difference between the construction site and the neighbor site in the past (as shown in Figure 123, type-1 cross sectional view). Instead of modeling the wall, the sloped excavation and the elevation difference; the part beside the wall is assumed at the same elevation of the construction site and the load caused by the elevation difference is reflected as surcharge load. One more simplification had to be made for type-5 system. Because of the architectural limitations, a pile-wall composite system with variable top elevation had to be applied for this part. The equivalent diameter is actually different for the wall and the piles; however same equivalent diameter is assigned for both in order to simplity data entry process. Moreover, fixed top elevation is applied at this part.

Hardening Soil Model is used for simulating the behavior of greywacke. As no water table was observed at the site, drained material type is selected.

In both 2D and 3D analyses, 15 nodded triangular elements are used. In 2D analyses, plane strain model is utilized. For simulation of the elevation difference between the construction site and the neighbor site, 100kPa surcharge load is applied. Interfaces are also utilized to simulate the interaction between the piles and the soil.

The finite element meshes used for 2D and 3D analyses are demonstrated in Figure 124 and Figure 125.

Soil parameters used for modeling are summarized in Table 4.

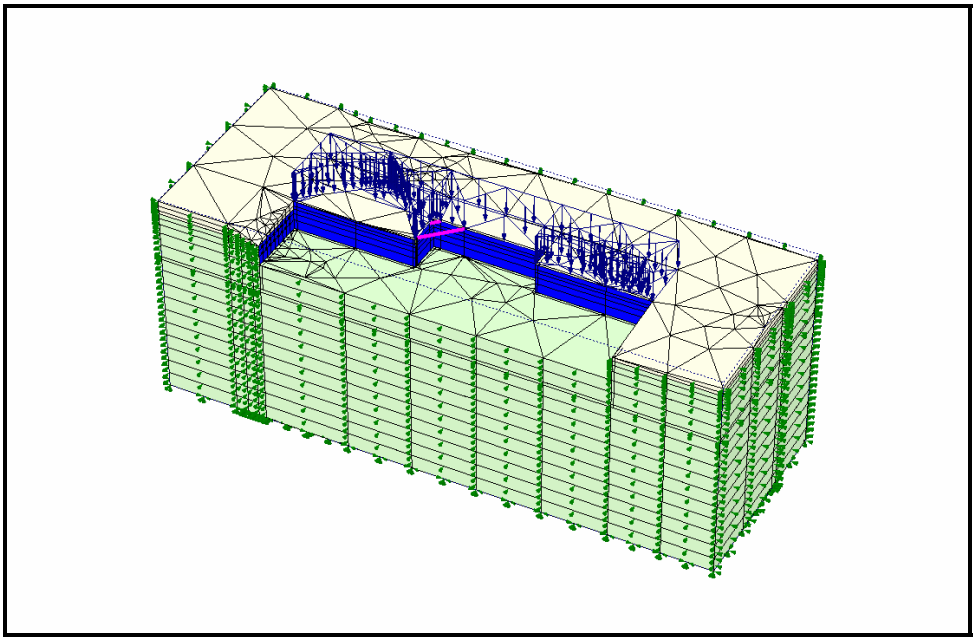

Figure 124. Finite element mesh used in 3D analyses

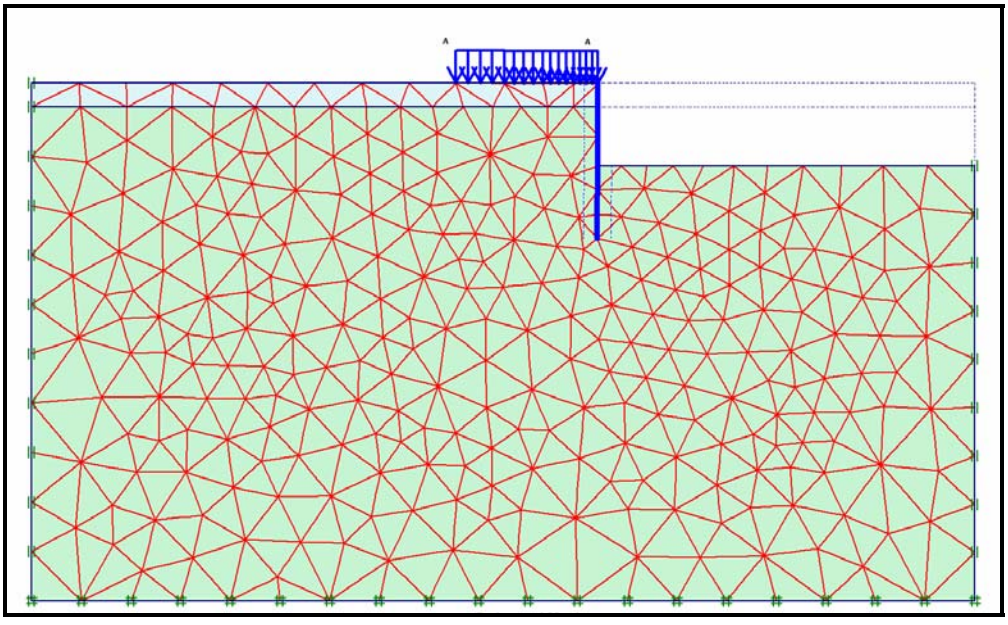

Figure 125. Finite element mesh used in 2D analyses

Table 4. Soil properties used in analyses

PARAMETER	NAME	ALTERED GRAYWACKE-1	ALTERED GRAYWACKE-2	UNIT
Material Model	*Model*	HSM	HSM	-
Material Behavior	*Type*	Drained	Drained	-
Unsaturated Soil Weight	γ_{unsat}	19	19	kN/m^3
Saturated Soil Weight	γ_{sat}	19	20	kN/m^3
Secant Stiffness for CD Triaxial Test	E_{50}^{ref}	50000	90000	kN/m^2
Tangent Oedometer Stiffness	E_{oed}^{ref}	50000	90000	kN/m^2
Unloading/Reloading Stiffness	E_{ur}^{ref}	150000	270000	kN/m^2
Power Stress Level Dependency of Stiffness	*Model*	0,5	0,5	-
Cohesion	c_{ref}	15	10	kN/m^2
Friction Angle	ϕ	24	33	°
Dilatancy Angle	ψ	0	3	°
Poisson's Constant	ν_{ur}	0,2	0,2	-
Interface Reduction Factor	R_{inter}	0,7	0,7	-

4.6. Results of Finite Element Analyses

Deflections, moments and horizontal effective stresses of type-1 are studied by using 2D and 3D finite element programs.

Deflections obtained from analyses are compared with measured data as shown in Figures 126, 127, 128, 129. Following results are obtained;

- Calculated deflections obtained from 3D analyses and measured deflections match.
- Calculated deflections, that are obtained from 3D without corner and plane strain analyses, are much higher than the measured values.
- The difference between deflections of 3D without corner and plane strain analyses is nearly 30mm.

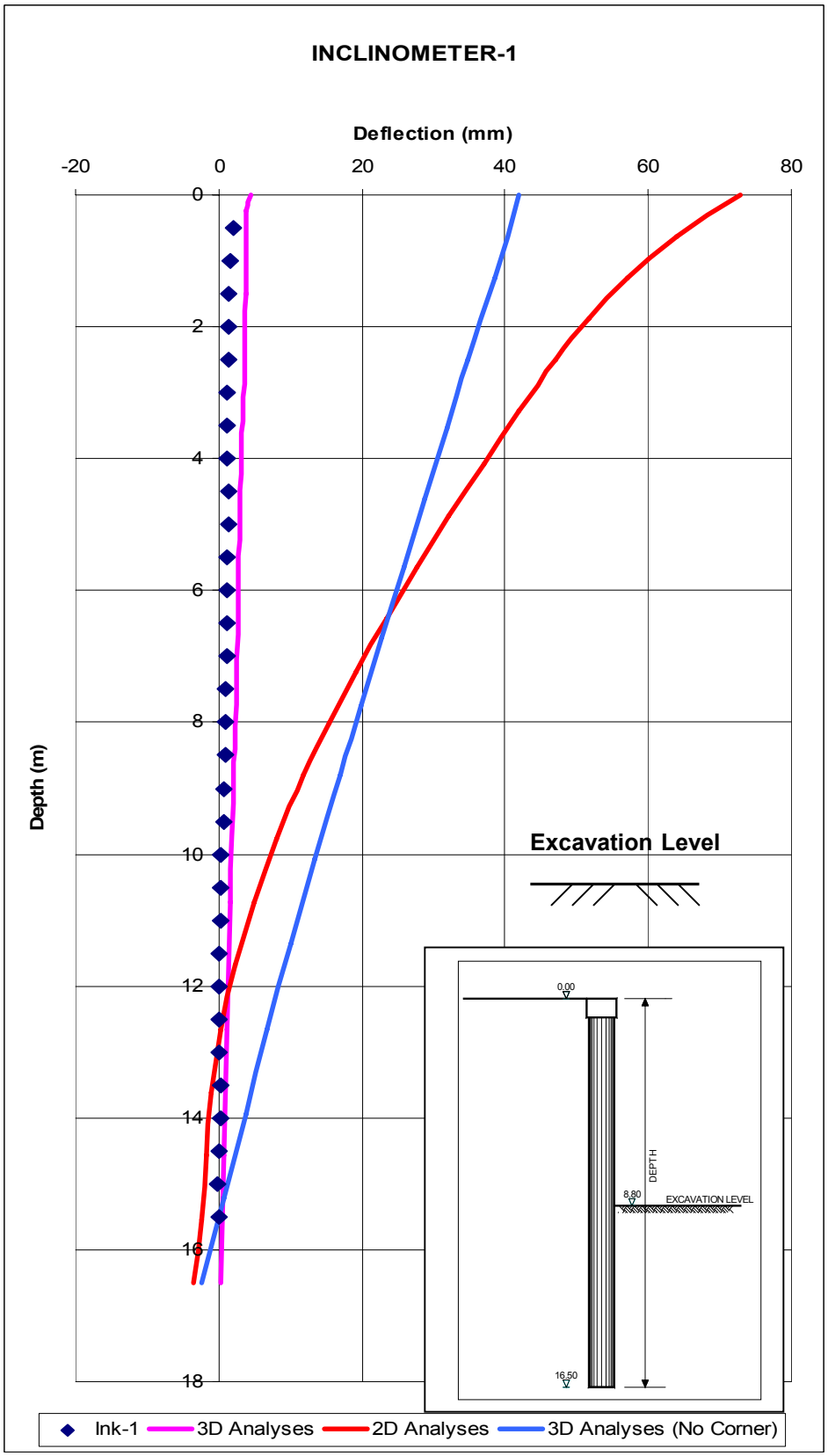

Figure 126. Deformation vs. depth plot for Inclinometer-1 section

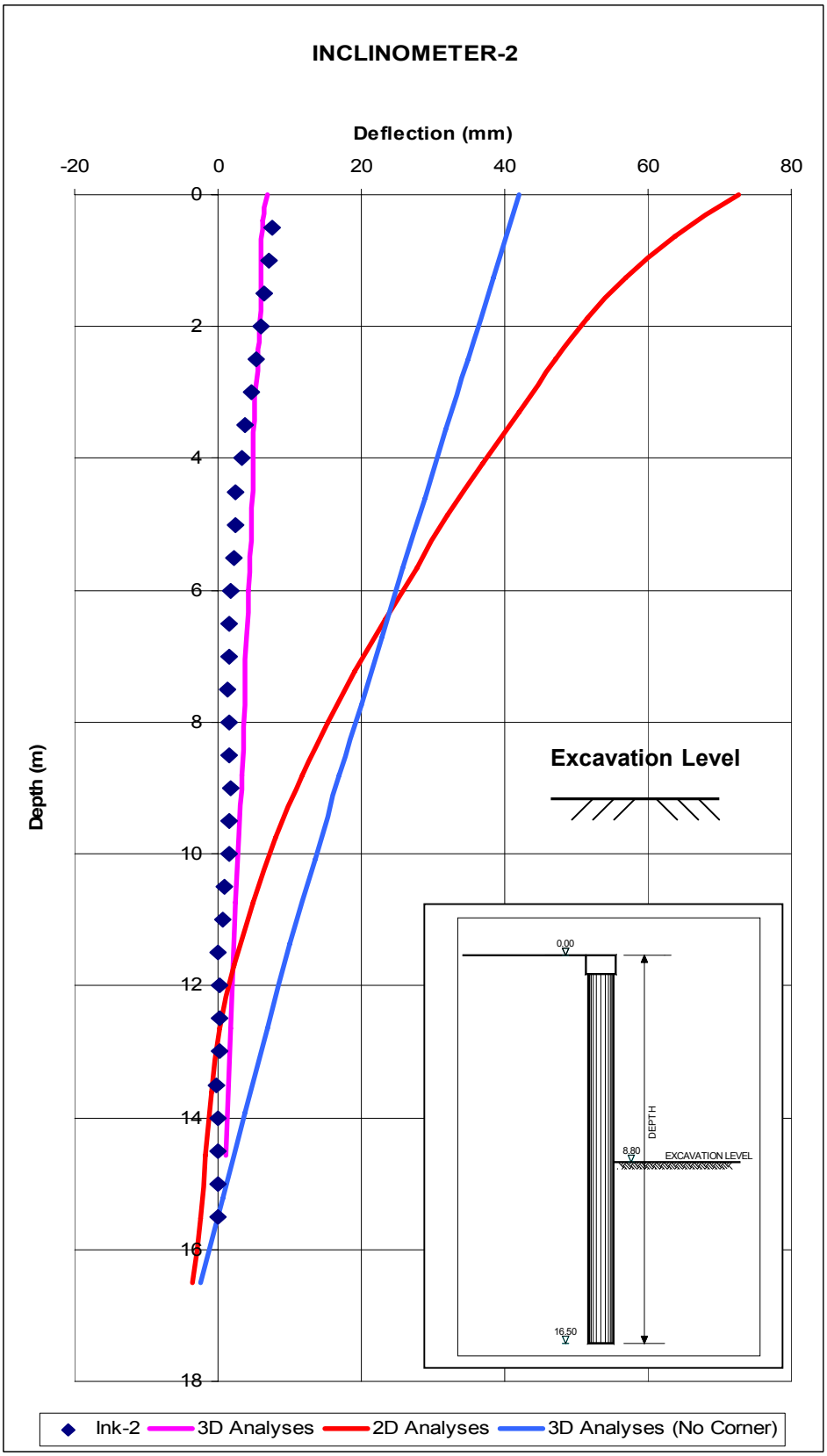

Figure 127. Deformation vs. depth plot for Inclinometer-2 section

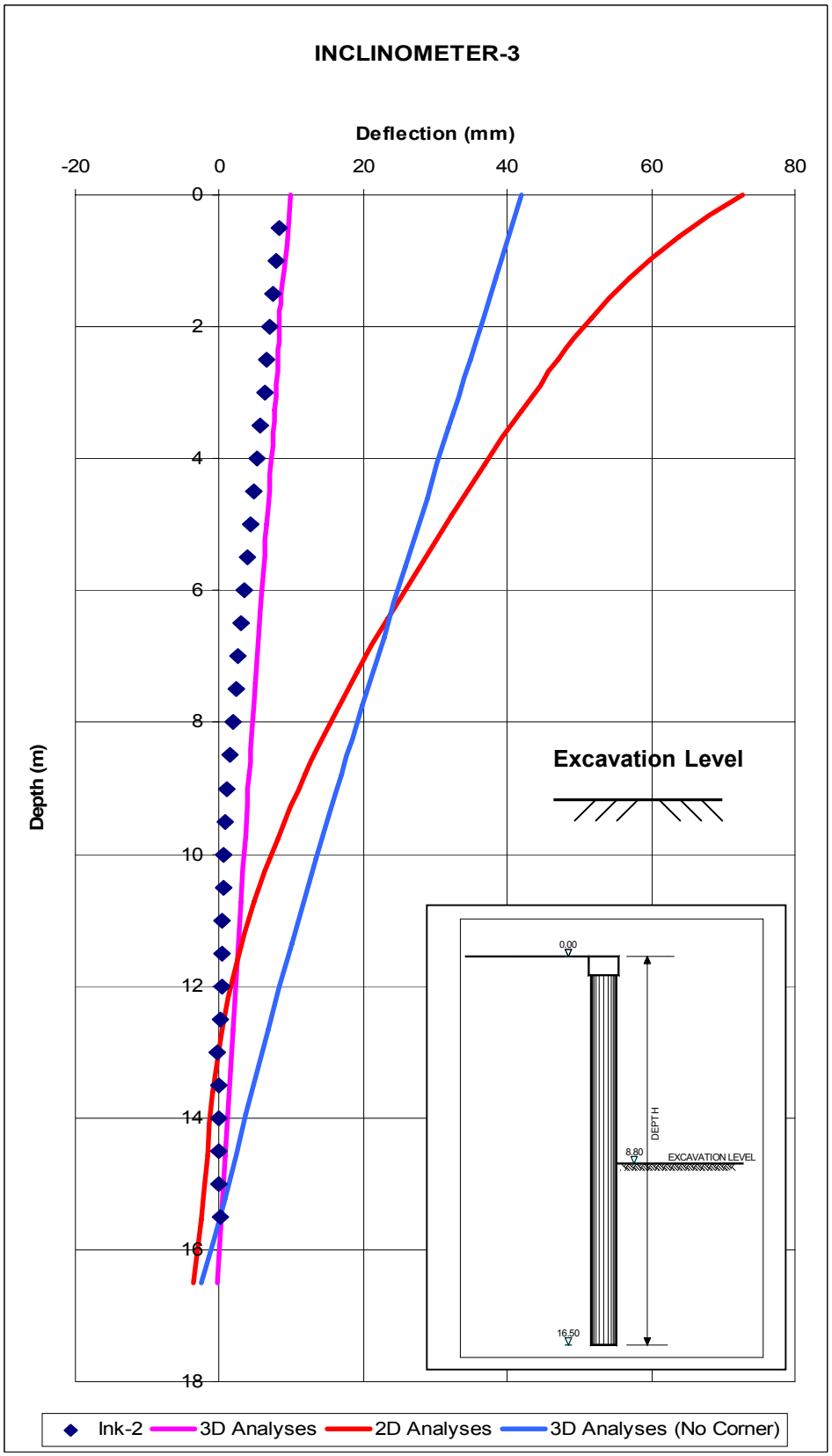

Figure 128. Deformation vs. depth plot for Inclinometer-3 section

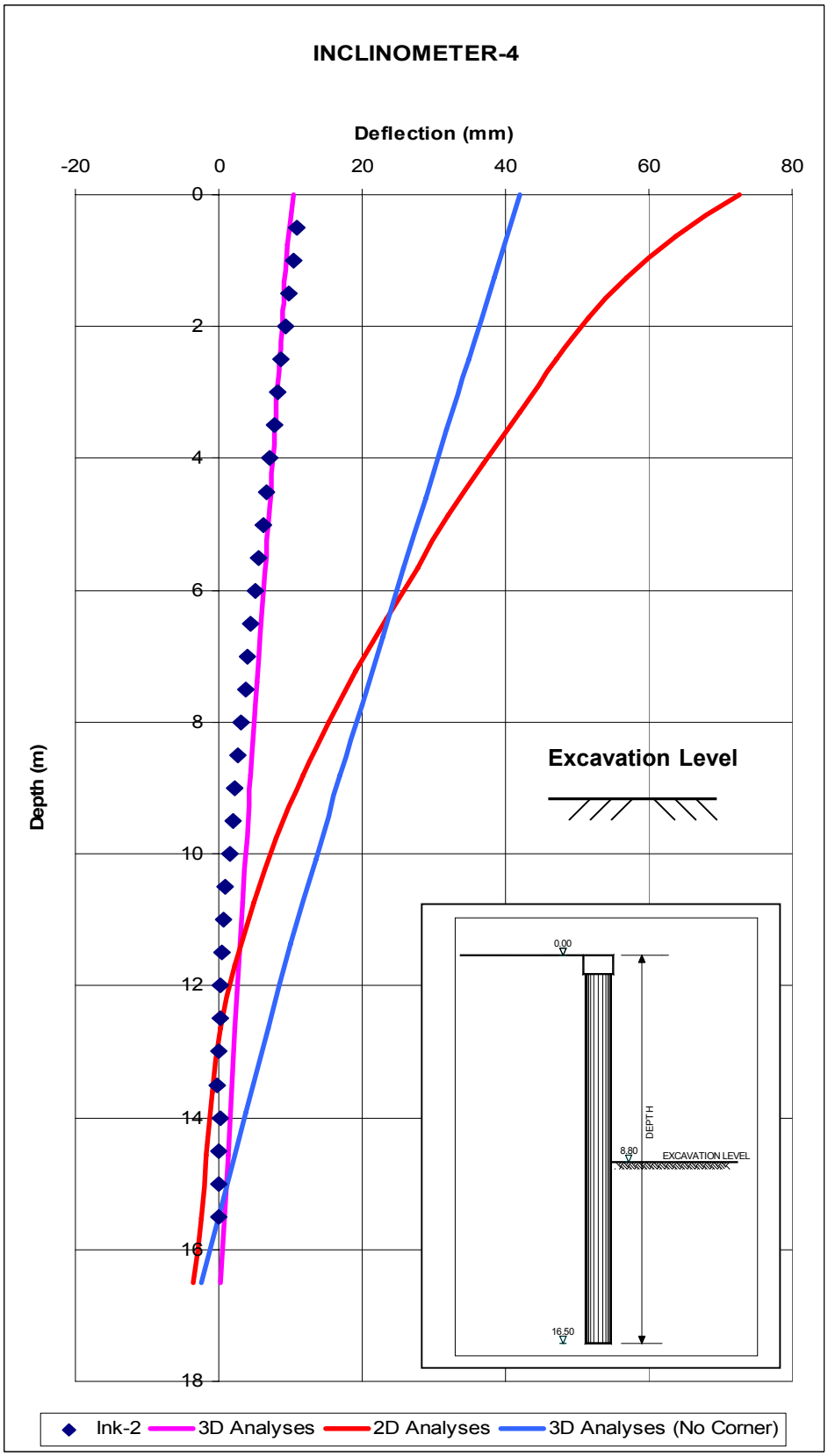

Figure 129. Deformation vs. depth plot for Inclinometer-4 section

Beside deflections, moments of different cross sections of the model are also compared as shown in Figure 130. Following results are obtained;

- Two types of moment diagrams are obtained from analyses; type-a: typical moment diagram of cantilever case, type-b: typical moment diagram of in-situ walls supported by struts. Typical views of these moment types are demonstrated in Figure 65 (in Section 3.5.1.).

- Type-a moment diagrams are obtained from plane strain and 3D without corner analyses. Absolute moment values of these two analyses are similar.

- Type-b moment diagrams are obtained from 3D with corner analyses. Examined cross sections have similar calculated moment values.

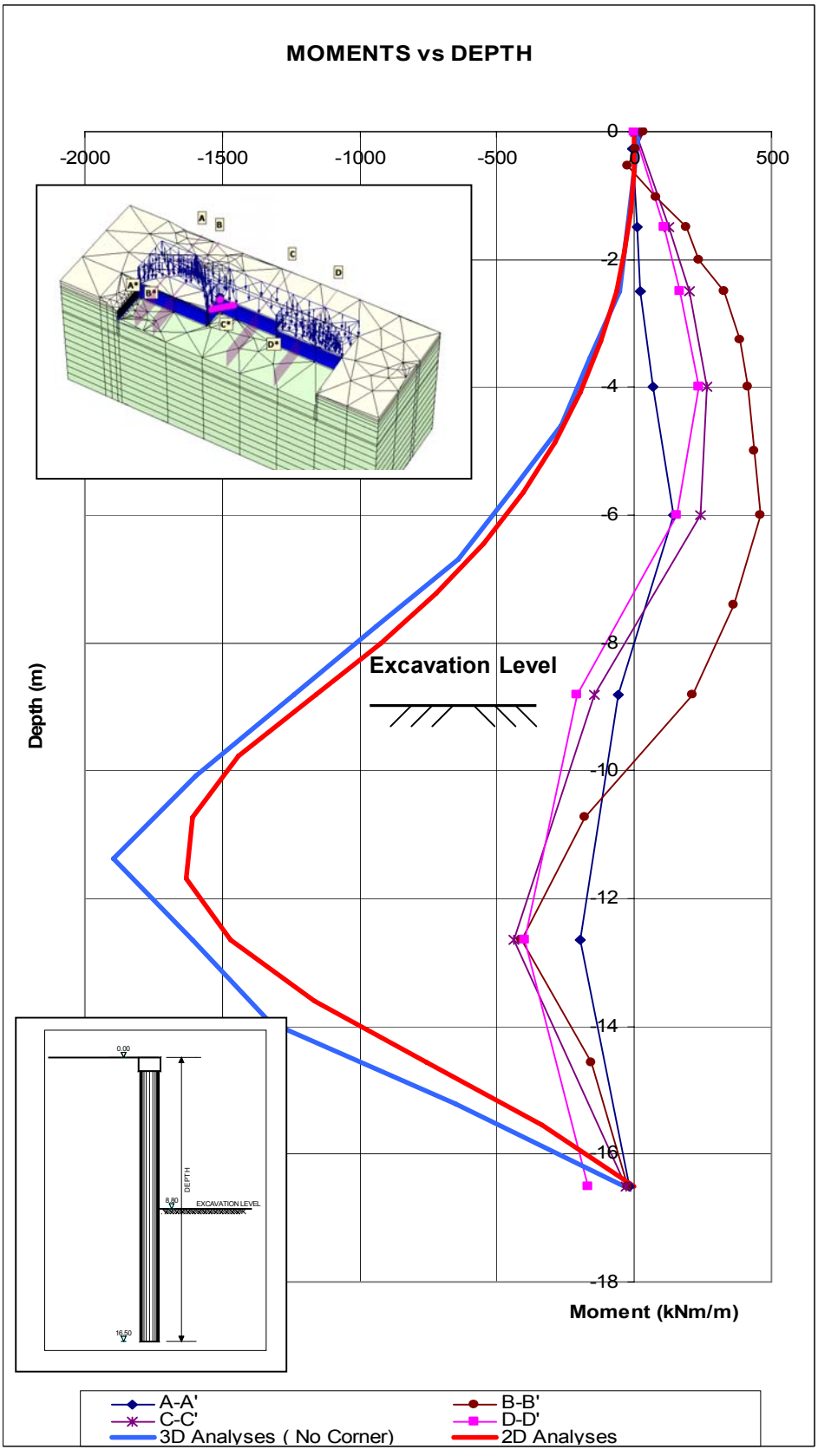

Figure 130. Moment vs. Depth plot for different sections

As moment diagram shape of 3D with corner analyses is similar with the moment diagrams of in-situ walls supported by struts, it is thought that whether the top beam of the piles which are perpendicular to observation piles behave like strut. To check this, plane strain analyses with modeling the corner as a strut is performed. In this analysis, stiffness value of top beam is assigned to strut, and also the distance between the piles which are perpendicular to the observation piles are assumed to be the distances between struts. Finite element meshes used in analysis is shown in Figure 131.

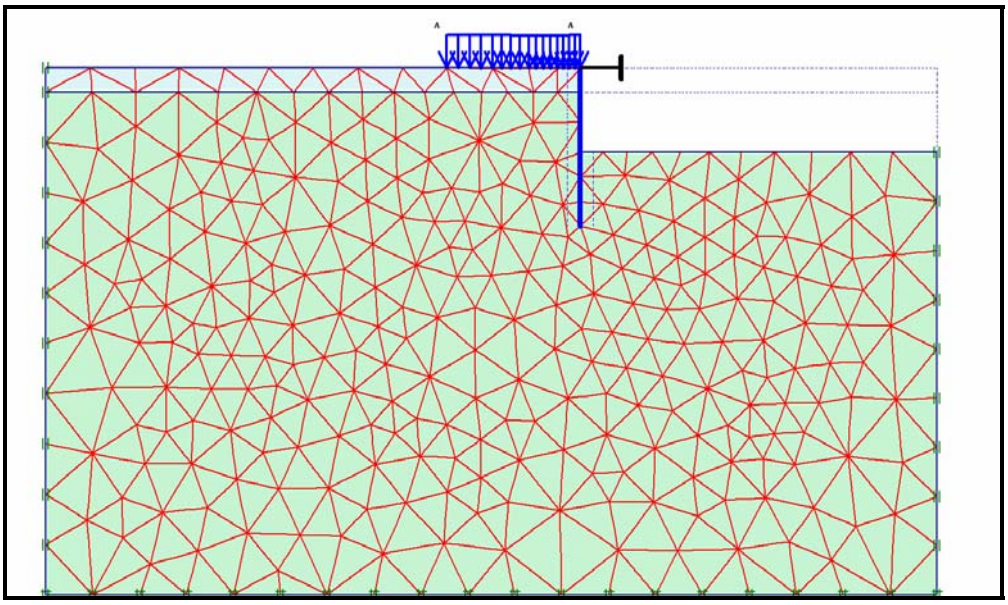

Figure 131. Finite element mesh used in plane strain analyses with strut solution

Deflections of these analyses are compared with measured and calculated values; moments are compared with calculated moments as shown in Figures 132, 133, 134, 135, 136.

Following results are obtained;

- Obtained deflections from modeling the corner as a strut analysis, match the measured values.

- Magnitude and shape of moment diagram obtained from plane strain with strut analysis is similar to the values obtained from 3D analyses.

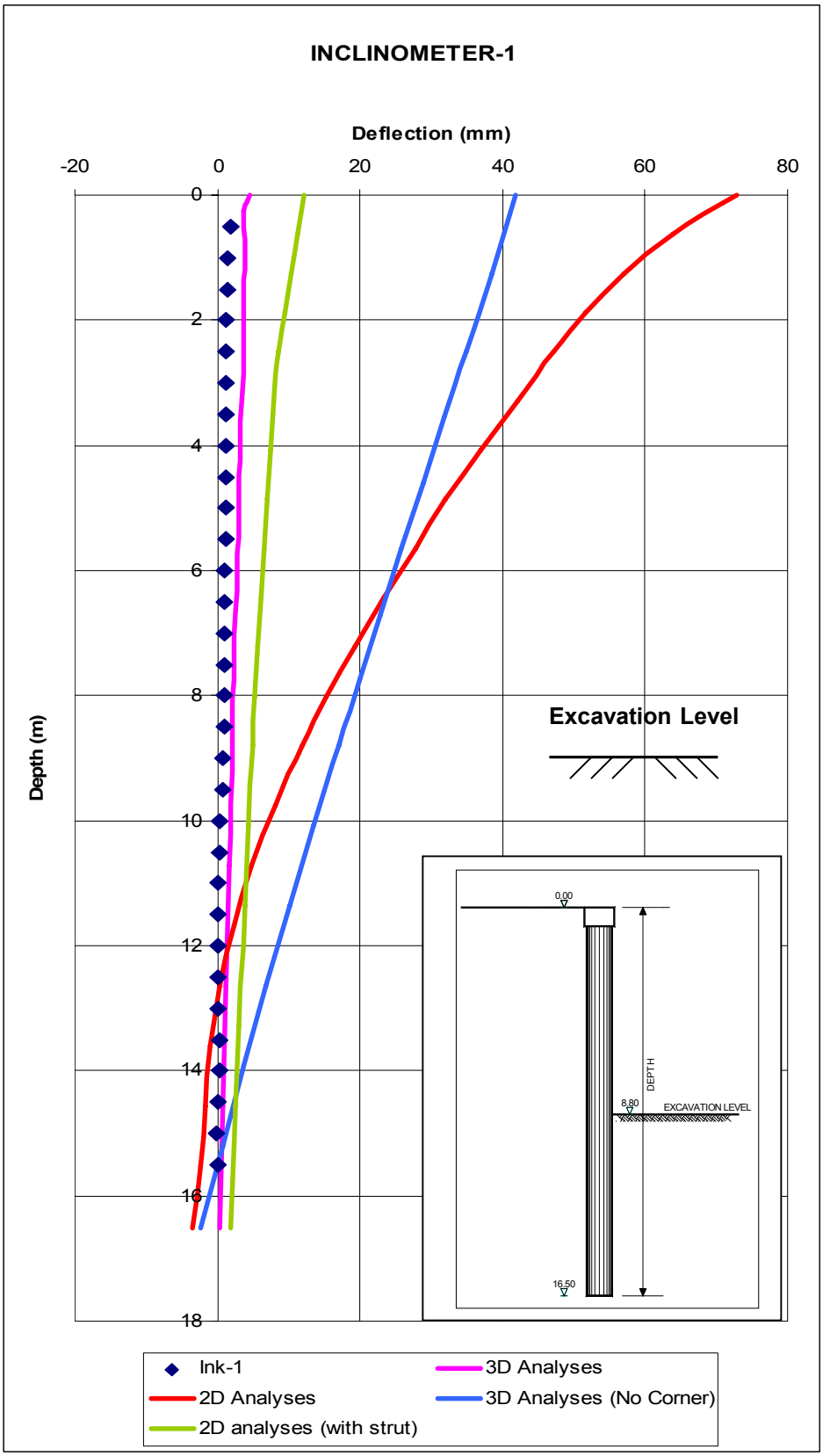

Figure 132. Deformation vs. depth plot for Inclinometer-1 section with strutted solution

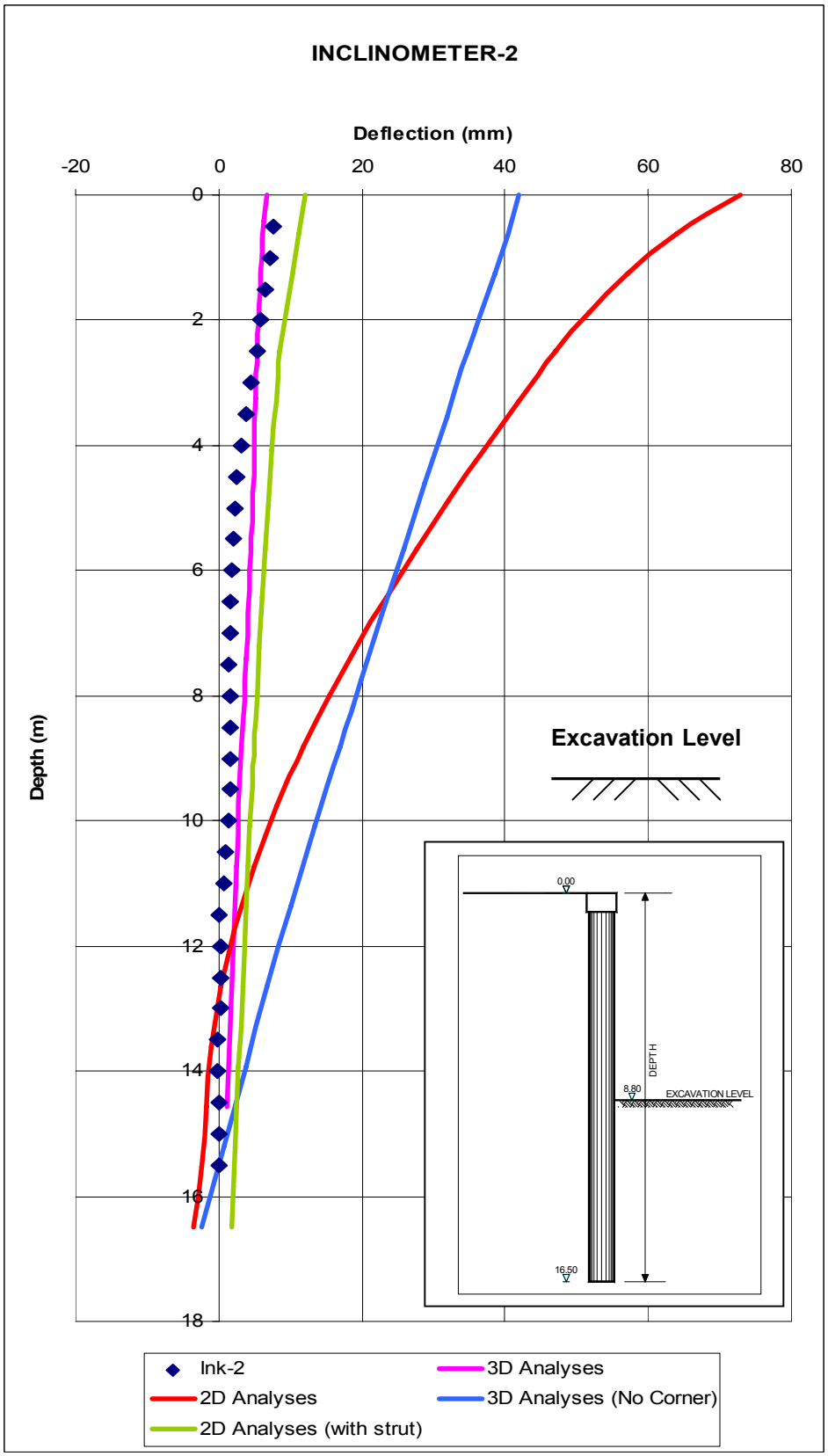

Figure 133. Deformation vs. depth plot for Inclinometer-2 section with strutted solution

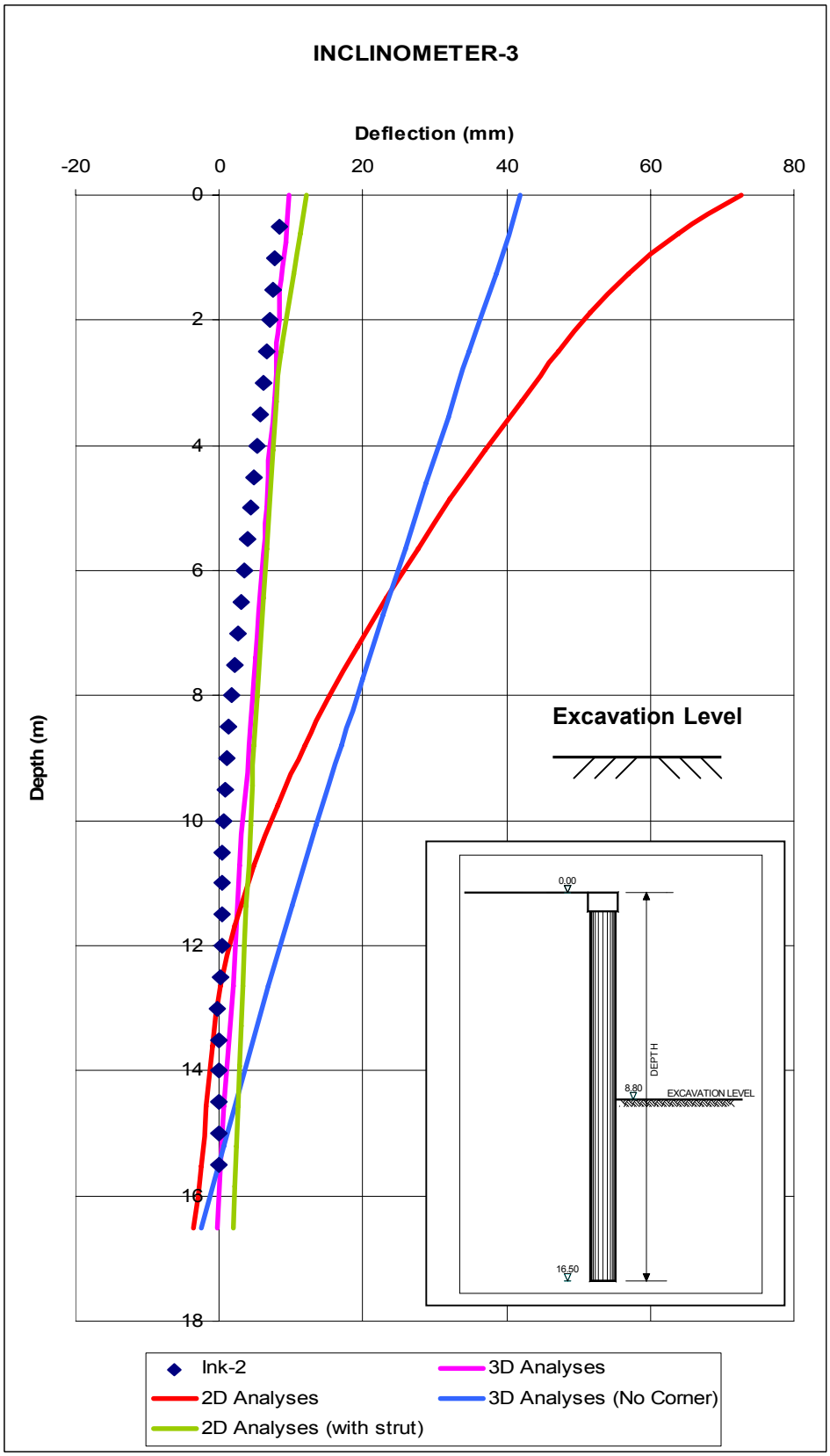

Figure 134. Deformation vs. depth plot for Inclinometer-3 section with strutted solution

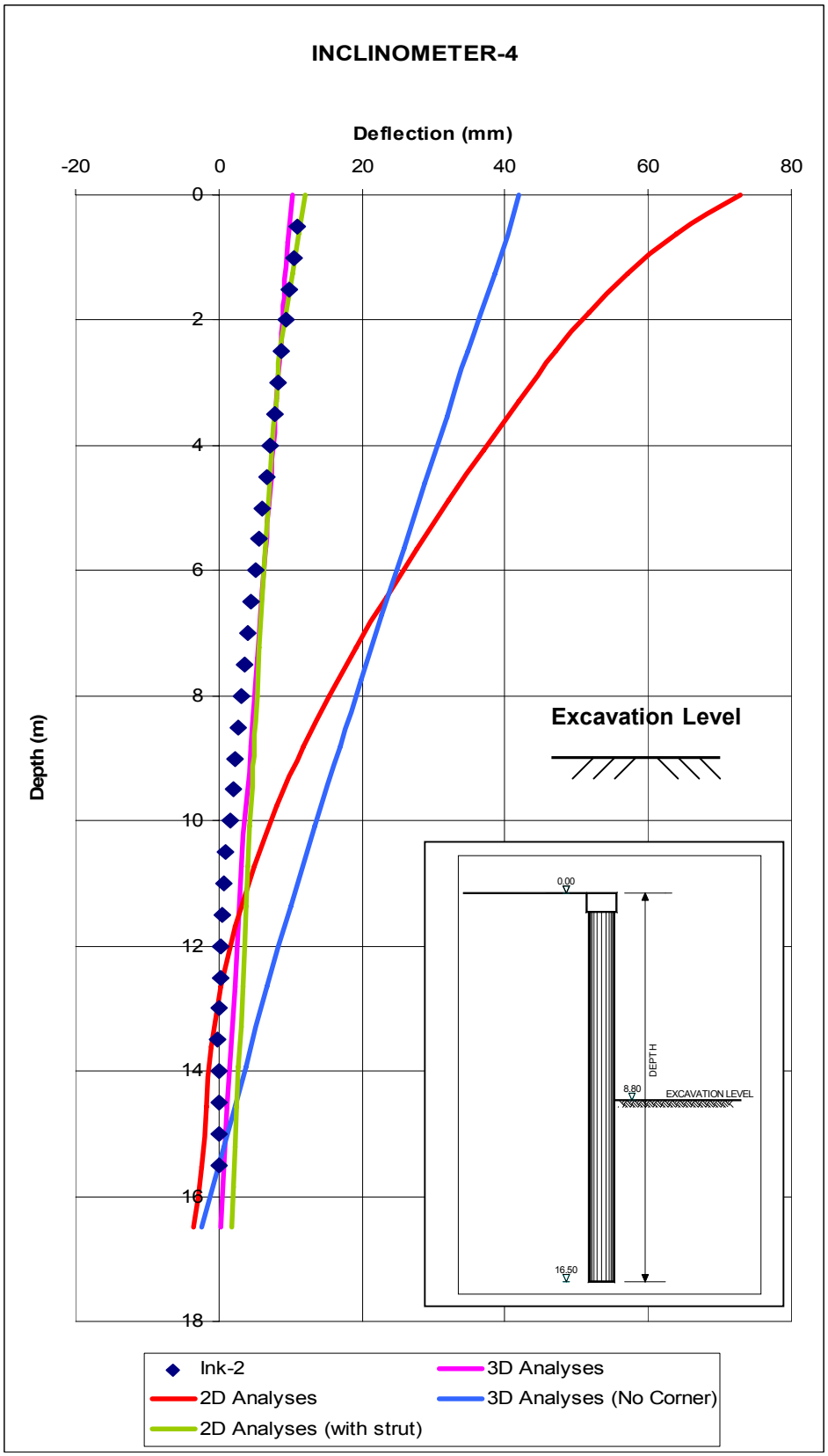

Figure 135. Deformation vs. depth plot for Inclinometer-4 section with strutted solution

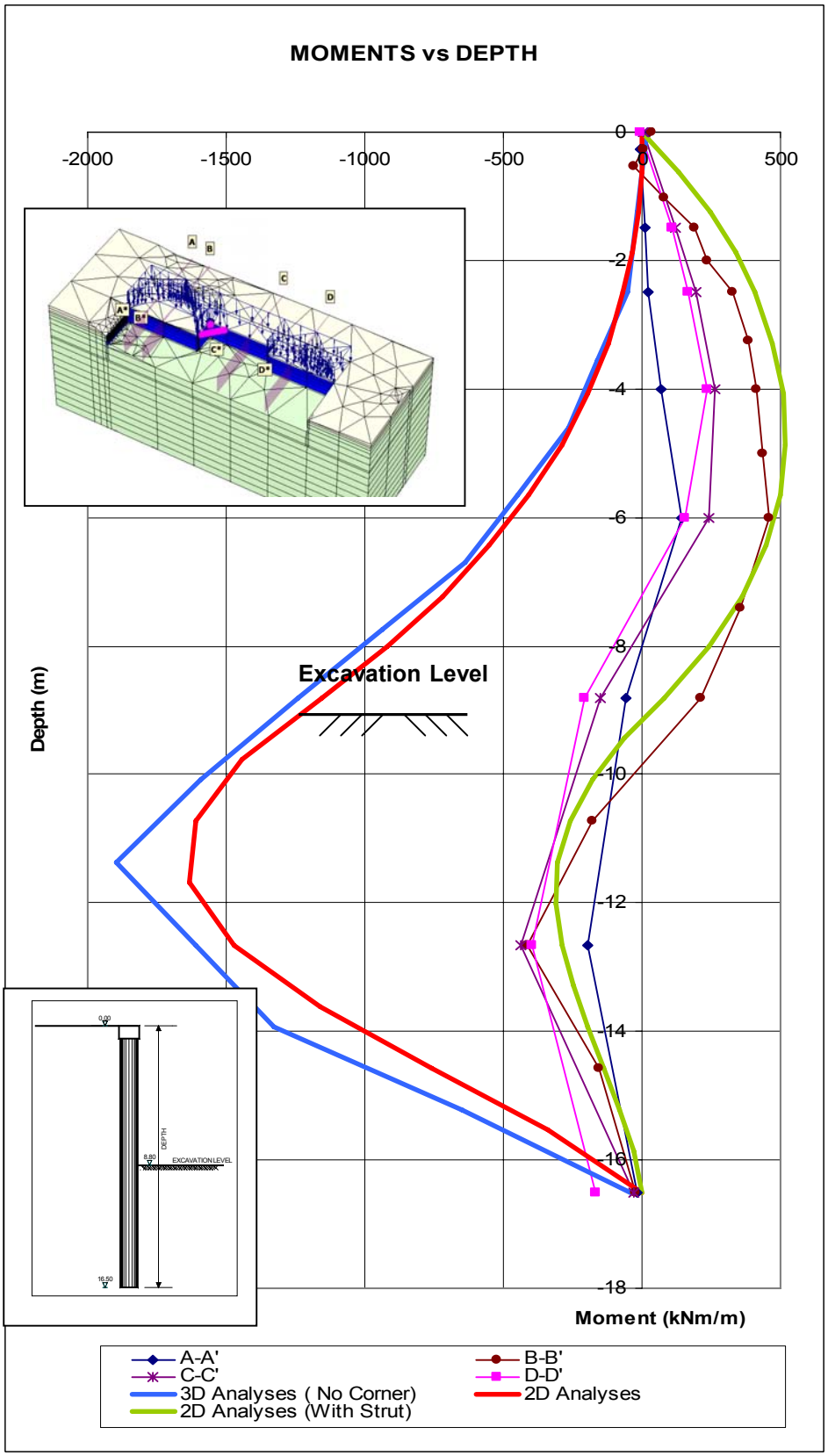

Figure 136. Moment vs. depth plot for different sections with strutted solution

In addition to moments and deflections, effective horizontal stresses of the cases are also examined as shown in Figure 137. Calculated effective horizontal stresses are compared with Rankine's active earth pressures and at rest earth pressures.

Following results are obtained;

- When obtained results of plane strain and 3D analyses are compared, 5-10 kPa differences are observed at some points.

- Calculated results can be approximated by active earth pressure line.

Effective horizontal stresses of plane strain analyses with modeling the corner as a strut is also examined and shown in Figure 138. Stresses of strut solution are compared with plane strain analyses, 3D analyses, and theories. Following results are obtained;

- When plane strain with and without strut solutions, and earth pressure theories are compared, the following results are found;

  0 – 4 m: The lateral pressure of strut solution is more than without strut solution. Also with strut solution values are coincide with at rest pressure line.

  4 – 9 m: With and without strut, effective horizontal stresses are similar and close to active earth pressure line.

  9 – 16.5m: Effective horizontal stresses of with strut solution are more than without corner solution. With strut solution results are in between at rest earth pressure and active earth pressure lines.

- Strut placed at 0m depth, restrict the deflections. This restriction causes an increase in effective horizontal stresses between 0-4m depths.

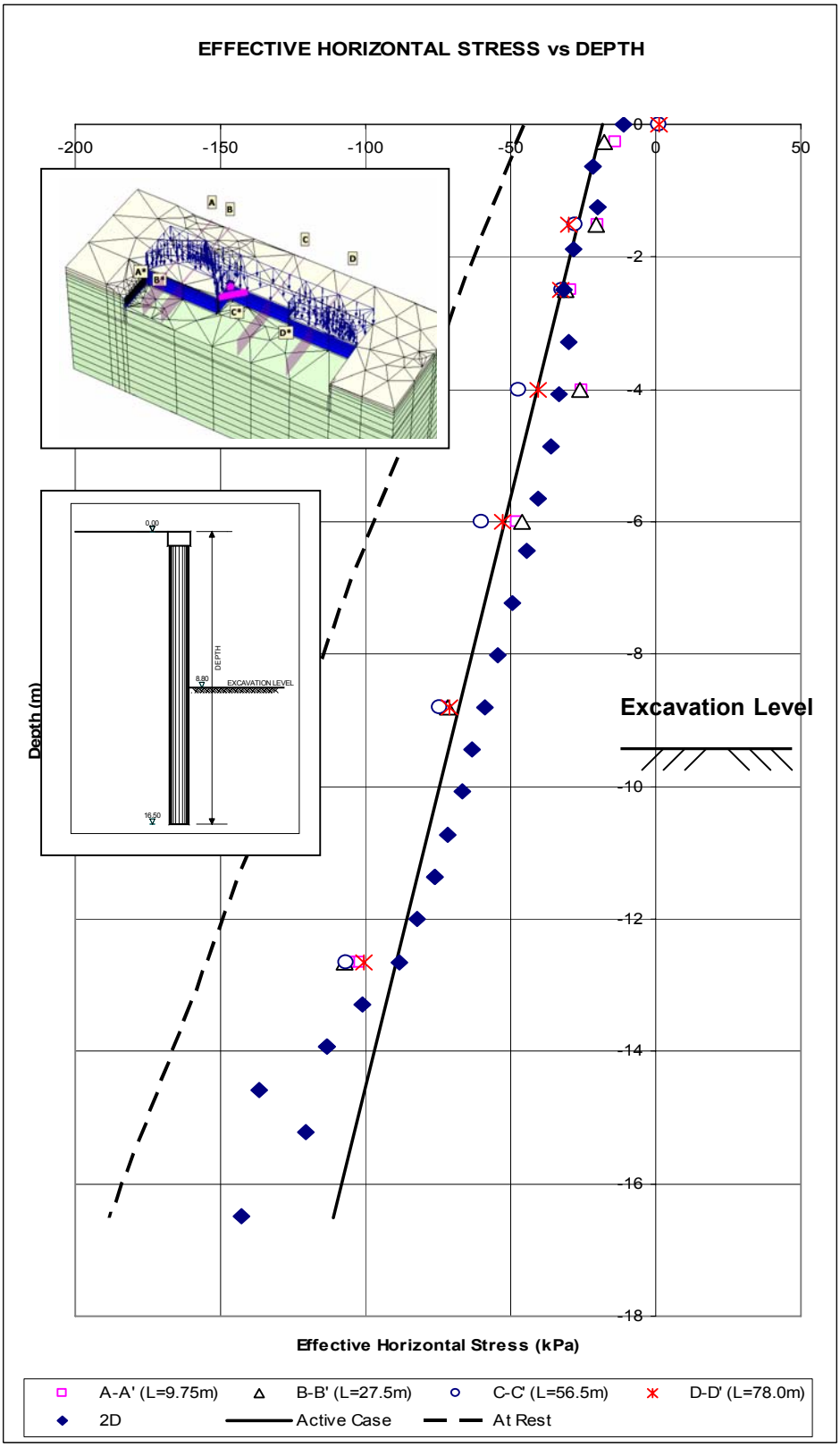

Figure 137. Effective horizontal stresses vs. depth plot for different sections

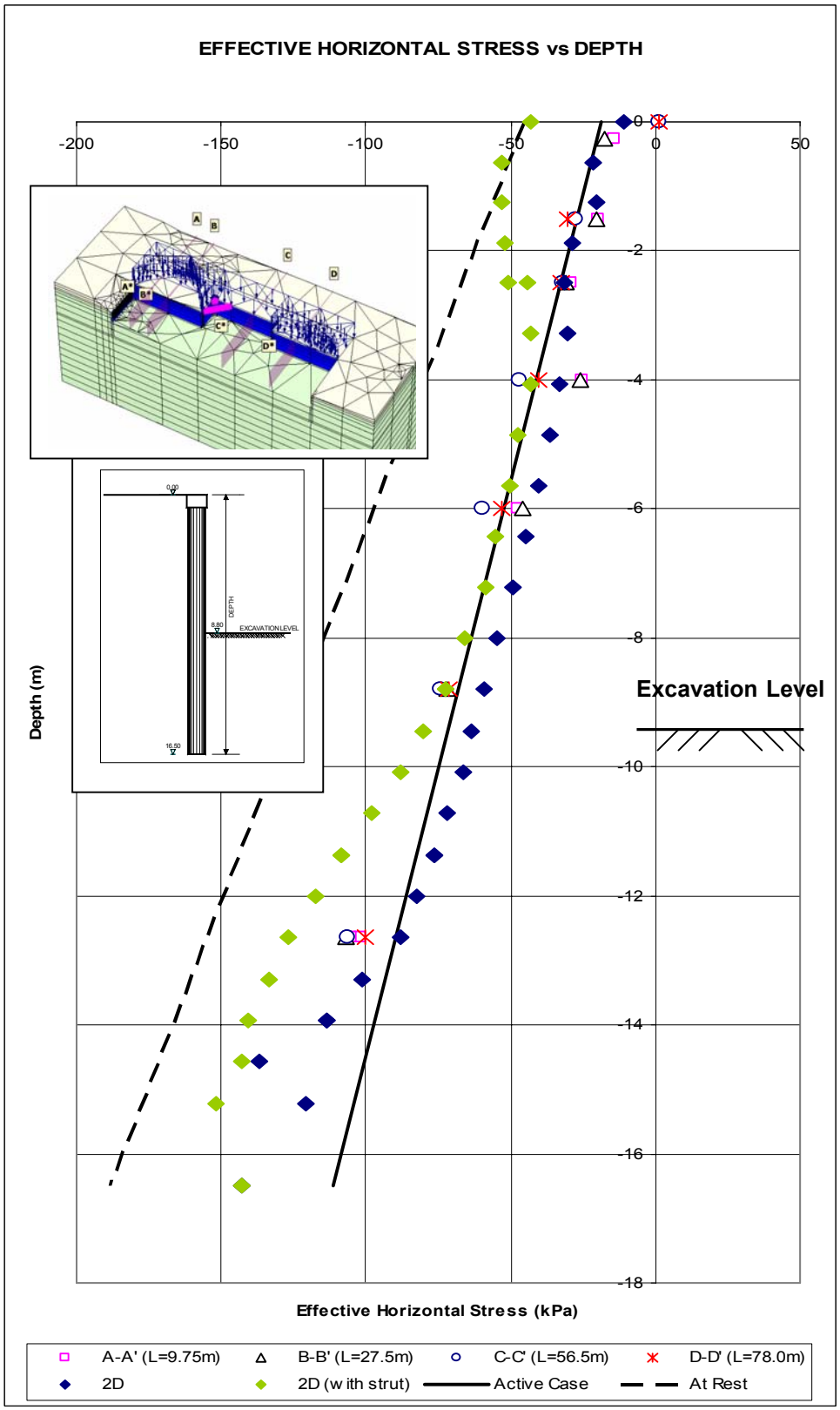

Figure 138. Effective horizontal stress vs. depth plot for different sections with strutted solution

CHAPTER 5

BEHAVIOR OF EKOL CONSTRUCTION EXCAVATION

5.1. General

Ekol construction site is surrounded by Konya Route and buildings. The area of the excavation pit is about 3330 m^2 in plan view as shown in Figures 139, 140. Excavation level is fixed at -16.75m. As a result of elevation differences of the site before construction, excavation depth of the site changes from 10.75m to 15.75m. The excavation depth of the part which is examined in scope of this section is 12.75m.

5.2. Subsoil Conditions

Four boreholes are drilled at the site as shown in Figure 139. Cross section view of soil profile is illustrated in Figure 141. General soil profile of the site is summarized as follows;

- 0-2m depth: Fill Material
- From 0-2m to 7-15m: Alluvium: composed of clayey gravel-clayey sand, contains clay interlayer.
- From 7-15m to End of borehole: Ankara Clay (Gölbaşı Formation): contains occasional gravel and sand interlayer.

Field and laboratory test results of ‘clayey gravel-clayey sand (Alluvium)’ and ‘clay (Gölbaşı Formation)’ are summarized in Tables 5 and 6.

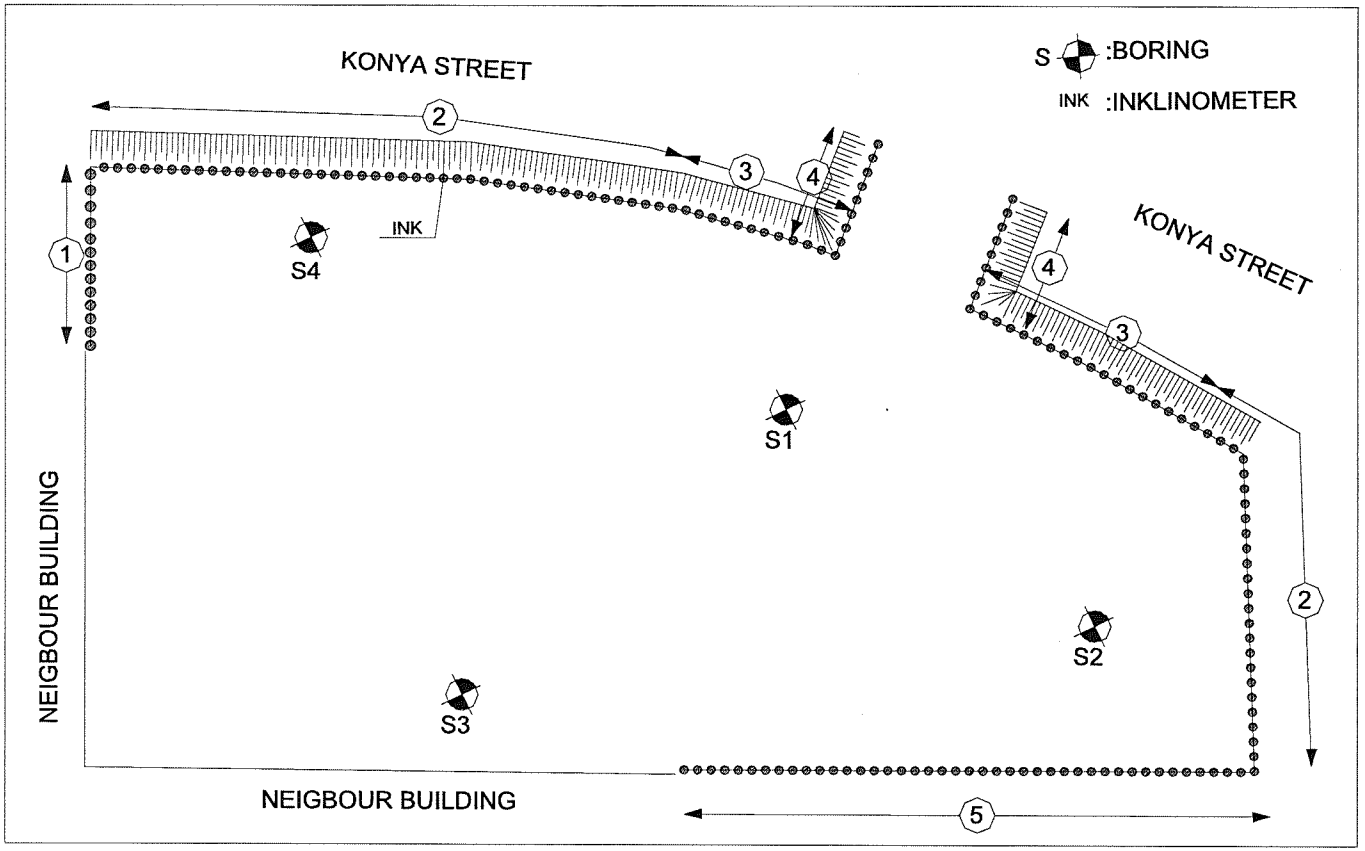

Figure 139. Plan view of the site, location of borings and inclinometers, support system types

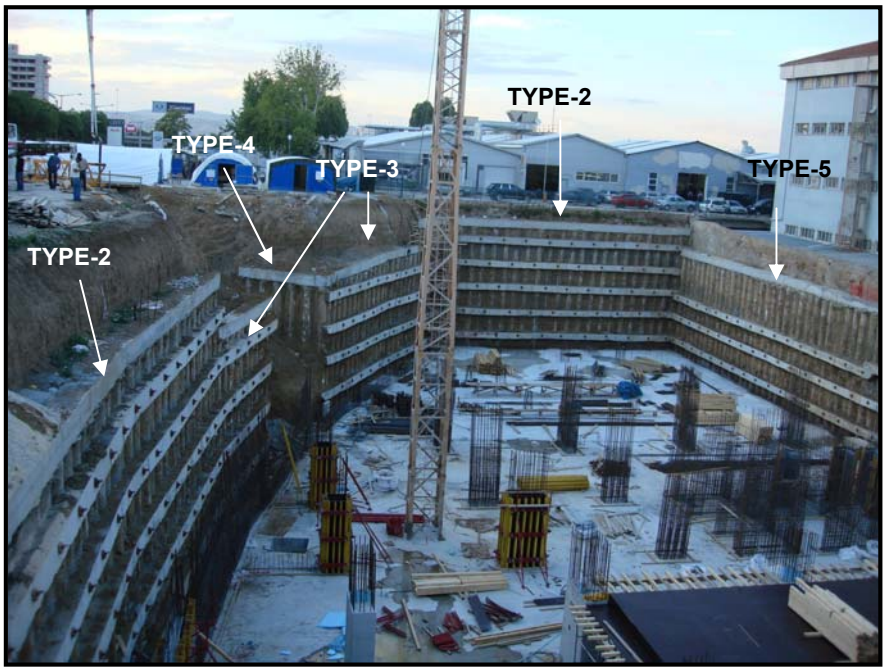

Figure 140. Views of the site

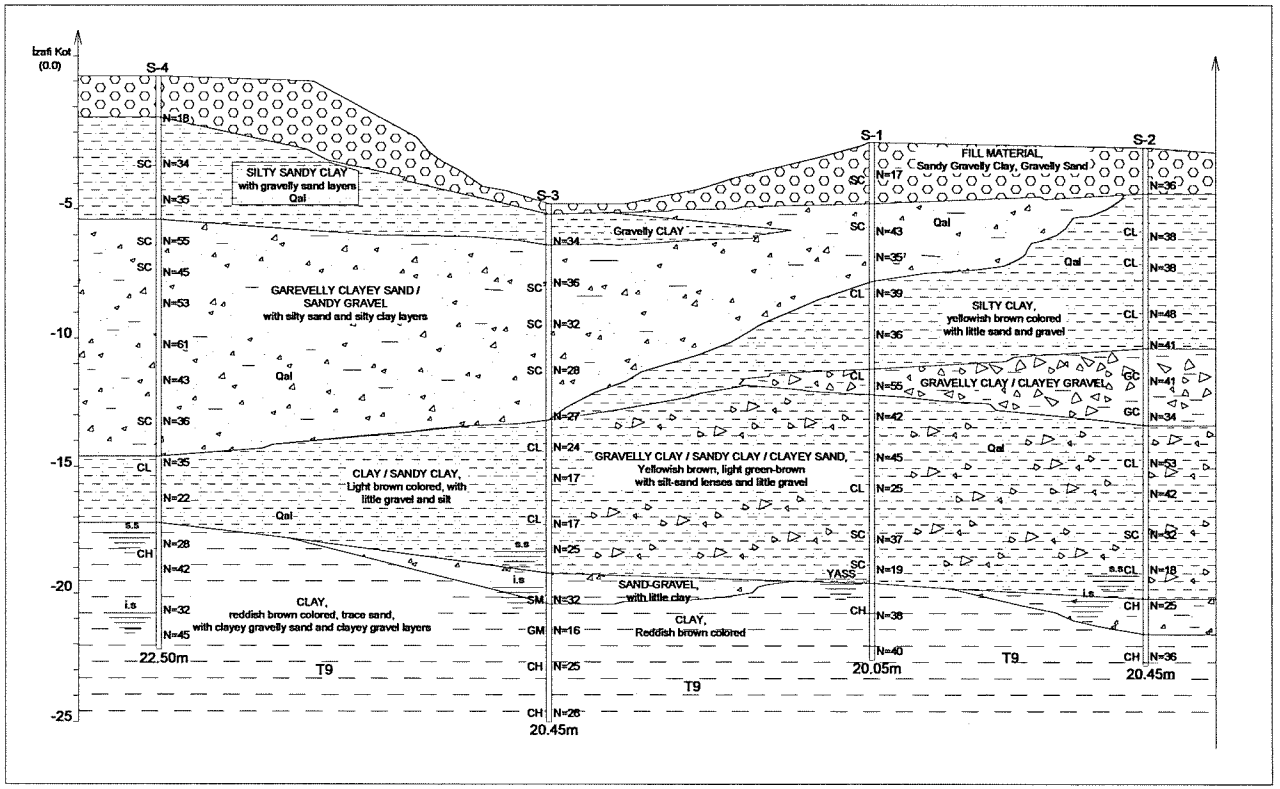

Figure 141. Cross sectional view of soil profile

Table 5. Field and laboratory results summary of Clayey Sand

USCS Soil Type	*CL,SC*
Fine content,	*F (%) = 12,7– 85,6 (representative value F (%) =45,0)*
Gravel content	*G (%) =0,0 – 52,7 (representative value G (%) = 24,0)*
Natural Water Content,	*w_n (%) = 4,0 – 31,7 (representative value w_n(%) =14,0)*
Liquid Limit	*LL (%) = 24,1 – 73,9 (representative value LL (%) =35,5)*
Plastic Limit	*PL (%) = 12,8– 30,5 (representative value PL (%) =15,5)*
Plasticity Index	*PI (%) = 10,5- 43,4 (representative value PI (%) = 20,0)*
SPT Values	N = 28-61 (*representative value* N =40)

Table 6. Field and laboratory results summary of Clay

USCS Soil Type	*CH*
Fine content,	*F (%) = 70,4– 87,7 (representative value F (%) =79,0)*
Gravel content	*G (%) =2,6 – 17,1 (representative value G (%) = 9,5)*
Natural Water Content,	*w_n (%) = 26,6 – 36,0 (representative value w_n(%) =30,0)*
Liquid Limit	*LL (%) = 56,9 – 82,9 (representative value LL (%) =70,0)*
Plastic Limit	*PL (%) = 20,2– 31,3 (representative value PL (%) = 26,0)*
Plasticity Index	*PI (%) = 36,7-51,6 (representative value PI (%) = 44,0)*
SPT Values	N = 17 - 53 (*representative value* N ≅ 32)

Boreholes except S4 are far from the part which is examined in scope of this part. Therefore, S4 is used for the model. A 13m thick alluvium layer is observed in S4. The subsoil of the site is assumed as a uniform layer (clayey sand-clayey gravel) and relevant soil parameters for this layer are derived because of the reasons below;

- As there is no other borehole along the excavation side, the continuity and thickness of clayey gravel- clayey sand (alluvium) layer is not certain.

- Fine content of alluvium is quite high. Also standard penetration results of clay and alluvium are quite similar.

- Only clayey sand-clayey gravel is observed during pile construction. Because of these reasons, the subsoil of the site is assumed as a uniform layer; clayey sand-clayey gravel.

Back analyses are performed for the retaining system near the Konya Street by using 3D finite element program. By increasing and decreasing modulus of elasticity, friction angle and cohesion values, the measured and calculated deformations are matched. According to the back analyses, parameters of clayey gravel-clayey sand are derived and summarized in Table 7.

Table 7. Derived parameters for clayey sand

Cohesion	$c' = 10$ kPa
Friction Angle	$\phi' = 32°$
Soil Weight	$\gamma = 21$ kN/m^3
Elastic Modulus	$E_s = 70.000$ kPa

5.3. Support System

Elevation differences in the site, foundation elevations and floor numbers of neighbouring buildings forced designers to design different type of support systems for this site.

Type numbers are assigned to the support systems as shown in Figure 139 and properties of the systems are described in Table 8. All anchors are constructed with 15° angle to the horizontal and a prestress of 360 kN per anchor prestresses is applied.

The cross sectional views of type-1 and type-2 systems are shown in Figure 142.

5.4. Monitoring System

The deflection behaviour of type-2 system is monitored by using one inclinometer placed inside the 65cm pile as shown in Figure 139. Distance of inclinometer pipe to the corner is 26m. One reference reading was taken at the beginning of the construction and one more reading was taken at the end of the construction period. No measurement was taken during the construction steps.

Measured deflections are demonstrated in Appendix C.

Table 8. Properties of support system type

Type number of the systems	Top elevation of the system	Bored pile diameter / spacing	Pile Length	Anchor levels /Length		Surcharge effect near the system
1	-1.00	80cm/120cm	19.75m	Level-1	-3.00 / 20.0m	-
				Level-2	-5.25 / 18.5m	
				Level-3	-7.50 / 17.5m	
				Level-4	-9.75 / 16.0m	
				Level-5	-12.00 / 14.5m	
				Level-6	-14.75 / 13.5m	
2	-4.00	65cm/100cm	15.75	Level-1	-5.25 / 18.5m	80kPa
				Level-2	-7.50 / 17.0m	
				Level-3	-9.75 / 15.5m	
				Level-4	-12.00 / 14.0m	
				Level-5	-14.75 / 13.0m	
3	-6.00	65cm/110cm	13.75	Level-1	-7.50 / 17.0m	80kPa
				Level-2	-9.75 / 15.5m	
				Level-3	-12.00 / 14.0m	
				Level-4	-14.75 / 13.0m	
4	-6.00	65cm/110cm	15.75	Level-1		80kPa
				Level-2		
				Level-3	-	
				Level-4		
				Level-5		
5	-6.00	65cm/100cm	13.75	Level-1	-9.75 / 15.0m	-
				Level-2	-12.00 / 14.0m	
				Level-3	-14.75 / 13.0m	

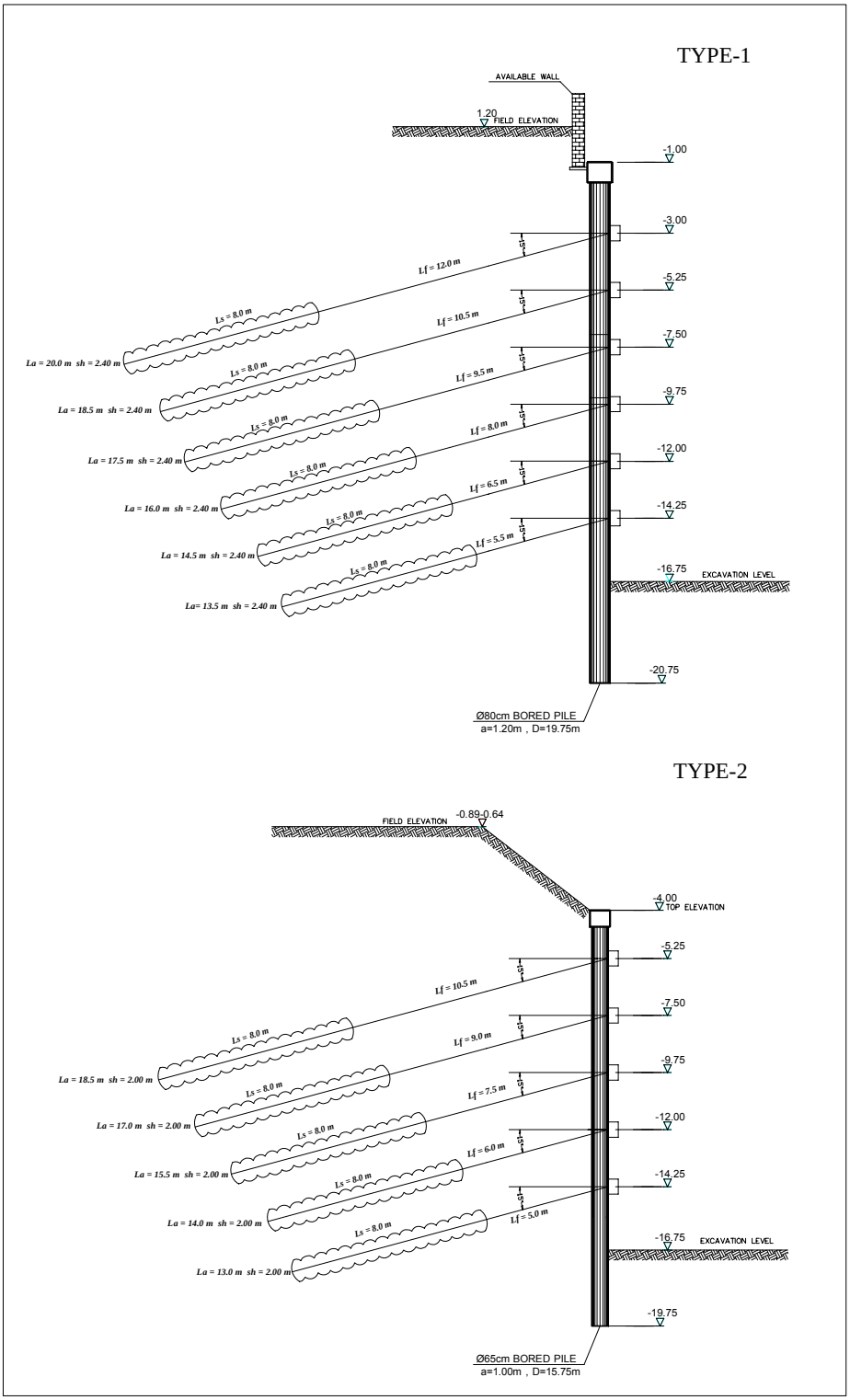

Figure 142. Cross-sections of Type-1 and Type-2

5.5. Finite Element Analyses

2D and 3D finite element analyses are used to simulate the part near the Konya Route. In 2D analyses; only type-2 system, where inclinometer is placed, is modelled. In 3D Analyses; in addition to type-2 system, type-1 and type-3 systems are also simulated in the same model by using the advantages of 3D analyses.

Some simplifications have to be made for modelling. The top elevations of type-1, type-2 and type-3 are different. To model this elevation difference, a sloped site had to be modelled by 3D program. As this process is time consuming, all of these three systems' top elevations are assumed to be -4.0 which is the real top elevation of type-2. Because of this assumption, the first level anchors of type-1 have to be ignored. The sloped excavation (near type-2) down to -4.0m depth is modelled by applying surcharge load.

Hardening Soil Model is used for simulating the behaviour of clayey sand. As no water table was observed at the site, drained material type is selected.

In both 2D and 3D analyses, 15 nodded triangular elements are used. In 2D analyses, plane strain model is utilized. For simulation of bevelled excavation down to -4.0m elevation, 80kPa surcharge load is applied. Interfaces are also utilized to simulate the interaction between the piles and the soil.

The finite element meshes used for 2D and 3D analyses are demonstrated in Figures 143, 144.

Soil parameters used for modelling are summarized in Table 9.

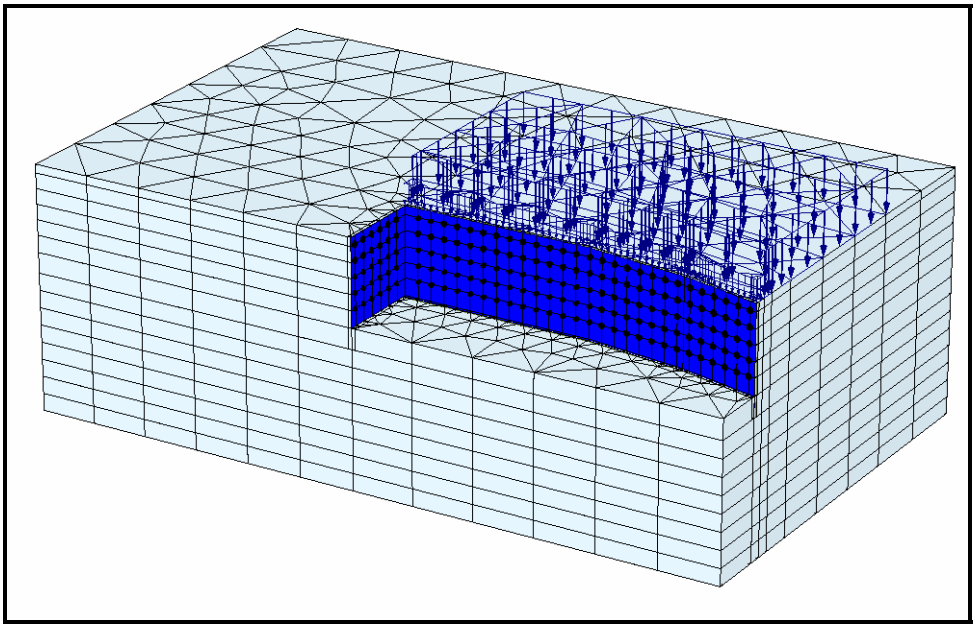

Figure 143. Finite element mesh used in 3D analyses

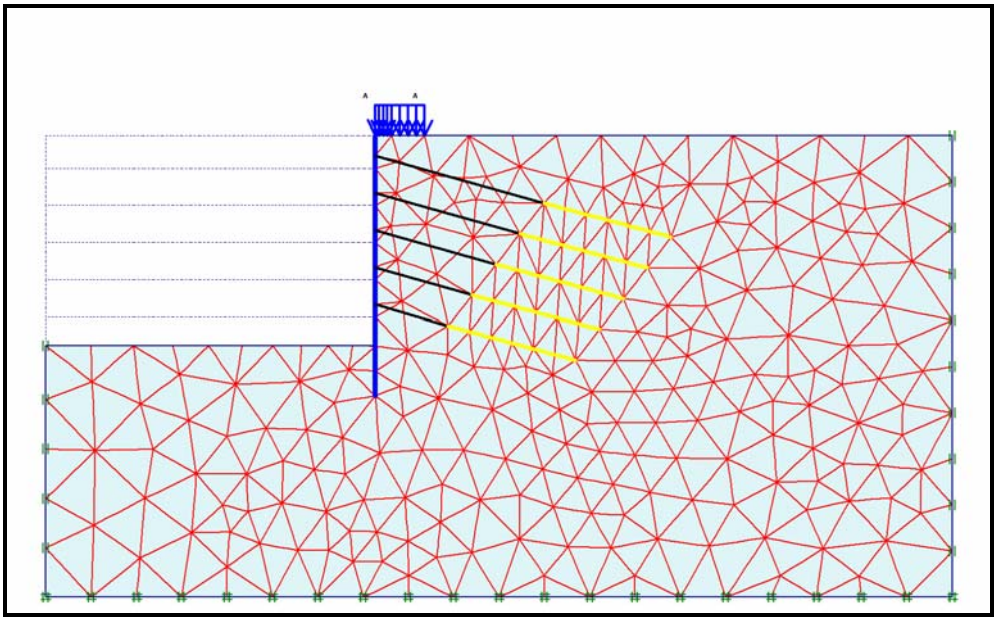

Figure 144. Finite element mesh used in 2D analyses

Table 9. Soil properties used in analyses

PARAMETER	*NAME*	*CLAYEY SAND*	*UNIT*
Material Model	*Model*	HSM	-
Material Behaviour	*Type*	Drained	-
Unsaturated Soil Weight	γ_{unsat}	21	kN/m^3
Saturated Soil Weight	γ_{sat}	21	kN/m^3
Secant Stiffness for CD Triaxial Test	E_{50}^{ref}	70000	kN/m^2
Tangent Oedometer Stiffness	E_{oed}^{ref}	70000	kN/m^2
Unloading/Reloading Stiffness	E_{ur}^{ref}	210000	kN/m^2
Power Stress Level Dependency of Stiffness	*Model*	0.5	-
Cohesion	c_{ref}	10	kN/m^2
Friction Angle	ϕ	32	°
Dilatancy Angle	ψ	0	°
Poisson's Constant	ν_{ur}	0.2	-
Interface Reduction Factor	R_{inter}	0.8	-

5.6. Results and Discussions of Finite Element Analyses

Input parameters for the FEM model are calibrated with the measured data. Three dimensional finite element analyses are performed to back calculate soil parameters by matching calculated and observed deformations. By increasing and decreasing elastic modulus, cohesion, and internal friction angle for soil, the measured and calculated deformations are matched as shown in Figure 145. Also by using the same soil parameters, plane strain analysis is performed. Following results are obtained;

- The deformation pattern of plane strain and 3D analyses are similar.
- There is 2-3mm difference between plane strain and 3D results for inclinometer section which is placed at 26m distance from the corner. It shows that corner effect diminishes about 26m distance from the corner.

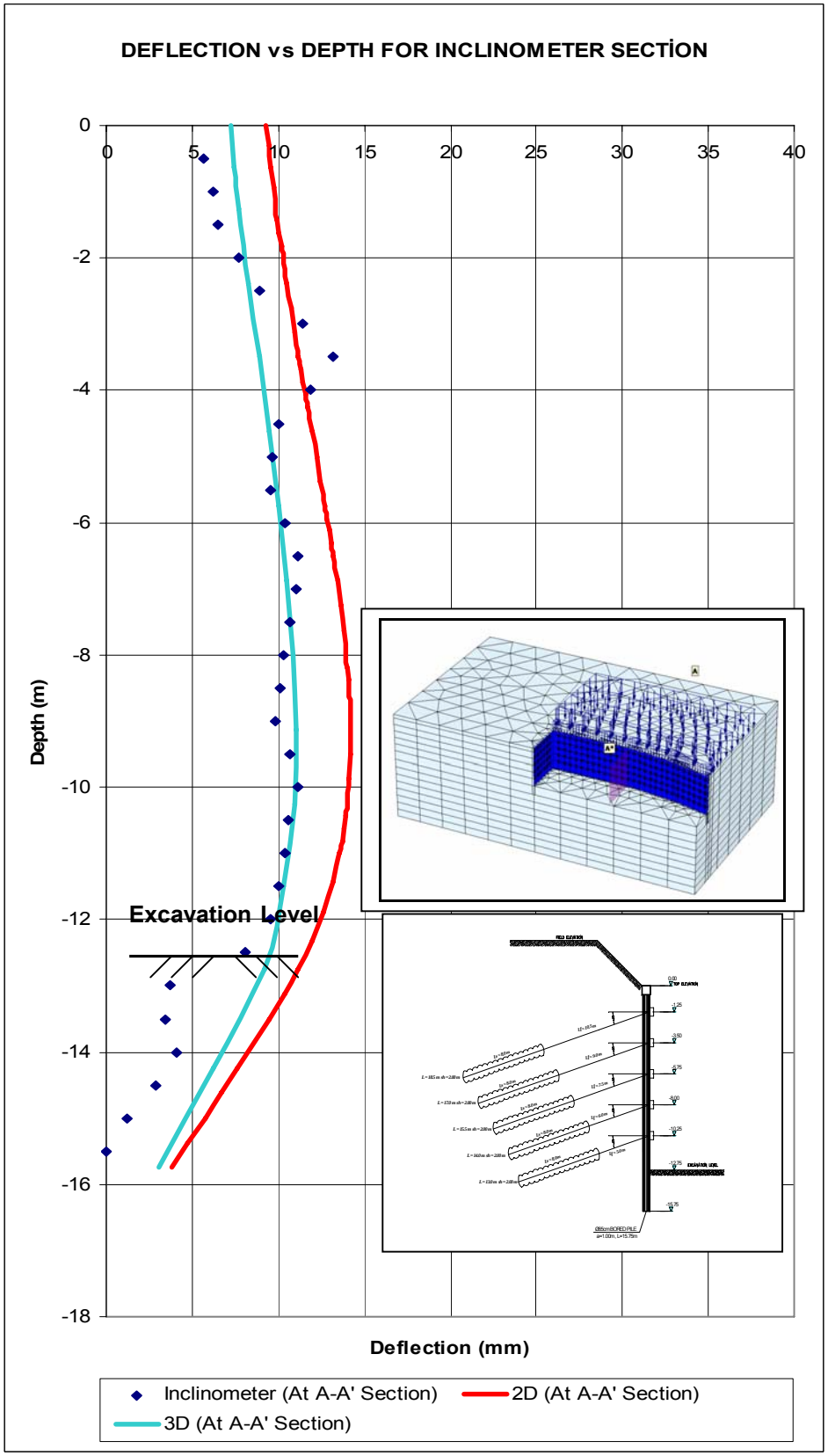

Figure 145. Deflection plot for inclinometer section

Deflection of several sections with different distances from the corner are specified in the three dimensional analyses. The results are shown in Figure 146. Following results are obtained;

- It is observed that corner effect on deflections diminishes at 10-20m distance from the corner. After this distance, deflections become constant.
- Deflections obtained from sections of which distances are more than 20m from the corner, match the measured values.
- Deflection of plane strain analysis is 4mm more than deflection of 3D analyses.

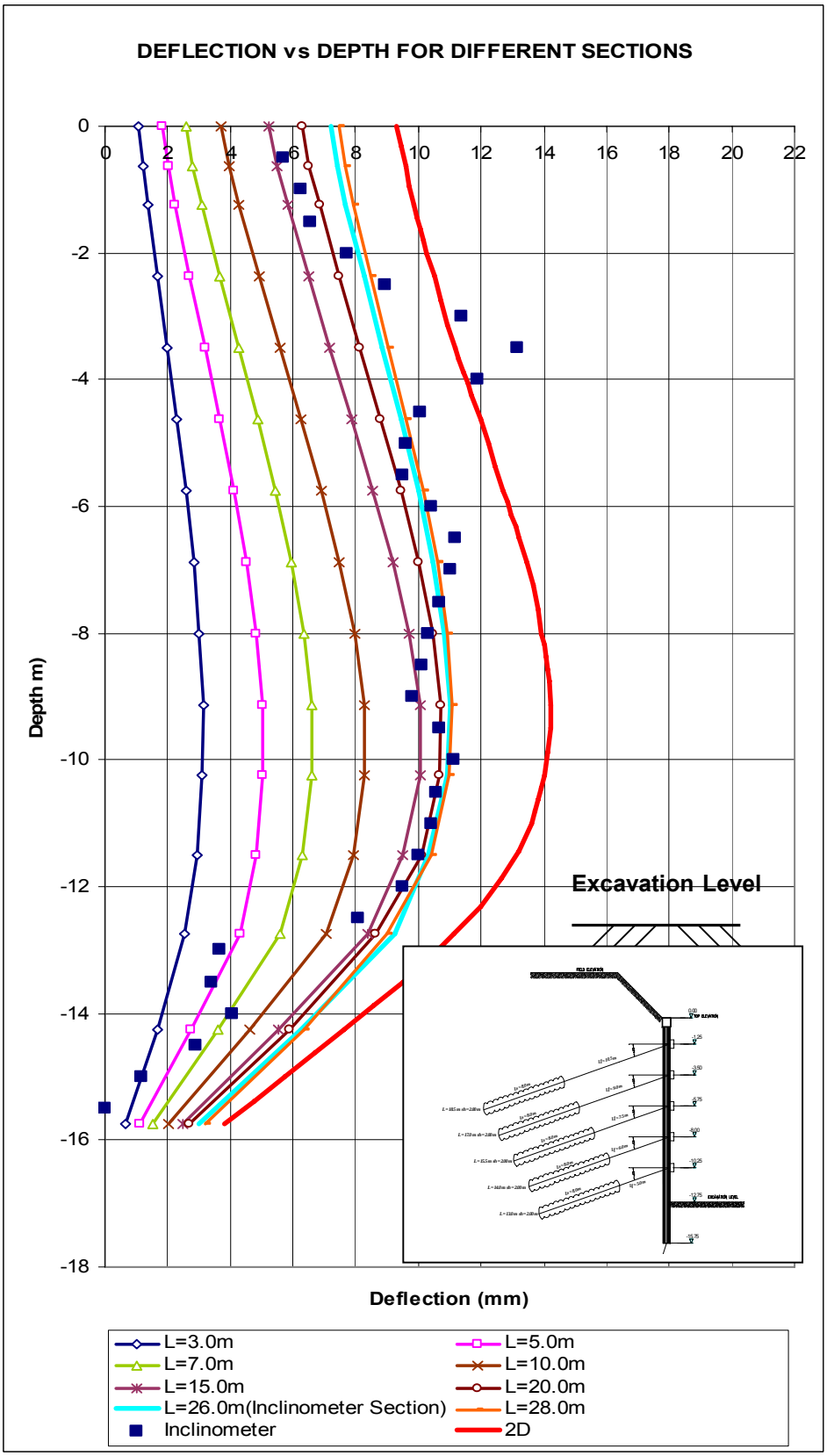

Figure 146. Deflections through the excavation side

Deflection over maximum deflection of 3D analyses ratio, which is the ratio of maximum wall displacement of a section to maximum wall displacement of in-situ wall vs. distance from corner graph is demonstrated in Figure 147. It can be seen that corner effect diminishes after 20m distance from the corner. Deflection of plane strain analysis is 28% more than maximum deflection of 3D analyses.

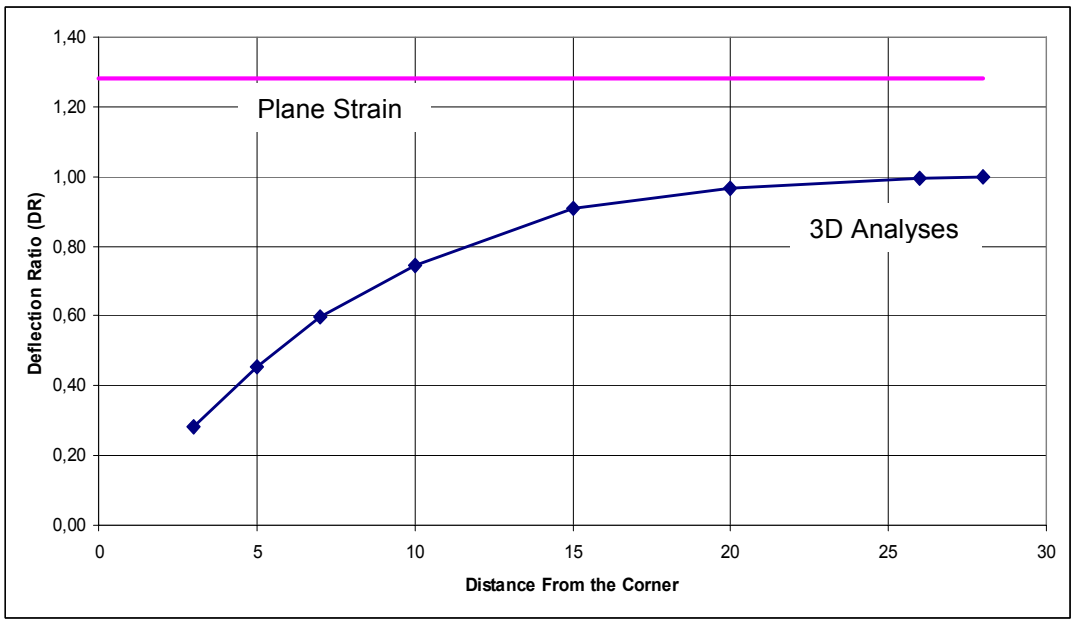

Figure 147. Deflection ratios of Ekol Construction excavation

Moment diagrams are shown in Figure 148. Following results are obtained;

- Up to 10m distance from the corner, moment increase. After this distance, moments become nearly constant.
- The maximum moment obtained from plane strain analyses is 80-100kNm/m smaller than the maximum moment obtained from 3D analyses.
- Fluctuations in moments are observed at anchor levels in plane strain analyses.

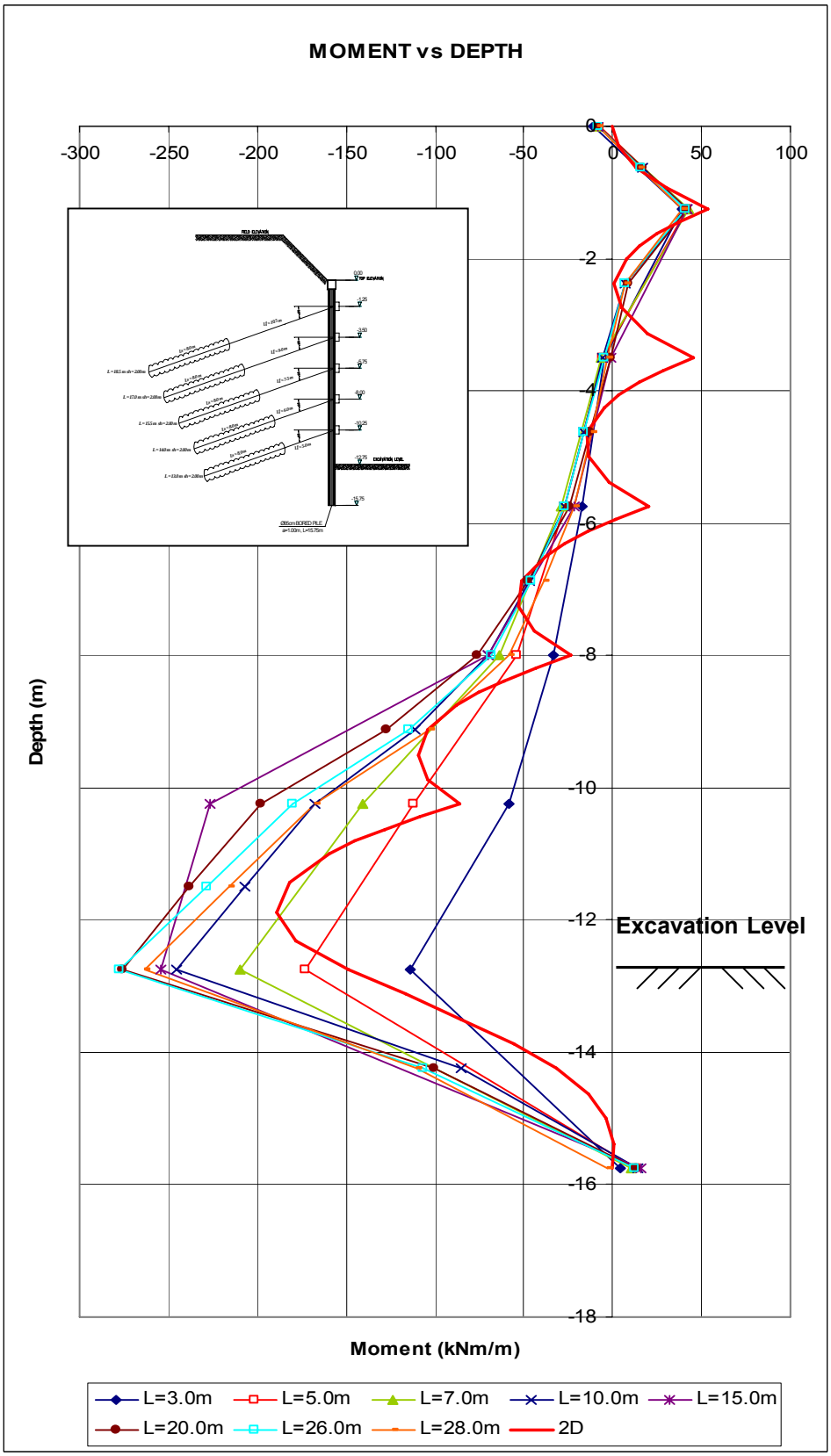

Figure 148. Moments through the excavation side

Moment over maximum moment ratios vs. distance from corner graph is shown in Figure 149. Following results are obtained;

- Corner effect on moment diminishes at 10m distance from the corner.
- Moment obtained from plane strain analysis is nearly 30% smaller than the maximum moment of three dimensional analyses.

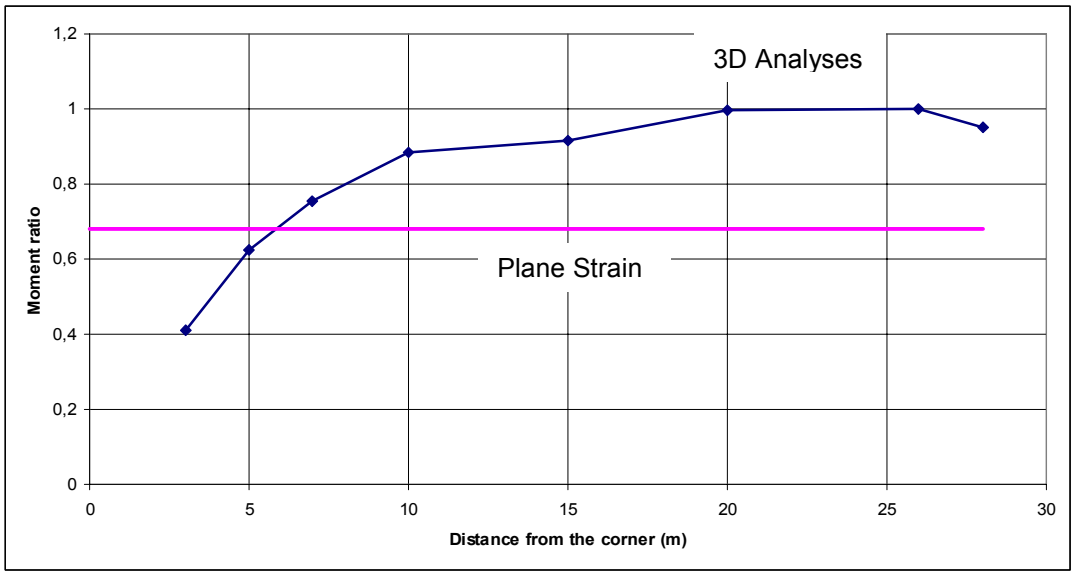

Figure 149. Moment ratios of Ekol Construction excavation

CHAPTER 6

CONCLUSIONS

As a result of analysis of corner effects on in-situ walls supporting deep excavations, the following conclusions can be drawn:

- For all support systems and all elastic modulus of soils, it is observed that corner effect on deflection and moment is observed up to 20m distance from the corner.
- Corner effect on effective horizontal stresses is not apparent.
- The anchor loads increase until 10-15m distance from the corner. After this distance they become nearly constant.
- It is observed that as elastic modulus of soil and stiffness of the support system increase, corner effect decrease.
- Moment diagram obtained around corner of cantilever systems in 3D analysis and diagrams obtained from the plane strain analyses by modeling the corner as a strut are quite similar. Ankara-Çankaya project is solved by modeling the corner as a strut in plane strain analyses; results of this analyses are alike field monitoring indicating that corner effects could be simulated by modeling the perpendicular pile wall as a strut in plane strain analysis.

In hypothetical analyses, constant excavation dimensions are used, but Ou, Chiou, Wu (1996) claimed that, as complementary and primary wall lengths change, corner effect changes. Effect of complementary and primary wall length on wall behavior may worth to investigate in future studies.

The field data used in this thesis is limited to wall deformations. To investigate corner effect on moment, anchor loads and effective horizontal forces; it is advisable to evaluate the moment, anchor loads and effective horizontal force measurements together with the wall displacement data.

REFERENCES

Bowles, J.E. (1988). *Foundation Analysis and Design*, McGraw-Hill, Singapore

Carder, D. R. (1995). '' Ground movements caused by different embedded retaining wall construction techniques.'' *Transport Res. Lab. Rep.* 172, Berkshire, U.K.

Cloug, G. W., and O'Rourke, T. D. (1990). ''Construction induced movements of in situ walls.'' *Proc., ASCE Conf. on Des. And Perf. of Earth Retaining Struct., Geotech.* Spec. Publ. No. 25, ASCE, New York, 439-470.

Çalışan, O. (2005). ''Design and measurements of 30m deep excavation'' Proc. *Prof İsmet Ordemir'i Anma Toplantısı ve 3. ODTÜ Geoteknik Mühendisliği Sempozyumu*, 74-81

Das, B.M. (1984). *Principles of Foundation Engineering*, PWS Publishers, Boston.

Erdinç, E. (2000). ''Performance of deep excavations in soft clays.'' Master Thesis, Middle East Technical University, Ankara.

Fernie, R., and Suckling, T. (1996). ''Simplified approach for estimating lateral movement of embedded walls in U.K. ground.'' *Proc., Int. Symp. Geo Aspects of Underground Constr. In Soft Ground*, City University, London, 131-136.

Kuruoğlu, Ö. (1998). ‘’FEM Analysis and evaluation of Field Measurements on Two Strutted Deep Excavations.’’ Master Thesis, Middle East Technical University, Ankara.

Lee, F.H., Yong, K.Y., Quan K.C.N., Chee,K.T. (1998). ‘’ Effect of corners in strutted excavations: field monitoring and case histories’’ *Journal of Geotechnical and Geoenviromental Engineering*, ASCE, Vol. 124, No. 5,339-349.

Lin, D.G., Chung, T.C., Phien-wej, N. (2003). ‘’Quantitative evaluation of multi strutted deep excavation in Bangkok subsoil’’ *Journal of The Southeast Asian Geotechnical Society*, 41-57.

Ou, C.Y., Chiou, D.C., Wu, T.S. (1996). ‘’Three-Dimensional finite element analysis of deep excavations’’ *Journal of Geotechnical Engineering*, ASCE, Vol. 122, No. 5, 337-345.

Ou, C. Y., Hsien. P. G., and Chiou, D. C. (1993). ‘’Characteristics of ground surface settlement during excavation.’’ *Can. Geotech. J.*, Ottawa, 30, 758-767.

Ou, C. Y., Lai, C. H. (1994) ’’Finite element analysis of deep excavation in layered sandy and clayey soil deposits’’ *Canadian Geotech. J.*, Vol. 31, 204-214.

Ou, C.Y., Shiau, B.Y., Wang, I.W. (2000). ‘’Three-Dimensional deformation behavior of the Taipei National Enterprise Center (TNEC) excavation case history’’ *Canadian Geotechnical Journal*, 37, 438-448

Whittle, A. J., Hashash, Y. M. A., Whitman, R. V. (1993). ‘’Analysis of deep excavation in Boston.’’ *Journal of Geotechnical Engineering, ASCE*, Vol. 119, No. 1, 69-89.

Wong, I. H., Poh, T. Y., and Chuah, H. L. (1997). ‘’Performance of excavations for depressed expressway in Singapore.’’ J. *Geotech. and Geoenvir. Engrg., ASCE*, 123(7), 617-625.

Toker Sondaj ve İnşaat Ltd. Şti. (2006). ‘’Ankara-Çankaya 6049 Ada 21 Parsel İksa Sistemi Açıklama Raporu.’’

Toker Sondaj ve İnşaat Ltd. Şti. (2007). ‘’ Ankara-Çankaya 9895 Ada 76 Parsel İksa Sistemi Açıklama Raporu.’’

APPENDIX A

BORING LOGS OF ANKARA-ÇANKAYA PROJECT

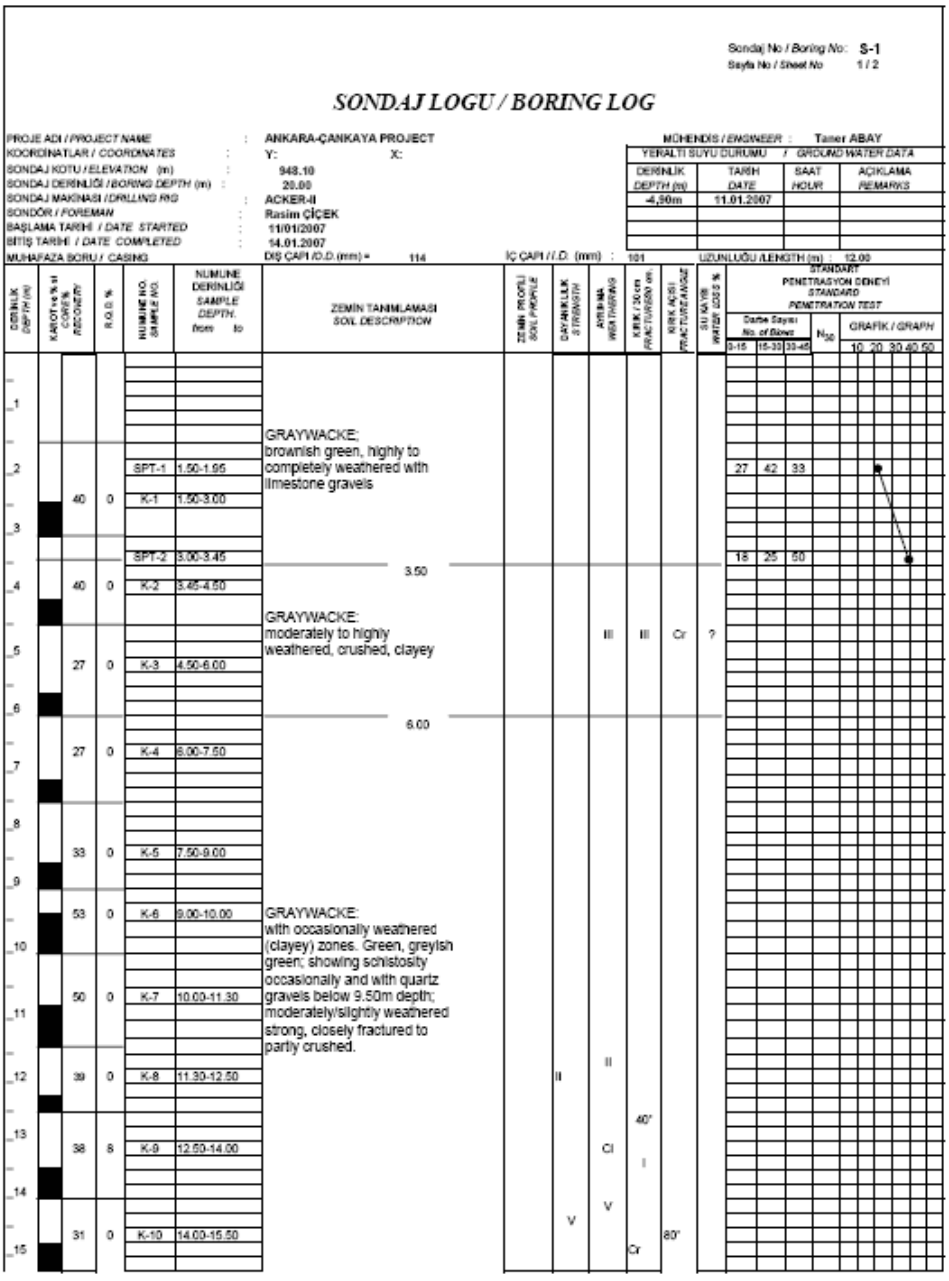

Sondaj No / *Boring No*: S-1
Sayfa No / *Sheet No* 1 / 2

SONDAJ LOGU / BORING LOG

PROJE ADI / *PROJECT NAME* : ANKARA-ÇANKAYA PROJECT
KOORDİNATLAR / *COORDINATES* : Y: X:
SONDAJ KOTU / *ELEVATION* (m) : 948.10
SONDAJ DERİNLİĞİ / *BORING DEPTH* (m) : 20.00
SONDAJ MAKİNASI / *DRILLING RIG* : ACKER-II
SONDÖR / *FOREMAN* : Rasim ÇİÇEK
BAŞLAMA TARİHİ / *DATE STARTED* : 11/01/2007
BİTİŞ TARİHİ / *DATE COMPLETED* : 14.01.2007
MUHAFAZA BORU / *CASING* : Dış ÇAPI / *O.D.* (mm) = 114 İÇ ÇAPI / *I.D.* (mm) : 101 UZUNLUĞU / *LENGTH* (m) : 12.00

MÜHENDİS / *ENGINEER* : Taner ABAY

YERALTI SUYU DURUMU / *GROUND WATER DATA*			
DERİNLİK *DEPTH* (m)	TARİH *DATE*	SAAT *HOUR*	AÇIKLAMA *REMARKS*
-4,90m	11.01.2007		

DERİNLİK *DEPTH* (m)	KAROT % / CORE % RECOVERY	R.Q.D. %	NUMUNE NO. SAMPLE NO.	NUMUNE DERİNLİĞİ *SAMPLE DEPTH* from	to	ZEMİN TANIMLAMASI *SOIL DESCRIPTION*	ZEMİN PROFİLİ *SOIL PROFILE*	DAYANIMLILIK *STRENGTH*	AYRIŞMA *WEATHERING*	KIRIK / 30 cm *FRACTURES/30 cm.*	KIRIK AÇISI *FRACTURE ANGLE*	SU KAYIPLARI *WATER LOSS* %	STANDART PENETRASYON DENEYİ *STANDARD PENETRATION TEST* Darbe Sayısı *No. of Blows* 0-15	15-30	30-45	N_{30}	GRAFİK / *GRAPH* 10 20 30 40 50
1																	
2			SPT-1	1.50	1.95	GRAYWACKE; brownish green, highly to completely weathered with limestone gravels							27	42	33		
	40	0	K-1	1.50	3.00												
3																	
			SPT-2	3.00	3.45								18	25	50		
						3.50											
4	40	0	K-2	3.45	4.50												
						GRAYWACKE: moderately to highly weathered, crushed, clayey			III	III	Cr	?					
5	27	0	K-3	4.50	6.00												
6						6.00											
7	27	0	K-4	6.00	7.50												
8																	
9	33	0	K-5	7.50	9.00												
	53	0	K-6	9.00	10.00	GRAYWACKE: with occasionally weathered (clayey) zones. Green, greyish green; showing schistosity occasionally and with quartz gravels below 9.50m depth; moderately/slightly weathered strong, closely fractured to partly crushed.											
10																	
11	50	0	K-7	10.00	11.30												
12	39	0	K-8	11.30	12.50			II	II								
13	38	8	K-9	12.50	14.00				CI	40°							
14										I							
15	31	0	K-10	14.00	15.50			V	V	Cr	80°						

PROJE / PROJECT : ANKARA-ÇANKAYA PROJECT
Sondaj No / Boring No : S-1
Sayfa No / Sheet No : 2 / 2

DERİNLİK DEPTH (m)	KAROT ve % KOZ % CORE & RECOVERY	R.Q.D. %	NUMUNE NO. SAMPLE NO.	NUMUNE DERİNLİĞİ SAMPLE DEPTH from to	ZEMİN TANIMLAMASI SOIL DESCRIPTION	ZEMİN PROFİLİ SOIL PROFILE	DAYANIMLILIK STRENGTH	AYRIŞMA WEATHERING	KIRIK / EKLEM FRACTURE/JOINTS	KIRILMA AÇISI FRACTURE ANGLE	SU KAYIŞ WATER LOSS %	STANDART PENETRASYON DENEYİ STANDARD PENETRATION TEST Darbe Sayısı No. of Blows 0-15 / 15-30 / 30-45	N30	GRAFİK / GRAPH 10 20 30 40 50
16	55	0	K-11	15.50-16.50	GRAYWACKE: with occasionally weathered (clayey) zones. Green, greyish green; showing schistosity occasionally and with quartz gravels below 9.50m depth; moderately/slightly weathered strong, closely fractured to partly crushed.		II	II	CI					
17	40	0	K-12	16.50-17.50										
18	34	10	K-13	17.50-18.50										
19	32	0	K-14	18.00-20.00										
20					20.00									
					End of boring									
21														
22														
23														
24														
25														
26														
27														
28														
29														
30														
31														
32														
33														

Sondaj No / *Boring No*: **S-2**
Sayfa No / *Sheet No* 1 / 2

SONDAJ LOGU / BORING LOG

PROJE ADI / *PROJECT NAME* : ANKARA-ÇANKAYA PROJECT
KOORDİNATLAR / *COORDINATES* : Y: X:
SONDAJ KOTU / *ELEVATION* (m) : 947.60
SONDAJ DERİNLİĞİ /*BORING DEPTH* (m) : 20.00
SONDAJ MAKİNASI /*DRILLING RIG* : ACKER-II
SONDÖR / *FOREMAN* : Rasim ÇİÇEK
BAŞLAMA TARİHİ / *DATE STARTED* : 14/01/2007
BİTİŞ TARİHİ / *DATE COMPLETED* : 17.01.2007
MUHAFAZA BORU / *CASING* DIŞ ÇAPI /*O.D.* (mm) = 114 İÇ ÇAPI / *I.D.* (mm) : 101 UZUNLUĞU /*LENGTH* (m) : 9.00

MÜHENDİS / *ENGINEER* : Taner ABAY

YERALTI SUYU DURUMU / *GROUND WATER DATA*

DERİNLİK *DEPTH (m)*	TARİH *DATE*	SAAT *HOUR*	AÇIKLAMA *REMARKS*

DERİNLİK *DEPTH (m)*	KAROT % *CORE % RECOVERY*	R.Q.D. %	NUMUNE NO *SAMPLE NO*	NUMUNE DERİNLİĞİ *SAMPLE DEPTH* from	to	ZEMİN TANIMLAMASI *SOIL DESCRIPTION*	ZEMİN PROFİLİ *SOIL PROFILE*	DAYANIKLILIK *STRENGTH*	AYRIŞMA *WEATHERING*	KIRIK / 30 cm *FRACTURES/30 cm*	KIRIKÇIĞI *FRACTURE ANGLE*	SU KAYBI *WATER LOSS* %	STANDART PENETRASYON DENEYİ *STANDARD PENETRATION TEST* Darbe Sayısı *No. of Blows* 0-15	15-30	30-45	N_{SP}	GRAFİK / *GRAPH* 10 20 30 40 50
1	100	0	K-1	0.0	1.50	GRAYWACKE / CLAYSTONE: yellow, grayish green, completely weathered (partly highly weathered)		IV	IV								
2			SPT-1	1.50	1.95								25	40	38		
	100	0	K-2	1.50	3.00			V	V								
3																	
			SPT-2	3.00	3.45								28	36	44		
4	51	0	K-3	3.00	4.50												
						4.00											
5	85	0	K-4	4.50	5.50	GRAYWACKE: brown, greenish brown moderately weathered, *closely fractured, clayeywith* quartz veins		III	III	CI							
						5.50											
6	95	0	K-5	5.50	6.20												
7	42	0	K-6	6.20	7.50												
8	40	22	K-7	7.50	8.00	GRAYWACKE (with occasionally weathered CLAYSTONE): green, brownish green; contains quartz veins and gravels, slightly weathered, closely fractured and crushed, fractures filled by clay and quartz weathered zones (claystone): are inform of gravelly clay.											
9	58	38	K-8	8.00	9.50												
10	33	10	K-9	9.50	10.50												
11	89	0	K-10	10.50	12.00												
12																	
13	57	8	K-11	12.00	13.50			II	II	CI	30°						
14											40°						
	50	20	K-12	13.50	15.00					I							
15																	

PROJE / PROJECT : ANKARA-ÇANKAYA PROJECT
Sondaj No / Boring No : S-2
Sayfa No / Sheet No : 2 / 2

DERİNLİK DEPTH (m)	KAROT ve % si CORE % RECOVERY	R.Q.D. %	NUMUNE NO. SAMPLE NO.	NUMUNE DERİNLİĞİ SAMPLE DEPTH from to	ZEMİN TANIMLAMASI SOIL DESCRIPTION	ZEMİN PROFİLİ SOIL PROFILE	DAYANIKLILIK STRENGTH	AYRIŞMA WEATHERING	KIRIK / 30 cm FRACTURES/30 cm	KIRIK AÇISI FRACTURE ANGLE	SU KAYBI WATER LOSS %	STANDART PENETRASYON DENEYİ STANDARD PENETRATION TEST				
												Darbe Sayısı No. of Blows			N_{30}	GRAFİK / GRAPH
												0-15	15-30	30-45		10 20 30 40 50
16	32	0	K-13	15.00-16.50	GRAYWACKE (with occasionally weathered CLAYSTONE): green, brownish green; contains quartz veins and gravels, slightly weathered, closely fractured and crushed, fractures filled by clay and quartz weathered zones (claystone): are inform of gravelly clay.		V	V		80°						
17	19	0	K-14	16.50-17.50			II	II								
18	50	0	K-15	17.50-18.50												
19	30	0	K-16	18.50-20.00												
20					20.00											
					End of boring											
21																
22																
23																
24																
25																
26																
27																
28																
29																
30																
31																
32																
33																

Sondaj No / *Boring No*: S-3
Sayfa No / *Sheet No*: 1 / 2

SONDAJ LOGU / BORING LOG

PROJE ADI / *PROJECT NAME* : ANKARA-ÇANKAYA PROJESİ
KOORDİNATLAR / *COORDINATES* : Y: X:
SONDAJ KOTU / *ELEVATION* (m) : 947.30
SONDAJ DERİNLİĞİ /*BORING DEPTH* (m) : 18.00
SONDAJ MAKİNASI /*DRILLING RIG* : ACKER-II
SONDÖR / *FOREMAN* : Rasim ÇİÇEK
BAŞLAMA TARİHİ / *DATE STARTED* : 18/01/2007
BİTİŞ TARİHİ / *DATE COMPLETED* : 19.01.2007
MUHAFAZA BORU / *CASING* DİŞ ÇAPI /*O.D.* (mm) = 114 İÇ ÇAPI / *I.D.* (mm) : 101 UZUNLUĞU /*LENGTH* (m) : 10.50

MÜHENDİS / *ENGINEER* : Taner ABAY

YERALTI SUYU DURUMU / *GROUND WATER DATA*

DERİNLİK *DEPTH (m)*	TARİH *DATE*	SAAT *HOUR*	AÇIKLAMA *REMARKS*

DERİNLİK *DEPTH (m)*	KAROT % *CORE %*	R.Q.D. %	NUMUNE NO. *SAMPLE NO.*	NUMUNE DERİNLİĞİ *SAMPLE DEPTH* from	to	ZEMİN TANIMLAMASI *SOIL DESCRIPTION*	ZEMİN PROFİLİ *SOIL PROFILE*	DAYANIKLILIK *STRENGTH*	AYRIŞMA *WEATHERING*	KIRIK (SU) sayısı *FRACTURE/SET no.*	KIRIKÇISI *FRACTURE ANGLE*	SU KAYBI *WATER LOSS %*	STANDART PENETRASYON DENEYİ *STANDARD PENETRATION TEST* Darbe Sayısı *No. of Blows* 0-15	15-30	30-45	N_{30}	GRAFİK / *GRAPH* 10 20 30 40 50
1						SANDY CLAY: with little gravel, brown (Altered Soil)											
2			SPT-1	1.50	1.90								12	17	50/10		
3						3.00											
			SPT-2	3.00	3.07								50/7				
4	100	0	K-1	3.00	4.50	GRAYWACKE: clayey, moderately weathered		III IV	III								
5						5.00											
6	53	11	K-2	4.50	6.00	GRAYWACKE: with quartz veins, showing schistosity below 6.50m depth, closely fractured and partly clayey especially between 5.50-6.00m 6.70-7.00m depth											
7	74	12	K-3	6.00	7.00			II	II	Cl Cr	40° ?						
8	47	35	K-4	7.00	8.50												
						8.50											
9	40	0	K-5	8.50	9.50												
10	38	0	K-6	9.50	10.50												
11	12	0	K-7	10.50	12.00	GRAYWACKE with occasional weathered zones (claystone) green, with quartz veins, strong, crushed, weathered zones in form of claystone is observed occasionally especially between 10.50-16.00m											
12																	
13	25	0	K-8	12.00	13.50			II	II	Cr	?						
14	23	0	K-9	13.50	15.00												
15								V	V								

PROJE / *PROJECT* : **ANKARA-ÇANKAYA PROJECT**
Sondaj No / *Boring No* : **S-3**
Sayfa No / *Sheet No* : **2 / 2**

DERİNLİK *DEPTH (m)*	KAROT ve % si *CORE & RECOVERY*	R.Q.D. %	NUMUNE NO. *SAMPLE NO.*	NUMUNE DERİNLİĞİ *SAMPLE DEPTH* from to	ZEMİN TANIMLAMASI *SOIL DESCRIPTION*	ZEMİN PROFİLİ *SOIL PROFILE*	DAYANIKLILIK *STRENGTH*	AYRIŞMA *WEATHERING*	KIRIK / 30 cm *FRACTURES/30 cm*	KIRIK AÇISI *FRACTURE ANGLE*	SU KAYBI *WATER LOSS %*	STANDART PENETRASYON DENEYİ *STANDARD PENETRATION TEST* Darbe Sayısı *No. of Blows* 0-15 / 15-30 / 30-45	N_{30}	GRAFİK / *GRAPH* 10 20 30 40 50
16	22	0	K-10	15.00-16.00	GRAYWACKE with occasional weathered zones (claystone) green, with quartz veins, strong, crushed, weathered zones in form of claystone is observed occasionally especially between 10.50-16.00m									
17	20	0	K-11	16.00-17.50										
18	40	0	K-12	17.50-18.00										
					18.00									
					End of Boring									
19														
20														
21														
22														
23														
24														
25														
26														
27														
28														
29														
30														
31														
32														
33														

APPENDIX B

INCLINOMETER RESULTS OF ANKARA-ÇANKAYA PROJECT

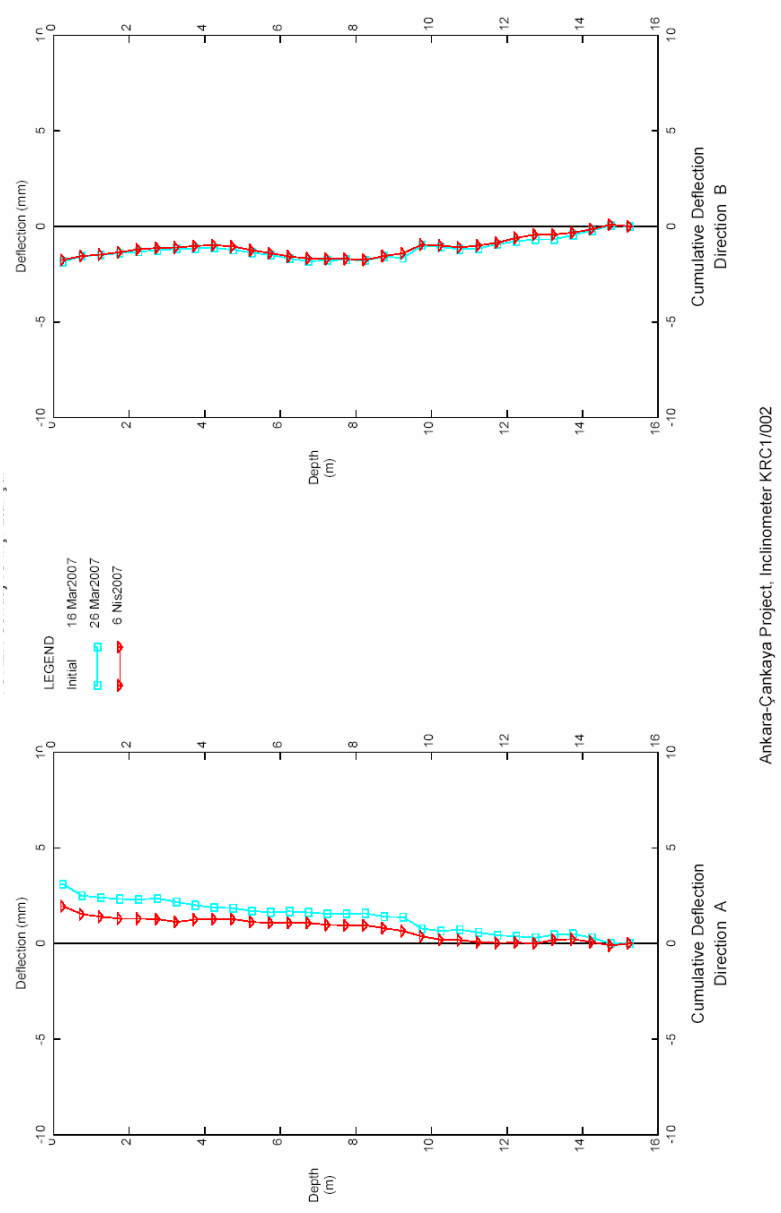

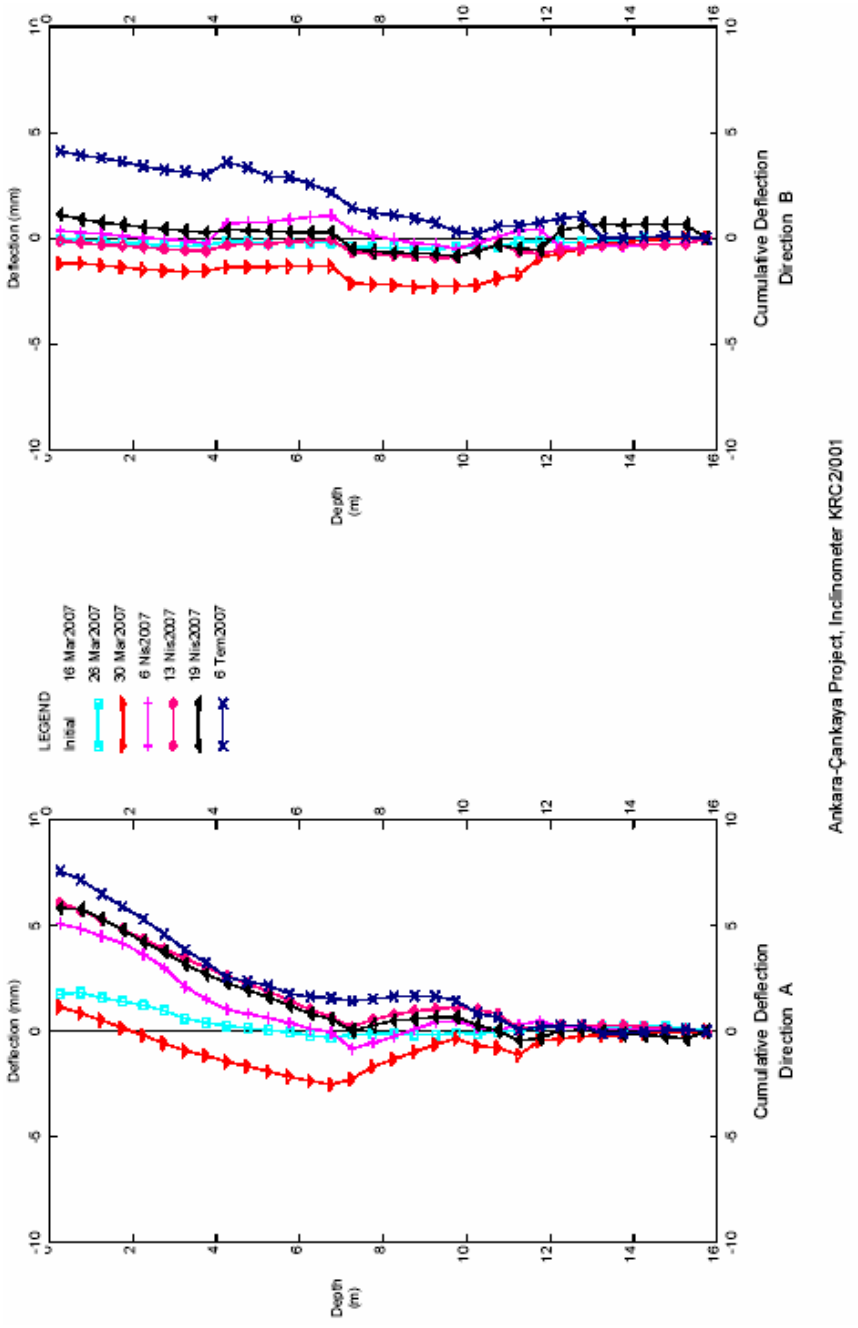
Ankara-Çankaya Project, Inclinometer KRC2/001
Cumulative Deflection
Direction A
Cumulative Deflection
Direction B
Deflection (mm)
Depth (m)
LEGEND
Initial
16 Mar2007
26 Mar2007
30 Mar2007
6 Nis2007
13 Nis2007
19 Nis2007
6 Tem2007

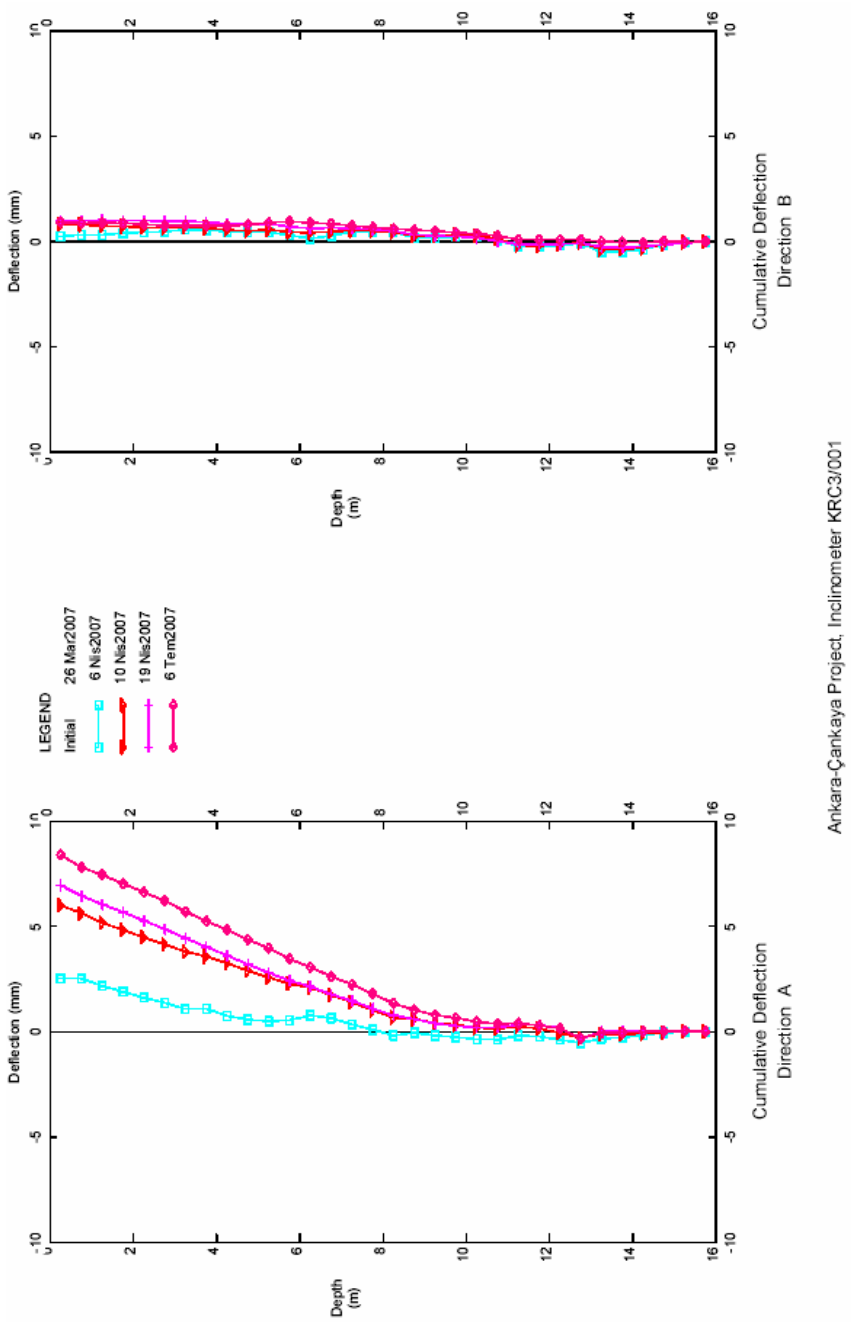
Ankara-Çankaya Project, Inclinometer KRC3/001
Cumulative Deflection
Direction A
Cumulative Deflection
Direction B
Deflection (mm)
Depth (m)
LEGEND
Initial
26 Mar2007
6 Nis2007
10 Nis2007
19 Nis2007
6 Tem2007

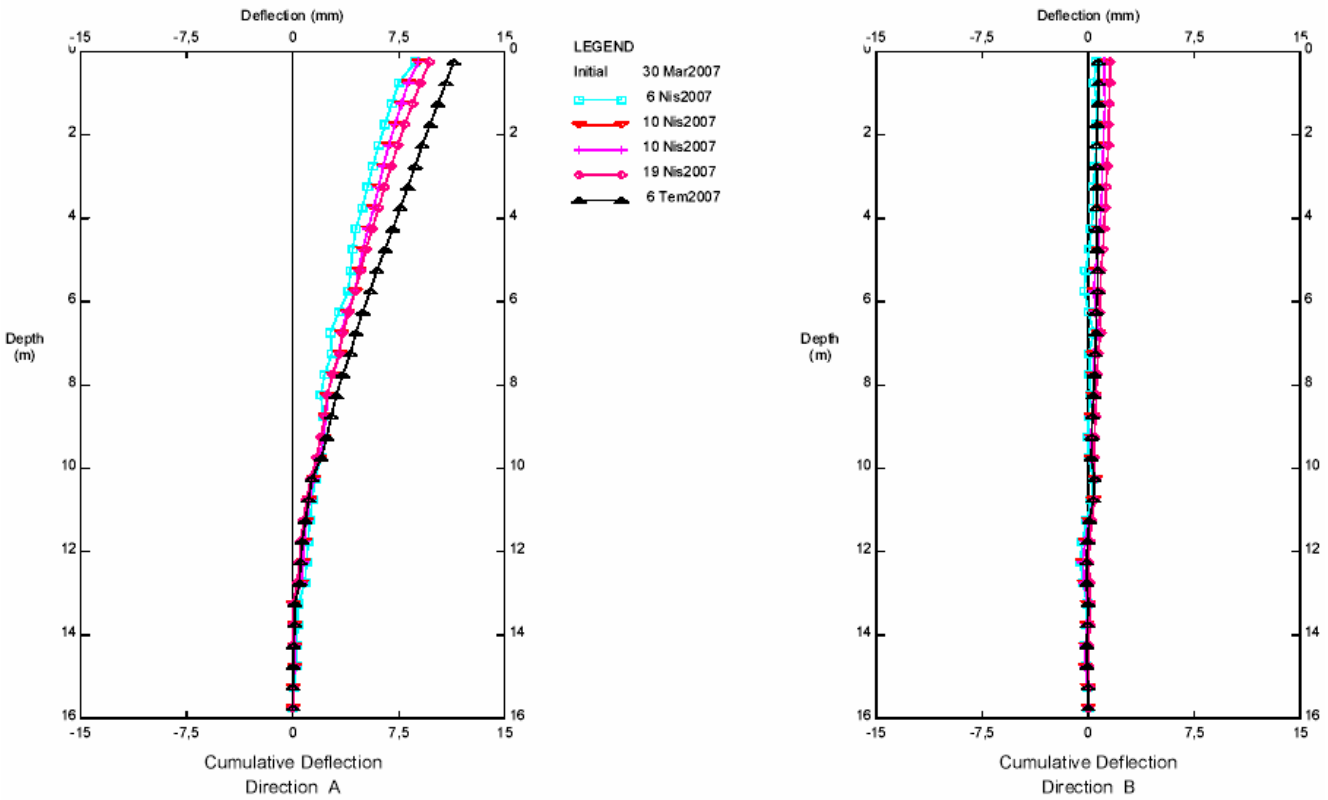

Ankara-Çankaya Project, Inclinometer KRC4/001

APPENDIX C

INCLINOMETER RESULTS OF EKOL CONSTRUCTION PROJECT